Design and Development of Renewable Plant Microbial Fuel Cell for Bioelectricity Generation

A Thesis

Submitted in Partial Fulfillment of the Requirements for the Degree of

DOCTOR OF PHILOSOPHY

by

Pranab Jyoti Sarma

(Roll No.: 156151005)

School of Energy Science and Engineering

Indian Institute of Technology Guwahati,

Guwahati – 781039, Assam, India

August 2023

The Thesis is dedicated

to

my Parents

SCHOOL OF ENERGY SCIENCE AND ENGINEERING

INDIAN INSTITUTE OF TECHNOLOGY GUWAHATI

STATEMENT

I do hereby declare that the content embodied in this thesis entitled "**Design and Development of Renewable Plant Microbial Fuel Cell for Bioelectricity Generation**" is the result of investigations carried out by me at the School of Energy Science and Engineering, Indian Institute of Technology Guwahati, Guwahati, India, under the guidance of **Prof. Kaustubha Mohanty**.

In keeping with the general practice of reporting scientific observations, due acknowledgements have been made whenever the work described is based on the findings of other investigations.

Pranab Jyoti Sarma

SCHOOL OF ENERGY SCIENCE AND ENGINEERING

INDIAN INSTITUTE OF TECHNOLOGY GUWAHATI

CERTIFICATE

This is to certify that **Mr. Pranab Jyoti Sarma** has been working under my supervision since July 2015. We hereby forward his PhD thesis entitled *"***Design and Development of Renewable Plant Microbial Fuel Cell for Bioelectricity Generation***"* to be submitted for the award degree of Doctor of Philosophy to IIT Guwahati. I certify that he has fulfilled all the requirements according to the rules of this institute and the investigations in his thesis have not been submitted elsewhere for a degree or diploma.

Date

IIT Guwahati

Dr. Kaustubha Mohanty

Professor and Head, Department of Chemical Engineering and Adjunct Professor, School of Energy Science and Engineering,
Indian Institute of Technology Guwahati

AKNOWLEDGEMENT

I would like to take this opportunity to express my heartful gratitude to all, who have directly or indirectly helped me in successful completion of my PhD. At the onset, Iam highly thankful to Indian Institute of Technology Guwahati for giving me the opportunity to carry out PhD work and providing me all the necessary support and facilities.

With immense gratitude I would like to acknowledge my Supervisor Prof. Kaustubha Mohanty, Head, Department of Chemical Engineering, IIT Guwahati, for his esteemed guidance, valuable suggestions and support throughout my PhD journey.

I owe my gratitude to the members of my Doctoral Committee, Prof. Mahuya De, Prof. Animes Golder and Prof. Vishal Trivedi for their valuable suggestions and advice throughout my research work.

I am thankful to School of Energy Science and Engineering (SESE) and all its staff members for providing me a wonderful environment to carry out my Ph. D work. I also thankful to Central workshop, Mechanical Depertment and Central Instruments Facility (CIF, IIT Guwahati) for providing with instrumental facilities.

I would like to gratefully acknowledge Ministry of Education for providing me with Financial Assistantship during my PhD tenure.

Throught this Phd Journey, many people I have came across has helped me immensely and I would like to give my warm thanks to my lab mates, Dr. Rajneesh Kumar, Pradeep Kumar, Nayan Moni Baishya, Aradhana Priyadarshini, Phenecia Shabong, Dr. Philip Bernstein Saynik, Dr. Madonna Roy, Dr. Sounak Bera, Saptaswa Biswas, Deepesh Singh Chouhan, Anindita Das, Himanshu Bhattacharyya, Dr. Parikshit Saikia, Dr. Manojit Ghosh, Dr. Ashif Iqbal, Arup Dutta, Jyotisman Pathak for their inspired support and help.

No words can suffice my deepest sense of gratitude to my parents, Mr. Biraj Kumar Sharma and Mrs. Manju Devi Sharma for their unconditional love, sacrifices, care and encouragement towards completion of my Ph. D Thesis. Special thanks to my sister, my brother in law, my in-laws for their constant motivations.

Last but not the least, I am sincerely grateful to my wife, Dr. Barasa Malakar for her unconditional support during my tough times and continuous motivation and encouragement. My PhD endeavor would not have been possible without them. Above all, I offer my gentle reverence to Almighty God.

Thank you all!!!

Pranab Jyoti Sarma

IIT Guwahati

August 2023

Abstract

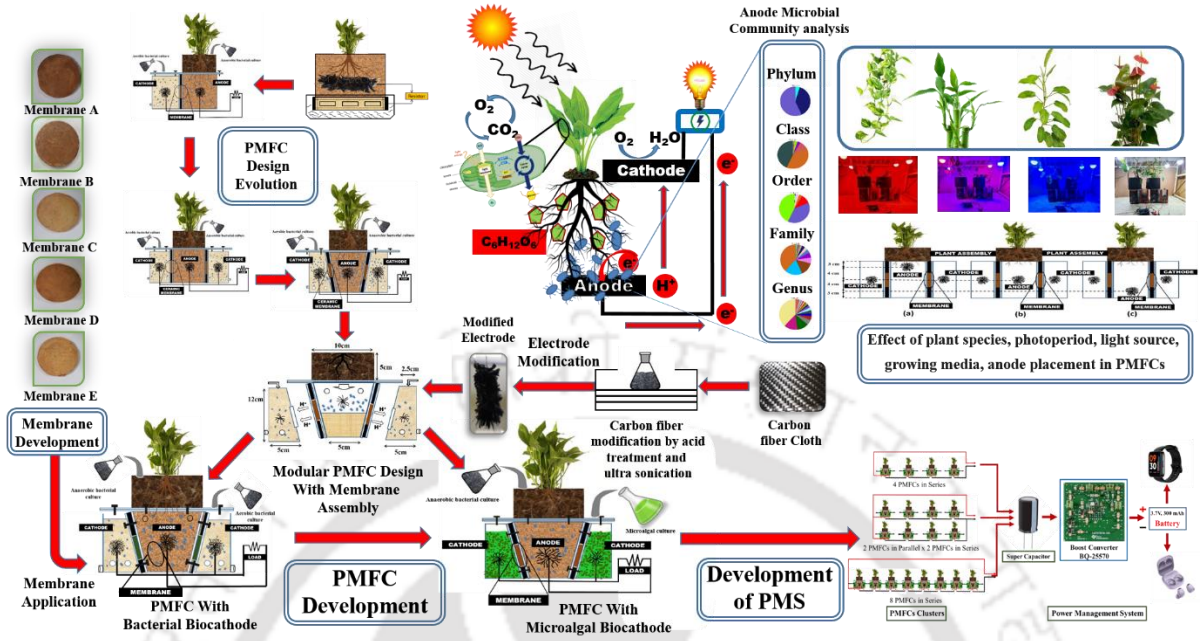

In recent times, mankind is undergoing a momentous transition, facing a significant energy demand while grappling with issues like biodiversity loss and climate change, which make our world challenging to inhabit. Presently, most of our energy needs are met by fossil fuels, but many countries are actively seeking green renewable energy sources for long-term sustainability in alignment with the UN's sustainable development goals (SDGs). While solar energy, wind energy, geothermal, and hydrothermal energy are promising renewable options, they come with drawbacks such as high energy-intensive processes, substantial capital requirements, geographical limitations, landscape transformation, and ecological disturbances.

To address these limitations, plant microbial fuel cells (PMFCs) emerge as a potential solution. They offer renewable, self-sustainable, green, eco-friendly, and cost-effective energy generation without requiring intensive processes or landscape alterations. PMFCs contribute to CO_2 reduction and leave a minimal carbon footprint, supporting a sustainable future with simultaneous power generation and biomass production.

Indoor air pollution is known to be a serious kind of pollution with associated many health implications. Many indoor plants have the ability to mitigate various indoor air pollutants. Therefore, this study explores the effectiveness of various indoor plants in mitigating indoor air pollution through PMFC operation. The bioelectricity generation pattern was observed for four indoor plants, with *Philodendron erubescens* showing the highest power density, followed by *Epipremnum aureum*, *Anthurium andreanum*, and *Dracaena braunii* with

maximum and minimum power density of 32.21 mWm^{-2} and 18.6 mWm^{-2} respectively. The total energy production per week was almost constant for these plants, with *P. erubescens* being the species with the best performance at 234 J. This is followed by *E. aureum, A. Andreanum* and *D. braunii* with 204 J and 187 J, 155 J respectively. A long-term performance study for over six month showed that the better root development and adaptability of plant species under moist conditions enhanced PMFC performance and stability, reducing the cell's internal resistance.

The study emphasizes the importance of different operating conditions in influencing plant growth and development, thereby impacting PMFC performance. The significance of photoperiod and light source is highlighted in their effect on electricity generation by indoor plants. The photoperiods of 16/8, 12/12 and 8/16 hours were tested using plant *P. erubescens* and the resulting power output was found to be 24.38 ± 0.8 mW m^{-2}, 23.64 ± 1.4 mW m^{-2} and 21.38 ± 0.4 mW m^{-2}, respectively. Since the photoperiod of 12/12-hour light and dark cycle closely resembles natural lighting process, therefore for optimum utilization of both the plants at bio anode and microalgae at the bio cathode the said photoperiod was used for all succeeding studies.

Similar to photoperiod, the source of light is equally important for photosynthesis. The voltage generation pattern by two indoor plant *E. aureum* and *P. erubescens* were studied under different lighting conditions i.e., Red, Blue, Red + Blue, and White light. The maximum power density was obtained under white light i.e., 26.42 ± 0.4 mW m^{-2} and 22.38 ± 0.4 mW $m^{-2}$from PMFC with *P. erubescens* and *E. aureum* respectively. A relatively lower power density of 15.32 ± 1.2 mW m^{-2} and 12.46 ± 1.4 mW m^{-2} were obtained for both the PMFCs under red light. Maximum biomass increase was seen for both plant and microalgal under white light with chlorophyll concentration increasing from 3.09 ± 0.046 µg mL^{-1} to 29.36 ± 1.6 µg mL^{-1}.

Also, the addition of novel plant growth media can influence plant growth and power generation in a PMFC leading to enhanced root and shoot development. The maximum power density and current density obtained were 27.41 mW m^{-2} 51.60 mA m^{-2} contributing to a 31% increase in power generation compared to PMFCs without growth media.

Electrode material plays a crucial role in PMFC performance, and carbon fiber, known for its eco-friendliness and adaptability to moist soil environments, was modified with acid treatment to improve biofilm development and power generation. Characterization studies were performed by FTIR, RAMAN, FESEM-EDS analysis. FTIR analysis indicates presence of significant peaks of alcohol and carboxyl functional groups on its surface after modification. These functional groups helped to enhance the electron transfer between electro-catalytic

surface of bacteria and the electrode, owing to the formation of hydrogen bonding between these functional groups of electrodes with peptide bonds present in bacterial cytochrome. Raman analysis shows the ID/IG ration of modified carbon fibre to be 0.89, which is lower than the unmodified part (1.02), indicating that acid modified carbon fibre has higher graphitic degree and lower disordered structure, that was beneficial for electrode performance. FESEM images confirms development of favourable environment for bacterial attachment to the electrode surface after modification with enhancement in fibrous nature of the material. This may have resulted from hydrogen bonding between the bacterial cytochrome and carboxyl group of the electrochemically oxidized carbon fibre. The modified carbon fiber showed significant enhancements in power density and current density without causing any adverse effect to the microorganisms and the plants. The biofilm development analysis through 16S rRNA gene amplicon high-throughput sequencing revealed the presence of Firmicutes (56.84%) and Bacteroidetes (38.45%) as the dominant bacteria.

The study also presents the development and comprehensive characterization of low-cost ceramic membranes, showcasing their potential to replace expensive commercial membranes without much compromise on PMFC properties and its performance. Different types of ceramic membranes were developed by blending natural clay with bentonite, flyash, Na_2CO_3, Na_2SiO_3, H_3BO_3 at various composition. Physical and chemical characterization were carried out by using TGA, XRD, FESEM, FTIR, water uptake, proton conductivity, oxygen and acetate diffusion and compared with Nafion117. Among all, the membrane B having composition of clay, bentonite, fly ash, Na_2Co_3, Na_2Sio_3 and H_3Bo_3 at a concentration of 40%, 20%, 20%, 10%, 3%, and 7%, respectively, demonstrated superior cation transport ability and reduced oxygen diffusion and substrate crossover, resulting in higher bioelectricity generation and overall improved PMFC performance. The membrane achieved a maximum power density of 22.38 mW m^{-2} which was 78% higher than PMFC with control membrane (100% clay). As a result, a decline in internal resistance was seen from 346 Ω to 234 Ω. The cost of making the ceramic membrane was estimated to be extremely low at ₹1,279 ft^{-2} in comparison to nafion117 (₹80,580 ft^{-2}), and it represent economically viable alternative. The membrane demonstrated extreme stability for long term operations involving more than six months.

Throughout the study, the PMFC setup underwent a design evolution from a membrane-less two-chamber design to a modular three-chamber structure. The introduction of a physical membrane improved ion transport and anaerobic environment creation minimize O_2 leakage to anode surface. Three chamber PMFC with narrow bottom anode chamber helps in creating favourable anaerobic environment with 26% decrease in O_2 concentration and increasing

power generation by 60 % with respect to membrane less two chamber design. The novel modular design of PMFC plays a significant role for ease of operation and maintenance of PMFCs during long term usage.

Incorporation of pre-acclimatized electrodes reduced start-up time significantly. The voltage generation pattern between the initial 20-60 days' time was very crucial as it depicted the nutrient transition period from synthetic nutrient to plants released nutrients through rhizodeposits. The use of SSN in PMFCs provided a smooth nutrient transition for microorganisms thereby obtaining continuous power generation. The study also explored the integration of bacterial and microalgal bio-cathodes, with microalgae enhancing power generation by 17 % as compared to bacterial counterpart. It also and reduce the need for energy-intensive mechanical aeration as microalgal bio cathode help to increase O_2 concentration in the cathode chamber with a maximum DO concentration recorded to be 10.7 ± 0.26 mg L^{-1}. Furthermore, the long term performance is also compromised due to electrode biofouling in bacterial bio cathode. This signifies the self-sustainable nature of PMFC, where plants-bacteria-microalgal mutual collaborative approach leads towards a better PMFC performance.

The study concludes with the design of an energy harvesting system using PMFCs connected in different cluster arrangements to understand the power generation pattern. Eight PMFCs, in series-parallel arrangements showed highest power output of 2.95 ± 0.08 mW among all which helps to charge a supercapacitor faster. Three different supercapacitors, viz., 2.2 F, 3.3F and 4.7F, are chosen and connected to the cluster and a comparative analysis was carried out through repeated charging-discharging cycles. It takes nearly ~18 hours to fully charge the supercapacitors from 0V to 2.7V. The plant recovery profile showcases almost~8.5 hours required to recover the voltage to its starting point. The DC/DC boost converter (BQ25570) provides a constant step-up voltage of 4.8V for 157 ± 5 seconds, while the supercapacitor of 4.7F discharge from 2.7V to 100 mV. It takes nearly 7days to fully charge a 300 mAh rechargeable battery. The battery was used to charge a smartwatch and a pair of wireless earbuds having 170 mAh and 43 mAh capacity in 120 minutes and 60 minutes, respectively. The study demonstrates the potential of PMFCs to power electronic gadgets for day-to-day applications, emphasizing their role as a sustainable and eco-friendly energy solution.

Keywords: Bio-electricity; Indoor plants; PMFC; Carbon fibre electrode; Ceramic membrane; Power management system

CONTENTS

LIST OF TABLES

LIST OF FIGURES

Chapter 3:

LIST OF ABBREVIATION

AC	Activated carbon
AEM	Anion-exchange membrane
AFC	Algal fuel cell
ATP	Adenosine triphosphate
Au	Gold
Ag	Silver
BES	Bioelectrochemical system
BFC	Biofuel cell
BPM	Bipolar membrane
CAGR	Compound annual growth rate
CAM	Crassulacean acid metabolism
CEM	Cation-exchange membrane
CM	Ceramic membrane
CNTs	Carbon nanotube
CPs	Conductive polymer
Chl	Chlorophyll
Chl-a	Chlorophyll-a
Chl-b	Chlorophyll-b
$C_6H_{12}O_6$	Glucose
CO_2	Carbon dioxide
Co_3O_4	Cobalt tetraoxide
COD	Chemical oxygen demand
COP	*Conference of the Parties*
CoTMPP	Cobalt tetramethoxyphenylporphyrin
CTCs	C-type Cytochromes
CV	Cyclic voltametry

DC	Direct current
DET	Direct electron transfer
D_A	Acetate diffusion coefficient
D_H	Proton diffusion coefficient
D_O	Oxygen diffusion coefficient
D_T	Doubling Time
DO	Dissolve oxygen
DCW	Dry cell weight
e^-	Electrons
EDTA	Ethylenediamine tetraacetic acid
EDX	Energy dispersive x-ray spectroscopy
EAB	Electroactive bacteria
EAM	Electrochemically active microbes
EIS	Electrochemical impedance spectroscopy
EMF	Electromotive force
ET	Electron transfer
EET	Extracellular electron transfer
EFB	Ecological floating bed
FDW	Fermented-distillery wastewater
FePc	Iron phthalocyanine
FESEM	Field emission scanning electron microscope
FTIR	Fourier transform infrared spectroscopy
FTS	Flow-through system
FR	Fumarate reductase
G^+	Gram-positive
G^-	Gram-negative
GAC	Granular activated carbon

SYMBOLS AND UNIT

A	Ampere
mA	Miliampere
V	Volt
mV	Mili Volt
W	Watt
GW	Giga Watt
μW	Microwatt
mW	Miliwatt
Wm^{-2}	Watt per meter square
Wm^{-3}	Watt per meter cube
$A\ m^{-2}$	Ampere per meter square
mAm^{-2}	Mili ampere per meter square
mAm^{-3}	Mili ampere per meter cube
mWm^{-2}	Mili watt per meter square
m^2g^{-1}	Meter square per gram
$g\ L^{-1}$	Gram per Litre
$mg\ L^{-1}$	Milligram per Litre
Hz	Hertz
kHz	Kilohertz
mHz	Megahertz
ºC	Degree Celsius
F	Farad
J	Joule
h	Hour
s	Second
ft	Feet
mL	Millilitre
w/w	Weight by weight
v/v	Volume by volume
d^{-1}	Per day

mg L^{-1} d^{-1}	Milligram per Litre per day
g	Gram
µg mL^{-1}	Microgram per Millilitre
µmol L^{-1}	Micromole per litre
g L^{-1}	Gram per litre
g mL^{-1}	Gram per Millilitre
wt %	Weight percentage/percent
min	Minute
mAh	Miliampere Hour
Mb	Megabyte
η_{phot}	Photosynthetic efficiency
Ω(ohm)	Ohmic resistance (ohm)
Ωm^{-2}	Resistance per metre square
Cm	Centimetre
mm	Milimetre
cm^{-1}	Per centimetre
cm s^{-1}	Centimeter per second
cm^2 s^{-1}	Centimeter square per second
nm	Nanometre
cm^2	cross-sectional area
Ω^{-1} cm^{-1}	specific conductivity
°/s	Degree per second
Å	Angstrom
λ	Lambda
θ	Theta
₹	Rupees
R_{int}	Internal resistance

Chapter I

Introduction

1.1 Global Energy Scenario

Mankind at present is going through tremendous energy crisis on global scale and thus, there is always a huge demand for an alternative form of energy that is renewable as well as sustainable (Imhoff et al., 2004; Solomon et al., 2007; Sharmina et al., 2017). More specifically, these forms of energy should be available in the form of electricity and fuels. The need for energy is increasing and is expected to keep on increasing in the coming decades. Currently most energy (81%) is generated by conversion of fossil fuels into electricity or fuels (Fig. 1.1).

Among all the sources of energy, coal has strengthened its role as the dominant energy source, maintaining its strong position in power generation as well as being the fuel of choice for many industries (especially heavy industries such as iron and steel). Coal demand nearly tripled between 2000 and 2019, accounting for half of primary energy demand growth. Today, coal meets 44% of India's primary energy demand, up from 33% in 2000. Coal has played a significant role in India's economic development while also contributing to air pollution and growing GHG emissions. Similar to global energy scenario, India's energy demand has tripled over the last three decades: the share of traditional biomass has fallen, leaving coal and oil dominant (Fig. 1.2).

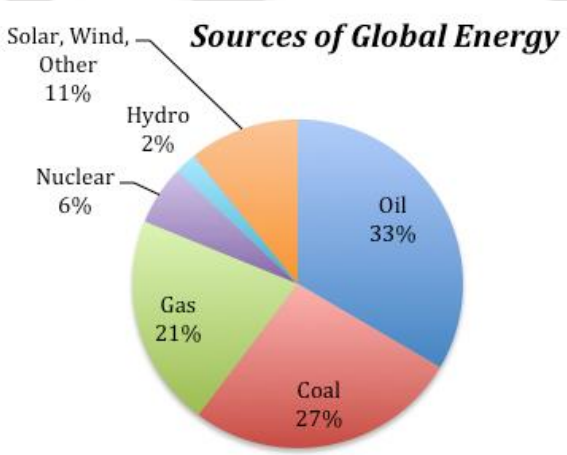

Fig. 1.1 The current contributions to our global energy from different sources (Source: International Energy Agency (iea.org)).

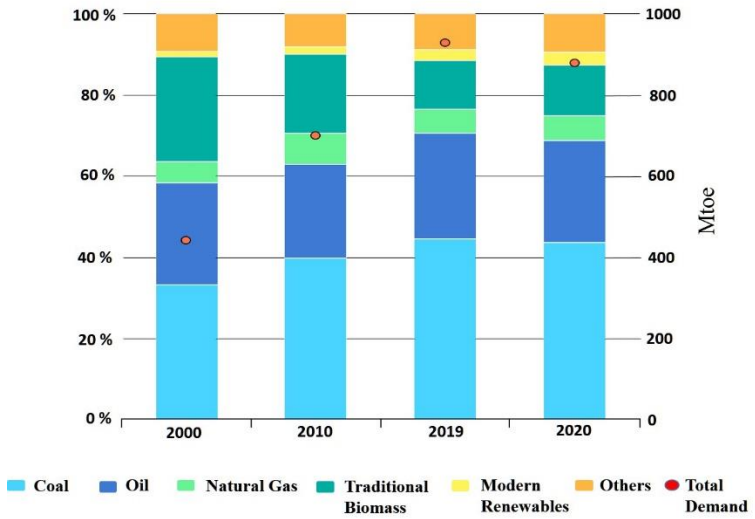

Fig.1.2 Total primary energy demand in India (Source: India Energy Outlook 2021, International Energy Agency; Mtoe = a million tonnes of oil equivalent).

1.2 Renewable energy and its importance

The major drawback of using fossil fuels is that their conversion into electricity or fuels is polluting the environment by emission of carbon dioxide, nitrogen oxides, sulphur dioxide, volatile organic compounds, heavy metals, and fine particles. These emissions result in all kind of environmental problems such as climate change, acid rain (Larssen et al., 2006) and public health issues. Furthermore, they can be considered to be not renewable (they are renewable but only on a time scale of millions of years), which inevitably resulting in depletion of these resources. To overcome these drawbacks, the ideal energy form of the future should be derived from renewable sources and converted into electricity or fuel via clean technologies.

Facilitation of transition to non-conventional sources holds the key towards global development aspiration and specially for developing countries like India. A revolutionary shift towards non-conventional sources can bring about transformational opportunities for sustainable economic development. Transition to renewable and green sources of energy is a crucial enabler for sustainable development and climate resilience paving its way towards creation of more equitable, inclusive and sustainable society. Five major non-conventional sources of energy prevailing today are as follows:

1.2.1 Solar Energy

Solar energy refers to the energy received from the sun in the form of light and heat. It can be harnessed by converting into electrical energy in solar plants. India, is a tropical country and its geographical location makes it a conductive source of energy. There has been a significant impact of the solar energy in India in recent years.

India has a favourable location in the solar belt (400S to 400N) making it one of the best recipient of solar energy with abundant availability. Its generation has increased by more than 18 times from 2.63 GW in March 2014 to 49.3 GW at the end of 2021 (India Energy Outlook 2021, International Energy Agency). Compared to conventional sources of energy, solar electricity offers a sustainable and environment friendly electricity supply for regular growing demand. There are now hybrid models where power is drawn from both the grid and solar cells thus reducing the dependency solely on grid which mainly runs on non-renewable source of energy.

1.2.2 Wind Energy

Wind power is a clean, reliable, renewable and cost–competitive sources of renewable energy that has been used for decades. Wind power generation along with solar power (Hybrid renewable power) is becoming quite popular now and many more wind turbines are getting installed globally. Conversion of wind energy has been expensive so far, along with the impact of a variable resource on the grid and siting. Hoverer, technology has advances rapidly in recent years to accommodate these factors.

1.2.3 Geothermal Power

Geothermal power is a renewable form of energy utilizing underground hot water or stream created by the natural heat beneath the earth's surface. Low-temperature geothermal sources can be utilised to heat and cool by installing heat pump systems. Hot water or steam from high temperature geothermal sources can be used to power turbines to produce clean and renewable electrical energy.

1.2.4 Hydropower

Hydropower harnesses the energy of water moving from higher to lower elevations. It can be generated from reservoirs and rivers. Reservoir hydropower plants rely on stored water in a reservoir, while run-of-river hydropower plants harness energy from the available

flow of the river. Hydropower reservoirs often have multiple uses - providing drinking water, water for irrigation, flood and drought control, navigation services, as well as energy supply. Hydropower currently is the largest source of renewable energy in the electricity sector. It relies on generally stable rainfall patterns, and can be negatively impacted by climate-induced droughts or changes to ecosystems which impact rainfall patterns. The infrastructure needed to create hydropower can also impact on ecosystems in adverse ways. For this reason, many consider small-scale hydro a more environmental-friendly option, and especially suitable for communities in remote locations.

1.2.5 Bioenergy

Bioenergy is produced from a variety of organic materials, called biomass, such as wood, charcoal, dung and other manures for heat and power production, and agricultural crops for liquid biofuels production. Most biomass is used in rural areas for cooking, lighting and space heating, generally by poorer populations in developing countries. Modern biomass systems include dedicated crops or trees, residues from agriculture and forestry, and various organic waste streams. Energy created by burning biomass creates greenhouse gas emissions, but at lower levels than burning fossil fuels like coal, oil or gas. Also it may change land use pattern and create competition for food sources. Apart from traditional bioenergy resources, there are other modern forms of bioenergy such as biodiesel, biohydrogen, bioethanol etc., developed from various agricultural waste feed stock and microalgal biomass which has gained considerable popularity in recent past due to being green, economical and non-competitive for food sources.

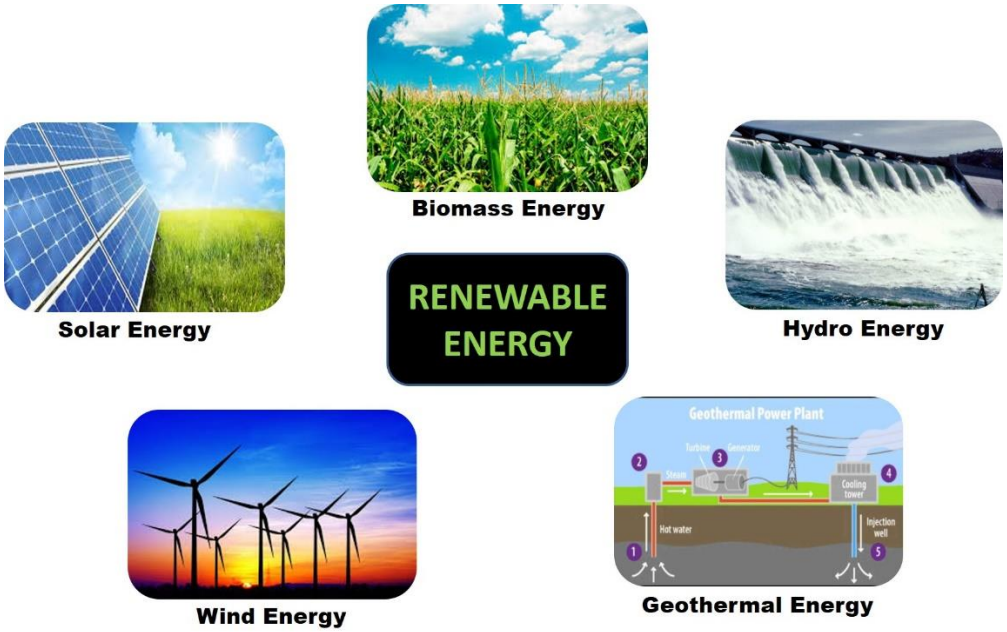

Fig. 1.3 Major forms of renewable energy.

1.3 Significance of Non-Conventional Sources of Energy

Transition to non-conventional sources of clean energy ensures the attainment of three Es that often find mention in energy policies-energy security, economic development and environmental sustainability. The shift towards non-conventional sources of energy will make this planet a better place to live. Apart from addressing the issue of climate change and global warming, transition to renewable sources of energy will reduce air pollution and will further contribute to better public health outcomes.

Additionally, the trust on non-conventional sources of energy can fetch economic gains for a country like India. The shift towards non-conventional sources of energy can bring down the cost of energy supply and can also ensure enhanced delivery of affordable clean energy that is accessible to all. The realisation of Govt of India's Aatmanirbhar Bharat Abhiyaan (https://aatmanirbharbharat.mygov.in/) also depends on the enhanced accessibility and affordability of green/clean energy sources.

Apart from environmental aspects, the economic benefits are also significant. The transition to renewable energy source will aid Indian economy to delink itself from volatile international oil prices. It can also ease out subsidy burden of government currently spend on conventional energy sources including kerosene. Further, the transition to non-conventional sources of energy results in more employment and entrepreneurship opportunities in the

domain of renewable energy. India can also lead in exports of non-conventional energy sources such as wind electric generators, biomass gasifiers, solar energy systems, electric vehicles etc. Further, India could also handhold other developing nations to explore the path of sustainable development via making best utilization of non-conventional sources of energy. As of 31st August 2022, renewable energy sources, including large hydropower, have a combined installed capacity of 163 GW (Invest India, 2022).

India ranks 3rd in renewable energy country attractive index in 2021 and 3rd largest energy consuming country in the world. India stands 4th globally in Renewable Energy Installed Capacity (including Large Hydro), 4th in Wind Power capacity and 4th in Solar Power capacity (as per REN21 Renewables 2022 Global Status Report). As per the central electricity authority report, the total installed capacity increased by CAGR 15.92% between financial year 2016-22. To combat climate change, India promised on five pledge (*Panchamrit*) at COP 26, Glasgow, which includes:

- India will get its non-fossil energy capacity to 500 GW by 2030;
- India will meet 50% of its energy requirement from renewable resources by 2030;
- India will reduce total projected carbon emissions by one billion tonnes from now onwards till 2030;
- By 2030, India will reduce the carbon intensity of its economy by less than 45%;
- By the year 2070, India will achieve the target of net-zero.

This is the India's largest expansion plan in renewable energy. India was the second largest market in Asia for new solar PV capacity and third globally (13 GW of additions in 2021). It ranked fourth for total installations (60.4 GW), overtaking Germany (59.2 GW) for the first time. India's installed renewable energy capacity has increased 396% in the last 8.5 years and stands at more than 174.53 Giga Watts (including large Hydro), which is about 42.5% of the country's total capacity (as of February 2023). India reported the highest year on year growth in renewable energy additions of 9.83% in 2022. The installed solar energy capacity has increased by 24.4 times in the last 9 years and stands at 63.3 GW as of Feb 2023. The installed renewable energy capacity (including large hydro) has seen an increase of around 128% since 2014 (India Energy Outlook 2021; Invest India, 2022).

1.4 Importance of Plant Microbial Fuel Cell Technology

The pursuit for alternative clean, green and sustainable energy technologies to fulfil energy requirements is a principle challenge in view of rising greenhouse gases (GHGs) levels

and to mitigate climate change issues and socioeconomic instability. There are also several challenges associated with the new technologies and their long term economic viability. Wind energy, solar energy and hydro power energy are interesting alternatives as future energy source because they are inexhaustible; however, their commercialization at a mass scale has some limitations. At the same time, environmental impact of both wind turbines (avian mortality, visual impacts, noise, electromagnetic interference) and solar panels (visual impacts, loss of green space and biodiversity, increasing dark surface, use of polluting metals) is negative and quite controversial (Campoccia et al., 2009; Kazmerski, 2006).

Amidst all such speculation, generation of bioelectricity employing microbial fuel cells (MFCs) are gaining serious attentions due its several benefits mainly waste to energy approach and greener in nature. MFCs generate electrical energy by utilizing the metabolic activities of electrochemically active microbes (EAM). It represents an innovative approach whereby EAM oxidises organic fraction of waste to be harnessed in the form of bioelectricity. In spite of being a wonderful technology, MFCs carry some major limitations which restrict its commercial applications; which includes:

1. The complete utilization of waste substrate by microbes in a MFC results into interruption of power generation process after a specific time duration;
2. The magnitude of voltage generated by a MFC is very limited, therefore it cannot be translated into a usable practical application.

The substrate for MFC technology being the organic fraction of waste biomass, therefore its continuous supply is desired to achieve continuous and sustainable output. Incorporation of plants in the anode chamber of the MFC is a good alternative to generate sustainable and green energy. A comparative difference between a MFC and a PMFC (plant MFC) is presented in Fig 1.4. Moreover, it is a source of electricity that are green and safe and can reduce the burden on food crop like corn and soybean for generation of bio-energy which is resulting in food crisis in many countries around the world (FAO, 2021).

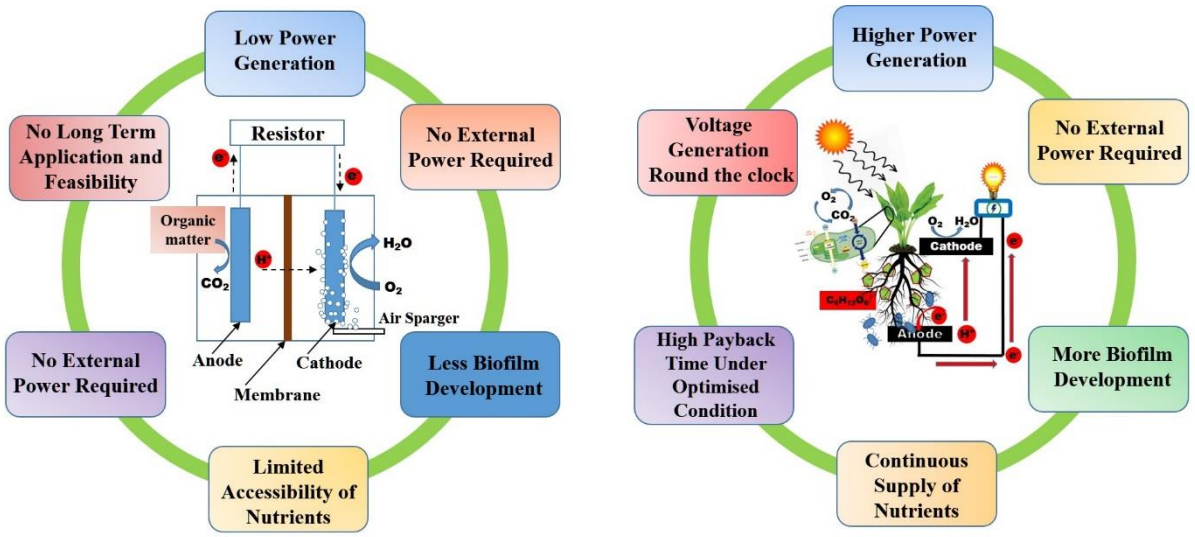

(a) (b)

Fig. 1.4 (a) Comparative representation of conventional MFC with its limitation (b) PMFC and its advantages over conventional fuel cells.

1.5 Principles of Plant Microbial Fuel Cell

The plant microbial fuel cell (PMFC) uses the activity of living plants and bacteria to generate electricity. The naturally occurring processes around the roots of plants helps to directly generate electricity in a PMFC. The plant utilizes sunlight and CO_2 to produce organic matter via photosynthesis, however a large portion of this organic matter remain in the soil as dead root material, lysates, mucilage and exudates. The bacteria living near the root surfaces can oxidize these organic matters releasing CO_2, protons and electrons. The electrons thus produced are donated by the bacteria to the anode of a microbial fuel cell. The anode is coupled, via an external load to a cathode. The released protons at the anode side travel through a membrane or spacer towards the cathode. At the cathode, oxygen is reduced together with protons and electrons to water (Strik et al., 2008). Thus, the PMFC technology works on two principles, excretion of unused organic compounds by plant roots i.e. rhizodeposition, and utilization of unused plant based food by electrochemically active bacteria for generation of bioelectricity in a microbial fuel cell (MFC) (Sarma et al., 2019; Timmers et al., 2013). The reactions taking place are shown below. A schematic presentation of a PMFC is shown in Fig. 1.5.

$$2C_6H_{12}O_6 + 6H_2O \rightarrow 6CO_2 + 24H^+ + 24e^- \text{ (Anode reactions)} \quad (1.1)$$

$$6O_2 + 24H^+ + 24e^- \rightarrow 12H_2O \text{ (Cathode reaction)} \quad (1.2)$$

$$C_6H_{12}O_6+6O_2 \rightarrow 6CO_2 + 6H_2O + \text{electricity (Overall reaction)} \quad (1.3)$$

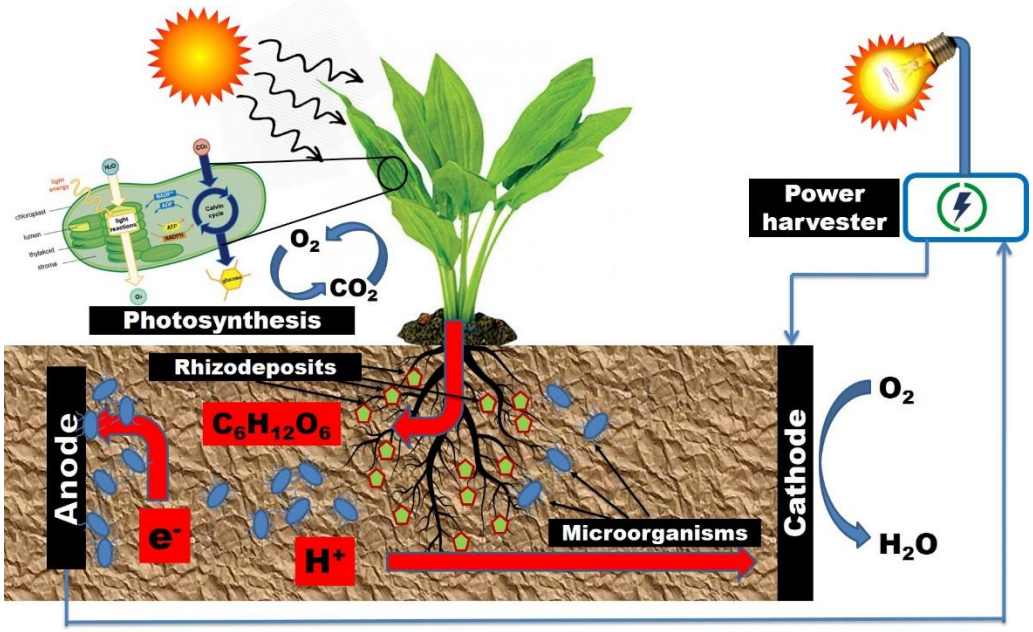

Fig.1.5 Schematic representation of working of a PMFC.

1.5.1 Photosynthesis

Photosynthesis is the first step towards electricity production. Photosynthesis is the conversion of light energy to chemical energy, stored as organic compounds and O_2 as by product. Therefore, considering O_2 as by product, photosynthesis is the leading O_2 supplier in the Earth's atmosphere. Photosynthesis is performed by many organisms viz., plants, algae, cyanobacteria etc. In the case of plants, light is absorbed by pigment-protein complexes located in the thylakoid membranes in the chloroplast. This process is known as light dependent reactions which convert light energy into adenosine triphosphate (ATP) and reduced nicotinamide adenine dinucleotide phosphate (NADPH). In addition to these reactions various other light dependent reactions converting ATP and NADPH into carbohydrates by incorporating CO_2 i.e., the Calvin-Benson-Bassham cycle (Johnson, 2016). In the plant kingdom, three photosynthesis pathways occur. Therefore, plants are organized into three groups: C3, C4, and Crassulacean Acid Metabolism (CAM) plants. Out of these, the C3 pathway is the oldest and most common: approximately 95% of terrestrial plants use this pathway (Bowes, 1993).

The amount of light from sun that a plant is able to convert into chemical energy is expressed as photosynthetic efficiency, η_{phot}. It is the energy content of the biomass that can be

harvested annually divided by the annual solar irradiance over the same area (Blankenship et al., 2011). Many external factors determine the photosynthetic efficiency: CO_2 concentration in the atmosphere, light intensity/availability, leaf nitrogen concentration, water availability, and temperature (Zhu et al., 2010; Seemann et al., 1987). Photosynthetic efficiency varies greatly between plants and locations, however under ideal conditions it varies around 4.6–6% (Zhu et al., 2010). In this process nearly 70 billion tons of annual carbon is fixed by plants globally out of total fixed carbon (450 billion tons) (Zheng et al., 2020). Various losses occur in the process leading to the resulting photosynthetic efficiency, which can be summarized in three categories: (1) absorption losses before light enters the photosynthesis process, (2) losses during the photosynthesis process, and (3) losses during secondary processing. Most energy lost is dissipated as heat, while a small fraction is emitted as fluorescence (Maxwell and Johnson, 2000).

1.5.2 Transport of carbohydrates to exoelectrogens

In the second step in the working principle of PMFCs, the product of the photosynthesis has various fates in the plant. A portion of the carbohydrates is stored as starch in the sink organs (roots, stems, flowers). This is used for respiration, plant metabolism and growth. However, a relative portion of photosynthates (about 75%) translocated below ground into roots and released into the soil as rhizodeposits where exoelectrogenic microorganisms use them for current production (Kuzyakov and Domanski, 2000; Warembourg et al., 2003; Jones et al., 2009; Lynch JM, Whipps, 1990). The rhizodeposits are released by the plants during all stages of plant growth and development, however it varies with age of the plant. It can be mainly categorised into four different types:

1) water soluble exudates, such as sugars, amino acids, organic acids, hormones and vitamins which leak from the root without the involvement of metabolic energy;

2) secretions, such as polymeric carbohydrates and enzymes which depend upon metabolic processes for their release;

3) lysates, released when cells autolyse including cell walls, and, with time whole roots;

4) gases such as ethylene and carbon dioxide.

Additionally, the degradation products of the roots including dying cells from the root cap, root debris and other low molecular weight organics (sugars, amino acids, organic acids) have been presented as an alternative source of substrate material to the exoelectrogenic microorganisms (Timmers et al., 2012; Bais et al., 2006; Pinton et al., 2007). Nearly 47.25

billion tons of fixed carbon are translocated to the roots and finally released into the rhizosphere in the form of exudates (sugars, organic acids, etc.), polymeric secretions rich in carbohydrates and enzymes, gases such as ethylene and CO_2, and dead cell materials into the rhizosphere by the process of rhizodeposition (Lynch JM, Whipps, 1990).

1.5.3 Conversion to electrical charges and current collection

The third step in the working principle of PMFCs is the conversion of the electron donors to electrical charges by exoelectrogens and current collection at the electrodes. A variety of losses occurs in this step including ohmic, activation, metabolic, and mass transport losses. The theoretical maximum open-circuit voltage (OCV) of any fuel cell corresponds to its electromotive force: $E_{emf} = E_{cat} - E_{an}$, where E_{cat} and E_{an} represent the cathode and anode potential respectively. Considering sucrose oxidation by exoelectrogens, it will be metabolized to carbon dioxide at the anode, with a release of hydrogen ions (protons) and electrons. The redox potential of the anodic half-reaction could go up to 0.430 V. At the cathode, the protons and electrons, together with oxygen, form water molecules worth 0.805 V, finally leading to the maximum electromotive force of 1.235 V (Schroder, 2007). However, in practice, the highest open circuit potential reached so far is 0.8 V (Liu et al., 2005).

References

Bais HP, Weir TL, Perry LG, Gilroy S, Vivanco JM (2006) The role of root exudates in rhizosphere interactions with plants and other organisms. Annu Rev Plant Biol. 57: 233–66

Blankenship RE, Tiede DM, Barber J, Brudvig GW, Fleming G, Ghirardi M (2011) Comparing photosynthetic and photovoltaic efficiencies and recognizing the potential for improvement. Science 332: 805–9

Bowes G (1993) Facing the inevitable: plants and increasing atmospheric CO_2. Annual Review of Plant Physiology and Plant Molecular Biology 44: 309–32

Campoccia A, Dusonchet L, Telaretti E, Zizzo G (2009) Comparative analysis of different supporting measures for the production of electrical energy by solar PV and Wind systems: Four representative European cases. Solar Energy 83(3): 287-297

FAO (2021) The state of food and agriculture. Food and Agriculture Organization of the United Nations, Rome

Imhoff ML, Bounoua L, Ricketts T, Loucks C, Harriss R, Lawrence WT (2004) Global patterns in human consumption of net primary production. Nature 429: 870-873

India Energy Outlook 2021, World energy outlook special report, International Energy Agency https://www.iea.org

Invest India (2022) National Investment Promotion and Facilitation Agency https://www.investindia.gov.in/sector/renewable-energy

Johnson MP (2016) Photosynthesis. Essays Biochem. 60: 255–73

Jones DL, Nguyen C, Finlay RD (2009) Carbon flow in the rhizosphere: carbon trading at the soil–root interface. Plant Soil 321: 5-33

Kazmerski LL (2006) Solar photovoltaics R&D at the tipping point: A 2005 technology overview. Journal of Electron Spectroscopy and Related Phenomena 150(2-3): 105-135

Kuzyakov Y, Domanski G (2000) Carbon input by plants into the soil. Review. J Plant Nutr Soil Sci. 163: 421–31

Larssen T, Lydersen E, Tang D, He Y, Gao J, Liu H, Duan L, Seip HM, Vogt RD, Mulder J, Shao M, Wang Y, Shang H, Zhang X, Solberg S, Aas W, Okland T, Eilertsen O, Angell V, Liu Q, Zhao D, Xiang R, Xiao J, Luo J (2006) Acid rain in China. Environmental Science and Technology 40(2): 418-425

Liu H, Cheng S, Logan BE (2005) Production of electricity from acetate or butyrate using a single-chamber microbial fuel cell. Environ Sci Technol. 39: 658–62

Lynch JM, Whipps JM (1990) Substrate flow in the rhizosphere. Plant Soil 129: 1-10

Maxwell K, Johnson GN (2000) Chlorophyll fluorescence—a practical guide. J Exp Bot 51: 659–68

Pinton R, Varanini Z, Nannipieri P (2007) The rhizosphere: biochemistry and organic substances at the soil-plant interface. CRC press

Schroder U (2007) Anodic electron transfer mechanisms in microbial fuel cells and their energy efficiency. Phys Chem Chem Phys 9: 2619–29

Seemann JR, Sharkey TD, Wang J, Osmond CB (1987) Environmental effects on photosynthesis, nitrogen-use efficiency, and metabolite Pools in leaves of sun and shade plants. Plant Physiol. 84: 796–802

Solomon S, Qin D, Manning M, Chen Z, Marquis M, Averyt KB, Tignor M, Miller HL Climate change 2007: the physical science basis; Contribution of Working Group I to the Fourth Assessment Report of the Intergovernmental Panel on Climate Change. IPCC

Sharmina M, McGlade C, Gilbert P, Larkin A (2017) Global energy scenarios and their implications for future shipped trade. Marine Policy 84: 12–21

Timmers RA, Strik DPBTB, Arampatzoglou C, Buisman CJN, Hamelers HVM (2012) Rhizosphere anode model explains high oxygen levels during operation of a *Glyceria maxima* PMFC. Bioresour Technol 108: 60–7

Warembourg FR, Roumet C, Lafont F (2003) Differences in rhizosphere carbon-partitioning among plant species of different families. Plant Soil 256: 347–57

Zhu XG, Long SP, Ort DR (2010) Improving photosynthetic efficiency for greater yield. Annu Rev Plant Biol. 61: 235–61

Chapter-II
Review of Literature

2.1 Background of Plant Microbial Fuel Cell Technology

The idea about the potential of microbes to generate electricity was put forward for the first time by Porter in 1910. Initially, not much attention was drawn; however, researchers gradually welcomed this technology's advent due to no environmental footprint associated with it. The main highlighting interest was the conversion of waste to energy by using microorganisms. With time, many advancements and modifications were made in the MFC technologies. A new horizon among MFCs was proposed in the form of PMFC, where plants were incorporated in the anode region to provide organic substrates for bacteria (Helder et al. 2010, 2013a, 2013b; Timmers et al. 2010; Arends et al. 2014; Chiranjeevi et al., 2019; Kuleshova et al., 2022). A detailed understanding of PMFC technology involves multidisciplinary expertise from studying microbes, plants, electrochemistry, and different engineering fields (Table 2.1). Therefore, exploration of these fields in PMFCs seems to be essential to understand the role and relationship that exists among them. The PMFC is a biosystem comprising biotic and abiotic components for producing biomass and bioenergy. Therefore, a holistic interrelationship is highly essential among the various factors in a PMFC.

Table 2.1 Role of the multidisciplinary field in PMFC.

Fields	Research Interest
Plant science	Choice of suitable plants based upon morphology and physiology Higher adaptation better rhizodeposition
Microbiology	Understanding the biofilm structure and microbial community involved, Studying better-adapted electrogens
Chemical engineering	Favorable electrochemistry, designing better electrode configuration, developing better membrane technology for easy ion transport, and reducing transmission loss
Electrical engineering	Obtaining the best possible combination for stacking and scale-up with building a suitable energy-storing device
Environmental engineering	Waste water treatment, heavy metal removal, Studying the impact of indoor plants on purifying air, and simultaneous energy generation

2.2 Electron transfer mechanism in Plant Microbial Fuel Cell

In the plant rhizosphere region, EAM uses organic substances for their growth and metabolism and, in turn, produces carbon dioxide (CO_2), protons (H^+), and electrons (e^-). The microbes transfer the electrons to the anode surface, which move towards the cathode through an external circuit to be reduced by oxygen. In the process, bioelectricity is produced, and water as a by-product. The reaction mechanism has been explained in Chapter-I. The electron transfer mechanism from EAM to the surface of the electrode is a complex one and is mainly assumed to be taking place in two ways (Bond et al., 2003).

(i) Indirect Electron Transfer: Certain bacteria secret mediators to shuttle the electrons from bacteria to the anode surfaces.

(ii) Direct Electron Transfer: Biofilm forming bacteria transfer electrons through membrane bound cytochromes or nanowires.

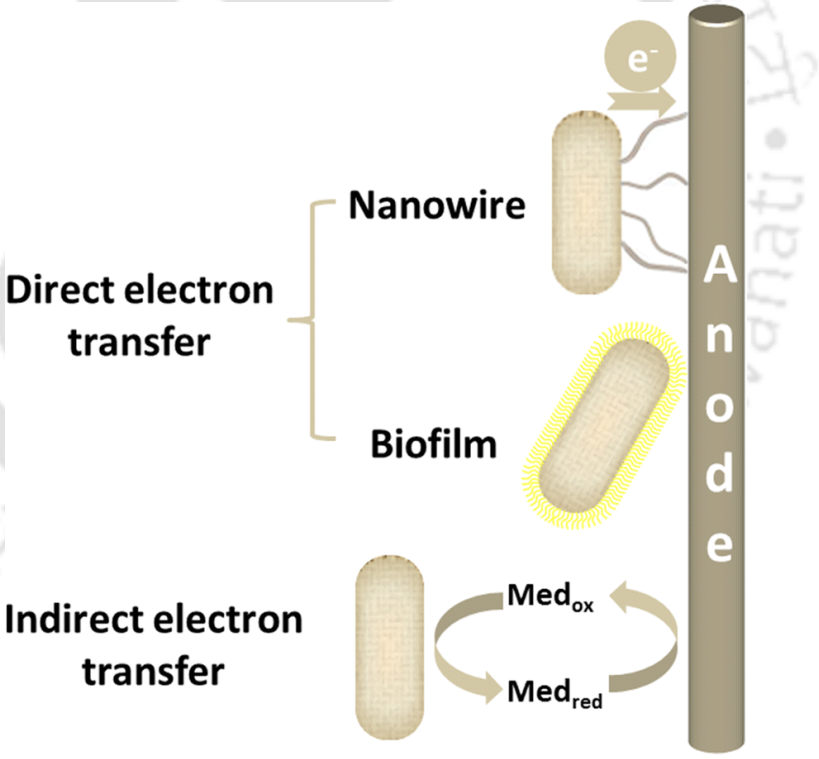

Fig. 2.1 The electron transfer mechanisms from exoelectrogens to the anode. Electrons from microbe's flow to the anode directly through nanowires or indirectly through an electron mediator. Med_{red} - reduced electron mediator; Med_{ox} -oxidized electron mediator (Source: Cao et al., 2019).

2.2.1 Indirect Electron Transfer (IET) through Mediators

The IET process takes place through the presence of a mediator (either exogenous or endogenous). Fermentative microbes in the rhizosphere, such as *Pseudomonas*, *Shewanella*, *Lactobacillus*, and *Enterococcus*, cannot transfer electrons directly to the anode. Hence these microbes require an external mediator (natural: flavins, melanin phenazines quinines, and cyanins; artificial: thionine, benzyl viologen) to assist the transfer of electrons from a bacterial cell to an anode surface by mediated electron transfer (Sekar and Ramaswamy,2013; Raghavulu et al., 2012). Some bacteria, such as *Pseudomonas aeruginosa*, secrete phenazines while few *Shewanella* sp. secrets flavins and $Fe^{3+,}$ which are helpful for electron movement from bacteria to anode surface (Ramaswamy and Mukherjee, 2012).

Moreover, several critical microbial metabolites, such as (formic acid, succinic acid, and biotin) are produced in the rhizospheric zone and are also known to mediate electron transfer (Schroder et al., 2007). These mediators can carry electrons from the microbial metabolism (with its reduced form) to the surface of a solid anode. Then, it is transformed to an oxidized compound and diffuses back to the cell. This complete cycle repeatedly occurs with the same combination.

ET mechanisms through a mediator are predominant in the case of sediment-MFC, where the electrons produced far away from the anode surface require electron mediators to reach the electron-accepting anode. Another example of mediated electron transfer is illustrated in Fig. 2.2 with the help of a bacterial electron transport chain. The electron transfer in the case of the electron transport chain begins with a biological transport molecule, i.e., NADH releasing a high energy electron (e^-) and a proton (H^+). The electron passes through the large protein molecules in the mitochondrial membrane following the red path. As the electron passes through each protein, it pumps hydrogen ions (H^+) through the membrane. In the case of a typical bacterial cell, the electron continues along the dotted red path, where it combines with oxygen to make water. However, in an MFC, the electron continues along the solid red path, which is picked up by a mediator molecule and taken to the electrode surface (Song et al., 2015).

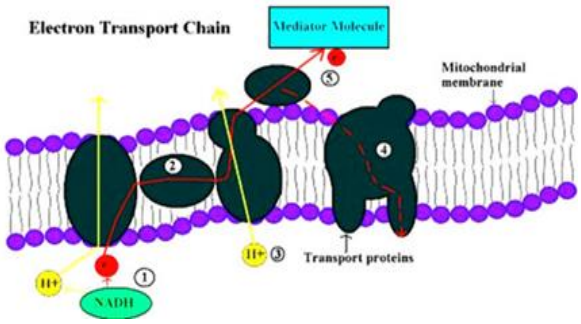

Fig. 2.2 Mediated based electron transfer in a bacterial cell (Source: Mercer/Campbell and Reece/Pearson Education, Inc).

2.2.2 Direct electron transfer (DET)

2.2.2.1 Electron transfer through membrane-bound Cytochromes

The transfer of an electron from the source (oxidized organic matter) to the anode's surface occurs directly or through cytochrome or via pilli present on the surface of bacteria. The process does not require a mediator to shuttle electrons from the enzyme active site to the electrode surface, minimizing complexity. As mentioned, the DET via outer membrane redox protein requires physical contact of bacterial biofilm with the anode. Pandit et al. (2014) studied the direct electron transfer to the electrode surface on *Shewanella putrefaciens* cultures during lactate metabolism. The outer cytochromes in *S. Putrefaciens* were important for mediating electrons to the anode surface and for generating bioelectricity (Wang and Ren, 2013).

Among the electro active microbes (EAMs), archaea and eubacteria comprise most of the population. They contain unique heme-containing membrane-bound proteins known as the C-type Cytochromes (CTCs), widely spread across the cell wall (Holmes et al., 2006). These proteins assume a most valuable role in the electron displacement technique for electricity harvesting by EAMs. *S. oneidensis* MR-1(model species) contains 42 putative CTCs, where 80% are situated in the external layer and involve 8-34% of the entire cell surface (Huang et al., 2011). In the periplasm of *S. Oneidensis*, numerous individual C-type cytochromes are involved in the electron transport mechanism (Schuetz et al., 2009).

A cytoplasmic membrane-bound tetra heme-CTC (CymA) belonging to NapC/NirT protein family with the N-terminal bound in the inward film and the C-terminal presented to the periplasm which directs the electrons from menaquinol to periplasm (Myers and Myers, 2000). CymA is of incredible significance as it takes an interest in numerous *Shewanella* anaerobic respiration forms. CymA can legitimately associate with numerous terminal reductases in the periplasm, such as fumarate reductase (FR) and nitrate reductase (NR). CymA

is a significant electron channel to periplasmic space. Similar to *Shewanella*, Geobacter also contains c-type cytochromes used for DET that exist on the bacterial cell surface, including OmcS, OmcE, and OmcB (Matsena and Chirwa, 2022)

Exoelectrogens are chiefly the Gram-negative (G^-) microscopic organisms since the Gram-positive (G^+) cell divider is ominous for EET (Extracellular electron transfer). However, G^+ microorganisms are the predominant dissimilatory metal-reducing bacteria (DMRB) in certain situations. A couple of Gram-positive species, for example, *Thermincola potens* are fit for performing direct electron transfer systems. Its genome has 32 putative CTC genes and a close arrangement on the external layer, thus building up an electron section for anode reduction (Logan, 2008).

2.2.2.2 Electron transfer through nanowires

The presence of some conductive appendages attached to the bacterial cell of *Geobacter sulfurreducens* and *Shewanella oneidensis* known as nanowires. These appendages allow microbes to reach and utilize more distant solid electron acceptors without physical whole-cell contact (Harnisch et al., 2011). The role of nanowires in metal-reducing bacteria *Shewanella oneidensis* were described by El-Naggar et al. (2010) and Gorby et al. (2006) to be involved in electron *transfer* to anode. These nanowires were conductive, serving as an alternative medium for extracellular electron transfer electrons. The nanowires are also responsible for developing a thicker electroactive biofilm at the anode surface, thus increasing anode performance (Harnisch et al., 2011).

2.3 Characterization of PMFCs

Characterization of the MFC/PMFC is defined by studying the potential generated by the cell and the reaction mechanism responsible for it. One of the most significant limitations of PMFCs is the low power output and the internal resistance of PMFC. These parameters have a substantial role in limiting the power output (Srivastava et al., 2015). Usually, the measured cell voltage produced in an MFC is represented through the following equations:

$$E_{cell} = E_{ocv} - IR_{int} \quad (2.1)$$

$$R_{int} = (E_{ocv} - E_{cell}) / \mathrm{I} \quad (2.2)$$

Where, E_{ocv} is the open-circuit voltage, E_{cell} is measured cell potential, and IR_{int} represents all the voltage losses, which is proportional to the system's current output and internal resistance (Srivastava et al., 2015).

Polarization curves represent a powerful tool for analyzing and characterizing fuel cells. A polarization curve represents the voltage as a function of current (density). Polarization curves are plots of electrode potential (or MFC voltage) as a function of current or current density. It can be recorded for the anode, the cathode, or the whole MFC using variable external resistance. A polarization curve can generally be divided into three zones: (*i*) starting from the OCV at zero current, there is an initial steep decrease of the voltage: in this zone, the activation losses are dominant; (*ii*) the voltage then falls more slowly, and the voltage drop is fairly linear with current: in this zone, the ohmic losses are dominant; (*iii*) there is a rapid fall of the voltage at higher currents: in this zone the concentration losses (mass transport effects) are dominant (Fig. 2.3a).

On the other hand, a power curve describes the power (or power density) as the function of the current (or current density) calculated from the polarization curve. Fig. 2.3b (solid line) shows a typical power curve based on a polarization curve (Fig. 2.3a). Initially, no power is produced as no current flows for open circuit conditions. From this point onward, the power increases with current to a maximum power point (MPP). Beyond this point, the power drops due to the increasing ohmic losses and electrode overpotentials to the point where no more power is produced (short circuit conditions).

In practice, the actual voltage output of an MFC is less than the predicted thermodynamic ideal voltage due to irreversible losses (i.e., overpotentials). The four major irreversibilities that affect MFC performance are: activation losses, ohmic losses, and mass transport losses. These losses are defined as the voltage required to compensate for the current lost due to electrochemical reactions, charge transport, and mass transfer processes in both the anode and cathode compartments (O'Hayre et al., 2015). The extent of these losses varies from one system to another. The real operational voltage output (V_{op}) of an MFC can be determined by subtracting the voltage losses associated with each compartment from the thermodynamically predicted voltage as follows:

$$E_{cell} = E_{ocp} - \eta_{cat} - \eta_{an} - I\,(RM) \tag{2.3}$$

Here η_{cat} is cathode over potential (V), and η_{an} is anode over potential (V), and *RM* is membrane resistance (Ωm^{-2}) (Liu et al., 2014). The anode and the cathode overpotential include losses in

the form of activation loss due to reaction kinetics, ohmic loss from ionic and electronic resistances, and concentration loss due to mass transport limitations. The above equation shows that cathode and anode overpotentials collectively limit the performance of MFCs and that the overall performance can be improved by optimizing both the anode and cathode.

2.3.1 Activation losses

Current production in MFCs depends mainly on the oxidation and reduction reaction kinetics at the anode and cathode, respectively. The reaction kinetics is limited by an activation energy barrier which impedes the conversion of the oxidant into a reduced form (i.e., Eq.1.1, Chapter-I). When current is drawn from a fuel cell, a portion of the anode and cathode potential is lost to overcome this activation barrier. The potential loss due to activation is called activation loss (i.e., activation overpotential) (O'Hayre et al., 2015).

Activation losses result in a characteristic, exponentially formed loss on the current–voltage curve at low current densities (Fig. 2.3). As more current is taken from the MFC, the activation loss increases and results in a lower cell potential (Larminie and Dicks, 2003). As with chemical and biological fuel cells, the activation losses dominate the performance of MFCs (Gil et al., 2003). The magnitude of activation overpotential depends on the reduction kinetics. Kinetic performance can be improved by decreasing the activation barrier and increasing the reaction interface area, temperature, or oxidant concentration.

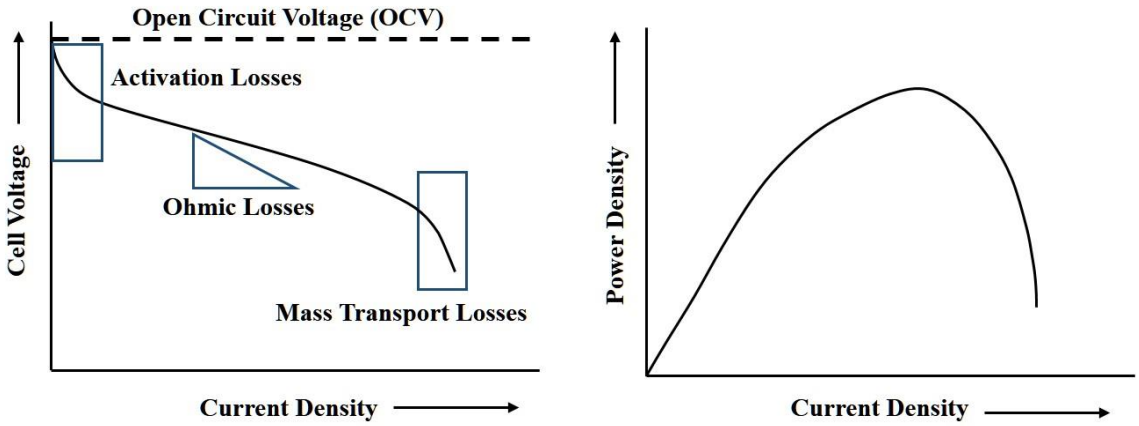

(a) (a)

Fig. 2.3 (a) Schematic potential losses displaying activation, ohmic, and mass transport losses in a polarization curve. (b) A typical power–current curve.

2.3.2 Ohmic losses

As in every electronic device, PMFC performance is also restricted by ohmic overpotentials, also known as intrinsic resistances resulting in voltage drop. This loss is the voltage required to drive the electron and proton transport processes. Since MFC conductors are not ideal, they have an intrinsic resistance to charge flow (Larminie and Dicks, 2003). The ohmic overpotential (η_{ohmic}), therefore, represents the voltage lost to accomplish charge transport (i.e., electrons and protons). This loss generally follows Ohm's law:

$$\eta_{ohmic} = iR_{ohmic} \tag{2.4}$$

Where, i is the current (A), and R_{ohmic} is the MFC's ohmic resistance (Ω). The ohmic resistance is a combination of both ionic, R_{ion}, and electronic, R_{elec} resistances and includes the resistance from the electrode, electrolytes, and interconnections:

$$R_{ohmic} = R_{ion} + R_{elec} \tag{2.5}$$

The electrolyte resistance usually dominates internal resistance since the ionic conductivity is orders of magnitude lower than the electrical conductivity of the electrode materials (O'Hayre et al., 2015). The ohmic resistance of the electrolyte, R_{ion}, can be expressed by

$$R_{ion} = l/AK \tag{2.6}$$

Where, l is the distance (cm) and A is the cross-sectional area (cm^2) over which the ionic conduction occurs. K is the specific conductivity Ω^{-1} cm^{-1} of the electrolyte (Larminie and Dicks, 2003).

The ohmic loss is more pronounced at medium current densities and, following Ohm's law, the operating voltage decreases linearly as the current increases (Fig. 2.3a). Reducing the ohmic losses is essential for improving the performance of MFCs.

2.3 Bacterial Metabolic losses

The electrochemical kinetics of bacterial metabolism allows electron transport from the electron donors at a low potential to a higher potential (Logan and Regan, 2006a). The bacteria will gain more energy if this potential difference is increased, leading to a lower MFC potential. The anode potential should therefore be kept as negative as possible. However, a too-low anode potential will enable other metabolic pathways, e.g., fermentation or methanogenesis, where

gas is produced instead of free electrons (Rismani-Yazdi et al., 2015). However, in the case of a plant microbial fuel cell, there is little control over the anode potential and, consequently, these losses.

2.3.4 Mass transport losses

As mentioned in equations (1.1) and (1.2) (Chapter-I), the concentrations of all elements part of the oxidation or reduction reaction should be high enough to limit the internal resistance. The process of supplying oxidants (i.e., O_2) and removing products (i.e., H_2O) at the cathode is governed by mass transport. Insufficient mass transport to or from the electrode causes reactant depletion or product accumulation. Reactant depletion affects cell voltage and the reaction rates, leading to a performance loss. This loss is the voltage required to drive mass transport processes, referred to as concentration loss or mass transport loss (O'Hayre et al., 2015). Mass transport losses occur at high current density, and the magnitude increases with increasing current density (Fig. 2.3a).

Mass transport limitations due to oxidant transport in the cathode compartment are typically much more severe than transport limitations in the anode compartment. Hence, when determining mass transport losses in fuel cell systems, only the limiting concentration for the oxidant is considered.

2.3.5 Reducing losses

The cell over potentials and internal losses impact the efficiency and power output of MFCs/PMFCs and represent a significant challenge for research and development (Zhao et al., 2006; Morris et al., 2007). Several studies have explored different approaches to improve the performance of the MFCs by lowering the overpotential. These approaches include using mediators, electrode modification with catalysts (metal-based, biocatalyst), and optimizing operational conditions. Anodic and cathodic ohmic losses can be minimized by increasing the conductivity of the electrolyte materials used and the proton-exchange membrane. Improvement can also be introduced by reducing the path distance between the cathode and anode electrodes.

On the other hand, mass transport is dependent on convection and diffusion. Mass transport in bulk electrolyte is dominated by convection (i.e., macroscopic flow). In contrast, diffusive transport at the electrode surface typically dominates mass transport. Maintaining high bulk concentrations and an even distribution of anaerobic and aerobic environments in the

anode and the cathode compartment can reduce mass transport losses. In addition, optimization of MFC operating conditions, electrode material, and anode and cathode compartment geometry can minimize mass transport limitations and performance losses.

2.4 Microbial community in PMFCs

Wide varieties of species of microorganisms are involved in generating bioelectricity in MFCs and PMFC is no different (Logan and Regan, 2006b). A wide-diverse species composition is seen in the natural microbial community in PMFCs (Timmers et al., 2012; Ueoka et al., 2016; Lu et al., 2015). The microbial community associated in the plant rhizosphere region varies with substrate composition, pH, electron donors, electron acceptors, availability of nitrogen, dissolved oxygen, humidity, temperature, plant species and their rhizodeposit, type of electrodes, etc. (Rusyn, 2021). More than 27 prominent bacterial families in PMFC demonstrated with *Glyceria maxima* in a synthetic medium (Timmers et al., 2012) and in the microbiome of natural paddy waterlogging (Ueoka et al., 2016). Molecular-genetic analyzes by Timmers et al., 2012 and Ueoka et al., 2016, found that the species composition of bacteria adhered to the anode and in the soil of the surrounding electrode space differ. Bacteria *Anaerolineaceae*, *Caldilineaceae*, *Geobacteraceae*, *Acidobacteriaceae* were observed in much higher quantities on the anode than the interelectrode space (Timmers et al., 2012; Ueoka et al., 2016). In the microbial population of PMFC, three main groups of rhizosphere microorganisms can be determined according to their function in generating bioelectricity and localization (Fig. 2.4) such as:

1. Anode microorganisms, which contain a maximal amount of exoelectrogenic microorganisms transferring electrons, formed during metabolism to the anode, and also associated electron-donor microorganisms that feed them (Kaku et al., 2008; Timmers et al., 2012; Kouzuma et al., 2014)
2. Cathode microorganisms, the called biocathode, mostly formed by electrotrophs, which accept electrons coming from the anode and reduce oxygen, nitrate or sulfate ion, etc., (Liu and Logan, 2004, Logan et al., 2019)
3. Microorganisms of the root surfaces and surrounding electrodes, so-called microorganisms of interelectrode space, where are located most of the microorganisms-cooperators of exoelectrogens that feed electroactive microorganisms, providing them with simple compounds as a result of the breakdown of complex organic compounds

of plant residues and root secretions, as well as a small number of electroactive microorganisms (Timmers et al., 2012; Ueoka et al., 2016).

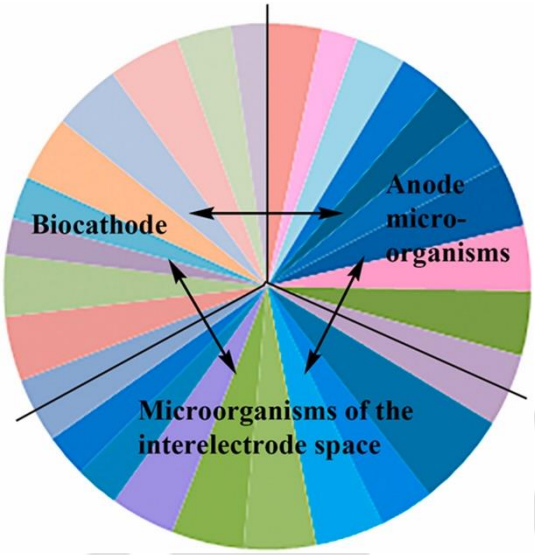

Fig. 2.4 Schematic representation of the PMFC microbial community, which includes a wide variety of species interrelated microorganisms of biocathode, anode, and interelectrode space (Source: Rusyn, 2021).

2.4.1 Microorganisms at Anode

The genus Geobacter has garnered significant attention in the study of Plant Microbial Fuel Cells (PMFCs) as one of the most extensively researched electroactive bacteria (Rusyn, 2021). Geobacter, specifically G. sulfurreducens, has been well-studied for its ability to colonize the MFC anode, form biofilm, and contribute to bioelectricity generation (Bond and Lovley, 2003; Qu et al., 2012). Studies have confirmed the presence of *Geobacter* and its species *G. sulfurreducens*, *G. metallireducens*, *G. grbiciae*, *G. hydrogenophilus*, in the anode-associated microbiome of PMFCs, especially in systems using different plant species like *G. maxima* and *O. sativa*. (De Schamphelaire et al., 2010; Timmers et al., 2012). Kouzuma et al. (2014) revealed the presence in the anode-associated microbiome of *G. psychrophilus* and syntrophically related species in sedimentary MFCs operating in paddy fields. 16S rRNA analysis of PMFS with *O. sativa* in waterlogged areas showed that bacteria of the family *Geobacteraceae*, *G. pelophilus* and *G. psychrophilus*, were present in the interelectrode substrate in a whole small amount <0.1%, while in anode samples there were 10 times more of them, 1.8–2.4% (Ueoka et al., 2016). In high-current PMFCs with plant *G. maxima*, the presence of *Geobacteriaceae* was notably higher than in low-current PMFCs, 0.74% vs. 0.13%, respectively (Timmers et al., 2012). The obtained data also indicate that even in a small

quantity, microorganisms play an essential role in bioelectricity production. The study of the species composition of the anode microbiome of PMFC with different species of plants, media, and electrode systems has demonstrated high biodiversity and the abundance of different prevailing species from families, mainly those other than *Geobacteriaceae* (Rusyn, 2021). This includes nitrogen-fixing bacteria such as *Rhizobiales, Beijerinckiaceae,* and *Natronocella acetinitrilica,* cable and sulfate-reducing bacteria of the family *Desulfobulbaceae* and non-cultivating archaebacteria, *Rhizobiales, Geobacter, Myxococcus, Deferrisom*a, *Desulfobulbus* and archaea, *Geobacter, Anaeromyxobacter and Anaerolineae*, *Anaerolineaceae* (Kaku et al., 2008; Timmers et al., 2012; Rusyn, 2021). *Geobacteriaceae* and fermentative bacteria *Anaerolineaceae* were prevailing on the anode in the constructed wetland PMFC with *C. indica* (Lu et al., 2015). Apart from the presence of bacteria, some fungi, such as *Aspegillus* spp. and *Penicillium* spp. were revealed in the anodic biofilm in PMFC with natural soil and plants suggesting the development of bacteria-fungi consortia (Rusyn, 2021). The anode microbial community in PMFCs shows high biodiversity, including various bacteria, archaea, and fungi species (*Aspegillus* and *Penicillium*), forming complex consortia. While *Geobacteriaceae* is an essential component, it is not always dominant among anodic microorganisms' (Lu et al., 2015). Other soil bacteria have also been found to significantly contribute to bioelectricity generation in MFCs. Overall, the range of anode electron-transferring microorganisms in PMFCs is extensive and presents a promising field for further research. Understanding the interactions and contributions of different microbial species in PMFCs can lead to advancements in bioelectricity production and optimization of these sustainable energy systems.

2.4.2 Microorganisms at Cathode

Unlike the anode, where the anaerobic oxidation of substrates and electron transfer process occurs through microbial biofilm on to electrode surface, various substances can be used as electron acceptors at the cathode (Clauwaert et al., 2007; Liu et al., 2004). However, oxygen is known to be a reliable electron acceptor because of its abundance and sustainable nature with high redox potential (Zhao et al., 2006). The reaction at the cathode can be carried out chemically or biologically (Wu et al., 2017). The most commonly used catalyst for oxygen reduction in MFCs is Pt, but its high cost and sensitivity to poisoning limit widespread applications in larger-scale systems. (Kiely et al., 2011; Saito et al., 2010). To make more cost-effective cathodes, various non-noble metal catalysts have been developed to replace Pt,

involving transition metal macrocyclic complexes such as cobalt tetramethoxyphenylporphyrin (CoTMPP) and iron phthalocyanine (FePc) (Zhao et al., 2005; Yu et al., 2007; Liew et al., 2014). Additionally, metal oxides such as MnO_2, (Liew et al., 2014), carbon materials (Zhang et al., 2009) as well as composite catalysts (Burkitt et al., 2016) were also used to replace Pt. While these materials can work well, their performance can be degraded over time. (Zhang et al., 2011).

2.5 Biocathode Design Techniques

Three methods were mainly used for designing oxygen reducing (OR) bio cathode. The first one is based on the natural ability of microorganisms to develop biofilms spontaneously on material surfaces. In this case, no polarization is applied to the electrode, the biofilm grows under open circuit conditions. Subsequently, electrochemical activity was observed when the biofilm-coated electrode was tested electrochemically (Cournet et al., 2010a; Cournet et al., 2010b; Erable et al., 2010; Xu et al., 2010). Such microbial bio-cathodes have notably been formed from seawater (Erable et al., 2010; Xu et al., 2010) and from laboratory cultures of single bacterial strains (Cournet et al., 2010a; Cournet et al., 2010b).

In a second way, a bio-cathode can be obtained by polarizing the electrode at a potential lower than the open circuit potential. The cathode polarization can be carried out directly from the operating MFC (Wang et al., 2014; Cristiani et al., 2013; Zhang et al., 2012; Chen et al., 2012) or by using a potentiostat at a constant potential (Quemener et al., 2016; Rimboud et al., 2015; Rimboud et al., 2016; Debuy et al., 2015; Rothballer et al., 2015; Milner et al., 2014; Glaven et al., 2013; Xia et al., 2012). This process is widely used to form effective OR-biocathodes in various environments, viz., sewage sludge or wastewater (Cristiani et al., 2013; Rothballer et al., 2015; Rothballer et al., 2015; Xia et al., 2012) industrial/agricultural wastes (Wang et al., 2014; Zhang et al., 2012), seawater and sediments (Debuy et al., 2015; Glaven et al., 2013), soil and/or derived leachate (Quemener et al., 2016; Rimboud et al., 2015; Rimboud et al., 2016).

Finally, the third technique is to obtain an OR-bio cathode by polarity reversion of already established bio anodes (Cheng et al., 2010). Generally, acetate-fed bio anodes can be turned into OR-bio cathodes after consecutive exhaustion of the acetate using oxygen. A practical benefit of reversible bio electrodes used in MFCs is that they can be periodically reversed to neutralize acidification at the anode and alkalinizing at the cathode. The pH

gradient formed between the anode and cathode can thus regularly be neutralized, which helps to maintain the MFC performance during long-term operation (Strik et al.,2010). Moreover, the biofilm acidification that occurs during the anode phase has been shown to favour the subsequent reduction of oxygen (Blanchet et al., 2014)

2.5.1 Aerobic bacterial Bio cathode

A diverse species of aerobic microorganisms that use oxygen as the terminal electron acceptor is used in the cathode. Among the bacterial population, Gammaproteobacteria predominated on the cathode of PMFC with *O. sativa* (Ahn et al., 2014). In another rice-based PMFC, *Rhodobacter gluconicum* was detected on the cathode (Kaku et al., 2008). It belongs to the purple non-sulfur anoxygenic phototrophic bacteria (Madigan et al., 2008), and its role in electrogenesis is still unclear. Among the diversity of bacterial orders on the cathode, uncultured bacteria were found, such as *Thiotrichales*, *Chromatiales*, *Legionellales*, *Methylococcales*, and *Acidithiobacillales*, belonged to Gammaproteobacteria (Ahn et al., 2014) including many bacterial species of purple sulfur bacteria that can oxidize sulfur compounds. *Acidiferrobacter thiooxydans*, an acidophilic, thermotolerant, facultatively anaerobic, and chemolithoautotrophic bacterium, occupied the highest proportion on the cathodes and occurred only when the circuit was connected (Ahn et al., 2014). These bacteria detected on the cathode apparently obtain energy from the oxidation of ferrous iron and reduces sulfur compounds to be used as terminal electron acceptors (Hallberg et al., 2011; Ahn et al., 2014). The16S rRNA gene-based microbial identification did not detect any archaeal, suggesting that archaea played a minor role in the cathodic reaction (Ahn et al., 2014). The composition of the microbial populations of the cathode operating under different conditions, such as soil-based PMFCs or waterlogged rice field/sediment-based PMFCs is qualitatively different due to the influence of other plant species on the microbiome. Other factors, such as substrate and light accessibility also play an important role. Large numbers of photoautotrophic purple bacteria are detected on the cathode of marshy PMFCs (Madigan et al., 2008) and are not adapted to metabolism and growth in the dark. The results of Ueoka et al. (2016) suggest that the cathodic microbial consortia is highly important and improvement in biocathode development is crucial for eliciting the maximum capacity of rhizosphere bacteria to generate bioelectricity in PMFC. Therefore, the identification and study of microbial community PMFC play a valuable role in understanding the mechanisms of microbial relationships in electrogenesis and creating optimal conditions for them during improving electro-biosystems.

2.5.2 Microalgae and cyanobacteria as Bio cathode

Green algae and cyanobacteria are valuable microorganisms in Plant Microbial Fuel Cells (PMFCs) as they can perform photosynthesis, producing dissolved oxygen levels higher than aeration, which reduces the cost and makes it more sustainable (Huang et al., 2011; Arun et al., 2020). Algae cultivated in the cathode can also reduce CO_2 generated from bacterial metabolism. The biofilm formed on the cathode surface plays a crucial role, and its formation rate depends on the cathode material (Zhou et al., 2011; Wu et al., 2013).

Various BFC technologies operated with algal and cyanobacteria biocathode can address wastewater treatment, desalination, CO_2 capture, bioremediation, bioenergy production, and high-value compound synthesis (Saratale et al., 2017; Enamala et al., 2020). Technological parameters like light, pH, and temperature influence biocathode performance. Microalgae and cyanobacteria in the cathode chamber can remove carbon, nitrogen, phosphorus compounds, antibiotics, and heavy metals for wastewater treatment. They can also produce biomass with high lipid content for biodiesel production (Elakkiya and Niju, 2020; Golub and Levtun, 2016) and carotenoids (Gouveia et al., 2014). The production of lipids can make the BFC technology more attractive due to simultaneous wastewater treatment and generation of bioelectricity and biodiesel (Nayak and Ghosh, 2019). Alternatively, the dead microalgae biomass may be used as a substrate at the anode in BFCs (Cui et al., 2014). For optimum growth of microalgal biomass, Wu et al. (2013) noted the requirement of a dark stage, because high levels of illumination and high oxygen concentration can inhibit photosynthesis and cause photooxidation. In the dark stage, less electricity is produced because oxygen is not produced and is consumed by algae for respiration. For the sustainable current generation, 50% of electrode immersion is proposed (Ling et al., 2019). Thus, in dark condition, oxygen from air become an electron acceptor at the cathode, while oxygen from the catholyte will be used by microalgae for respiration. Commault et al. (2014) obtained a maximum power density of 11 mWm^{-2} (projected anode area) using a mixed algal community, including yellow–green algae, diatoms, and cyanobacteria while operating MFC for over six months without feeding.

However, there are challenges, such as the high cost of CO_2 as a feedstock for algal growth (Chi et al., 2011). The performance of MFCs with biocathode containing diverse microorganisms shows promise for increased power density and wastewater treatment efficiency (Wetser et al., 2015; Yadav et al., 2020). Overall, microalgal biocathodes have great potential for sustainable current generation, wastewater treatment, and biofuel production in BFC technologies.

2.6 Operational Factors influencing PMFC performance

Various researchers highlighted many factors influencing a PMFC's performance (Long et al., 2021; Jiang et al., 2021). Apart from the species of plant affecting the bioelectricity generation, various other operational parameters affect PMFC performance such as reactor design and its configuration, light source and its intensity, placement of electrodes and membranes, type of available microbial inoculum, plant growth promoters in use, etc (He et al., 2021). In addition to these, many minor lacunas in the systems (Chu et al., 2021; Liu et al., 2021) must be thoroughly investigated before moving towards ideal design and performance criteria (Zhang and Liu, 2021) for PMFC. This is a sincere attempt to discuss those missing aspects of PMFC Research.

2.6.1 Effect of light intensity

Photosynthesis is the most significant factor and precursor of bioelectricity production in PMFCs. It depends on carbon dioxide concentration and photosynthetic active radiation (PAR) light intensity (Neogi et al., 2021). Maqsud et al. (2015) reported that time and solar radiation are crucial factors affecting a PMFC. Electromagnetic radiation in the wavelength range of 400 – 700 is considered PAR (Dou and Niu, 2020). The incidence rays from the sun arrive in two ways, as direct flux manner and diffuse fluxes manner or both. A direct flux is formed when the light photons pass through the atmosphere remain unscattered. When photons are scattered due to various barriers like molecules in the air, aerosols, and clouds, the flux formed is known as diffuse flux. While this flux reaches out to the vegetation canopy, the photons hitting other plant elements and leaves undergo automatic removal from incidence light. This photon flux that strikes the plant parts is termed the intercepted PAR flux and is popularly called interception of radiation (IPAR) (Kukal and Irmak, 2020). This fraction of IPAR radiation has the potential to carry out photosynthesis efficiently. Some fraction of radiation of IPAR also gets reflected, while some portion results in transmission by elements of interception, and hence it is not utilized for photosynthesis reaction. So, the merely absorbed photons in the region of the vegetation canopy are termed as absorbed PAR (APAR) flux and might be used for photosynthesis reaction (Kumar et al., 2021). This value of APAR is naturally less than IPAR; hence, a constant coefficient of 0.85 is required for calculation (Kukal and Irmak, 2020). APAR = 0.85 IPAR is the general relation between APAR and IPAR considered for analyses. Also, among the PAR radiation, the spectra' blue and red regions are known to be essential for plant growth. Therefore, finding and analyzing the PAR data for the region where

PMFC assembly is to be set up and operated is recommended. It will help to understand and optimize the photosynthesis activity of the plants and hence power generation in PMFC.

2.6.2 Effect of electrode material and surface area

Anode is assumed to be the heart of an MFC from where all the reaction mechanism starts. Therefore, the Electrode material used for anode in PMFC should be conductive, biocompatible, chemically stable, and affordable for application (Sonawane et al., 2020). Different forms of electrodes of carbon like compact graphite plates, cloth made up of fibrous material, granules or rods of different dimensions, foam-shaped objects, and paper felt are advisable as anode for MFC application (Salehmin et al., 2021). Electrodes with higher surface area are recommended as they can provide more site for bacterial attachment and biofilm formation. But it is essential to maintain the porous nature to allow the protons to reach ion exchange membrane and cross it, resulting in the circuit's completion and maintenance of redox gradient in the system (Li et al., 2021). Electrodes with ideal configuration for MFC should possess two criteria, the first one is greater availability of surface area for adherence of bacterial community and the second one is efficiency in current collection. A detailed discussion on the different types of electrode materials for anode and cathode and their modification strategies can be found in section 2.8.

2.6.3 Effect of additives on the performance of PMFC

The performance of a PMFC is critically dependent on the interaction of plants and microbes; therefore, the health of the plant and the microbes present is highly important. The widespread implementation of PMFC technology has opened new arenas for researchers to study the performance of PMFC concerning the use of different additives, including plant growth promoters. Different researchers across the globe identified various additives for increasing the resultant power of MFCs. It isn't easy to compare and interpret their performance accurately due to use of different electrode materials, different configurations, and designs of MFC, different sources and types of substrates used, and other environmental parameters (Gadkari et al., 2020). But the ultimate aim of introducing additives in the substrate was to amplify and enhance MFC's overall performance and sustained output. Some of the relevant and recent additives are discussed below.

2.6.3.1 Substrate salinity

The performance of a cell is significantly affected by substrate salinity. Till a specific limit, cell performance increases with substrate salinity. However, beyond that extent, the exoelectrogens lose their ability to survive (Guo et al., 2021). This exact concentration of substrate salinity at which MFC performance is maximum changes from MFC to MFC and the type of bacterial community present (Guo et al., 2021).

As per recent reports, a higher concentration of salts in the solution releases higher numbers of protons and electrons. As a result, the anolyte's pH decreases, inhibiting exoelectrogens' growth (Bejjanki et al., 2021). In an another recent study, on performance evaluation of MFC with wastewater from sewage and reverse osmosis (RO) concentrate using *Luffa aegyptiaca* anode, it was found that more proportion of RO concentrate was responsible for more power generation and hence could be considered as component of feed in MFC (Thakur and Das, 2021). Therefore, this aspect must be worked thoroughly while designing a highly efficient PMFC setup (Merino-Jime-nez et al., 2017).

2.6.3.2 Biochar addition

Applying coconut-based biochar is a cost-effective additive component in MFC to enhance power production (Ayyappan et al., 2018). The application of biochar for developing low-cost electrodes (Anode and Cathode), electrocatalysts, and efficient proton exchange membranes was critically reviewed (Chakraborty et al., 2020). It was reported that biochar and copper-based electrodes produced maximum power compared to other metal and biochar treatments (Senthilkumar and Naveenkumar, 2021). A study also reported the development of a biochar-based biocatalyst by synchronous carbonization and graphitization of eggplant biomass. It has witnessed an excellent electrochemical performance in a neutral medium with a maximum power density of 667 mWm^{-2}, more than the traditionally used Pt catalyst with a power density of 621 mWm^{-2} (Zha et al., 2020). Therefore, incorporating different compositions of biochar in MFCs/PMFCs studies could be beneficial for the overall performance of a cell. However, more studies need to be carried out to draw authentic conclusions.

2.6.3.3 Plant growth promoter

PMFC technology is a concurrent bioelectricity generation process where in biomass growth and electricity is produced simultaneously (Helder et al., 2010). Therefore, the good

health of a plant is highly crucial, and it influences the amount of rhizodeposits released for the microbes, thereby affecting energy recovery from a PMFC. Therefore, a balanced growth media consisting of all significant macro and micronutrients is vital for plants in a PMFC. Hoagland growth media is a popular liquid-based balanced media used in aquaponics plant culture and as an anolyte in PMFCs where the plant is directly grown (Helder et al., 2010; Helder et al., 2012a; Timmers et al., 2010). On the other hand, commercially available potting mix and a natural sandy loam soil were also used to enrich microbial community and plant growth in PMFCs (Khudzari et al., 2018).

2.6.4 Effect of the long operational period

PMFC is a relatively new technology, and most of the plant species employed to date are the wild grass species or plants with very little commercial value (Shaikh et al., 2020). Also the efficiency of PMFCs were not studied for long duration. Certain factors affect the rhizodeposition potential of the plants, such as plant physiology and age. Therefore, with time the structure of a microbial community in rhizosphere changes and due to limited rhizodeposits, the potential of PMFC decreases, restricting its use for longer duration (Gomathy et al., 2021). Another most important factor that is responsible for low power output in the long run is the rise in the value of internal resistance of the anode with time due to biofilm formation on the surface (Munjal et al., 2020). The thicker biofilm decreases the electrodes' porosity and restricts the ability to exchange protons across the membrane. Similarly, biofouling of membrane is another concern regarding the performance of a BFC (Discussed in detail in Section). Due to this overall process, the net redox potential is reduced, resulting in less power magnitude. Hence, it is required to replace the electrodes after specific time duration to maintain the power sustainability of PMFC in long run (Jadhav et al., 2021). All these aspects must be addressed so that resultant enhancements should be reproducible and scalable technologically.

2.6.5 Effect of cell architecture

The cell architecture plays an essential role in the operation and performance of an MFC/PMFC. Most importantly, the design should allow the development of anaerobic conditions at the anode while favouring the build-up of aerobic conditions at the cathode. Regarding design architecture two most commonly used types of PMFC seen were Tubular design and Flat-plate design (Described in Section 2.7). Subsequently, very little information is available regarding architectural design evolution.

As part of cell architecture, the nature of the electrode (material, displacement and spacing) plays an essential role in bioelectricity generation. In addition to the selection of materials and their modifications, proper electrode spacing in the deep root zone of the plant is crucial; at times, the roots might cover the anode making it unavailable for biofilm formation. A study by Deng et al. (2014) on the effect of electrode positions on various soils and water interface depicted that MFCs with a soil depth of 5 cm and a water interface of 3 cm has the highest power density of 0.72 mWm^{-2} along with reduced ohmic resistance. Like the electrode, membrane design (shape, thickness) and its placement inside a cell are equally essential to enhance MFC performance and decrease the cell's internal resistance. More in-depth work on the architectural designing of MFC/PMFC is expected in future.

2.7 Architecture of PMFC reactor

For the practical applicability of any design, various factors come into play: design language, cost-effectiveness, ease of operation and handling, environment friendliness long-term management to name a few. Construction cost poses a hurdle that needs to be overcome for practical use of MFCs. The significant cost involves the material cost of making the setup including cost of electrode, membranes, nutrients, mediators etc. For efficacious PMFC construction, using a non-catalysed carbon-based electrode and a proton exchange membrane remains key. However, the uniqueness about construction of PMFC is the non-requirement of periodic nutrient input as bioelectricity is driven by rhizodeposition of the living plants. Following the working principles of an MFC, the basic PMFC design can be divided into

1. Single-chamber PMFC where one chamber serves as both anode and cathode with membrane-less operation.
2. Double-chamber PMFC wherein anode and cathode chambers are separated by a proton-exchange membrane (PEM) to facilitate a proton's movement towards the cathode. The PEM also helps to prevent catholyte and O_2 diffusion to the anode.
3. Three-chamber PMFC, wherein one anode chamber sandwiched between two cathode chambers. The chambers being separated by a proton-exchange membrane (PEM).

Apart from the chamber structures, some of the essential factors that need to be considered while designing architecture of PMFCs are placement of anode, the distance between anode, cathode and membrane, and the dimensions of the electrodes, etc. The efficiency of a PMFC can be improved through inclusion of different substrates, inoculums,

efficient proton exchange membranes, decreasing cell resistances, etc. Among the various types of designs, a tubular model and a flat-plate model are the two PMFC designs, used in different studies for bioelectricity generation. The sustainability and practicality of the system depends upon its cost-effectiveness, long term operation, ease of handling and environmental friendliness.

2.7.1 Tubular Model PMFC

The tubular design PMFC is a robust and efficient setup that can be integrated into large cultivated areas to maximize power generation without disturbing the top layer of soil. This design was first developed by Timmers et al. in 2013 and consists of a tubular-shaped anode with a membrane attached at the bottom and the cathode beneath it (Fig 2.5a). Electrons generated by rhizodeposits breakdown are received at the anode and move through the external circuit to the cathode, while protons pass through the membrane and are reduced at the cathode. A variety of materials can be used for construction of tubular design PMFCs. A glass based setup was designed by Strik et al. (2008) where in a glass tube filled with graphite granules was used as the anode compartment. A proton exchange membrane was attached to the bottom of the glass tube. The cathode compartment was made up of a glass beaker containing graphite and surrounding the anode compartment. Polyvinyl chloride (PVC) is one of the most easily found component to be directly used for designing a tubular PMFC. A T-shaped PVC socket is used, where in PVC disk were fixed inside at both the ends to create water tight compartments. A tubular filtration membrane was fixed between the two disk. The anode was located outside the ultrafiltration membrane while the cathode was located inside the membrane, constituting graphite granules and felts respectively (Timmers et al., 2013).

A study similar to Strik et al. (2008) was carried out by Ruud et al. (2010) with plant *S. anglica;* however, with a different current collector, i.e., golden wire glued to a Teflon-coated copper wire connected to both anode and cathode. Similarly, *S. anglica* and *P. australis* were grown in salt marshes and peat soil respectively in a vertical PVC tube placed in wetlands. The bottom was covered with a PVC cap. Anodes and cathodes were made of graphite felt attached to a cation exchange membrane linked to a golden wire as a current collector (Wetser et al., 2015). Arends et al. (2014) used plexiglass material for making tubular PMFC containers and affixed with graphite interlaced with carbon rods as anode and cathode. This was used to study greenhouse gas emissions in rice paddy fields. Helder et al. (2010) used a plexiglass cylinder like the anode compartment filled with graphite granules. A cation exchange membrane was

placed at the bottom of the anode compartment. The anode chamber was placed inside a glass beaker acting as a cathode compartment with gold wire is woven graphite felt. Low-density polyethylene containers filled with red soil and planted with *P. setaceum* was used as PMFC for wastewater treatment and bioelectricity generation. Non-catalyzed graphite discs as anodes were placed vertically in the soil near the rhizosphere while the cathode was kept at the top exposed to air (Chiranjeevi et al., 2019). A centrifuge tube was also used as tubular PMFC. The tube was placed inside a lightproof plastic container filled with fresh paddy soil with an anode at the bottom and air cathodes on the soil's surface (Chen et al.2012). A PMFC was constructed by Lu et al. (2015) using a polymethyl methacrylate cylinder perforated graphite disk anode at the bottom of the reactor. An annular carbon cloth was tied on the container wall with a nylon mesh that acts as an open air cathode. A tube within a tube-type tubular design PMFCs was applied to a wetland with silicon tubes for gas diffusions by Wetser et al. (2017) where anode was wrapped around an ultrafiltration membrane. The cathode is wrapped around a silicon tube and inserted in the inner circle of the membrane-anode assembly (Wetser et al. 2017). Sophia and Sreeja, (2017) used a clay-based ceramic tubular structure for the PMFC study. The anode chamber was a cylindrical structure made of kaolinite and montmorillonite mix acting as membrane for ion transport. Carbon brush anodes were as anodes and covered with hydrated carbon cloth acting as air cathode, connected using copper wires. Although tubular designs were popular among researchers, a major limitation with the tubular model is that the average transport distance for a proton from the anode through the membrane to the cathode is relatively long, hindering power generation process.

2.7.2 Flat-Plate Model PMFC

Another design of PMFC setup not very widely used is a flat-plate configuration which consists of a cation exchange membrane sandwiched between the anode and cathode compartment (Fig.2.5b). The design being vertically flat, the anode and the cathode can be placed next to each other, separated by a membrane. The flat-plate configuration helps to reduce the distance between the electrodes. Hence, protons have less distance to travel in the flat plate setup. This configuration decreases ion transport resistance and membrane resistance (Helder et al., 2012b).

To carry out a comparative analysis with tubular design, Helder et al. (2012b) designed a flat plate PMFC. They studied the effect of internal resistance on bioelectricity generation for a longer period, i.e., 703 days. The setup used graphite felt for both anode and cathode. The

power and current densities per geometric planting area with the flat plate design (0.22 W m^{-2} and 0.15 A m^{-2}) were found to be higher than the tubular design (0.44 W m^{-2} and 1.6 A m^{-2}) A three chamber PMFC setup was designed for the first time by Wetser et al. (2015). The design had one anode chamber sandwich between two cathode chambers. The anode and cathode were composed of graphite felt, and the chambers were separated by a bipolar membrane (BPM). A long-term operation was carried out for 151 days which, with a maximum power production of 240 mWm^{-2}. In recent studies on flat plate PMFC, the activated carbon and marine sediments (in different compositions) were used as the anode in *Spartina anglica* operated PMFC, with results showing activated carbon concentration 33% (AC 33%) setup outperformed with enhanced power output (1.04 mWm^{-2} PGA) and current output (16.1 mAm^{-2}PGA) than all other compositions (Helder et al., 2012b). Flat plate design is indisputably the more efficient design regarding the area and material utilization for power production in PMFC setup. However, the main bottleneck remains the field scale application and scale-up challenge. Flat plate design is incompatible with application in natural ecosystems like constructed wetlands and paddy fields. Thus, future research in PMFC design should be aligned toward efficient flat plate design and feasible scalability.

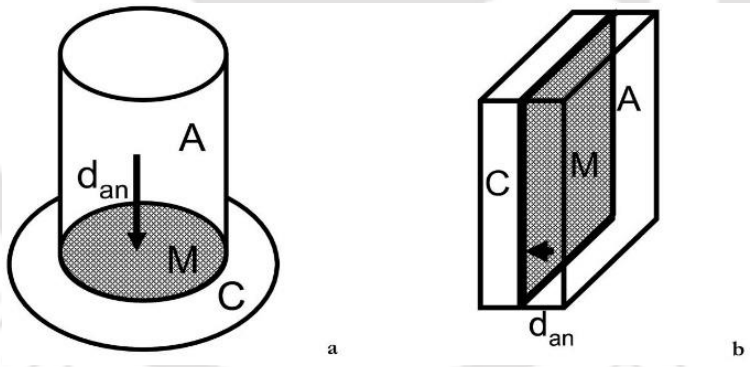

Fig. 2.5 Tubular (a) and flat-plate (b) design of a Plant Microbial Fuel Cell, in which A= anode, C = cathode, M= membrane, d_{an} = average distance between anode and membrane. Distance between anode and membrane is shorter in flat-plate design than in tubular design. (Source: Helder et al., 2012).

2.8 Electrode material

Electrodes is the most crucial element of an MFC for power generation; therefore, choice of materials is essential for effective microbial adhesion and biofilm development. Though the criteria for material selection for anode and cathode differ, in general, both should possess the following properties:

2.8.1 Properties of Electrode

Surface area

Internal resistance is the primary cause of ohmic losses, which reduces the overall performance of an MFC, and surface area and porosity significantly influence the overall internal resistance of a cell. It can be minimized by increasing the effective surface area, while keeping the volume constant. Moreover, high surface area enhances electrode kinetics by providing more reaction sites (Di Lorenzo et al., 2010).

Electrochemical properties

Electrode materials should possess high electrical conductivity with low interfacial impedance to facilitate the adequate flow of electrons through the circuit. The cathode should also maintain ionic conductivity to facilitate triple-phase boundary reaction (Sun et al., 2015).

Material stability and cost-effectiveness

The prevailing oxidizing and reducing environment in a MFC, microbial growth and attachment on electrode surfaces often lead to the decomposition of the electrode materials. Thus, the electrode material should be stable and durable with high mechanical strength to provide long-term performance with minimum fouling or degradation. Furthermore, electrode material should be low-cost, easily available, and sustainable for the technology's economic viability at a large scale (Wang et al., 2013).

Biocompatibility

Anode materials should be highly biocompatible to facilitate effective bacterial adhesion and biofilm formation without altering the properties of anolyte and catholyt and should cause adverse effect on microbial consortium. It should be resistance to corrosion and environmentally friendly thereby increasing overall MFC performance (Tao et al., 2016).

Carbonaceous and metallic-based materials are the main types of electrode adopted, which possess all the above-mentioned characteristics (Rimboud et al., 2014; Wei et al., 2011). Carbon is one of a trusted material where it can be used as electrode effectively which is available in numerous forms of structure such as carbon cloth, carbon paper, carbon fiber, carbon rod, carbon felt, granular activated carbon, carbon nanotube-based composites, and graphene based nano-composites. Carbon can be used in any type of MFC because of its flexibility in its size and shape. Cost of carbon electrode is significantly cheaper for

commercialisation. Among metals based materials, stainless steel plate, stainless steel mesh, stainless steel scrubber, silver sheet, nickel sheet, copper sheet, gold sheet and titanium plate were used as commercially available electrode material.

2.8.2 Classification of electrodes

Electrodes used in MFC applications could be classified commonly on the basis of their configuration into plane electrodes and three-dimensional electrode (Tiquia-Arashiro et al., 2020). Structurally a carbon based electrodes can be classified into a brush like structure, fully packed arrangement structure and plane type of structure (Kumar et al., 2021).

Plane type of structure

The most common plane structure used as electrodes are carbon paper, carbon sheet, carbon cloth and graphite plates (Cai et al., 2020). Among all these types of electrode there are some advantages and disadvantages associated like graphite plates or sheets possess greater strength as compared to paper of carbon (der Kuan et al., 2021). Also roughed graphite electrodes produce more power than the flat graphite electrodes (Malakooti et al., 2021). A cheaper and more feasible alternative for carbon cloth and carbon paper could be carbon mesh treated with ammonia gas.

Packed structure

For generation of a larger surface area for bacterial attachment, irregularly shaped packing materials such as graphite granules, granular rods, granular activated carbon (GAC) were used in anode chamber (Tan et al., 2021). For better performance in long run and to make complete bed conductive packing material were placed next to each other (Govender et al., 2020). As porosity of these packed electrode is ranging from 30% to 50%, but after certain time interval clogging of pores takes place which decreases the overall performance of MFC in long run (Caizan-Juanarena et al., 2020).

A comparative study of carbon felt as well as graphite granules of 2 and 5 mm reported graphite material to be a superior material for anode with a power generation up to 386 Wm^{-3} (Caizan-Juanarena et al., 2020). Similarly, a higher power density by 2.5 times was reported in GAC over carbon cloth as anode in MFC system (Matsena et al., 2021), which showed the potential of GAC in power generation and its applicability.

Brush structure

Another type of electrode structure is a brush structure which is designed to achieve a high surface area, efficient current collection and higher magnitude of porosities makes graphite brush electrodes as ideal choice for anode in MFC (Kaur et al., 2020). These type of electrode was first introduced by Logan, in 2007. These brush electrodes were designed by twisting the carbon fibers of desired length over two non-corrosive titanium wires. It can be made into different dimensions by varying the diameter and length of the electrode to achieve the desired surface area. (Yaqoob et al., 2020; Nandy, 2018).

2.8.3 Electrodes for Anode

Anode in an MFC functions as an electrode that allows electrons released from an anaerobic process to the load. Anode surface area (or projected area) also affects the overall performance because the anodic surface is the site for microorganism attachments and electrons' release (Logan, 2006). The important key criteria for selection of a material for anode depends on its biocompatibility, convenient microbial adhesion, electrochemical efficiency and electron transfer mechanism from microbial cell to the electron acceptor (Dumitru and Scott, 2016; Loubna et al., 2019). Therefore, the material for anode development should improve the attachment of electro active microorganisms to the electrode surface as well as current collection. Materials possessing good intrinsic biocompatibility for microbial inoculums, its growth and attachment to the surface and excellent conductivity for electron transfer are desired. Other properties, includes large surface area, highly porous structure, long-term stability, and favourable surface modification, are also utmost necessity. Therefore, one of the major objectives in the MFC research is to design and synthesize low-cost advance electrode materials with increased efficiency, and improved durability. To improve the electron transfer mechanisms in MFC, there are various strategies applied such as, application of bioactive redox compounds, modification of anode etc. (Nosek et al., 2020; Zhao et al., 2010).

As mentioned previously, carbon remains one of the trusted material along with other metal based materials were also commonly used as anode for MFCs (Wang et al., 2009; Wei et al., 2011; Wen et al., 2013). Anode is the conductor of electron and carbon materials which are used as anode has little electro catalytic activity which limits their performance; Thus, modification of carbon materials is the main approach to improve their conductivity (Wang et al., 2015). Semiconductors as well as their composite material have been used to modify the anodes in order to improve their electrochemical properties (Narayanasamy and Jayaprakash,

2020). Nanostructured metal oxides are also commonly used for anode modification as they possess high surface area, good biocompatibility, chemical stability and electro-conductive properties (Liu et al., 2020a).

2.8.3.1 Modification of anode electrodes

Anode modifications therefore be done for dual objectives of increasing active surface area for bacterial attachment and improving electrical conductivity of surface (Scott et al. 2007). The anode modification thus provides sufficient support and conductive surface for bacterial growth and bio-film development. Surface modification can be achieved by three different treatment methods on carbon fiber brushes: acid soaking (CF-A), heating (CF-H), and a combination of both processes (CFAH) (Feng et al. 2010). The combined heat and acid treatment exhibited improved power production which was higher by 34% than the untreated one, 25% higher than only acid treatment and 7% higher than heat treatment alone. Nitric acid treated activated carbon fiber improved the power density of a MFC considerably (Zhu et al. 2011) which was accounted to surface charge increment. Similarly, formic acid treated carbon cloth enhanced the bacterial attachment thereby increasing the system performance by 38.1 % than untreated one (Liu et al., 2014). Alternate treatment of anodes in acid and base was also practiced by researchers (Deepika et al., 2015). The acid pre-treatments (Nitric acid) was found to be promising for granular cathode carbon which exhibited 1050 mV higher than previously reported values (Erable et al. 2009).

Apart from acid treatment, a variety of materials such as semiconductors, metal oxides, carbon nanostructures and conductive polymers have been extensively explored as anode modifiers as coatings due to their excellent biocompatibility, chemical stability, good electron conductivity and high specific surface area. Some significant developments made towards developing anode materials are mentioned in Table 2.2. It represents the overview of MFC performance using modified anodes. Some anode modifications strategies can be classified broadly into following categories

1. Modifications using Carbon nanotube (CNTs) and conductive polymer (CPs)
2. Graphene based modifications
3. Modifications using metal/metal oxides

2.8.3.1.1 Anode modification using carbon nanotube (CNTs) and conductive polymers (CPs)

CNTs have exhibited very promising properties for uses as electrode material because of their large specific surface area, extraordinarily high conductivity and mechanical flexibility. However, due to their inhibitory or even toxic effect on microorganism, they are rarely used in MFC in unmodified form. Hence, various modifications on CNT are done to make it biocompatible. Qiao et al. (2007) reported that anode modification with CNT and polyaniline composites reduces cellular toxicity and also improves the electrocatalytic activity and reported a power density of 42 mWm^{-2} which was 1.2-fold higher than that of unmodified electrode. Liu et al., (2020b) modified multi-walled carbon nanotube with graphene oxide nanoribbons containing oxygen and nitrogen separately by microwave and ammonia treatment respectively. As a result, the power density increased from 970 mWm^{-2} to 3291 mWm^{-2} and 3444 mWm^{-2}, respectively primarily due to the improved biofilm adhesion. The specific surface area was known to increase from 18.1 to 49 m^2g^{-1} and 72.4 m^2g^{-1} due to the formation of micropores and macropores structures on the surface.

Conductive polymers are organic polymers that have potential of electricity conduction. They can be metallic conductors or semiconductors. Polyaniline (PANI) is a conductive polymer and has desirable use for MFC anode preparation due to its high electrical conductivity, facile processability, hydrophilicity, good biocompatibility and high stability (Qiao et al., 2007). The positive charge on outer surface of PANI facilitates its interaction with negatively charged bacterial cell membrane that leads to high bacterial density on its surface. Several researchers have combined PANI with metal oxide or graphene or graphene oxide to improve its specified surface area and reluctant conductivity. Metal oxides accelerate the electron transfer between anode and bacterial cells, thus improving the efficiency of MFC. Along with graphene and/or graphene oxide, PANI improves biocompatibility, thus influencing the bacterial adhesion capacity and extracellular electron transfer (EET) efficiency (Khilari et al., 2015; Huang et al., 2016; Fu et al., 2020; Jian et al., 2020; Rajesh et al., 2020).

2.8.3.1.2 Anode modification using graphene

Graphene has large specific surface area, high electronic conductivity and good biocompatibility, thus have application as electrode material (ElMekawy et al., 2017; Yuan and He, 2015). Various researchers have used graphene modified electrodes in MFC due to its above-mentioned properties and found improvement in power generation in comparison to

respective bare electrode. Liu et al. (2012) modified carbon cloth with graphene oxide and observed a 2.7 fold increased in power generation in MFCs. Zhang et al. (2011) modified stainless steel mesh (SSM) using porous graphene and PTFE (Polytetrafluoroethylene) paste and used as anode in MFC reactor fabricated using two round polymethylmethacrylate templates and observed improved MFC performance. The maximum power density of 2668 mWm^{-2} was reported when modified electrode was used which is 18 times larger than that obtained from the MFC with the SSM anode (without modification). Xiao et al. (2012) tested different shapes of graphene modified anodes and observed that graphene oxide shape which deliver higher surface area also deliver higher power density. Zhao et al. (2013a) have reported that when anode is modified using graphene could achieve 4.2 times higher power density over bare carbon paper anode. Geetanjali et al. (2019) modified the carbon cloth using NiWO4/GO and used as anode electrode in a single chambered MFC of 0.8 ml volumetric capacity operated using simulated wastewater sample and reported a power density of 1458 mWm^{-2} which is 8.5 fold more than bare electrode reported by them.

2.8.3.1.3 Anode modification using metal/metal oxides

Semiconducting metal oxide have great potential to work as anode catalyst in MFCs due to its high rate of redox reaction and electrical conductivity. Metal oxide such as TiO_2, MnO_2, FeO_2, Fe_2O_3 have properties such as structural stability, low cost, nontoxicity and good biocompatibility (Priya et al., 2020) and widely used as catalyst to improve the performance of MFC. Precious metals such as Pt or Au or Ag are widely employed in industries dealing with electrochemistry processes owing to their catalytic activity and high conductivity (HaoYu et al., 2007). However, the high cost of these metals makes them unsuitable to be used as anodic material in MFCs. The catalytic activity of semiconducting metals (PANI or graphene-based catalyst) or non-noble metals (such as Fe-based or Co-based catalysts) and their oxide nanoparticles is almost comparable to that of the precious metals, which can explicitly reduce the ohmic resistance and enhance the attachment of exo-electrogenic bacteria on the surface of the anode (Hindatu et al., 2017). Therefore, the topic needs to be widely explored in terms of the use of such semi conducting materials which have promising catalytic activity, conductivity and are not cost intensive.

One such promising material suitable for modification of anode can be Ti or TiO_2 which has high biocompatibility, anti-corrosion properties, optical and dielectric properties and reduced cost as compared to other metals. Thus, this metal oxide is a prospective material to

be used for modifying anode electrode. Some of the anode modification along with their power generation are tabulated in brief in Table 2.2.

Table 2.2 Modification of anode and its performance in term of power output

MFC Type	Electrode material	Anode modifier	Volume of the reactor	Power density (control) mWm^{-2}	Power density (modified) mWm^{-2}	References
Single chamber	Carbon cloth	Graphene + PAni	28	454 ± 47	884 ± 96	Huang et al. (2016)
Single chamber	Carbon cloth	PAni	28	454 ± 47	589 ± 38	Huang et al. (2016)
Dual chamber	Carbon cloth	NCP (Nickel oxide/ CNT/PAni)	500	1.5	2.5	Nourbakhsh et al. (2017)
Dual chamber	Carbon felt	PAni	250	166	216	Rajesh et al. (2020)
Single chamber	Carbon cloth	PDA-rGO	28	2337 ± 15	2047 ± 58	Li et al. (2020a)
Dual chamber	Carbon felt	Graphene/Fe_2O_3	250	129 ± 4	334 ± 4	Fu et al. (2020)
Dual chamber	Carbon cloth	Titanium suboxide/ Graphene/PAni	288	163.	2073	Li et al. (2020b)
Single Chamber	Carbon cloth	Graphene	28	454 ± 47	634 ± 78	Huang et al. (2016)
Dual Chamber	Carbon cloth	PPy-MnO_2	120	598.4 ± 31.5	2139.7 ± 67.5	Zhao et al. (2020)
Single Chamber	Carbon felt	Ru/Fe	40	0.223	0.6	Qiu et al. (2020)
Dual Chamber	Graphite plate	$FeMoO_4$	250	75.8 ± 1.5	106.2 ± 2	Mohamed et al. (2020)
Dual Chamber	Carbon felt	WO_3	50	0.49 ± 0.11	3.21 ± 0.22	Das and Ghangrekar (2020)

2.8.4 Electrodes for Cathode

Unlike anode, performance of a MFC depends on various cathode properties, redox potential being the most important one. Other desirable cathode properties include low corrosion, good electrical conductivity, high porosity and high specific surface area. The cathode materials should possess high redox potential so as to capture protons easily, which improves the performances of MFCs (Zhou et al., 2011). In MFC operation, O_2 is an important molecule to act as an electron acceptor in the cathode chamber. Slow oxygen-reduction reaction (ORR) kinetics, an important issue in MFC operation, also directly affects the power generation efficiency. To maintain high rate of ORR, platinum (Pt) based catalysts are preferably utilized as cathode catalyst in MFC due to their potency in reducing the *Ea* (activation energy) of cathode reducing reactions (Mohan et al., 2014).

Generally, carbon materials are used as cathode such as carbon cloth, carbon felt, and carbon paper (Merino-Jimenez et al., 2016). Other material such as graphite sheet, graphite paper steel mesh, or other are preferred less than the carbon based material due to their less efficacy in increasing ORR rate. To improve the performances of MFCs, the cathode can be modified using active catalyst. Pt is most popularly used catalyst and supposed to reduce the activation energy and increase the cathodic reaction rate (Li et al., 2017a). Considerably the high cost and very limited availability of platinum hinders its use to large scale MFC. Surface modification can also be achieved by acid soaking, heating, and a combination of both processes on carbon fiber material (Feng et al. 2010). Researchers have used several modifications to develop a cheap and highly active noble catalyst for its potential and specific application as a cathode catalyst in MFC operation.

2.8.4.1 Modification of cathode electrodes using non-Pt catalysts

Many other cathode catalysts have been researched so far that can have manifested similar performances as platinum used as catalyst. Moon et al. (2006) used graphite felt coated with Pt as cathode in their microbial fuel cell and reported a power density of 150 mWm^{-2}, which was thrice times higher when graphite felt used without modification (Bare graphite felt). As Pt is very expensive metal so this can't be used for realistic application. Activated carbons have been reported with comparable performance to Pt-doped carbon cathodes (Zhang and Zhao, 2009). Cheng et al. (2006) found that the potential did not change noticeably (maximum of 19%) when the Pt loading on the cathode ranged from 0.1 to 2 mg cm^{-2}. This finding resulted in the Pt modified cathode still being competitive and cost-effective. Li et al.

(2017b) used $NiCo_2O_4$/carbon composite as catalyst to improve the oxygen reduction rate of cathode (carbon cloth) in MFC and reported a power density of 1249.86 mWm^{-3}. Sonawane et al. (2019) used PANI/Cu hybrid as catalyst to improve the performance of carbon cloth electrode and used as cathode in MFC and obtained a power density of 0.101 ± 0.01 mWm^{-2}. Li et al. (2019a) modified bacterial cellulose by doping with Cu and P heteroatoms. It was freeze-dried and subjected to high-temperature pyrolysis. Doping resulted in changes in functional group and an increase in the number of active sites, thereby increasing the oxygen reduction reaction catalytic activity. The bacterial cellulose-based catalyst was coated on to an air diffusion layer (Ma et al., 2018) and utilized as the cathode in MFC with activated sludge as the inoculum. The results of this study were compared with another similar work that employed a platinum-based catalyst (Li et al., 2019a). A maximum power density of 1177.31 mWm^{-2} was obtained for the Cu-P-Co doped bacterial cellulose-based catalyst, while the Pt-based catalyst achieved a power density of 1044.93 mWm^{-2}. The recent modifications of different cathode electrode are elaborated in Table 2.3 with the power generation and COD removal values reported in the literatures.

Table 2.3 Modification of cathode and its performance in term of power output

MFC Type	Electrode material	Catalyst	Volume of the reactor	Power density (control) Wm^{-3}	Power density (modified) Wm^{-3}	References
Dual chamber	Carbon felt	Co–N-CNT	80	2.9	5.1	Turk et al. (2018)
Cylindrical chamber	Carbon cloth	Co_3O_4	80 (A) & 250	2.96 ± 0.20	6.62 ± 0.33	Bhowmick et al. (2019)
Single chamber	Carbon cloth	$MnCo_2O_4$/ PPy	-	1.77	6.11	Khilari et. al. (2014)
Dual chamber	Carbon felt	Rh/AC	70	3.65	9.36	Rajesh et al. (2020)
Single chamber		MnO_2	900	0.491	1.64	Noori et al. (2016)
Single chamber	Carbon cloth	Co/FeTMPP	100	-	33.4	Zhao et al. (2013b)

2.9 Membrane for MFCs

Membranes are an important constituent of a MFC configuration, where in its main objective is to prevent oxidation and reduction reactions happening in the same place, i.e., oxidation of organic matter by anaerobic microbes should be separated from reduction of O_2 at the other side as described redox reaction in Chapter I. Otherwise if the redox reaction occurs in the same place, it will get short-circuited. Therefore, the use of a membrane or separator is essential for the configuration. On the other hand, the membrane must have the ability to function as a channel, allowing the flow of ionic species generated by oxidation. In contrast, generated electrons migrate through an external wired connected circuit from the anode to the cathode. Nafion-117 membranes are one of the most commonly used proton exchange membranes (PEMs) available commercially. Its excellent proton conductivity makes Nafion the choice of researchers for use in fuel cells (Venkatesan et al., 2014; Sangeetha et al., 2019; Logan,2008 Logan and Regan, 2006a; Kim et al., 2014; Rabaey and Verstraete, 2005).

The performance of any membrane depends on its physical and chemical properties. In the case of membranes with pores in their structure, membrane performance is the function of pore size and the number of pores (porosity). Nevertheless, there are nonporous membranes where porosity is conceptualized as the phase-separation degree between hydrophobic and hydrophilic phases, playing a significant role in membrane performance. The size of ion clusters (size of ion transport channel/pathways), and ion exchange hydrophobic and hydrophilic phases, play a significant role in membrane performance. The size of ion clusters (size of ion transport channel/pathways) and ion exchange capacity (IEC) are other important factors to consider when evaluating nonporous membrane performance. Porous membranes do not have functional groups; therefore, they do not have IEC (Sun et al., 2021). Thus, depending on the presence of pores, membranes have been classified into porous and nonporous membranes. The nonporous membranes, also called ion-exchange membranes (IEMs), are in turn classified into three groups based on the type of ion that is transferred: cation-exchange membranes (CEMs), anion-exchange membranes (AEMs), and bipolar membranes (BPMs). On the other hand, porous membranes have been grouped into ultrafiltration membranes, microfiltration membranes, ceramic membranes and pore filter materials (Sangeetha et al., 2019; Li et al., 2011; Scott, et al., 2016).

2.9.1 Function of Membranes in Microbial Fuel Cells

The membranes used inside an MFC carries out several essential functions. It should have a high ionic conductivity, increasing an MFC's performance. Its primary purpose is to act as a barrier between the anode and cathode to prevent short circuit. It must perform as ion-conducting channel (protons, anions, or both) from anode to the cathode or vice versa (Fig.2.6). For non-porous membranes like IEM, should have hydrophilic properties to provide ion transport channels. However, for a porous membrane it may have hydrophobic properties. The membranes must inhibit oxygen (O_2) diffusion from cathode to anode with high selectivity. This is necessary for maintenance of anaerobic conditions in the anode chamber required for metabolic activities of electrochemically active microbes (EAM) (Scott, (2016); Hernandez-Flores et al., 2016). In case of use of PEMs, it should selectively avoid transfer of other electron acceptors viz., sulphates, nitrates, H_2O_2, ammonia, ferricyanide permanganate, trichloroethene, perchlorate and few heavy metals, that may irreversibly alter the anodic microbial community structure and in turn favour development of other non-electrochemically active microbes (Logan, 2008; Catal et al., 2009; Wang and Ren, 2014; Mathuriya and Yakhmi 2014). Similarly, for the cathode side, the membrane should not favour fuel crossover, i.e., it should prevent the transfer of soluble low molecular weight organics from anode to cathode (Logan, 2008). Also, in cases when different microorganisms were used in both the chambers, the membrane should also prevent crossover or exchange of microbes across the chambers. Apart from these functions, the membrane should exhibit good mechanical and chemical stability to prevent membrane oxidation and microbial degradation (Velez-Perez et al., 2020).

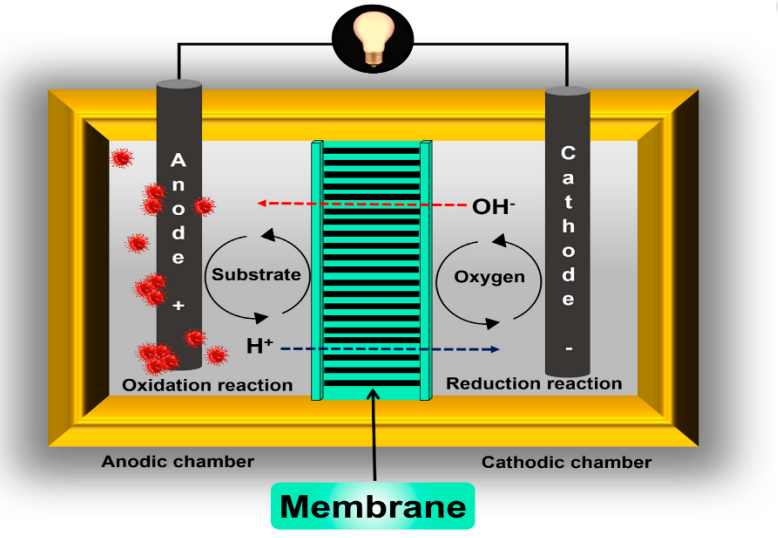

Fig.2.6 Membrane functions (Source: Ramirez-Nava et al., 2021)

2.9.2 Disadvantages of Using Membranes in Microbial Fuel Cells

An ideal membrane should meet all the criteria as described in section. However, chemical composition of the membranes along with physiochemical and microbiological features of anolyte and catholyte with which membrane is continuously engages, certain deviations in the membrane characteristics may takes place from time to time. Major disadvantages associated with use of membranes are the following (Ramirez-Nava et al., 2021):

2.9.2.1 Increasing in Total Internal Resistance of the Cell

The total internal resistance of a cell, R_{int} is one of the main factors related to the power generation. The R_{int} of an MFC is the sum of the resistances caused by design factors and physico-chemical properties of the materials used in the construction of the MFC (Sangeetha et al., 2019; Leong et al., 2013). The membrane itself, depending on its nature (organic, inorganic, or mixed compound) and the number of pores, contributes significantly to increasing the total R_{int} of an MFC. The resistance imparted by a membrane is associated with its capacity to exchange ions across the chamber i.e., ion exchange capacity (IEC). The IEC is affected by operating conditions of the cell: temperature, electrolyte type, pH, and concentration of the electrolyte solution. A low proton diffusion from the anode to the cathode will be reflected by low MFC performance.

Porous membranes are generally considered to have lower resistance, e.g., microfiltration membranes. However, a low resistance value does not reflect positive MFC performance as these membrane has high oxygen and fuel crossover values that translates into low MFC performance in terms of power output (Leong et al., 2013). On the other hand, non-porous membranes are known to have high value membrane resistance. However, despite this disadvantage, non-porous membranes are preferred instead of porous membranes. While using a non-porous membrane, a thinner one is not recommended for MFC use in spite of its property to increase conductivity with decreasing thickness. Sun and Zhang (2019), demonstrated that thinner membranes such as Nafion-212 and Nafion-115, in comparison to NF-117, have a higher permeability to electro-active species, an undesirable effect. Moreover, usually, thinner IEMs have lower mechanical properties. Thus, the use of thinner nonporous membranes will not improve the overall membrane performance.

2.9.2.2 Oxygen Diffusion

Oxygen is the primary electron acceptor at the cathode because of its high redox potential (Krauskopf and Bird (2003); Velez-Perez et al., 2020). However, the presence of oxygen in the anodic chamber negatively affects the MFC's performance (Watson et al., 2011). The presence of facultative bacteria as biocatalysts in the anode acts on dissolved oxygen before the anodic substrate. This will lead to aerobic oxidation process which is undesirable (Harnisch and Schroder, (2009); Leong et al., 2013; Watson et al., 2011). The job of an ideal membrane is to prevent diffusion of oxygen from the cathode chamber to the anode chamber. Unfortunately, nonporous membranes (including Nafion membranes) fail to meet this requirement. That is because oxygen has a significant solubility in water. For instance, Qu et al. (2012), used an air cathode based single chamber MFC with a membrane filter as separator and a pure culture of *Geobacter sulphurreducens*, where it was found that the dissolved oxygen concentration at the anode reached 6 mg L^{-1}, a concentration close to oxygen saturation levels. Consequently, growth of *G. sulfurreducens* was inhibited. The ion-exchange functionality in nonporous membranes is maximized when the membranes have been fully hydrated. Therefore, OD is associated with the need to keep the membrane hydrated (Scott, (2016); Leong et al., 2013). In general, porous membranes have a greater tendency to allow the passage of oxygen from the cathode to the anode due to the presence of pores compared to nonporous membranes. However, considering IEMs need to be hydrated to acquire their functionality, it will be difficult to synthesize a membrane that avoids OD entirely.

2.9.2.3 Substrate Crossover

In theory, nonporous membranes do not allow non-ionic species to cross to the cathode. However, in the anode, different pure compounds such as acetates, butyrates, and propionates, and wastewater with a large amount of dissolved low molecular weight organic compounds, have been evaluated as fuels or substrates resulting in susceptibility to the substrate/fuel crossover phenomenon. It is a similar phenomenon to that experienced by oxygen diffusion, however in the opposite direction. This phenomenon is observed when dissolved organic compounds are used as a source of energy by biocatalysts may diffuse through across the membranes from the anaerobic to the aerobic cathode chamber (Sangeetha et al., 2019; Scott, (2016); Leong et al., 2013). The hydrophilic nature of the membrane favors the embedding of aqueous organic substrate into the membrane and crossover towards the cathode as a function of the current concentration gradient.

Unlike ions, organic compounds are considerably larger in size. Therefore, in the case of nonporous membranes, the occurrence of substrate crossover is practically negligible, except in AEMs which has characteristic positively charged ionic groups. Consequently, negatively charged organic compounds has the tendency to diffuse across AEMs at a slower rate. On the other hand, porous membranes having larger pores induces the substrate crossover phenomenon at a higher speed.

When the substrate migrates from the anodic to the cathodic chamber, several effects are observed:

1. The amount of substrate available at the anode for the microorganism's decreases;
2. The substrate is oxidized at the cathode by aerobic bacteria producing electrons for the ORR that is carried out at the cathode;
3. Biofouling is generated at the cathode surface and reduces oxygen interactions with the active cathode surface.

The power generation decreases due to each of these mentioned activities (Sangeetha et al., 2019; Scott, (2016); Leong et al., 2013).

2.9.2.4 Biofouling

This phenomenon is characterized by the adherence of organic compounds used as on the membrane surface, exposed towards the interior of the anode section (anodic biofouling) or towards cathode section (cathodic biofouling). Both porous and non-porous membranes go through the process of biofouling. Diffusion of O_2 from cathode to anode followed by long term operational period leads to organic matter oxidizing under aerobic conditions, favoring the proliferation of aerobic microorganisms on the membrane (Scott, (2016); Leong et al., 2013). Aerobic oxidation is carried out at a higher speed than anaerobic oxidation processes. Also, in this process, a large amount of energy (65%) is applied to generate new cells that will be translated into a greater quantity of sludge, while in anaerobic conditions, the amount of energy employed to create new cells is considerably lower (10%).This aerobic oxidative microenvironment generated on the surface of the membrane causes: (i) substrate consumption at a higher speed susceptible to conversion into electrical energy, (ii) a negative oxygen gradient due to the aerobic bacteria demand; the latter leads to more oxygen passing from the cathode to the anode, and (iii) an additional barrier between the anolyte and the membrane, the biofilm results in increasing overall internal resistance of the cell.

In case of cathodic biofilm formation, substrate crossover from anode play an important role favouring biofouling on the surface of the membrane exposed to the cathodic section. Depending on the porosity, cathodic biofouling will be mostly observed in porous membranes. However, in AEMs (nonporous membranes), this phenomenon has also been observed, although to a lesser extent, since some low molecular weight organic acids can cross the membrane (Sangeetha et al., 2019).

Therefore, biofouling is a process that depends on substrate crossover, O_2 diffusion, membrane porosity, and MFC operational time. The greater the substrate or oxygen crossover and operating time, the greater the thickness of the biofouling will be. This will increase the thickness of the membrane, while increasing the overall internal resistance of the cell; therefore, the MFC performance will decrease (Sangeetha et al., 2019; Leong et al., 2013).

2.9.2.5 pH Splitting

This phenomenon associated with a wide variation in pH between the anodic and cathodic chambers during MFC operation. Based on the type of anolyte and membrane use, a characteristics pH gradient can be observed between chambers as a result of pH splitting. The presence of any cation-rich anolyte (105 times higher than the H^+ concentration) such as NH_4^+, Na^+, K^+, Mg_2^+, and Ca_2^+, and a CEM, leads to splitting effects compared to the use of an AEM. The high concentration of cations will compete directly against H^+ ions for crossing over to cathode. These cations will first pass before the H^+ ions, causing its accumulation in the anode resulting in acidification of the anode chamber. Under acidic conditions, anaerobic bacterial oxidation is inhibited, resulting in decreased proton and electron generation. Besides, in the absence of H^+ transfer to the cathode the pH of the catholyte increases, thereby decreasing MFC performance. AEMs represent a good option for eliminating this phenomenon because the anions of the AEM are responsible for transferring H^+ ions. In MFCs using this type of membrane, pH splitting is practically not observed (Sangeetha et al., 2019; Leong et al., 2013).

2.9.2.6 Water Loss by Evaporation

The hydrophilic nature of the membrane facilitates water transport and water evaporation. In a single chamber MFC, it was observed that for every H^+ transferred to the cathode, $3H_2O$ molecules pass through the membrane (Scott, (2016)). Hernández-Flores et al. (2017) operated two single chamber MFC using different membranes. The first used Nafion-117 as a PEM, while the second operated using Zirfon as an AEM. In both designs, the cathode

section aerated by natural convection and exposed to an environment with a low humidity percentage favored water loss by evaporation.

2.9.2.7 Undesirable Ions Crossing

In the case of nonporous membranes specifically in CEMs and AEMs, the permeability of H+ and OH- ions is not 100% efficient and depends on the concentration of other ions present in the anolyte and catholyte. In the case of CEM, the presence of other cations NH_4^+, Na^+, K^+, Mg_2^+, and Ca_2^+ will compete with H^+, and there is a possibility that they will cross the membrane and generate pH splitting. Besides, in the case of AEM, anions other than OH^-, such as Cl^- and SO_4^{2-}, can pass through these membrane types. The transfer of ions other than those desired becomes a problem throughout the operation of the membrane system (Sangeetha et al., 2019; Hernandez-Flores et al., 2019).

2.9.2 Types of membranes

While designing the MFC architecture, the choice of material for the membrane is very critical as its nature, geometry, and properties significantly decrease the overall internal resistance of the cell and contribute towards its performance and also its practical application (Ramirez-Nava et al., 2021). Membranes used in MFCs can be classified into Porous and Non-Porous membranes and are described in detail as follows:

2.9.2.1 Non-Porous membranes

2.9.2.1.1 Cation-Exchange Membranes (CEMs)

CEMs are characteristically designed to allow the passage of positive ions through them selectively. Their chemical composition is characterized by the presence of negatively charged such as SO_3^-, COO^-, PO_3^{2-}, HPO_3^- and $C_6H_4O^-$ among others, when the membrane is hydrated (Sangeetha et al., 2019). Membranes such as Nafion-117, Hyflon, Zirfon, Ultrex, and CMI-7000 are some types of membrane that have been used in MFCs as CEMs (Sangeetha et al., 2019; Leong et al. 2013; Kazemi et al., 2012; Pandit et al., 2018).

The main characteristic of these membranes is that a negatively charged sulfonate functional group is attached to the hydrophobic structure of fluorocarbon; the hydrophilic nature of the sulfonate group promotes the transport of protons through the membrane (Sangeetha et al., 2019; Leong et al., 2013). Among all the CEMs, Nafion-117 is the most widely used in MFCs due to its high proton conductivity and low ohmic resistance, translating

into high power output. Ultrex CMI-7000 membranes have also produced power densities similar to those of NF-117 (Leong et al., 2013). Despite their excellent characteristics, unfortunately, this membrane has certain limitations:

1. High cost. Cost is one of the most critical disadvantages since it represents a percentage greater than 50% of the system's total cost. It is one of the criteria that prevents MFC technology from being scalable (Christgen et al., 2015);
2. Sensitivity to cations. Many cations present in the anolyte competes with H^+ ions, thus decreasing proton conducting capacity;
3. Permeability to oxygen. A significant amount of oxygen can pass through the membrane from the cathode to the anode chamber;
4. Biofouling—a phenomenon that is associated with the adherence of a mixture of substrate with microorganisms and metabolic products of bacteria on the surface of the membrane, generating a barrier between the soluble transferable H^+ and the membrane (Sangeetha et al., 2019; Chae et al., 2008; Kim et al., 2007).

2.9.2.1.2 Anion-Exchange Membranes

Contrary to CEMs, anion exchange membranes (AEMs) have the characteristics and properties to allow negative ions to pass through them. They are an important group of membranes and the second most-used group of membranes in MFCs, only after CEMs. The presence of positive charges (cations) such as NH_4^+, NHR_2^+, NR_2H^+, NR_3^+, PR_3^+, and SR_2^+ on the surface of the polymer matrix helps in the transfer of negative ions accross it (Sangeetha et al., 2019; Scott, (2016)).

The main demand for AEMs are in alkaline fuel cells, where PEMs like Nafion and PTFE unable to meet expectations. In MFCs AEMs mainly allow anions such as OH^-, Cl^-, SO_4^- and has the characteristic property to inhibit cation transfer. Using an AEM instead of a CEM is based on the existing interference due to the passage of cations, different from the cation of interest (H^+), through the CEM. This interference reduces the pH in the anode chamber and inhibits microbial activity; consequently, a high pH in the cathode chamber represents a reduction in the cathode potential (Mahendiravarman and Sangeetha, (2017); Rossi et al., 2020). Fumasep membranes are a group of AEMs; some have been evaluated as separators in MFCs (Scott, (2016)). AEMs used in MFCs are inexpensive and highly porous, e.g., fiberglass and nylon (Li et al., 2011; Zhang et al., 2010; Guo et al., 2010). A polyvinyl chloride coating is applied to increase the mechanical stability of the AEMs. Kim et al. (2007) reported an

improvement in power density of 610 mWm^{-2} while using an AEM in MFCs as compared to the typical Nafion at 514 mWm^{-2}.

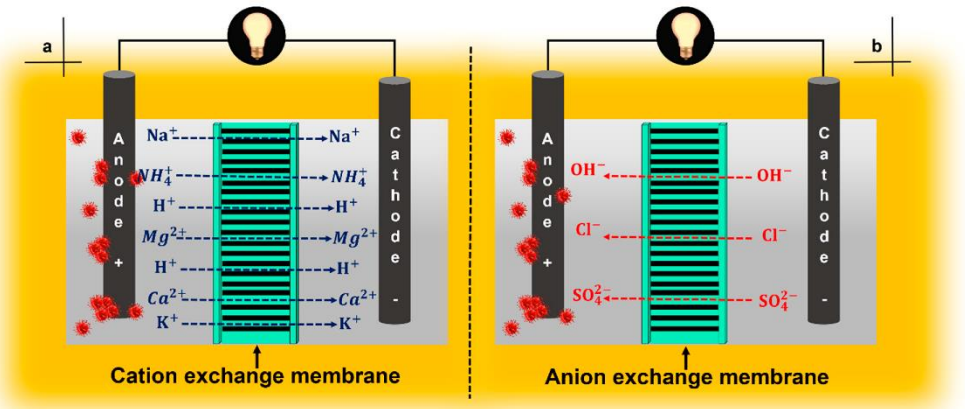

(a) (b)

Fig. 2.7 Main ions transported in a microbial fuel cell working with (a) a cation-exchange membrane and (b) an anion-exchange membrane (Source: Ramirez-Nava et al., 2021).

2.9.2.1.3 Bipolar Membrane

A third category of the non-porous membrane is made by the union of a CEM with an AEM with an objective to transport H^+ and OH^- simultaneously and contribute to a load balance. Heijne et al. (2006) used an MFC with a BPM and operated it continuously, achieving ferric iron reduction on a graphite electrode at the cathode. On the other hand, Kim et al. (2017) carried out a comparative performance study between a PEM and a BPM using two dual chamber MFCs for Cr^{6+}removal from wastewater. Apart from these reported studies, the BPMs are not very popular for use in an MFC. However, they are mainly used in electrodialysis processes where water molecules dissociate into H^+ and OH^- and move in opposite directions (Logan 2008).

2.9.2.2 Porous Membranes

As compared to non porous membranes, these types of membranes are considered to be low cost alternatives. On the other hand, porous membranes are not very selective permeable to ions as compared to IEMs (Sangeetha et al., 2019).

The function of porous membranes is based on their pore size and porosity. H^+/OH^- ions and other large molecules are transferred directly through the electrolyte solution that has become embedded in the membrane's pores. The high porosity of these membranes is reflected by its low R_{int} value, which provides a great advantage in terms of its performance in MFCs. However, the porosity also undesirably affects the performance of the membranes such as its susaptability to oxygen and substrate crossover leading to biofouling (Leong et al. 2013; Scott et al., 2016). Based on the pore sizes, at least four types of porous membranes can be applied: UFM, MFM, CMs, and pore filter materials. Apart from these, glass wool has also been used as a porous membrane due to its low cost for wastewater treatment and bioelectricity generation.

2.9.2.2.1 Ultrafiltration Membranes (UFMs)

Ultrafiltration membranes are mainly used for treatment of water and waste water for separating particulate pollutants based on their molecular weights. The membrane permeable to cations and anions is also used in dual chamber MFCs. However, while using such membranes in MFCs oxygen diffusion and substrates, crossover is noticed, reflected by its low performance. Some UFMs evaluated based on their molecular weights were UFM-0.5K, UFM-1K, and UFM-3K; all presented a high R_{int} value (especially the UFM-0.5K) and low power density values of 5 mWm^{-2}. On the other hand, when an AEM and a CEM was used under similar condition, a better performance was observed (33–38 mWm^{-2}) (Sangeetha et al., 2019; Logan and Rabaey, 2012).

2.9.2.2.2 Microfiltration Membrane (MFMs)

Like the UFMs, MFMs are also largely used for waste water treatment and sludge separation. They are known to be stable for long-term operations; hence these attractive characteristics propose to use of these membranes in MFCs as separators. Due to its porosity, different types of ions and neutral molecules can pass through this membrane. Some examples of cheap MFMs that have functioned in MFCs are nylon mesh, cellulose filters, and polycarbonate filters. However, these membranes also suffer from similar problems as UFMs: O_2 diffusion, fuel crossover, and a high R_{int} (Sangeetha et al., 2019; Scott et al., 2016).

2.9.2.2.3 Ceramic Membranes (CMs)

In recent times, ceramic membranes are gaining popularity for use in MFCs due to its versatility and low cost of manufacturing (Behera et al., 2010a; Behera and Ghangrekar.,2010). The composition of the membranes can be customized based on porosity, and permeability giving it a hydrophilic character. The composition of membranes includes various cations such as Ca^{2+}, Mg^{2+}, K^{+}, Na^{+}, $H^{+,}$ and Al^{3+}, where the first four cations are referred to as the base cations, whereas the last two are referred to as acidic cations. The presence of acidic cations is important for proton transfer (Sangeetha et al., 2019).

Park and Zeikus (2003) first reported the use of ceramic membranes on a single chamber MFC obtaining a maximum power density of 788 mWm^{-2} using sewage sludge as the biocatalyst. Behera and Ghangrekar (2010) also demonstrated the potential of CMs as separators in MFCs, generating a volumetric power output of 16.8 Wm^{-3}. In the same year, (Behera et al. 2010a; Behera et al. 2010b) used commercial earthen pots to test their efficiency in pollutant removal and electricity production at different pH_s using WW from rice mills as substrate. Winfield et al. (2013a) investigated ceramic and terracotta materials' properties, focusing on the material's porosity, wall thickness and the hydration of the cathode. They showed that the cylindrical, clay-based MFCs produced significantly higher current and power. Compostable starch-based bags (BioBag) and ceramic were compared with a commercially available cation exchange membrane to understand the practical applicability in terms of cost and operational stability of eco-friendly materials. Despite the limited life span of around 8 months, the starch bags proved to be an effective material for the microbial environment (Winfield et al., 2013b). The performance of different low-cost CMs was recently compared against commercial PEM in MFC by Pasternak et al. (2016). The finding showcased the highest volumetric power of 6.93, 6.85, 4.98 and 2.60 mWm^{-3}obtained from pyrophyllite, earthenware, mullite, and alumina, respectively. Merino-Jimenez et al. (2017), (2019) report advances in using ceramic cylinders with different porosities.

The various studies showed that ceramic membranes can be used in MFCs as a viable low-cost, sustainable, and widely available alternative. Another advantage of CMs is that they provide the chassis of the MFCs, thus decreasing overall reactor cost. However, an increase in R_{int} in long-term usage in MFCs is one of the major concerns of this type of membrane.

2.9.2.2.4 Coarse-Pore Filters

Certain materials, such as porous fabrics, glass fiber, cellulose filters, agar–agar membranes, nylon mesh, and non-woven paper fabric filters, have been used as separators in Microbial Fuel Cells (MFCs) due to their property of not obstructing charge transfer, as well as their cost-effectiveness (Hernández-Flores et al., 2015; Hernández-Flores et al., 2016; Li et al., 2011; Choi et al., 2013). The use of these materials provides insulation and prevents short circuiting in MFCs. However, some of these materials have the drawback of higher oxygen and substrate exchange, leading to biofouling issues in the long term (Zhang et al., 2009).

Researchers have explored various separator materials to optimize MFC performance. Fan et al. (2007) used J-cloth fabric as a separator, reducing internal resistance (Rint) and achieving impressive volumetric power outputs in both batch and continuous flow modes. Canvas has also shown promise as an effective separator material for MFCs (Zhuang et al., 2009). Fiberglass has been found to be a superior material compared to J-cloth due to its non-degradability, as reported by Zhang et al. (2009).

Choi et al. (2013) used a non-woven paper fabric filter (NWF) as a separator in MFCs and compared its performance with a Nafion-117 separator. The MFC with NWF demonstrated higher power generation (1027 mWm-3) and showed stable cell performance for over 300 days, outperforming the Nafion-117 separator (609 mWm-3), which experienced biofilm formation and chemical precipitation on its surface.

2.9.3 Membrane-Less Microbial Fuel Cells

To address the limitations associated with using membranes in Microbial Fuel Cells (MFCs), researchers have explored membrane-less MFC configurations. The presence of nonporous or porous membranes in MFCs can lead to various issues such as increased internal resistance (Rint), biofouling, and decreased performance, while also significantly raising the setup costs (Logan, 2008; Du et al., 2008; Santoro et al., 2020; Leong et al., 2013). To overcome these challenges, the option of operating MFCs without membranes has been considered.

The concept of membrane-less MFCs was first explored by Liu & Logan (2004), who experimented with single-chamber MFCs using Nafion-117 and without a spacer between carbon electrodes, using domestic wastewater and glucose as substrates. Subsequent studies, such as those conducted by Santoro et al. (2013), reported the successful operation of membrane-less single-chamber MFCs with human urine as the substrate.

The presence of oxygen at the anode in MFCs competes for electrons generated during oxidation, while crossover fuel towards the cathode reduces the available anodic fuel load for anaerobic oxidation by electrochemically active bacteria. This crossover of fuel also harvests electrons through the external circuit of the system, affecting overall MFC performance (Logan and Regan 2006; Yang et al., 2010; Liu and Logan, 2004; Logan, 2008; Li et al., 2011; Liu et al., 2005). Overall, membrane-less MFCs offer a potential solution to overcome membrane-related challenges and enhance the efficiency of MFC systems for various applications.

2.10 Variations in PMFCs

2.10.1 PMFCs with vascular plants

Plants utilized in Plant Microbial Fuel Cells (PMFCs) are those that can thrive in waterlogged conditions, avoiding oxygen interruption in the anode and promoting anaerobic conditions. Different grass species, including both C3 and C4 plants, have been explored for PMFCs. C3 plants, like Glyceria maxima, utilize the Calvin cycle but suffer from energy loss during photosynthesis due to photorespiration. In contrast, C4 plants, such as Arundinella anomala, Spartina anglica, and Arundo donax, use the C4 pathway, which enhances their photosynthetic efficiency and rhizodeposition, making them more suitable for PMFCs (Chiranjeevi et al., 2019).

Salt-tolerant plants have also been studied for PMFCs, and the use of rice plants in paddy fields has shown promising results due to their flooded and anaerobic conditions. Marshy grasses, like Spartina anglica and Arundinella anomala, have demonstrated high biomass production, salt resistance, and adaptability, making them the most promising plants for PMFC applications (Helder et al., 2010). A. donax, although following the C3 pathway, exhibits high photosynthetic rates and rapid growth, making it an ideal energy crop for bioenergy production in PMFCs (Angelini et al., 2009).

The field of PMFCs has evolved significantly over the years, with a substantial increase in maximum power density yields. The combination of wetland plants and microbial fuel cells in CW-MFCs offers an innovative approach to wastewater treatment and bioenergy generation concurrently (Fang et al., 2013). The continued research and exploration of various plant species hold promising potential for the development of sustainable and efficient PMFC technology.

2.10.2 Constructed wetland-MFC (CW-MFC)

Wetlands, often considered as waste lands, are ecologically essential for sustaining diverse species and playing a significant role in carbon and nitrogen cycles. Unfortunately, wetland water pollution has become a concern due to uncontrolled waste dumping, harming aquatic life and biodiversity. Constructed wetland-based Plant Microbial Fuel Cells (CW-MFCs) offer a promising solution to combat water pollution, combining the advantages of MFCs and constructed wetlands.

In CW-MFCs, wastewater is received and then discharged in the presence of plants, which act as natural aerators (Xu et al., 2016; Fernandez et al., 2014). This hybrid system utilizes two biological approaches to degrade organic matter, benefiting from both MFCs and constructed wetlands (Corbella et al., 2014; Doherty et al., 2015). The system capitalizes on the redox gradient that naturally exists between the electrodes, depending on the influent flow direction and wetland depth (Doherty et al., 2015).

The key difference between a typical PMFC and a wetland-based PMFC is the source of Electron-Accepting Materials (EAMs). In PMFCs, EAMs are fed by rhizodeposits, whereas in CWs, EAMs are fed with both rhizodeposits and wastewater from treatment facilities (Strik et al., 2008; Doherty et al., 2015). This dual feeding system allows CW-MFCs to achieve both wastewater treatment and bioenergy generation simultaneously (Fang et al., 2013).

CW-MFCs generate power through microbial oxidation of organic matter released by aquatic plants via rhizodeposits (Timmers et al., 2012). Plant roots inserted into the cathode release O2 via the rhizosphere, enhancing CW-MFC performance (Dong et al., 2011). Additionally, plant biomass absorbs dissolved nutrients and heavy metals, providing the dual benefits of bioelectricity generation and wastewater treatment (Ju et al., 2014; Song et al., 2011).

The development of CW-MFCs has seen progress with various systems, such as vertical flow subsurface, horizontal subsurface flow, and surface flow with floating macrophytes, tested for treating different types of wastewater. Reported maximum power densities for CW-MFCs range from $35 mWm^{-2}$ to $184.75 \pm 7.50 mWm^{-3}$, demonstrating their potential as effective solutions for wastewater treatment and bioenergy production (Mohan et al., 2013; Yadav et al., 2012; Villasenor et al., 2013; Oon et al., 2017).

2.10.3 Macrophyte based PMFC system

Macrophytes are multicellular aquatic plants that grow submerged or floating through the surface of marine, estuarine or in fresh water ecosystems (Pieterse and Murphy,1990, O'Hare et.al., 2018). They form important parts of aquatic habitats as they provide shelter (Suren et.al., 2000), food (Gross et.al., 2001) or influence the hydrology and sediment dynamics of aquatic systems. The macrophyte based PMFC represents an ecologically engineered system in which macrophytes are used as the biota. Macrophytes manufacture their food via photosynthesis, where rhizodeposits and released exudates are used as supplemental organic matter (OM) in the CW-MFC for the generation of electricity (Liu et.al., 2013). The Macrophytes have major effects on the removal efficiencies of pollutants (N, P and heavy metals) as well as some communities of microbial (Vymazal, 2011). During photosynthesis, the O_2 excreted from macrophytes is used to construct efficient biocathodes for PMFCs (Zhao et.al., 2013a). Mohan et al. (2010) used submerged and emergent macrophytes with filter feeders to treat domestic sewage (DS) and fermented-distillery wastewater (FDW) from a hydrogen producing bioreactor, where the system could significantly remove COD, nitrate and turbidity. Later, a submerged and emergent macrophyte based sediment microbial fuel cell (SESMFC) was developed by Chiranjeevi et al. (2013) to generate bioelectricity with concurrent wastewater treatment. Similarly, Kokabian and Gude, (2013) tested different macrophyte-based Sediment-MFC with aquatic plants *Limnobium laevigatum*, *Pistia stratiotes,* and *Lemna minor* and obtained a volumetric power density of 80.22 mW m^{-3}.

The above has clearly demonstrated the potential of this aquatic species to generate bioelectricity and requires further research as to its future application. Finally, aquatic plants and algae proved to be efficient in treating both wastewater and fermented distillery wastewater.

2.10.4 Bryophyte based PMFC system

Bryophytes are plants known to be more tolerant to dehydration than other plants because of not having vascular tissues (Bombelli et al., 2016; Turetsky, 2003, Piyare et al., 2017). This unique physiological characteristic enables them to accumulate water and nutrients to survive in a wide range of adverse temperature and habitats. Bryophytes do not have roots; however, they possess hair-like rhizoids, which helps them to bind to different surfaces on which they grow. In this way, they stabilize soils and prevent nutrient loss by erosion. The bryophyte biomass can be a source of organic matter for microbes, if placed in the anode

chamber, thus influencing carbon/nitrogen cycling between the atmosphere and PMFC to generate power (Bombelli et al., 2016; Turetsky, 2003). The first bryophyte based PMFC was reported by Hubenova and Mitov (2011) using the forest moss *Dicranum montanum*. Similarly, a moss plant *Physcomitrella patens* was studied in a bryo PMFC by Bombelli et al. (2016) to generate bioelectricity and obtained a maximum power output of 6.7 ± 0.6mWm^{-2}.

2.10.5 Algae-based PMFC system

Algal-based Plant Microbial Fuel Cells (PMFCs), also known as photosynthetic PMFCs, are considered self-sustaining. Algae in a PMFC can serve as either an electron donor or acceptor, enabling carbon capture in the anode or cathode, respectively (Gajda et al., 2015). Algal biomass proves to be an efficient source for producing bioelectricity without any pre-treatment. When used with activated sludge or wastewater in the anode, algae become part of the wastewater microbiome, aiding in substrate oxidation and nutrient removal (Wang et al., 2010; Wu et al., 2014).

The use of algae in the anode chamber has shown comparable bioelectricity generation to other organic substrates like acetate. However, the complex substrate of microalgae with slow electron release can hinder its effective utilization in the anode. Pre-treatment techniques like sonication, thermal treatment, or microwave treatment can overcome this limitation and enhance algal biomass utilization (Rashid et al., 2013; Kondaveeti et al., 2014; Gadhamshetty et al., 2013).

While inorganic substitutes like acetate have been more effective in catalyzing substrate oxidation at the anode, algae have proven advantageous in the cathode chamber of MFCs. They reduce the requirement for aeration as they produce oxygen through photosynthesis, and after growth, harvested algal biomass can be used as biofuel, reducing net expenditure in wastewater treatment (Christenson and Sims, 2011; Arora et al., 2021). Algal biomass can also transport cations like ammonium ions, aiding biomass growth and potentially lowering the cost of MFC technology (Gajda et al., 2015).

Algal biofilms have been directly used at the cathode, but operating parameters like light intensity, algal biomass concentration, and carbon dioxide supply influence PMFC performance (Jadhav et al., 2019; Jadhav et al., 2017). Efficient ways of using wastewater for chlorella biofilm growth on stainless steel mesh cathodes have been explored (Ma et al., 2017). However, increasing biomass concentration under high light intensity may decrease coulombic efficiency (Bazdar et al., 2018). In general, higher light intensity and biomass concentration with high light/dark frequencies result in higher power density in PMFCs (Ma et al., 2017).

In conclusion, algal-based PMFCs offer promising opportunities for sustainable bioelectricity generation, with potential applications in wastewater treatment and cost-effective energy production. Nevertheless, optimizing operating parameters and exploring innovative approaches will be essential for realizing the full potential of algal-based PMFC technology.

2.11 Approaches for improving power generation in PMFCs

The practical appliaction of PMFC technology is a small step towards greener future. During the last decade, the advancement in MFC/PMFC technology has opened up new dimensions in the biotechnology field for sustainable and cost-effective bioelectricity generation. However, MFC/PMFCs generate very low voltages (Prasad and Tripathi, 2018b, Zabihallahpoor et al., 2015, Ren et al., 2012). In the case of PMFCs, it improves comparatively; however, the power generated by PMFCs are still insufficient to run any electronic device. To increase the output voltage, making large MFC/PMFC is ineffective because the voltage does not increase proportionally to the surface area of the anode. Over the last few years, many researchers have carried out various innovations in terms of modification and use of novel products to design and develop electrodes, membranes, reactor assembly, etc., to increase power generation (As explained in previous sections). In the proceess, overall cost of MFCs increases (Kim et al., 2007). MFC/PMFC have definitely evolved over these years; however, voltage generation is still very low.

2.11.1 PMFC stack as a power source

MFCs are complex biological systems, and building a reliable model is challenging. Also, the characteristics of the cell keep changing with the environmental and operational conditions affecting the overall power output. Due to thermodynamics limitations a single MFC generates a very low voltage ($\leq$ 1.16V), which is not enough to power electronic devices such as led lighting, cell phone charging, wireless sensors, etc. LED lighting and sensors, for example, require a voltage level between 3.0 V to 5.0 V. Therefore, connecting multiple MFCs in a series has a higher chance of voltage generation. Parallel and series connections to the MFC were designed to amplify the output voltage (approximately 3 V) for the sensor (Paule et al., 2015) and LED lighting (Prasad and Tripathi, 2018a; Mateo et al., 2018). A stack of six MFCs configured as a vertical cascade demonstrated higher power in parallel combination but exhibited considerable voltage loss under a series connection (Zhuang et al., 2012). The voltage of MFC may be enhanced by connecting some of MFC in parallel and series combinations, but this strategy requires a considerable number of MFC, which take up a wide area. Limited

studies have been performed on stacked MFCs, and most reported energy loss due to voltage reversal. Aelterman et al. (2006) studied the stacked MFC by connecting six MFC units (total volume of 1.9 L) in series and parallel with acetate as substrate. The reactor produced a power density of 51 Wm^{-3} when connected in series, while parallel connection demonstrated a power of 59 Wm^{-3}. The performance of individual MFC units showed unequal voltages, with some having negative voltage leading to voltage reversal. The other group designed a novel serpentine-type stack MFC using 40 tubular air cathodes with a total volume of 10 L with brewery wastewater as substrate. The stack produced a power of 4.1 Wm^{-3} when connected in series, whereas a series-parallel connection generated 1.5 times more power than series connection (Zhuang et al., 2012).

2.11.2 Development of power management system (PMS) for PMFCs

As mentioned previously, series connections of MFC amplify the voltage; however, the current output becomes low, and the cell goes through the problem of voltage reversal because of the nonlinear nature of MFCs. Parallel connections help maximize current output, but the overall operational voltage remains unamplified. Moreover, series-parallel combinations require a large number of MFC, which take up a wide area.

The main disadvantage of MFCs/PMFCs has low voltage with an irregular variation. The problem cannot be solved by stacking MFCs. Therefore, introducing a power management system (PMS) comes into play. It raises the voltage of the MFC to the voltage required for the electronic device. Each type of MFC has a different maximum efficiency operating point. Also, for MFCs to be compatible with conventional electronic components, some technical limitations must be overcome. In this regard, a programmable maximum power point tracking (MPPT) technology was applied along with DC-DC booster, capacitors and Voltage Complementary Oxide Semiconductor (LVCMOS) to optimize the power transfer from the PMFC.

Nevertheless, a very little or no study was reported for power enhancement using PMFC (Areej et al., 2014). Recently, a PMFC stack was established by installing multiple anodic chambers in an algal raceway pond. During long-term operation, the highest power density of the stack with capacitors reached 2.34 Wm^{-3}, which was 77% higher than that without capacitors (1.32 Wm^{-3}) (Yang et al., 2019). More study is required with P-MFC for successful commercialization of the technology.

2.12 Applications of PMFCs

The biggest highlighting fact about PMFCs is the continuous supply of organic matter at the anodes in the form of rhizodeposits for long-term in-situ bioelectricity generation (Deng et al., 2012). However, this new technology has the potential for diverse applications including few already in use, such as monitoring of environmental conditions (Donovan et al., 2008), biosensing of plant maturity (Chen et al., 2012), bioremediation of polluted waters, recovery of heavy metals from contaminated environments (Habibul et al.,2016), generation of bioelectricity from paddy field, rhizosphere and wetlands (Kouzuma et al., 2014). Beside, many related products are emerging (Strik et al., 2011; Gude et al., 2013). More than 50% of companies around the world are willing to consider sustainable solutions for their systems rather than paying more for non-sustainable solutions. Social acceptability of PMFCs will be very high in developing countries by decentralized application with more than 1.2 billion people worldwide accessing electricity production. The main applications of PMFCs are discussed below and represented in Fig.

2.12.1 PMFCs for wireless energy-neutral sensing

Wireless sensor networks (WSNs) and the Internet of Things (IoT) are among the hottest research topics in the 21st century and blooming industrial trends. They offer unique benefits in smart healthcare, smart homes, environmental monitoring, and security services. The 4th industrial revolution is expected to be driven by emerging concepts of artificial intelligence (AI) and IoT (Rapanyane and Sethole, 2020; Williams et al., 2017). In this context, Plant Microbial Fuel Cells (PMFCs) present a sustainable and green option for powering these systems for wireless sensing (Schievano et al., 2017; Rosa et al., 2021).

To apply PMFCs effectively for power applications, implementing a power management system becomes essential to provide continuous power for IoT-based sensors in a setup (Rosa et al., 2019). This is a significant development that enables battery-less operation of sensor nodes for 'temperature data acquisition' and 'cloud-based data storage.' For instance, Rosa et al. (2021) designed an array of PMFCs powered by Areca bamboo palm (*Dypsis lutesens*) to achieve long-range transmission from the sensor nodes with the help of a power management system.

The concept of 'floating gardens' was introduced by Schievano et al. (2017), combining sediment MFCs and PMFCs for accurate remote monitoring of water bodies. This setup generates power for remote environment sensors, facilitating data transmission for over a year.

Piyare et al. (2017) developed a wake-up radio receiver-based sensor that uses power from PMFCs for transmission and sensing applications. Additionally, Xu et al. (2021) introduced graphene quantum dots (GQDs) to catalyze PMFCs, enhancing the 5G and WiFi signal range. A continuous electrical power output of 320 mWm-2 was achieved by PMFCs, which serves as a power supply for IoT uses, such as Bluetooth connections, and also amplifies the 5G signal. Consequently, this technology has the potential to reduce the number of 5G base stations, saving square meter areas, and expanding the 5G signal range to remote areas without excessive infrastructure and power needs.

Thus, PMFCs show promise in powering low-energy devices like wireless sensors for IoT applications. They can be particularly useful for sensing applications in remote areas where providing a power source might be technically and economically challenging.

2.12.2 Flow-through system based PMFCs

PMFCs find practical applications in eco-electrogenic engineered systems (EES), such as FTS (Fishpond Treatment Systems), which aim to tackle pollution problems by treating wastewater and recycling in wetlands while simultaneously generating power (Chiranjeevi et al., 2013; Mohan et al., 2011; Lu et al., 2015; Moulin et al., 2001; Habibul et al., 2016). The integration of PMFCs into FTSs allows for the creation of artificial wetlands, mimicking natural ecosystems, which can be utilized to reconstruct wetlands while incorporating fishponds. This approach proves beneficial in restoring ecosystems that have been impacted by significant mining activities, rehabilitating lakes and rivers, and remediating hazardous waste sites. Furthermore, FTS interventions, as part of EES, offer ecologically sound solutions to modify and improve deteriorating existing ecosystems, thereby addressing various environmental concerns (Mitsch and Jorgensen, 1989).

2.12.3 Ecological floating bed for pollutant removal

PMFCs have been employed in Ecological floating bed (EFB) due to its reputation of green economy, convenience, and efficiency in treating diverse eutrophic landscape wastewater. The application has been proven to be eco-friendly with high organics removal and stable power generation capabilities than other treatment systems (Habibul et al., 2016). PMFC technology was also employed in low-cost wastewater treatment units (Lu et al., 2015). An easily constructed low-cost miniature ecological system embedded with a P-MFC showed maximum chemical oxygen demand (COD), color, and turbidity removal Chiranjeevi et al.,

2013; Strik et al., 2008). A variety of nutrients from the water such as C, N, P can be removed by plants through the process of water self-purification, plant uptake, microbial assimilation, adsorption-sedimentation and other pathways. Under the comprehensive actions of various pathways, the eutrophication can be avoided by decreasing the pollutant concentration in water and inhibiting the growth of phytoplankton (Wang et al., 2020). There are many researches focused on the selection of plant species in EFB. A variety of plants such as windmill grass, goldfish algae, water hyacinth and water spinach were used by Yang et al., (2021) for nitrogen removal and bioelectricity generation.

2.12.4 PMFCs in Agriculture

Agriculture is the backbone of the Indian economy and the primary earning sector of most Indians in rural India. Sustaining a fast increasing world population with present-day agricultural practices will be a task looking for limited water and land resources. Science and technology have a more significant role in next-generation sustainable agriculture. Continuous monitoring of plant health and its requirements (water, soil, nutrients, pH, and temperature) is vital for smart farming (Jayaraman et al., 2016). Apart from traditional income from agricultural products, farmers can generate revenue by producing electricity during cultivation processes by applying PMFC technology as a decentralized system.

2.12.4.1 PMFCs for next-generation farming

Next-generation farming stands to be revolutionized by the implementation of Plant Microbial Fuel Cells (PMFCs), which can serve as biosensors and power sources for wireless embedded electronics. These PMFC-powered sensors have the capability to continuously monitor environmental parameters and plant health. A study by Brunelli et al. (2016) explored a PMFC-powered wireless sensor that can monitor parameters like light intensity, soil moisture, and plant physiological activities, while sending the data remotely. This advancement allows Wireless Sensor Networks (WSNs) to monitor, acquire, and store precise agricultural data, aiding in optimizing irrigation practices and providing comprehensive crop production requirements for precision agriculture (Srbinovska et al., 2017).

PMFCs harness power from root exudates, directly correlated with photosynthetic activity, making them highly efficient and energy-neutral sensors (Kaku et al., 2008). Additionally, PMFCs find application in monitoring water content in farming setups, facilitating efficient water resource utilization and preventing wastage (Kuleshova and Gall,

2021). By integrating PMFCs into IoT-based sensor networks, smart and connected farming practices (Mat et al., 2016) become achievable, further contributing to sustainable food production to meet the growing demands of the global population (Tapia et al., 2017; Yoon et al., 2018; Stafford, 2000). This integration of PMFC technology into modern agriculture has the potential to revolutionize farming practices, leading to more efficient resource utilization and improved food production for a rapidly growing world population.

2.12.4.2 Hydroponic cultivation system

Hydroponics-based vegetable cultivation is recognized as an advanced form of agricultural system gaining popularity worldwide due to its resource-efficient nature and production of high-quality food. This system utilizes nutrient-laden water to nourish plants, eliminating the need for soil and relying on natural precipitation. The hydroponic approach maximizes agricultural efficiency in limited land space, making it suitable for integration into energy harvesting systems (Lee and Miller, 2018). By combining hydroponics with energy harvesting, aquaponics can be achieved, integrating fish farming with soilless vegetable cultivation.

Yadav et al. (2020) integrated a drip hydroponics-microbial fuel cell (MFC) system design with multiple small reactors using domestic wastewater and cocopeat as a support material for *Cymbopogon citratus*. Cocopeat, known for its high water retention ability, can hold up to 8-9 times its weight in water, making it ideal for the hydroponic system. Additionally, its natural rooting hormones and anti-fungal properties make it a valuable element in this setup. The integrated system not only achieved maximum power densities of 31.88 mWm-2 but also efficiently removed pollutants from wastewater, providing a sustainable solution.

Similarly, Paucer and Sato (2022) designed a hydroponic-MFC system to remove and recover nutrients (phosphorus, P, and nitrogen, N) from wastewater while simultaneously producing edible plants. The MFC-Hyp system they developed exhibited a remarkable power density of 250.7 mWm^{-2}. This innovative system efficiently recovers nutrients from wastewater, enabling the growth of edible plants and offering ease of operation, thereby showing potential for large-scale application.

Therefore, hydroponics coupled with microbial fuel cells presents an environmentally friendly and efficient approach for vegetable cultivation, wastewater treatment, and energy

generation, making it a promising solution for sustainable agriculture and resource management.

2.12.4.3 Paddy field PMFC

The cultivation of rice as one of the major food products has opened up possibilities for a dual application of rice-based Plant Microbial Fuel Cells (PMFCs), which have been extensively studied in numerous works (Takanezawa et al., 2010; Moqsud et al., 2015; Ueoka et al., 2016; Srivastava et al., 2018; Chen et al., 2011; Kouzuma et al., 2014). These PMFCs have proven to be successful in not only providing bioelectricity but also in reducing methane gas emissions when installed in wetlands and paddy fields (Wetser et al., 2015; Arends et al., 2014).

The unique anoxic-oxic interface created at the soil/sediment-water interface and the presence of rhizodeposits in the paddy ecosystem create suitable conditions for the installation and operation of PMFCs, as demonstrated by Kiran et al. in 2020. This has led to the development of innovative applications, such as floating gardens based on O. sativa-based PMFCs, which were showcased at the EXPO2015 world exposition in Milan. These floating gardens not only powered the supply of environmental sensors and data transmitters but also showcased the potential of PMFCs in powering other devices. Additionally, PMFCs based on marshy grasses, particularly S. anglica, have been equally employed for similar purposes (Wetser et al., 2015).

Further advancements in PMFC technology have been made by researchers at Wageningen University, who have been experimenting with various new tubular designs. They have successfully applied PMFCs in diverse environments, including wetland systems, marshes, river deltas, and floodplains, enabling power generation and facilitating multifunctional commercial use of land. This initiative has led to the creation of a spin-off company named "Plant-e," which was established in 2013 to explore the commercial potential of these PMFC applications.

2.12.4.4 Green rooftop PMFC

Green rooftop PMFC combines the advantages of green rooftops and power generation, restoring green cover, and increasing biodiversity while producing electricity. This concept is getting popular nowadays, which can be easily transformed in to efficient power house. It works well with grass species covering extensive areas and does not necessarily require a membrane, making it cost-effective and productive. It makes effective use of a space rooftop

that is otherwise not used productively. The green electricity roof offers numerous benefits, including aesthetics, rainwater retention, biodiversity preservation, improved oxygen content, insulation, and reduced urban temperatures (Borker et al., 2017; Sarma and Mohanty 2019). The rooftop PMFCs installed by Helder et al., (2013) at Wageningen University, The Netherlands was used to test the resilience in harsh winter conditions. Tapia et al. (2017) used green rooftop PMFC to test its bio-sensing capabilities. The study proved to be an efficient biosensor for estimation of water content making PMFCs suitable for semi-arid ecosystems. The technology is weather-independent, generating electricity day and night with minimal maintenance. With further improvements, it holds potential for year-round electricity production (Helder et al., 2013b). The application of PMFCs is represented schematically in Fig.2.8.

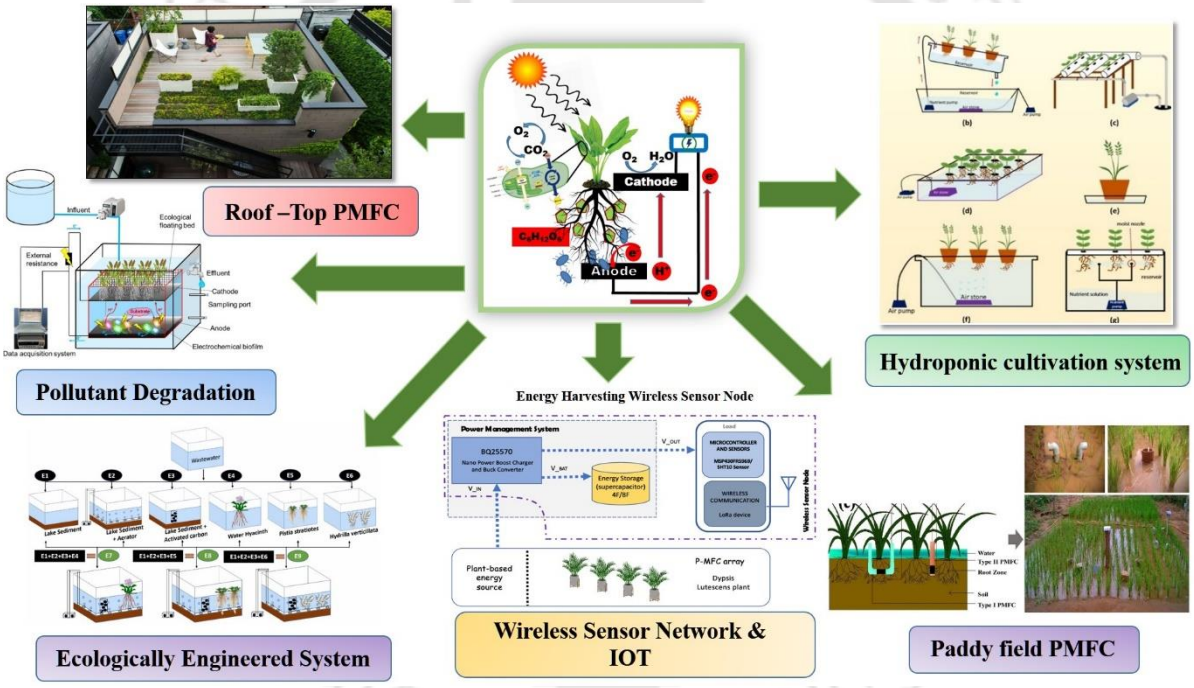

Fig.2.8 Application of Plant Microbial fuel cells

2.13 Knowledge Gap

The literature survey above highlights a significant number of studies focused on the development of Microbial Fuel Cells (MFCs); however, the technology of Plant Microbial Fuel Cells (PMFCs) remains relatively unexplored, with untapped potential. While a considerable portion of PMFC-based research has concentrated on bioelectricity generation from wetland and paddy-based plants, there is a scarcity of reports on PMFCs operated with indoor plants.

Indoor air pollution is a pressing global issue, and NASA recommends the use of indoor plants to improve air quality by removing toxic substances and absorbing CO_2. As these indoor plants are easy to grow, research is now exploring their capacity for bioelectricity generation alongside their environmental benefits.

Enhancing the design of PMFC reactors is essential for improving performance, efficiency, and operational ability while reducing maintenance requirements. So far, only two types of reactors, namely flat-plate and tubular systems, have been reported, leaving ample room for further improvement.

The high operational costs of MFC technology, including nutrient requirements, expensive chemical catalysts, electrode modifications, and commercially available membranes, make the overall system unsustainable. A cost-effective approach is necessary for the long-term sustainable bioelectricity generation of PMFCs, involving the development of affordable electrodes and membranes.

Although the development of bio-cathodes has been a crucial achievement in MFC research, their implementation in PMFC studies has been limited. Exploring the performance of microalgal bio-cathodes in PMFCs could be beneficial, as plants and microalgae share similar photosynthetic requirements. The use of membranes has been underrepresented in the literature due to the presence of soil in PMFCs. However, their addition can physically separate the anode and cathode, creating anaerobic and aerobic environments on each side, leading to improved overall cell performance.

Long-term operational behavior of PMFCs without external nutrient input is also an area with limited research, indicating the need for continuous improvement for sustainable operation. Currently, practical applications of PMFCs are primarily limited to low-power requirements in sensors and IoT-WSN devices. Nevertheless, the potential for diversifying its applicability through efficient power management systems (PMS) and powering more advanced electronic devices remains promising. Overall, exploring these areas can unlock the full potential of PMFC technology in various environmental and technological applications.

2.14 Research Hypothesis

Plant microbial fuel cell has the potential to become an alternate form of renewable and sustainable energy. The thesis work is targeted to improve the performance and power generation ability from indoor PMFCs by incorporating the following:

- Identify best performing indoor plants in a PMFC by studying different operating parameters.
- Enhancing proton transfer ability across chambers with the incorporation of novel low cost ceramic membrane, thereby finding an alternative to expensive commercial nafion membrane.
- Design and develop modern and modular PMFC setup for ease of operation.
- Develop a power management system to store energy from PMFCs under low power output to be able to utilize to run electronic devices.

2.15 Objectives

This research aims to design and develop a Plant Microbial Fuel cell for sustainable bioelectricity generation. Throughout the study, the following objectives were established and accomplished.

- Design, develop and characterize different plant-based microbial fuel cells.
- Studies on the effect of different operating parameters on performance of plant microbial fuel cells.
- Performance evolution studies considering bacterial and microalgal bio cathode and identification of the microbial community present in PMFC.
- Development and comprehensive characterization of low-cost hybrid clay based ceramic membrane for power enhancement in plant based microbial fuel cells.
- Development of power management system for energy harvesting from PMFCs to run small electronic devices.

References

Aelterman P, Rabaey K, Pham HT, Boon N, Verstraete W (2006) Continuous Electricity Generation at High Voltages and Currents Using Stacked Microbial Fuel Cells. Environ. Sci. Technol. 40: 3388–3394

Angelini LG, Ceccarini L, Nassi o Di Nasso N, Bonari E (2009) Comparison of Arundo donax L. and Miscanthus x giganteus in a long-term field experiment in Central Italy: analysis of productive characteristics and energy balance. Biomass and Bioenergy 33: 635–643

Areej A, AL-Janabi J, Saad F (2014) Microbial Fuel Cell (MFC) Technique for Electricity Production. Lap Lambert Academic Publishing GmbH KG

Arends JB, Speeckaert J, Blondeel E (2014) Greenhouse gas emissions from rice microcosms amended with a plant microbial fuel cell. Applied Microbiology and Biotechnology 98: 3205–3217

Arora K, Kaur P, Kumar P, Singh A, Patel S, Li X, Yung YU, Bhatia SK, Kulshrestha S (2021) Valorization of wastewater resources into biofuel and value-added products using microalgal system. Front. Energy Res. 9:646571

Arun S, Sinharoy A, Pakshirajan K, Lens PNL (2020) Algae based microbial fuel cells for wastewater treatment and recovery of value-added products. Ren. Sust. Energy Rev. 132: 110041

Atoche A, Becerra-Nunez G (2021) Arrays of plant microbial fuel cells for implementing self-sustainable wireless sensor networks. IEEE Sensor. J. 21(2).

Ayyappan CS, Bhalambaal VM, Kumar S (2018) Effect of Biochar on Bio-electrochemical Dye degradation and Energy Production. Bioresour. Technol. 251:65-70.

Bazdar E, Roshandel R, Yaghmaei S, Mardanpour MM (2018) The effect of different light intensities and light/dark regimes on the performance of photosynthetic microalgae microbial fuel cell. Bioresour Technol. 261: 350-360.

Behera M, Jana PS, Ghangrekar MM (2010a) Performance evaluation of low cost microbial fuel cell fabricated using earthen pot with biotic and abiotic cathode. Bioresour. Technol. 101: 1183–1189

Behera M, Jana PS, More TT, Ghangrekar MM (2010b) Rice mill wastewater treatment in microbial fuel cells fabricated using proton exchange membrane and earthen pot at different pH. Bioelectrochemistry 79: 228–233

Behera M, Ghangrekar MM (2010) Electricity generation in low cost microbial fuel cell made up of earthenware of different thickness. Water Sci. Technol. 64: 2468–2473.

Bhowmick GD, Das S, Verma HK, Neethu B, Ghangrekar MM (2019) Improved performance of microbial fuel cell by using conductive ink printed cathode containing Co_3O_4 or Fe_3O_4. Electrochim. Acta 310: 173–183

Bejjanki D, Muthukumar K, Radhakrishnan TK, Alagarsamy A, Pugazhendhi A, Naina Mohamed S (2021) Simultaneous bioelectricity generation and water desalination using Oscillatoria sp. as biocatalyst in photosynthetic microbial desalination cell. Sci. Total Environ. 754: 142215

Bombelli P, Dennis RJ, Felder F, Cooper MB, Madras Rajaraman Iyer D, Royles J, Harrison ST, Smith AG, Harrison CJ, Howe CJ (2016) Electrical output of bryophyte microbial fuel cell systems is sufficient to power a radio or an environmental sensor. R Soc Open Sci. 3(10):160249

Bond DR, Lovley DR (2003) Electricity production by *Geobacter sulfurreducens* attached to electrodes. Appl Environ Microbiol 69(3):1548–55

Borker M, Suchithra TV, Srinivas M, Jayaraj S (2017) Sustainable bioelectricity generation from living plants. In: Patra, J.K., Vishnuprasad, C.N., Das, G. (Eds.), Microbial Biotechnology. Springer, Singapore 399–412

Brunelli D, Tosato P, Rossi M (2016) Flora health wireless monitoring with plant-microbial fuel cell. Procedia Eng. 168: 1646–1650

Burkitt R, Whiffen TR, Yu EH (2016) Iron phthalocyanine and MnOx composite catalysts for microbial fuel cell applications. Appl. Catal. B Environ. 181: 279-288

Caizan-Juanarena L, Sleutels T, Borsje C, Ter Heijne A (2020) Considerations for application of granular activated carbon as capacitive bioanode in bioelectrochemical systems. Renew. Energy. 157: 782–792

Cao Y, Mu H, Liu W, Zhang R, Guo J, Xian M Liu H (2019) Electricigens in the anode of microbial fuelcells: pure cultures versus mixed communities. Microb. Cell Fact. 18:39

Catal T, Bermek H, Liu H (2009) Removal of selenite from wastewater using microbial fuel cells. Biotechnol. Lett. 31: 1211–1216

Chae KJ, Choi M, Ajayi FF, Park W, Chang IS, Kim IS (2008) Mass transport through a proton exchange membrane (Nafion) in microbial fuel cells. Energy Fuels 22: 169–176

Chakraborty I, Sathe SM, Dubey BK, Ghangrekar MM (2020) Waste-derived biochar: Applications and future perspective in microbial fuel cells. Bioresour. Technol. 312: 123587

Chen Z, Huang YC, Liang JH, Zhao F, Zhu YG (2012) A novel sediment microbial fuel cell with a biocathode in the rice rhizosphere. Bioresour. Technol.108: 55–59

Cheng S, Liu H, Logan BE (2006) Power densities using different cathode catalysts (Pt and CoTMPP) and polymer binders (Nafion and PTFE) in single chamber microbial fuel cells. Environ. Sci.Technol. 40 (1): 364–369

Christenson L, Sims R (2011) Production and harvesting of microalgae for wastewater treatment, biofuels, and bioproducts. Biotechnol. Adv. 29: 686-702

Christgen B, Scott K, Dolfing J, Head IM, Curtis TP (2015) An evaluation of the performance and economics of membranes andseparators in single chamber microbial fuel cells treating domestic wastewater. PLoS ONE 10: 0136108

Chi Z, O'Fallon JV, Chen S (2011) Bicarbonate produced from carbon capture for algae culture. Trends Biotechnol. 29: 537-541

Chiranjeevi P, Chandra R, Mohan SV (2013) Ecologically engineered submerged and emergent macrophyte based system: an integrated eco-electrogenic design for harnessing power with simultaneous wastewater treatment. Ecol. Eng. 51: 181-190

Chiranjeevi P, Yeruva DK, Kumar AK, Mohan SV, Varjani S (2019) Chapter 3.8 -plant-microbial fuel cell technology. In: Mohan SV, Varjani S, Pandey A (Eds.), Microbial Electrochemical Technology, Biomass, Biofuels and Biochemicals. Elsevier 549–564

Choi S, Kim JR, Cha J, Kim Y, Premier GC, Kim C (2013) Enhanced power production of a membrane electrode assembly microbial fuel cell (MFC) using a cost effective poly [2,5-benzimidazole] (ABPBI) impregnated non-woven fabric filter. Bioresour. Technol. 128: 14–21

Chu N, Zhang L, Hao W, Liang Q, Jiang Y, Zeng RJ (2021) Rechargeable microbial fuel cell based on bidirectional extracellular electron transfer. Bioresour. Technol. 329: 124887.

Clauwaert P, Rabaey K, Aelterman P, De Schamphelaire L, Ham TH, Boeckx P, Boon N, Verstraete W (2007) Biological denitrification in microbial fuel cells. Environ. Sci. Technol. 41 (9): 3354−3360

Commault AS, Laczka O, Siboni N, Tamburic B, Crosswell JR, Seymour JR, Ralph PJ (2017) Electricity and biomass production in a Bacteria-Chlorella based microbial fuel cell treating wastewater. Journal of Power Sources 356: 299-309

Corbella C, Garfi M, Puigagut J (2014) Vertical redox profiles in treatment wetlands as function of hydraulic regime and macrophytes presence: surveying the optimal scenario for microbial fuel cell implementation. Sci Total Environ. 470: 754–8

Cui Y, Rashid N, Hu N, Rehman MSU, Han JI (2014) Electricity generation and microalgae cultivation in microbial fuel cell using microalgae-enriched anode and biocathode. Energy Conv. Manag. 79: 674–680

Das S, Ghangrekar MM (2020) Tungsten oxide as electrocatalyst for improved power generation and wastewater treatment in microbial fuel cell. Environ. Technol. 41 (19): 2546–2553

De Schamphelaire L, Cabezas A, Marzorati M, Friedrich MW, Boon N, Verstraete W (2010) Microbial community analysis of anodes from sediment microbial fuel cells powered by rhizodeposits of living rice plants. Appl Environ Microbiol. 76(6)

Deepika J, Meignanalakshmi S, Thilagaraj RW (2015) The optimization of parameters for increased electricity production by a microbial fuel cell using rumen fluid. International Journal of Green Energy 12 (4):333–38

Deng H, Wu YC, Zhang F, Huang ZC, Chen Z, Xu HJ, Zhao F (2014) Factors affecting the performance of single-chamber soil microbial fuel cells for power generation. Pedosphere 24: 330–338

Deng H, Chen Z, Zhao F (2012) Energy from plants and microorganisms: progress in plant–microbial fuel cells. Chem. Sus. Chem. 5(6): 1006–11

Der Kuan Y, Ciou CW, Shen MY, Wang CK, Fitriani RZ, Lee CY (2021) Bipolar plate design and fabrication using graphite reinforced composite laminate for proton exchange membrane fuel cells. Int. J. Hydrog. Energy. 46: 16801–16814

Di Lorenzo M, Scott K, Curtis TP, Head IM (2010) Effect of increasing anode surface area on the performance of a single chamber microbial fuel cell. Chem. Eng. J. 156 (1): 40–48

Doherty L, Zhao Y, Zhao X, Hu Y, Hao X, Xu L (2015a) A review of a recently emerged technology: constructed wetland–microbial fuel cells. Water Res 85: 38–45

Doherty L, Zhao X, Zhao Y, Wang W (2015b) The effects of electrode spacing and flow direction on the performance of microbial fuel cell-constructed wetland. Ecol Eng. 79: 8–14

Dong C, Zhu W, Zhao Y, Gao M (2011) Diurnal fluctuations in root oxygen release rate and dissolved oxygen budget in wetland mesocosm. Desalination 272(1–3): 254–8

Donovan C, Dewan A, Heo D, Beyenal H (2008) Batteryless, wireless sensor powered by a sediment microbial fuel cell. Environ Sci Technol. 42(22): 8591–6

Dou H, Niu G (2020) Plant responses to light. In: Plant Factory. Kozai T, Niu G, Takagaki M, Eds.; Elsevier: Amsterdam, The Netherlands,153–166

Du Z, Li Q, Tong M, Li S, Li H (2008) Electricity generation using membrane-less microbial fuel cell during wastewater treatment. Chin. J. Chem. Eng. 16:772–777

Du F, Xie B, Dong W, Jia B, Dong K, Liu H (2011) Continuous flowing membrane-less microbial fuel cells with separated electrode chambers. Bioresour. Technol. 102: 8914–8920

Dumitru A, Scott K (2016) Anode materials for microbial fuel cells. In: Scott K, Yu EH (Eds.), Microbial Electrochemical and Fuel Cells. Woodhead Publishing 117–152

Elakkiya E, Niju S (2020) Simultaneous treatment of lipid rich ghee industry wastewater and power production in algal biocathode based microbial fuel cell. Energy Sour. A: Recovery, Utilizat. Environ. Effects: 1–11

ElMekawy A, Hegab HM, Losic D, Saint CP, Pant D (2017) Applications of graphene in microbial fuel cells: the gap between promise and reality. Renew. Sustain. Energy Rev. 72: 1389–1403

El-Naggar MY, Wanger G, Leung KM, Yuzvinsky TD, Southam G, Yang J, Lau WM, Nealson KH, Gorby YA (2010) Electrical transport along bacterial nanowires from Shewanella oneidensis MR-1. PNAS 107: 18127–18131

Enamala MK, Dixit R, Tangellapally A, Singh M, Dinakarrao SMP, Chavali M, Pamanji SR, Ashokkumar V, Kadier A, Chandrasekhar K (2020) Photosynthetic microorganisms (Algae)

mediated bioelectricity generation in microbial fuel cell: concise review. Environ. Tech. Innov. 19: 100959

Erable B, Duteanu N, Kumar SMS, Feng Y, Ghangrekar MM, Scott K (2009) Nitric acid activation of graphite granules to increase the performance of the non-catalyzed oxygen reduction reaction (ORR) for MFC applications. Electrochemistry Communications 11 (7):1547–49

Fan Y, Hu H, Liu H (2007) Enhanced coulombic efficiency and power density of air-cathode microbial fuel cells with an improved cell configuration. J. Power Sources 171: 348–354

Fang Z, Song HL, Cang N, Li XN (2013) Performance of microbial fuel cell coupled constructed wetland system for decolorization of azo dye and bioelectricity generation. Bioresour Technol. 144:165–71

Feng Y, Yang Q, Wang X, Logan BE (2010) Treatment of carbon fiber brush anodes for improving power generation in air–cathode microbial fuel cells J. Power Sources, 195 (7): 1841-1844

Fernandez F, Lobato J, Villasenor J, Rodrigo M, Canizares P (2014) Microbial fuel cell: the definitive technological approach for valorizing organic wastes. Environment, Energy and Climate Change I. Springer; 287–316

Fu L, Wang H, Huang Q, Song TS, Xie J (2020) Modification of carbon felt anode with graphene/Fe_2O_3 composite for enhancing the performance of microbial fuel cell. Bioproc. Biosyst. Eng. 43 (3): 373–381

Gadhamshetty V, Belanger D, Gardiner CJ, Cummings A, Hynes A (2013) Evaluation of Laminaria based microbial fuel cells (LbMs) for electricity production. Bioresour Technol. 127: 378-385

Gadkari S, Fontmorin JM, Yu E, Sadhukhan J (2020) Influence of temperature and other system parameters on microbial fuel cell performance: Numerical and experimental investigation. Chem. Eng. J. 388: 124176

Gajda I, Greenman J, Melhuish C, Ieropoulos I (2015) Self-sustainable electricity production from algae grown in a microbial fuel cell system. Biomass and Bioenergy 82: 87-93

Geetanjali Rani R, Sharma D, Kumar S (2019) Optimization of operating conditions of miniaturize single chambered microbial fuel cell using $NiWO_4$/graphene oxide modified anode for performance improvement and microbial community dynamics. Bioresour. Technol. 285: 121337

Gil GC, Chang IS, Kim BH, Kim M, Jang JK, Park HS, Kim HJ (2003) Operational parameters affecting the performannce of a mediator-less microbial fuel cell. Biosens. Bioelectron. 18: 327-334

Golub N, Levtun I (2016) Impact of sound irradiation on Chlorella vulgaris cell metabolism. East. Eur. J. Enter. Techn. 10: 27–31

Gomathy M, Sabarinathan KG, Subramanian KS, Ananthi K, Kalaiyarasi V, Jeyshri M, Dutta P (2021) Rhizosphere: Niche for Microbial Rejuvenation and Biodegradation of Pollutants. Springer, Singapore 1–22

Gorby YA, Yanina S, McLean JS, Rosso KM, Moyles D, Dohnalkova A, Beveridge TJ, Chang IS, Kim BH, Kim KS, Culley DE, Reed SB, Romine MF, Saffarini DA, Hill EA, Shi L, Elias DA, Kennedy DW, Pinchuk G, Watanabe K, Ishii S, Logan B, Nealson KH, Fredrickson JK, (2006) Electrically conductive bacterial nanowires produced by *Shewanella oneidensis* strain MR-1 and other microorganisms. PNAS 103: 11358–11363

Govender N, Cleary PW, Kiani-Oshtorjani M, Wilke DN, Wu CY, Kureck H (2020) The effect of particle shape on the packed bed effective thermal conductivity based on DEM with polyhedral particles on the GPU. Chem. Eng. Sci. 219: 115584

Gouveia L, Neves C, Sebastião D, Nobre BP, Matos CT (2014) Effect of light on the production of bioelectricity and added-value microalgae biomass in a Photosynthetic Alga Microbial Fuel Cell. Biores.Tech. 154: 171–177

Gross EM, Johnson RL, Hairston Jr., NG (2001) Experimental evidence for changes in submersed macrophyte species composition caused by the herbivore Acentria ephemerella (Lepidoptera). Oecologia 127(1):105–14

Gross J, Alviso CT, Pekala RW (1996) Structural evolution in carbon aerogels as a function of precursor material and pyrolysis temperature. MRS Online Proceedings Library Archive 431

Gude V, Kokabian B, Gadhamshetty V (2013) Beneficial bioelectrochemical systems for energy, water, and biomass production. JMBT 6:2

Guo D, Zhuo YZ, Lai AN, Zhang QG, Zhu AM, Liu QL (2016) Interpenetrating anion exchange membranes using poly (1-vinylimidazole) as bifunctional crosslinker for fuel cells. J. Membr. Sci. 518: 295–304

Guo F, Luo H, Shi Z, Wu Y, Liu H (2021) Substrate salinity: A critical factor regulating the performance of microbial fuel cells, a review. Sci. Total Environ. 763: 143021

Habibul N, Hu Y, Wang YK, Chen W, Yu HQ, Sheng GP (2016) Bioelectrochemical chromium (VI) removal in plant-microbial fuel cells. Environ. Sci. Technol. 50(7): 3882-3889

HaoYu E, Cheng S, Scott K, Logan B (2007) Microbial fuel cell performance with non-Pt cathode catalysts. J. Power Sources 171 (2): 275–281

Harnisch F, Aulenta F, Schroder U (2011) Microbial fuel cells and Bioelectrochemical systems: Industrial and Environmental Biotechnologies based on extracellular electron transfer. Comprehensive biotechnology (Second Edition) 6: 643-659

He J, Xin X, Pei Z, Chen L, Chu Z, Zhao M, Wu X Li B Tang X, Xiao X (2021) Microbial profiles associated improving bioelectricity generation from sludge fermentation liquid via microbial fuel cells with adding fruit waste extracts. Bioresour. Technol. 337: 125452

Heijne AT, Hamelers HVM, De Wilde V, Rozendal RA, Buisman CJ (2006) A Bipolar membrane combined with ferric iron reduction as an efficient cathode system in microbial fuel cells. Environ. Sci. Technol. 40: 5200–5205

Helder M, Strik DP, Hamelers HV, Kuhn AJ, Blok C, Buisman CJN (2010) Concurrent bioelectricity and biomass production in three plant-microbial fuel cells using *Spartina anglica*, *Arundinella anomala* and *Arundo donax*. Bioresource Technology 101: 3541–3547

Helder M, Strik DPBTB, Hamelers HVM, Kuijken RCP, Buisman CJN (2012a) New plant-growth medium for increased power output of the Plant-Microbial Fuel Cell, Bioresource Technology 104: 417–423

Helder M, Strik DP, Hamelers HV, Buisman CJ (2012b) The flat-plate plant-microbial fuel cell: the effect of a new design on internal resistances. Biotechnol. Biofuels 5:70.

Helder M, Chen WS, Harst EJ (2013a) Electricity production with living plants on a green roof: environmental performance of the plant microbial fuel cell. Biofuels, Bioproducts and Biorefining 7: 52–64

Helder M, Strik DP, Timmers RA, Raes SMT, Hamelers HVM, Buisman CJN (2013b) Resilience of roof-top plant-microbial fuel cells during Dutch winter. Biomass Bioenergy 51: 1–7

Hernandez-Flores G, Poggi-Varaldo HM, Romero-Castanon T, Solorza-Feria O, Rinderknecht-Seijas N (2017) Harvesting energy from leachates in microbial fuel cells using an anion exchange membrane. Int. J. Hydrogen Energy 42: 30374–30382

Hernandez-Flores G, Poggi-Varaldo HM, Solorza-Feria O (2016) Comparison of alternative membranes to replace high cost Nafion ones in microbial fuel cells. Int. J. Hydrogen Energy 41: 23354–23362

Hernandez-Flores G, Poggi-Varaldo HM, Solorza-Feria O, Romero-Castanon T, Rios-Leal E, Galindez-Mayer J, Esparza-García F (2015) Batch operation of a microbial fuel cell equipped with alternative proton exchange membrane. Int. J. Hydrogen Energy 40:17323–17331

Hindatu Y, Annuar MSM, Gumel AM (2017) Mini-review: anode modification for improved performance of microbial fuel cell. Renew. Sustain. Energy Rev. 73: 236–248

Holmer M, Gribsholt B, Kristensen E (2002) Effects of sea level rise on growth of *Spartina anglica* and oxygen dynamics in rhizosphere and salt marsh sediments. Marine Ecology Progress Series 225: 197–204

Huang L, Li X, Ren Y, Wang X (2016) In-situ modified carbon cloth with polyaniline/ graphene as anode to enhance performance of microbial fuel cell. Int. J. Hydrogen Energy 41 (26): 11369–11379

Huang L, Regan JM, Quan X (2011) Electron transfer mechanisms, new applications, and performance of biocathode microbial fuel cells. Bioresource Technology 102: 316–323

Hubenova Y, Mitov M (2011) Bacterial mutalism in the mosses roots applicable in Bryophyta-microbial fuel cell. Commun Agric Appl Biol Sci.76(2):63

Jadhav DA, Deshpande PA, Ghangrekar MM (2017) Enhancing the performance of single-chambered microbial fuel cell using manganese/palladium and zirconium/palladium composite cathode catalysts. Bioresource Technology 238: 568–574

Jadhav DA, Mungray AK, Arkatkar A, Kumar SS (2021) Recent advancement in scaling-up applications of microbial fuel cells: From reality to practicability. Sustain. Energy Technol. 45, 101226

Jadhav DA, Neethu B, Ghangrekar MM (2019) Microbial carbon capture cell: advanced bio-electrochemical system for wastewater treatment, electricity generation and algal biomass production. In: Gupta, S.K., Bux, F. (Eds.), Application of Microalgae in Wastewater Treatment. Springer International Publishing, Cham. 317–338

Jayaraman P, Yavari A, Georgakopoulos D, Morshed A, Zaslavsky A (2016) Internet of things platform for smart farming: experiences and lessons learnt, Sensors 16: 1884

Jian M, Xue P, Shi K, Li R, Ma L, Li P (2020) Efficient degradation of indole by microbial fuel cell based Fe_2O_3-polyaniline-dopamine hybrid composite modified carbon felt anode. J. Hazard Mater. 388: 122123

Jiang J, Wang H, Zhang S, Li S, Zeng W, Li F (2021) The influence of external resistance on the performance of microbial fuel cell and the removal of sulfamethoxazole wastewater. Bioresour. Technol. 336: 125308

Ju X, Wu S, Huang X, Zhang Y, Dong R (2014) How the novel integration of electrolysis in tidal flow constructed wetlands intensifies nutrient removal and odour control. Bioresour Technol. 169:605–13

Kaku N, Yonezawa N, Kodama Y, Watanabe K. (2008) Plant/microbe cooperation for electricity generation in a rice paddy field. Appl Microbiol. Biotechnol. 79(1):43–49

Kaur R, Marwaha A, Chhabra VA, Kim KH, Tripathi SK (2020) Recent developments on functional nanomaterial-based electrodes for microbial fuel cells. Renew. Sustain. Energy Rev. 119: 109551

Kazemi S, Fatih K, Mohseni M, Wang H (2012) Investigating Separators to Improve Performance of Flat-Plate Microbial Fuel Cells. In Meeting Abstracts: The Electrochemical Society; The Electrochemical Society: Pennington, NJ, USA, 3593

Khandelwal A, Vijay A, Dixit A, Chhabra M (2018) Microbial fuel cell powered by lipid extracted algae: a promising system for algal lipids and power generation. Bioresour. Technol. 247: 520-527

Khilari S, Pandit S, Das D, Pradhan D (2014) Manganese cobaltite/polypyrrole nanocomposite-based air-cathode for sustainable power generation in the single-chambered microbial fuel cells. Biosens. Bioelectron. 54: 534–540

Khilari S, Pandit S, Varanasi JL, Das D, Pradhan D (2015) Bifunctional manganese ferrite/polyaniline hybrid as electrode material for enhanced energy recovery in microbial fuel cell. ACS Appl. Mater. Interfaces 7 (37): 20657–20666

Khudzari J M, Kurian J, Gariépy Y, Tartakovsky B, Raghavan GSV (2018) Effects of salinity, growing media, and photoperiod on bioelectricity production in plant microbial fuel cells with weeping alkaligrass. Biomass and Bioenergy 109:1–9

Kiely PD, Rader G, Regan JM, Logan BE (2011) Long-term cathode performance and the microbial communities that develop in microbial fuel cells fed different fermentation end products. Bioresour. Technol. 102 (1): 361−366

Kim BH, Chang IS, Gadd GM (2007) Challenges in microbial fuel cell development and operation. Appl. Microbiol. Biotechnol. 76 (3): 485–494

Kim C, Lee CR, Song YE, Heo J, Choi SM, Lim DH, Cho J, Park C, Jang M, Kim JR (2017) Hexavalent chromium as a cathodic electron acceptor in a bipolar membrane microbial fuel cell with the simultaneous treatment of electroplating wastewater. Chem. Eng. J. 328: 703–707

Kim JR, Cheng S, Oh SE, Logan BE (2007) Power generation using different cation, anion, and ultrafiltration membranes in microbial fuel cells. Environ. Sci. Technol. 41:1004–1009

Kim Y, Shin SH, Chang IS, Moon SH (2014) Characterization of uncharged and sulfonated porous poly (vinylidene fluoride) membranes and their performance in microbial fuel cells. J. Membr. Sci. 463, 205–214

Kiran KV, Manmohan K, Sreelakshmi PM, Manju P, Gajalakshmi S (2020) Resource recovery from paddy field using plant microbial fuel cell. Process Biochemistry 99: 270–281

Kondaveeti S, Choi KS, Kakarla R, Min B (2014) Microalgae *Scenedesmus obliquus* as renewable biomass feedstock for electricity generation in microbial fuel cells (MFCs). Front Environ Sci & Eng. 8 (5): 784-791

Kouzuma A, Kaku N, Watanabe K (2014) Microbial electricity generation in rice paddy fields: recent advances and perspectives in rhizosphere microbial fuel cells. Appl Microbiol Biotechnol 98(23): 9521–26

Kukal MS, Irmak S (2020) Interrelationships between water use efficiency and light use efficiency in four row crop canopies. Agrosystems, Geosciences & Environment. 3 (1)

Kuleshova TE, Gall NR (2021) Dynamics of bioelectric potential in the root zone of plants during irrigation. Eurasian Soil Sci. 54:381–388

Kuleshova TE, Rao A, Bhadra S, Garlapati VK, Sharma S, Kaushik A, Goswami P, Sreekirshnan TR, Sevda S (2022) Plant microbial fuel cells as an innovative, versatile agro-technology for green energy generation combined with wastewater treatment and food production Biomass and Bioenergy 167:106629

Kumar S, Saeed G, Zhu L, Hui KN, Kim NH, Lee (2021) 0D to 3D carbon-based networks combined with pseudocapacitive electrode material for high energy density supercapacitor: A review. Chem. Eng. J. 403: 126352

Kumar Y, Singh R, Kumar A (2021) Study of PAR interception, energy balance studies and microclimatic profiles in potato (*Solanum tuberosum*) cultivars under varying planting dates. Int J Chem Stud 9(1):2475-2491

Larminie J, Dicks A (2003) Fuel Cell Systems Explained (2nd ed.), John Wiley & Sons, New York 406

Lee R, Miller A, Knight R, Fierer N (2018) A Novel Approach to Harvesting Energy from Agriculture in Microbe-Polluted Water: The Implementation of Plant Microbial Fuel Cells in Hydroponic Chambers 1. Columbia Undergraduate Science Journal (CUSJ) 75

Leong JX, Daud WRW, Ghasemi M, Liew KB, Ismail M (2013) Ion exchange membranes as separators in microbial fuel cells for bioenergy conversion: A comprehensive review. Renew. Sustain. Energy Rev. 28: 575–587

Li B, He Z, Wang M, Wang X, (2017a) PtSnP/C and PtSn/C as efficient cathode catalysts for oxygen reduction reaction in microbial fuel cells. Int. J. Hydrogen Energy 42 (8): 5261–5271

Li H, Ma H, Liu T, Ni J, Wang Q (2019a) An excellent alternative composite modifier for cathode catalysts prepared from bacterial cellulose doped with Cu and P and its utilization in microbial fuel cell. Bioresour. Technol. 289, 121661

Li Q, Liu Z, Sun YI, Yang S, Deng C (2021) A review on temperature control of proton exchange membrane fuel cells. Processes 9 (2): 235

Li S, Cheng C, Thomas A (2017b) Carbon-based microbial-fuel-cell electrodes: from conductive supports to active catalysts. Adv. Mater. 29 (8): 1602547

Li WW, Sheng GP, Liu XW, Yu HQ (2011) Recent advances in the separators for microbial fuel cells. Bioresour. Technol. 102: 244–252

Li Y, Liu J, Chen X, Yuan X, Li N, He W, Feng Y (2020a) Enhanced electricity generation and extracellular electron transfer by polydopamine–reduced graphene oxide (PDA–rGO) modification for high-performance anode in microbial fuel cell. Chem. Eng. J. 387: 123408

Li Z, Yang S, Song YN, Xu H, Wang Z, Wang W, Zhao Y (2020b) Performance evaluation of treating oil-containing restaurant wastewater in microbial fuel cell using in situ graphene/polyaniline modified titanium oxide anode. Environ. Technol. 41 (4): 420–429

Liew KB, Daud WRW, Ghasemi M, Leong JX, Lim SS, Ismail M (2014) Non-Pt catalyst as oxygen reduction reaction in microbial fuel cells: A review. Int. J. Hydrogen Energy. 39:4870–4883

Ling J, Xu Y, Lu C, Lai W, Xie G, Zheng L, Li G (2019) Enhancing stability of microalgae biocathode by a partially submerged carbon cloth electrode for bioenergy production from wastewater. Energies 17: 3229

Liu H, Logan BE (2004) Electricity generation using an air-cathode single chamber microbial fuel cell in the presence and absence of a proton exchange membrane. Environ. Sci. Technol. 38 (14): 4040−4046

Liu H, Cheng S, Logan BE (2005) Power generation in fed-batch microbial fuel cells as a function of ionic strength, temperature, and reactor configuration. Environ. Sci. Technol. 39:5488–5493

Liu J, Qiao Y, Guo CX, Lim S, Song H, Li CM (2012) Graphene/carbon cloth anode for high-performance mediatorless microbial fuel cells. Bioresour. Technol. 114: 275–280.

Liu S, Song H, Li X, Yang F (2013) Power generation enhancement by utilizing plant photosynthate in microbial fuel cell coupled constructed wetland system. Int. J Photoenergy 172010

Liu S, Song H, Wei S, Yang F, Li X (2014) Bio-cathode materials evaluation and configuration optimization for power output of vertical subsurface flow constructed wetland microbial fuel cell systems. Bioresour. Technol. 166: 575–583

Liu W, Cheng S, Guo J (2014) Anode modification with formic acid: A simple and effective method to improve the power generation of microbial fuel cells. Applied Surface Science 320:281–86

Liu Y, Zhang X, Zhang Q, Li C, (2020a) Microbial fuel cells: nanomaterials based on anode and their application. Energy Technol. 8 (9): 2000206

Lu L, Xing D, Ren Z (2015) Microbial community structure accompanied with electricity production in a constructed wetland plant microbial fuel cell. Bioresour. Technol. 195: 115-120

Logan BE (2006) Critical review microbial fuel cells: Methodology and technology. Environment Sciences Technological 40 (17):5181–5192

Logan BE (2008) Microbial Fuel Cells. John Wiley & Sons: Hoboken, NJ, USA.

Logan BE, Rabaey K (2012) Conversion of wastes into bioelectricity and chemicals by using microbial electrochemical technologies. Science 337: 686–690

Logan BE, Regan JM (2006a) Microbial challenges and harnessing the metabolic activity of bacteria can provide energy for a variety of applications, once technical and cost obstacles are overcome. Environ. Sci. Technol. 5172–5180

Logan BE, Regan JM (2006b) Electricity-producing bacterial communities in microbial fuel cells. Trends Microbiol. 14:512–8

Logan BE, Rossi R, Ragab A, Saikaly PE (2019) Electroactive microorganisms in bioelectrochemical systems. Nat Rev Microbiol. 17(5):307–19

Long S, Zhao L, Chen J, Kim J, Huang CH, Pavlostathis SG (2021) Tetracycline inhibition and transformation in microbial fuel cell systems: Performance, transformation intermediates, and microbial community structure. Bioresour. Technol. 322: 124534

Loubna E, Elabed A, Ibnsouda S, El Abed S (2019) Challenges of microbial fuel cell architecture on heavy metal recovery and removal from wastewater. Front. Energy Res. 7: 1

Ma H, Peng C, Jia Y, Wang Q, Tu M, Gao M (2018) Effect of fermentation stillage of food waste on bioelectricity production and microbial community structure in microbial fuel cells. Royal Soc. open sci. 5 (9): 180457

Ma J, Wang Z, Zhang J, Waite TD, Wu Z (2017) Cost-effective Chlorella biomass production from dilute wastewater using a novel photosynthetic microbial fuel cell (PMFC) Water Research 108: 356-364

Mahendiravarman E, Sangeetha D (2017) Application of polysulphone based anion exchange membrane electrolyte for improved electricity generation in microbial fuel cell. Mater. Chem. Phys. 199: 528–536

Malakooti A, Abdualla H, Sadati S, Ceylan H, Kim S, Cetin K (2021) Experimental and theoretical characterization of electrodes on electrical and thermal performance of electrically conductive concrete. Compos. B Eng. 109003

Mat I, Mohd Kassim MR, Harun AN, Mat Yusoff I (2016) IoT in precision agriculture applications using wireless moisture sensor network. In: 2016 IEEE Conf. Open Syst., IEEE, 24–29

Mateo S, Cantone A, Canizares P, Fernandez-Morales FJ, Scialdone O, Rodrigo MA (2018) Development of a module of stacks of air-breathing microbial fuel cells to light-up a strip of LEDs. Electrochim. Acta 274: 152–159

Mathuriya AS, Yakhmi JV (2014) Microbial fuel cells to recover heavy metals. Environ. Chem. Lett. 12: 483–494

Matsena MT, Chirwa EMN (2022) Advances in Microbial fuel cell technology for zero carbon emission energy generation from waste. Biofuels and Bioenergy 321-358

Matsena MT, Mabuse M, Tichapondwa SM, Chirwa EMN (2021) Improved performance and cost efficiency by surface area optimization of granular activated carbon in air-cathode microbial fuel cell. Chemosphere 281: 130941

Merino-Jimenez I, Celorrio V, Fermin DJ, Greenman J, Ieropoulos I (2017) Enhanced MFC power production and struvite recovery by the addition of sea salts to urine. Water Res. 109: 46–53

Merino-Jimenez I, Greenman J, Ieropoulos I (2017) Electricity and catholyte production from ceramic MFCs treating urine. Int. J. Hydrogen Energy 42: 1791–1799

Merino-Jimenez I, Gonzalez-Juarez F, Greenman J, Ieropoulos I (2019) Effect of the ceramic membrane properties on the microbial fuel cell power output and catholyte generation. J. Power Sources 429: 30–37

Merino-Jimenez I, Santoro C, Rojas-Carbonell S, Greenman J, Ieropoulos I, Atanassov P (2016) Carbon-based air-breathing cathodes for microbial fuel cells. Catalysts 6 (9): 127

Min B, Kim J, Oh S, Regan JM, Logan BE (2005) Electricity generation from swine wastewater using microbial fuel cells. Water Res. 39 (20): 4961-4968

Mitsch WJ, Jorgensen SE (1989) Ecological Engineering: An Introduction to Ecotechnology. John Wiley & Sons, Inc., New York, USA

Mohamed SN, Thomas N, Tamilmani J, Boobalan T, Matheswaran M, Kalaichelvi P (2020) Bioelectricity generation using iron (II) molybdatenanocatalyst coated anode during treatment of sugar wastewater in microbial fuel cell. Fuel 277: 118119

Mohan SV, Mohanakrishna G, Chiranjeevi P, Peri D, Sarma PN (2010) Ecologically engineered system (EES) designed to integrate floating, emergent and submerged macrophytes for the treatment of domestic sewage and acid rich fermented-distillery wastewater: evaluation of long-term performance. Bioresour Technol. 101(10): 3363–70

Mohan SV, Mohanakrishna, G, Chiranjeevi P (2011) Sustainable power generation from floating macrophytes based ecological microenvironment through embedded fuel cells along with simultaneous wastewater treatment. Bioresour. Technol. 102: 7036-7042

Mohan SV, Velvizhi G, Modestra JA, Srikanth S (2014) Microbial fuel cell: critical factors regulating bio-catalyzed electrochemical process and recent advancements. Renew. Sustain. Energy Rev. 40: 779–797

Mohamed SN, Hiraman PA, Muthukumar K, Jayabalan T (2020) Bioelectricity production from kitchen wastewater using microbial fuel cell with photosynthetic algal cathode. Bioresour. Technol. 295:122226

Mohnish B, Suchithra TV (2018) Electricity generation from living plants using microbial fuel cells. IJET 7, 534

Moon H, Chang IS, Kim BH (2006) Continuous electricity production from artificial wastewater using a mediator-less microbial fuel cell. Bioresour. Technol. 97 (4): 621–627

Moqsud MA, Yoshitake J, Bushra QS, Hyodo M, Omine K, Strik DPBTB (2015) Compost in plant microbial fuel cell for bioelectricity generation. J Waste Manag 36: 63–9

Morris JM, Jin S, Wang JQ, Zhu CZ, Urynowicz MA (2007) Lead dioxide as an alternative catalyst to platinum in microbial fuel cells. Electrochem. Commun. 9: 1730-1734

Moulin L, Munive A, Dreyfus B, Boivin-Masson C (2001) Nodulation of legumes by members of the b-subclass of Proteobacteria. Nature 411: 948-950

Munjal M, Tiwari B, Lalwani S, Sharma M, Singh G, Sharma RK (2020) An insight of bioelectricity production in mediator less microbial fuel cell using mesoporous Cobalt Ferrite anode. Int. J. Hydrog. Energy. 45: 12525–12534

Myers JM, Myers CR (2000) Role of the Tetraheme Cytochrome CymA in anaerobic electron transport in cells of shewanella putrefaciens MR-1 with normal levels of menaquinone. Journal of Bacteriology 182: 67–75

Nandy A (2018) Configurations of Microbial Fuel Cells Different approaches for harnessing bioenergy from microbial fuel cells, In Progress and recent trends in microbial fuel cells, 25-45

Narayanasamy S, Jayaprakash J (2020) Application of carbon-polymer based composite electrodes for Microbial fuel cells. Rev. Environ. Sci. Biotechnol. 19: 595–620

Nayak JK, Ghosh UK (2019) Post treatment of microalgae treated pharmaceutical wastewater in photosynthetic microbial fuel cell (PMFC) and biodiesel production. Biomass Bioenergy 131: 105415

Neogi S, Bhattacharyya P, Nayak AK (2021) Characterization of carbon dioxide fluxes in tropical lowland flooded rice ecology. Paddy Water Environ. 1: 3

New T, Xie Z (2008) Impacts of large dams on riparian vegetation: applying global experience to the case of China's Three Gorges Dam. Biodivers Conserv 17: 3149– 3163

Nguyen HTH, Min B (2020) Leachate treatment and electricity generation using an algae-cathode microbial fuel cell with continuous flow through the chambers in series. Sci. Total Environ. 723: 138054

Nitisoravut R, Regmi R (2017) Plant microbial fuel cells: a promising biosystems engineering. Renewable and Sustainable Energy Reviews 76: 81–89

Noori MT, Ghangrekar MM, Mitra A, Mukherjee CK (2016) Enhanced power generation in microbial fuel cell using MnO2-catalyzed cathode treating fish market wastewater. In: Kumar S, Khanal SK, Yadav YK (Eds.), Proceedings of the First International Conference on Recent Advances in Bioenergy Research. Springer, New Delhi 285–294

Nourbakhsh F., Mohsennia M, Pazouki M (2017) Nickel oxide/carbon nanotube/ polyanilinenanocomposite as bifunctional anode catalyst for high-performance Shewanella-based dual-chamber microbial fuel cell. Bioproc. Biosyst. Eng. 40 (11): 1669–1677

Nosek D, Jachimowicz P, Cydzik-Kwiatkowska A (2020) Anode modification as an alternative approach to improve electricity generation in microbial fuel cells. Energies 13: 6596

O'Hare MT, Baattrup-Pedersen A, Baumgarte I, Freeman A, Gunn ID, Lazar AN (2018) Responses of aquatic plants to eutrophication in rivers: a revised conceptual model. Front. Plant Sci. 9: 451

O'Hayre R, Cha SW, Colella W, Prinz FB (2005) Fuel Cell Fundamentals. John Wiley & Sons, New York 409

Oon YL, Ong SA, Ho LN, Wong YS, Dahalan FA, Oon YS (2017) Role of macrophyte and effect of supplementary aeration in up-flow constructed wetland-microbial fuel cell for simultaneous wastewater treatment and energy recovery. Bioresour Technol. 224:265–75

Osorio de la Rosa E, Vazquez Castillo J, Carmona Campos M, Barbosa Pool G, Becerra Nunez G, Castillo Atoche A (2019) Plant microbial fuel cells–based energy harvester system for self-powered IoT applications. Sensors 19: 1378

Osorio-de-la-Rosa E, Vazquez-Castillo J, Castillo-Atoche A, Heredia-Lozano J Castillo-Atoche A, Becerra-Nunez G, Barbosa R (2021) Arrays of Plant Microbial Fuel Cells for Implementing Self-Sustainable Wireless Sensor Networks. In *IEEE Sensors Journal* 21(2):1965-1974

Pandit S, Das D (2018) Principles of Microbial Fuel Cell for the Power Generation. Capital Publishing Company (Eds.) New Delhi, India

Pandit S, Khilari S, Roy S, Pradhan D, Das D (2014) Improvement of power generation using Shewanella putrefaciens mediated bioanode in a single chambered microbial fuel cell: Effect of different anodic operating conditions. Bioresource Technology 166: 451-457

Park DH, Zeikus JG (2003) Improved fuel cell and electrode designs for producing electricity from microbial degradation. Biotechnol. Bioeng. 81: 348–355

Paule S, Ondel O, Roos C, Robert F (2015) Energy harvest with mangrove benthic microbial fuel cells. Int. J. Energy Res. 39 (4): 543–556

Pasternak G, Greenman J, Ieropoulos I (2016) Comprehensive study on ceramic membranes for low-cost microbial fuel cells. ChemSusChem 9: 88–96

Pieterse AH, Murphy KJ (1990) Aquatic weeds: the ecology and management of nuisance aquatic vegetation. first ed. Oxford: Oxford University Press

Piyare R, Murphy AL, Tosato P, Brunelli D (2017) Plug into a plant: using a plant microbial fuel cell and a wake-up radio for an energy neutral sensing system IEEE Proceedings of 2017 IEEE 42nd conference on local computer networks workshops (LCN workshops) Singapore: IEEE Press; 18–25

Potter MC (1911) Electrical effects accompanying the decomposition of organic compounds. Proc R Soc Lond B 84: 260–276

Prasad J, Tripathi RK (2018a) A Dc-Dc Boost Converter for Sediment Microbial Fuel Cell Energy Harvesting. 2nd IEEE International Conference on Power Electronics, Intelligent Control and Energy Systems (ICPEICES), Delhi, India 712-716

Prasad J, Tripathi RK (2018b) Energy harvesting from sediment microbial fuel cell using different electrodes. Int. J. ChemTech Res. 11 (07): 219–225

Priya AD, Deva S, Shalini P, Setty YP (2020) Antimony-tin based intermetallics supported on reduced graphene oxide as anode and MnO_2@ rGO as cathode electrode for the study of microbial fuel cell performance. Renew. Energy 150: 156–166

Qiao Y, Li CM, Bao SJ, Bao QL (2007) Carbon nanotube/polyaniline composite as anode material for microbial fuel cells. J. Power Sources 170 (1): 79–84

Qiu B, Hu Y, Liang C, Wang L, Shu Y, Chen Y, Cheng J (2020) Enhanced degradation of diclofenac with Ru/Fe modified anode microbial fuel cell: kinetics, pathways and mechanisms. Bioresour. Technol. 300: 122703

Qu Y, Feng Y, Wang X, Logan BE (2012) Use of a coculture to enable current production by *Geobacter sulfurreducens*. Appl. Environ. Microbiol. 78: 3484–3487

Rabaey K, Verstraete W (2005) Microbial fuel cells: Novel biotechnology for energy generation. Trends Biotechnol. 23: 291–298

Raghavulu SV, Babu PS, Goud RK, Subhash GV, Srikanth S, Mohan SV (2012) Bioaugmentation of an electrochemically active strain to enhance the electron discharge of mixed culture: process evaluation through electro-kinetic analysis. RSC Adv;2(2):677–88

Rajesh PP, Noori MT, Ghangrekar MM (2020) Improving performance of microbial fuel cell by using polyaniline-coated carbon–felt anode. J. Hazard. Toxic, and Radioactive Waste 24 (3): 04020024

Ramaswamy N, Mukerjee S (2012) Fundamental mechanistic understanding of electrocatalysis of oxygen reduction on Pt and Non-Pt surfaces: acid versus Alkaline Media. Advances in Physical Chemistry

Ramirez-Nava J, Martinez-Castrejon M, Garcia-Mesino RL, Lopez-Diaz JA, Talavera-Mendoza O, Sarmiento-Villagrana A, Rojano F, Hernandez-Flores G (2021) The Implications of Membranes Used as Separators in Microbial Fuel Cells. Membranes 11: 738

Rapanyane MB, Sethole FR (2020) The rise of artificial intelligence and robots in the 4th Industrial Revolution: implications for future South African job creation. Contemp. Soc. Sci. 15: 489–501

Rashid N, Cui YF, Rehman MSU, Han JI (2013) Enhanced electricity generation by using algae biomass and activated sludge in microbial fuel cell. Sci. Total Environ. 456: 91-94

Ren H, Lee HS, Chae J (2012) Miniaturizing microbial fuel cells for potential portable power sources: Promises and challenges. Microfluid. Nanofluidics 13 (3): 353–381

Rimboud M, Pocaznoi D, Erable B, Bergel A (2014) Electroanalysis of microbial anodes for bioelectrochemical systems: basics, progress and perspectives. Phys. Chem. Chem. Phys. 16: 16349-16366

Rismani-Yazdi H, Carver SM, Christy AD, Yu Z, Bibby K, Peccia J (2013) Suppression of methanogenesis in cellulose-fed microbial fuel cells in relation to performance, metabolite formation, and microbial population. Bioresour. Technol. 129: 281-288

Rossi R, Wang X, Logan BE (2020) High performance flow through microbial fuel cells with anion exchange membrane. J. Power Sources 475: 228–633

Rusyn I (2021) Role of microbial community and plant species in performance of plant microbial fuel cells. Renewable and Sustainable Energy Reviews 152: 111697

Ruud AT, Strik DPBTB, Hamelers HVM, Buisman CJN (2010) Long-term performance of a plant microbial fuel cell with Spartina anglica. Appl. Microbiol. Biotechnol. 86: 973-981

Saito T, Merrill MD, Watson VJ, Logan BE, Hickner MA (2010) Investigation of ionic polymer cathode binders for microbial fuel cells. Electrochim. Acta 55 (9): 3398−3403

Salehmin MNI, Lim SS, Satar I, Daud WRW (2021) Pushing microbial desalination cells towards field application: Prevailing challenges, potential mitigation strategies, and future prospects. Sci. Total Environ. 143485

Sangeetha D, Kugarajah V, Sugumar M (2019) Membranes for Microbial Fuel Cells. In Microbial Electrochemical Technology: Sustainable Platform for Fuels, Chemicals and Remediation, Biomass, Biofuels, Biochemicals; Elsevier: Amsterdam, The Netherlands, 143–194

Santoro C, Ieropoulos I, Greenman J, Cristiani P, Vadas T, Mackay A, Li B (2013) Power generation and contaminant removal in single chamber microbial fuel cells (SCMFCs) treating human urine. Int. J. Hydrogen Energy 38: 11543–11551

Santoro C, Salar Garcia MJ, Walter XA, You J, Theodosiou P, Gajda I, Ieropoulos I (2020) Urine in bioelectrochemical systems: An overall review. Chem Electro Chem 7: 1312–1331

Saratale RG, Kuppam C, Mudhoo A, Saratale GD, Periyasamy S, Zhen G, Kook L, Bakonyi P, Nemestóthy N, Kumar G (2017) Bioelectrochemical systems using microalgae – a concise research update. Chemosphere 177: 35–43

Sarma PJ, Mohanty K (2019) An insight into plant microbial fuel cells. In: Krishnaraj, R.N., Sani, R.K. (Eds.), Bioelectrochemical Interface Engineering. Wiley 137–148

Schroder U (2007) Anodic electron transfer mechanisms in microbial fuel cells and their energy efficiency. Phys. Chem. Chem. Phys. 9: 2619–2629

Schievano A, Colombo A, Grattieri M, Trasatti SP, Liberale A, Tremolada P (2017) Floating microbial fuel cells as energy harvesters for signal transmission from natural water bodies. J. Power Sources 340: 80–88

Schuetz B, Schicklberger M, Kuermann J, Spormann AM, Gescher J (2009) Periplasmic electron transfer via the c-Type Cytochromes MtrA and FccA of *Shewanella oneidensis* MR-1. AEM 75: 7789–7796

Scott K (2016) Membranes and Separators for Microbial Fuel Cells. In Microbial Electrochemical and Fuel Cells: Fundamentals and Applications; Elsevier Ltd.: Newcastle upon Tyne, UK, 153–178

Sekar N, Ramasamy RP (2013) Electrochemical impedance spectroscopy for microbial fuel cell characterization. J Microb Biochem Technol S. 6(2)

Senthilkumar K, Naveenkumar M (2021) Enhanced performance study of microbial fuel cell using waste biomass-derived carbon electrode. Biomass Convers. Biorefin. 1–9

Shaikh R, Rizvi A, Quraishi M, Pandit S, Mathuriya AS, Gupta PK, Singh J, Prasad R (2020) Bioelectricity production using plant-microbial fuel cell: Present state of art. S. Afr. J. Bot. 140: 393-408

Sonawane JM, Ezugwu CI, Ghosh PC (2020) Microbial Fuel Cell-Based Biological Oxygen Demand Sensors for Monitoring Wastewater: State-of-the-Art and Practical Applications. ACS Sensors 5: 2297–2316

Sonawane JM, Pant D, Ghosh PC, Adeloju SB (2019) Fabrication of a carbon paper/polyaniline-copper hybrid and its utilization as an air cathode for microbial fuel Cells. ACS Appl. Energy Mater. 2 (3): 1891–1902

Song X, Yan D, Liu Z, Chen Y, Lu S, Wang D (2011) Performance of laboratory-scale constructed wetlands coupled with micro-electric field for heavy metal-contaminating wastewater treatment. Ecol Eng. 37(12):2061–5

Sophia AC, Sreeja S (2017) Green energy generation from plant microbial fuel cells (PMFC) using compost and a novel clay separator. Sustain. Energy Technol. Assess. 21: 59–66

Spencer DF, Liow PS, Chan WK, Ksander GG, Getsinger KD (2006) Estimating *Arundo donax* shoot biomass. Aquatic Botany 84: 272–276

Srbinovska M, Gavrovski C, Dimcev V, Krkoleva A, Borozan V (2015) Environmental parameters monitoring in precision agriculture using wireless sensor networks. J. Clean. Prod. 88: 297–307

Srivastava P, Yadav AK, Mishra BK (2015) The effects of microbial fuel cell integration into constructed wetland on the performance of constructed wetland. Bioresour. Technol. 195: 223–230

Srivastava P, Gupt S, Garaniya V, Yadav A (2018) Up to 399 mV bioelectricity generated by a rice paddy-planted microbial fuel cell assisted with a blue-green algal cathode. Environ Chem Lett. 17:1045–51

Stafford JV (2000) Implementing precision agriculture in the 21st century. J. Agric. Eng. Res. 76: 267–275

Strik DPBTB, Hamelers HVM, Snel JFH, Buisman CJN (2008) Green electricity production with living plants and bacteria in a fuel cell. International Journal of Energy Research 32: 870–876

Strik DP, Timmers RA, Helder M, Steinbusch KJ, Hamelers HV, Buisman CJ (2011) Microbial solar cells: applying photosynthetic and electrochemically active organisms. Trends Biotechnol 29(1):41–9

Sudirjo E, Buisman CJN, Strik DPBTB (2019) Activated carbon mixed with marine sediment is suitable as bioanode material for Spartina anglica sediment/plant microbial fuel cell: plant growth, electricity generation, and spatial microbial community diversity. Water 11: 1810

Sun D, Cheng S, Wang A, Li F, Logan BE, Cen K (2015) Temporal-spatial changes in viabilities and electrochemical properties of anode biofilms. Environ. Sci.Technol. 49 (8): 5227–5235

Sun CY, Zhang H (2019) Investigation of Nafion series membranes on the performance of iron-chromium redox flow battery. Int. J. Energy Res. 43: 8739–8752

Sun C, Negro E, Nale A, Pagot G, Vezzu K, Zawodzinski TA, Meda L, Gambaroe C, Di Noto V (2021) An efficient barrier toward vanadium crossover in redox flow batteries: The bilayer [Nafion/(WO_3) x] hybrid inorganic-organic membrane. Electrochim. Acta 378: 133–138

Suren AM, Smart GM, Smith RA, Brown SL (2000) Drag coefficients of stream bryophytes: experimental determinations and ecological significance. Fresh wat. Biol. 45(3):309–17

Takanezawa K, Nishio K, Kato S, Hashimoto K, Watanabe K (2010) Factors affecting electric output from rice-paddy microbial fuel cells. Biosci Biotechnol Biochem 74:1271–3

Tan SM, Ong SA, Ho LN, Wong YS, Abidin CZA, Thung WE, Teoh TP (2021) Polypropylene biofilm carrier and fabricated stainless-steel mesh supporting activated carbon: Integrated configuration for performances enhancement of microbial fuel cell. Sustain. Energy Technol. Assess. 46: 101268

Tao Y, Liu Q, Chen J, Wang B, Wang Y, Liu K (2016) Hierarchically three-dimensional nanofiber-based textile with high conductivity and biocompatibility as a microbial fuel cell anode. Environ. Sci.Technol. 50 (14): 7889–7895

Tapia NF, Rojas C, Bonilla CA, Vargas IT (2017) Evaluation of Sedum as driver for plant microbial fuel cells in a semi-arid green roof ecosystem. Ecological Engineering 108: 203–210

Tapia NF, Rojas C, Bonilla C, Vargas IT (2017) A new method for sensing soil water content in green roofs using plant microbial fuel cells. Sensors 18: 71

Terada A, Yuasa A, Kushimoto T, Tsuneda S, Katakai A, Tamada M (2006) Bacterial adhesion to and viability on positively charged polymer surfaces. Microbiology (Reading, England) 152: 3575–3583

Thakur S, Das B (2021) Performance evaluation of microbial fuel cell with sewage wastewater and RO concentrate using composite anode made of Luffa aegyptiaca. nviron. Prog. Sustain. Energy. 40

Tiquia-Arashiro SM, Pant, D (2020) In (eds) Microbial electrochemical technologies. CRC Press

Timmers RA, Rothballer M, Strik DP, Engel M, Schulz S, Schloter M (2012) Microbial community structure elucidates performance of *Glyceria maxima* plant microbial fuel cell. Appl Microbiol Biotechnol. 94(2):537–48

Timmers RA, Strik DP, Hamelers HV (2010) Long-term performance of a plant microbial fuel cell with *Spartina anglica*. Applied Microbiology and Biotechnology 86: 973–981

Timmers RA, Strik DP, Hamelers HV (2013) Electricity generation by a novel design tubular plant microbial fuel cell. Biomass Bioenergy 5: 60–67

Turetsky MR (2003) The role of bryophytes in carbon and nitrogen cycling. Bryologist 106(3):395–409

Turk KK, Kruusenberg I, Kibena-Poldsepp E, Bhowmick GD, Kook M, Tammeveski K (2018) Novel multi walled carbon nanotube based nitrogen impregnated Co and Fe cathode catalysts for improved microbial fuel cell performance. Int. J. Hydrogen Energy 43 (51): 23027–23035

Ueoka N, Sese N, Sue M, Kouzuma A, Watanabe K (2016) Sizes of anode and cathode affect electricity generation in rice paddy-field microbial fuel cells. J Sustain Bioenergy Syst 6(1):10–5

Vazquez-Larios AL, Solorza-Feria O, Vazquez-Huerta G, Esparza-Garcia FJ, Rios-Leal E, Rinderknecht-Seijas N, Poggi- Varaldo HM (2010) A new design improves performance of a single chamber microbial fuel cell. J. New Mater. Electrochem. Syst. 13:219–226

Velasquez-Orta SB, Curtis TP, Logan BE (2009) Energy from algae using microbial fuel cellS. Biotechnol Bioeng. 103 (6):1068-1076

Velez-Perez LS, Ramirez-Nava J, Hernandez-Flores G, Talavera-Mendoza O, Escamilla-Alvarado C, Poggi-Varaldo HM, Solorza-Feria O, Lopez-Diaz JA (2020) Industrial acid mine drainage and municipal wastewater co-treatment by dual-chamber microbial fuel cells. Int. J. Hydrogen Energy 45: 13757–13766

Venkatesan PN, Sangeetha D (2014) Characterization and performance study of sulfonated poly ether ether ketone/Fe3O4nanocomposite membrane as electrolyte for microbial fuel cell. Chem. Eng. J. 243: 564–571

Villasenor J, Capilla P, Rodrigo MA, Canizares P, Fernandez FJ (2013) Operation of a horizontal subsurface flow constructed wetland-microbial fuel cell treating wastewater under different organic loading rates. Water Res. 47(17):6731–8

Vymazal J (2011) Plants used in constructed wetlands with horizontal subsurface flow: a review. Hydrobiologia 674(1):133–56

Walter XA, Greenman J, Taylor B, Ieropoulos IA (2015) Microbial fuel cells continuously fuelled by untreated fresh algal biomass. Algal Res.11: 103-107

Wang H, Liu D, Lu L, Zhao Z, Xu Y, Cui F (2012) Degradation of algal organic matter using microbial fuel cells and its association with trihalomethane precursor removal. Bioresour Technol. 116: 80-85

Wang X, Feng Y, Liu J, Lee H, Li C, Ren N (2010) Sequestration of CO_2 discharged from anode by algal cathode in microbial carbon capture cells (MCCs). Biosens. Bioelectron. 25: 2639–2643

Wang X, Feng Y, Ren N, Wang H, Lee H, Li N, Zhao Q (2009) Accelerated start-up of two-chambered microbial fuel cells: effect of anodic positive poised potential. Electrochim. Acta 54 (3): 1109–1114

Wang H, Park JD, Ren ZJ (2015) Practical energy harvesting for microbial fuel cells: a review. Environ. Sci.Technol. 49 (6): 3267–3277

Wang H, Ren ZJ (2013) A comprehensive review of microbial electrochemical systems as a platform technology. Biotechnology Advances 31: 1796–1807

Wang H, Ren ZJ (2014) Bioelectrochemical metal recovery from wastewater: A review. Water Res. 66: 219–232

Wang P, Gao M, Pan H, Zhang J, Liang C, Wang J (2013) A facile synthesis of Fe_3O_4/C composite with high cycle stability as anode material for lithium-ion batteries. J. Power Sources 239: 466–474

Wang WH, Wang Y, Sun LQ, Zheng YC, Zhao JC (2020) Research and application status of ecological floating bed in eutrophic landscape water restoration. Sci. of Tot. Env. 704: 135434

Watson VJ, Saito T, Hickner MA, Logan BE (2011) Polymer coatings as separator layers for microbial fuel cell cathodes. J. Power Sources 196: 3009–3014

Wei L, Han H, Shen J (2012) Effects of cathodic electron acceptors and potassium ferricyanide concentrations on the performance of microbial fuel cell. Int. J. Hydrog. Energ. 37: 12980–12986

Wei J, Liang P, Huang X (2011) Recent progress in electrodes for microbial fuel cells. Bioresour. Technol. 102 (20): 9335–9344

Wen Z, Ci S, Mao S, Cui S, Lu G, Yu K, Chen J (2013) TiO_2 nanoparticles-decorated carbon nanotubes for significantly improved bioelectricity generation in microbial fuel cells. J. Power Sources 234: 100–106

Wetser K, Dieleman K, Buisman C, Strik DPBTB (2017) Electricity from wetlands: tubular plant microbial fuels with silicone gas-diffusion biocathodes. Apenergy, 185: 642-649

Wetser K, Liu J, Buisman C, Strik D (2015) Plant microbial fuel cell applied in wetlands: spatial, temporal and potential electricity generation of *Spartina anglica* salt marshes and Phragmites australis peat soils. Biomass Bioenergy 83:543–50

Wetser K, Sudirjo E, Buisman CJ, Strik DP (2015) Electricity generation by a plant microbial fuel cell with an integrated oxygen reducing biocathode. Appled Energy 137: 151–157

Wijte AHBM, Mizutani T, Motamed ER, Merryfield ML, Miller DE, Alexander DE (2005) Temperature and endogenous factors cause seasonal patterns in rooting by stem fragments of the invasive Giant Reed, Arundo donax (Poaceae). International Journal of Plant Sciences 166: 507–517

Williams JM, Khanna R, Ruiz-Rosero JP, Pisharody G, Qian Y, Carlson CR (2017) Weaving the wireless web: toward a low-power, dense wireless sensor network for the industrial IoT. IEEE Microw. Mag. 18:40–63

Winfield J, Greenman J, Huson D, Ieropoulos I (2013a) Comparing terracotta and earthenware for multiple functionalities in microbial fuel cells. Bioproc. Biosyst. Eng. 36: 1913–1921

Winfield J, Chambers LD, Rossiter J, Ieropoulos I (2013b) Comparing the short and long term stability of biodegradable, ceramic and cation exchange membranes in microbial fuel cells. Bioresour. Technol. 148: 480–486

Wu J, Chen W, Yan Y, Gao K, Liao C, Li Q, Wang X (2017) Enhanced oxygen reducing biocathode electroactivity by using sediment extract as inoculum. Bioelectrochemistry 117: 9–14

Wu XY, Song TS, Zhu XJ, Wei P, Zhou CC (2013) Construction and operation of microbial fuel cell with Chlorella vulgaris biocathode for electricity generation. Appl. Bioch. Biotech. 171: 2082–2092

Xiao L, Damien J, Luo J, Jang HD, Huang J, He Z (2012) Crumpled graphene particles for microbial fuel cell electrodes. J. Power Sources 208: 187–192

Xu L, Zhao Y, Doherty L, Hu Y, Hao X (2016) The integrated processes for wastewater treatment based on the principle of microbial fuel cells: a review. Crit. Rev. Environ. Sci. Technol. 46(1):60–91

Xu Y, Lu Y, Zhu X (2021) Toward plant energy harvesting for 5G signal amplification. ACS Sustain. Chem. Eng. 9 1099–1104

Yadav AK (2010) Design and development of novel constructed wetland cum microbial fuel cell for electricity production and wastewater treatment. In: Cerioni AM, Motta R, editors. Proceedings of 12th international conference on wetland systems for water pollution control (IWA); venice, Italy. Palombi: 321

Yadav AK, Dash P, Mohanty A, Abbassi R, Mishra BK (2012) Performance assessment of innovative constructed wetland-microbial fuel cell for electricity production and dye removal. Ecol Eng. 47:126–31

Yadav G, Sharma I, Ghangrekar M, Sen R (2020) A live biocathode to enhance power output steered by bacteriamicroalgae synergistic metabolism in microbial fuel cell. Journal of Power Sources 449: 227560

Yadav RK, Chiranjeevi P, SukrampaL, Patil SA (2020) Integrated drip hydroponics-microbial fuel cell system for wastewater treatment and resource recovery. Bioresource Technology Reports (9):100392

Yang XL, Li T, Xia YG, Singh RP, Song HL, Zhang H, Wang YW (2021) Microbial fuel cell coupled ecological floating bed for enhancing bioelectricity generation and nitrogen removal. Int. J. Hyd. Eng. 46(20): 11433-11444

Yang Y, Sun G, Xu M (2010) Microbial fuel cells come of age. J. Chem. Technol. Biotechnol. 86: 625–632

Yang Z, Zhang L, Nie C, Hou Q, Zhang S, Pei H (2019) Multiple anodic chambers sharing an algal raceway pond to establish a photosynthetic microbial fuel cell stack: voltage boosting accompany wastewater treatment. Water Research 164: 114955

Yaqoob AA, Ibrahim MNM, Rodríguez-Couto S (2020) Development and modification of materials to build cost-effective anodes for microbial fuel cells (MFCs): An overview. Biochem. Eng. J. 107779

Yoon TH, Song HJ, Jung WY, Kim JE, Kim KJ, Kim HH (2018) Monitoring plant health using a plant microbial fuel cell. Bull. Kor. Chem. Soc. 39 1193–1197

Yu E, Cheng S, Scott K, Logan B (2007) Microbial fuel cell performance with non-Pt cathode catalysts. Journal of Power Sources 171: 275-281

Yuan H, He Z (2015) Graphene-modified electrodes for enhancing the performance of microbial fuel cells. Nanoscale 7 (16): 7022–7029

Zabihallahpoor A, Rahimnejad M, Talebnia F (2015) Sediment microbial fuel cells as a new source of renewable and sustainable energy: present status and future prospects. RSC Adv. 5 (114): 94171–94183

Zha Z, Zhang Z, Xiang P, Zhu H, Zhou B, Sun Z, Zhou S (2020) One-step preparation of eggplant-derived hierarchical porous graphitic biochar as efficient oxygen reduction catalyst in microbial fuel cells. RSC Adv. 11:1077–1085

Zhang F, Cheng SA, Pant D, Van Bogaert G, Logan BE (2009) Power generation using an activated carbon and metal mesh cathode in a microbial fuel cell. Electrochem. Commun. 11 (11): 2177− 2179

Zhang F, Pant D, Logan BE (2011) Long-term performance of activated carbon air cathodes with different diffusion layer porosities in microbial fuel cells. Biosens. Bioelectron. 30 (1), 49−55

Zhang LL, Zhao XS (2009) Carbon-based materials as supercapacitor electrodes. Chem. Soc. Rev. 38: 2520-2531

Zhang LX, Liu CS, Zhuang L, Li, WS, Zhou SG, Zhang JT (2009) Manganese dioxide as an alternative cathodic catalyst to platinum in microbial fuel cells. Biosens. Bioelectron. 24 (9): 2825−2829

Zhang Q, Liu L (2021) Cathodes of membrane and packed manganese dioxide/titanium dioxide/graphitic carbon nitride/granular activated carbon promoted treatment of coking wastewater in microbial fuel cell. Bioresour. Technol. 321: 124442

Zhang Y, Mo G, Li X, Zhang W, Zhang J, Ye J (2011) A graphene modified anode to improve the performance of microbial fuel cells. J. Power Sources 196 (13): 5402–5407

Zhang X, Cheng S, Wang X, Huang X, Logan BE (2009) Separator characteristics for increasing performance of microbial fuel cells. Environ. Sci. Technol. 43: 8456–8641

Zhang XY, Cheng SA, Huang X, Logan BE (2010) The use of nylon and glass fiber filter separators with different pore sizes in air-cathode single-chamber microbial fuel cells. Energy Environ. Sci. 3: 659–664

Zhao F, Harnisch F, Schroder U, Scholz F, Bogdanoff P, Herrmann I (2005) Application of pyrolysed iron(II) phthalocyanine and CoTMPP based oxygen reduction catalysts as cathode materials in microbial fuel cells. Electrochem. Commun. 7 (12):1405−1410

Zhao F, Harnisch F, Schrorder U, Scholz F, Bogdanoff P, Herrmann I. (2006) Challenges and constraints of using oxygen cathodes in microbial fuel cells. Environ. Sci. Technol. 40: 5193-5199

Zhao P, Kumamoto A, Kim S, Chen X, Hou B, Chiashi S (2013a) Self-limiting chemical vapor deposition growth of monolayer graphene from ethanol. J. Phys. Chem. C 117 (20): 10755–10763

Zhao X, Tian T, Guo M, Liu X, Liu X (2020) Cauliflower-like polypyrrole@ MnO_2 modified carbon cloth as a capacitive anode for high-performance microbial fuel cells. J. Chem. Technol. Biotechnol. 95 (1): 163–172

Zhao Y, Collum S, Phelan M, Goodbody T, Doherty L, Hu Y (2013b) Preliminary investigation of constructed wetland incorporating microbial fuel cell: batch and continuous flow trials. Chem. Eng. J. 229: 364–370

Zhao Y, Watanabe K, Nakamura R, Mori S, Liu H, Ishii K, Hashimoto K (2010) Three-dimensional conductive nanowire networks for maximizing anode performance in microbial fuel cells. Chem. Eur. J 16 (17): 4982–4985

Zhou M, Chi M, Luo J, He H, Jin T (2011) An overview of electrode materials in microbial fuel cells. Journal of Power Sources 196: 4427–4435

Zhu N, Chen X, Zhang T, Pingxiao W, Ping L, Jinhua W (2011) Improved performance of membrane free single-chamber air-cathode microbial fuel cells with nitric acid and ethylenediamine surface modified activated carbon fiber felt anodes. Bioresource Technology 102 (1):422–26

Zhuang L, Zheng Y, Zhou S, Yuan Y, Yuan H, Chen Y (2012) Scalable microbial fuel cell (MFC) stack for continuous real wastewater treatment. Bioresource Technology 106: 82–88

Zhuang L, Zhou S, Wang Y, Liu C, Geng S (2009) Membrane-less cloth cathode assembly (CCA) for scalable microbial fuel cells. Biosens. Bioelectron. 24: 3652–3656

Chapter-III

Study of Various Operating Parameters and Electrode Modification for Performance Enhancement in Plant Microbial Fuel Cells (PMFCs)

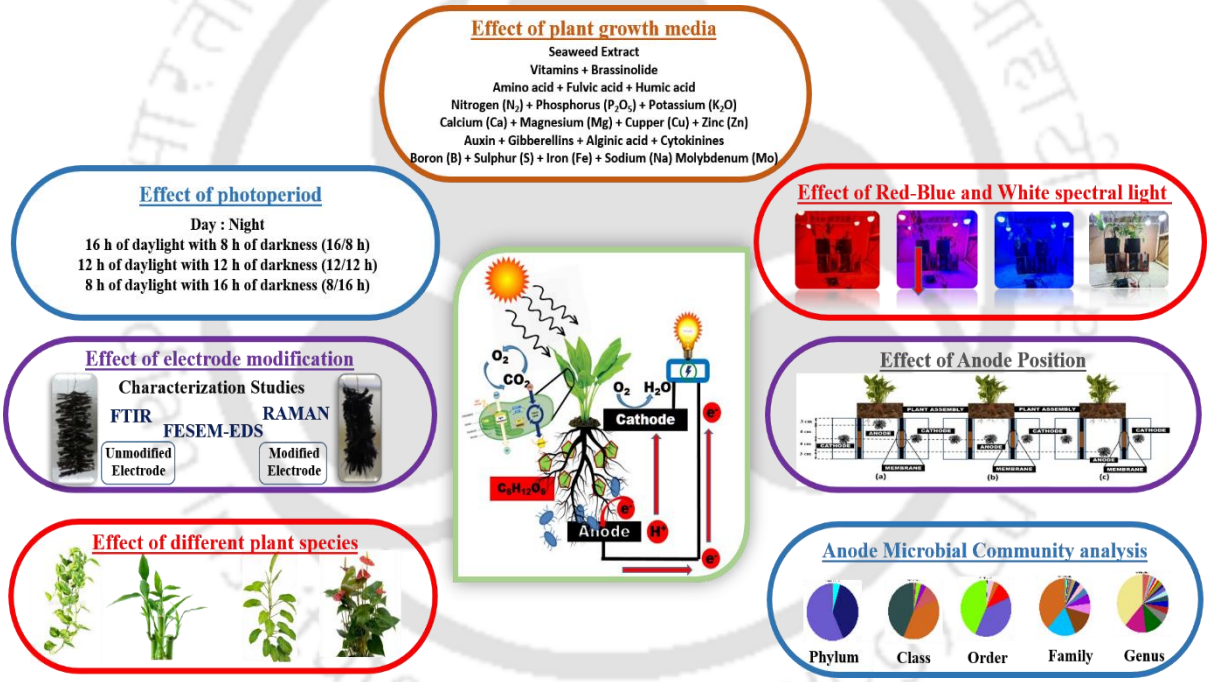

3.1 Overview

Indoor air pollution is known to be one of serious type of pollution prevailing in the indoor environment. To combat this, the easiest way is to grow indoor plants which are known to purify the indoor air by absorbing various air pollutants and are also believed to bring happiness and prosperity by purifying indoor atmosphere (Claudio 2011; Wolverton et al.,1989). Therefore, for this study, four different indoor plants were selected to obtain dual benefit of purifying indoor air and bioelectricity generation at the same time. These plants are easily available, requires minimal maintenance and has a high growth rate. The plants also provide no competition with food production, do not require direct sunlight and grows well in the range of 18-25 ^{o}C temperature. Different plants behave differently when intergraded in a PMFC environment. Therefore, this chapter highlights a fascinating comparative study of four different indoor plant species to find out best performer in terms of bioelectricity generation without compromising on growth.

In addition to plant species, a variety of factors plays a crucial role for improving bioelectricity generation capabilities in a PMFC including photoperiod, light source, growing media, setup design, electrode modification and its placement, presence of microbial community to name a few. The health of the plants in a PMFC plays a vital role for bioelectricity generation, owing to the fact that a healthy plant is equipped to perform photosynthesis in a better way and thus release nutrients for the microbes to breakdown. From the perspective of plant physiological, lights play a substantial role on plant photosynthesis and growth (Shuai et al., 2016). Several researchers have investigated the application of red and blue LEDs on the growth behaviour and photosynthetic activity of indoor plants (Pennisi et al., 2019; Piovene et al., 2015; Carvalho et al., 2016; Bantis et al., 2016). However, direct correlation study of different light source affecting bioelectricity generation in PMFCs was not performed previously.

Over the past decades, numerous electrode materials have been tested, and various modifications strategies showcases increase in surface area for improved biofilm development, thus enabling improved electron transfer rates. However, most of the electrode materials, including metals, graphite, carbon, composite, employed in the past and their modification strategies are complex and involves high cost and are practically unpromising. Also, the use of two different materials for anode and cathode separately increases the complexity of the MFC setup. On the other hand, the implementation of carbon fibre-based electrode for both anode and cathode is environmentally friendly and well suited for PMFC condition (Maqsud et al.,

2015). Placement of anode is as important as electrode modification as its placement close to plant roots does vitiates the PMFC performance owing to O_2 release through root exodus. An ideal PMFC setup should facilitate anaerobic oxidation at the anode and proper transport of proton towards cathode side.

Therefore, this study presents a comprehensive documentation of use of different types of indoor plants in PMFC, influence of numerous operating parameters on bioelectricity generation potential of PMFCs including study of effect of different photo periods, effect of red-blue-white light sources, role of composite plant growth media, role of electrode modification and anode location and finally carrying out microbial community analysis associated with bioelectricity generation in PMFCs.

3.2 Materials and Methods

3.2.1 Effect of plant species on bioelectricity generation in PMFC

To study the effect of plants species on bioelectricity generation in PMFCs, four different indoor plants viz., *Anthurium andreanum*, *Dracaena braunii*, *Epipremnum aureum* and *Philodendron erubescens* were incorporated in a three chamber PMFC with microalgal biocathode and comparative analysis was carried out (Fig. 3.1). The plants were grown in a plant assembly containing mixture of soil, compost and cow dung in 3:2:1 ratio. The chambers were separated by a ceramic membrane made up of Clay-55%, Bentonite-15%, Flyash-15%, Na_2Co_3-8%, Na_2Sio_3-2% and H_3Bo_3-5%. The electrodes used were the modified carbon fibre brush (Mentioned in detail in section 3.2.6). Anode chamber is filled with anaerobic microbial culture containing all the essential nutrients (Mentioned in detail in section 5.2.3.1). Nitrogen purging was done to maintain anaerobic conditions. Similarly, cathode chambers were inoculated with microalgal culture of *Chlorella sorokiniana* (Mentioned in detail in section 5.2.3.3). All PMFCs studies were conducted under indoor lightning conditions and maintained at a temperature of 23 ± 2 °C. The pH of the cathodic chamber was maintained around 7-7.5 by periodically purging CO_2 while anodic chamber was monitored using soil survey instruments (DSMM600, UX General Tools and Instruments, New York, USA). Detail regarding PMFC design evolution and development of biocathode and ceramic membranes were discussed in subsequent chapters.

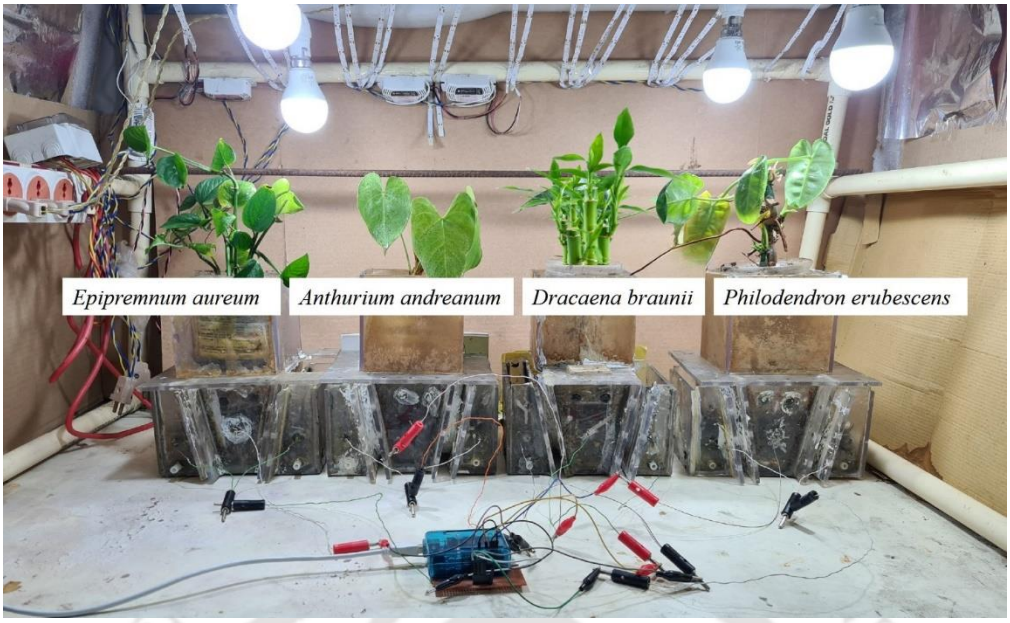

Fig. 3.1 Different plants used in PMFC.

3.2.2 Effect of Photoperiod on bioelectricity generation

To study the effect of photoperiods on the performance of the PMFCs, three different photoperiods were used, viz., 16 h of daylight with 8 h of darkness (16/8 h), 12 h of daylight with 12 h of darkness (12/12 h), and 8 h of daylight with 16 h of darkness (8/16 h). The photoperiod tests were conducted in a three chamber PMFC having microlagal bio-cathode with plant *Philodendron erubescens.* The test run was carried out in the following order: 16/8 h → 12/12 h → 8/16 h. The change of photoperiod was not done abruptly, instead 1 h per day change in photoperiod was implemented to reduce the light-related stress on the plants and were kept in a particular photoperiod for at least a month.

3.2.3 Effect of Red-Blue and White spectral light on PMFC performance

Red and blue lights is known to significantly affect the photosynthetic properties of plants (Lan et al., 2013; Wang et al., 2016). Therefore, to study and understand its effect on plant growth and in turn bioelectricity generation capabilities in PMFCs, four different light treatments (100% red, 100% blue, 50% blue + 50% red, 100% white) were applied with LED glow lights at 610 nm and 435 nm for red and blue spectrum respectively (Fig. 3.2). Each experimental conditions were fulfilled by four 9 W glow lights (Bajaj Electricals Ltd., India) with an average light intensity of 1200 lux measured during the light phase by using LUX meter (Lutron LX 101, Taipei, Taiwan). The light intensity was kept constant throughout the study. Two different plants viz., *Epipremnum aureum* and *Philodendron erubescens* were grown under the 12:12 h light/dark cycle at 23 ± 2 ^{o}C under indoor conditions in a three

chamber PMFC with microlagal bio-cathode. The initial and final total chlorophyll content (a and b) of microalgae *Chlorella sorokiniana* were measured by spectrophotometric method similar to previously studied PMFC with *Chlamydomonas reinhardtii* (Lan et al., 2013; Malakar et al., 2022). To calculate the concentration of chlorophyll in the sample, modified Arnon's equations were used as mentioned below.

Chlorophyll a: $16.72 \times A_{665} - 9.16 \times A_{652}$ (3.1)

Chlorophyll b: $34.09 \times A_{652} - 15.28 \times A_{665}$ (3.2)

Total Chlorophyll ($\mu g\ mL^{-1}$) = Chlorophyll a + Chlorophyll b (3.3)

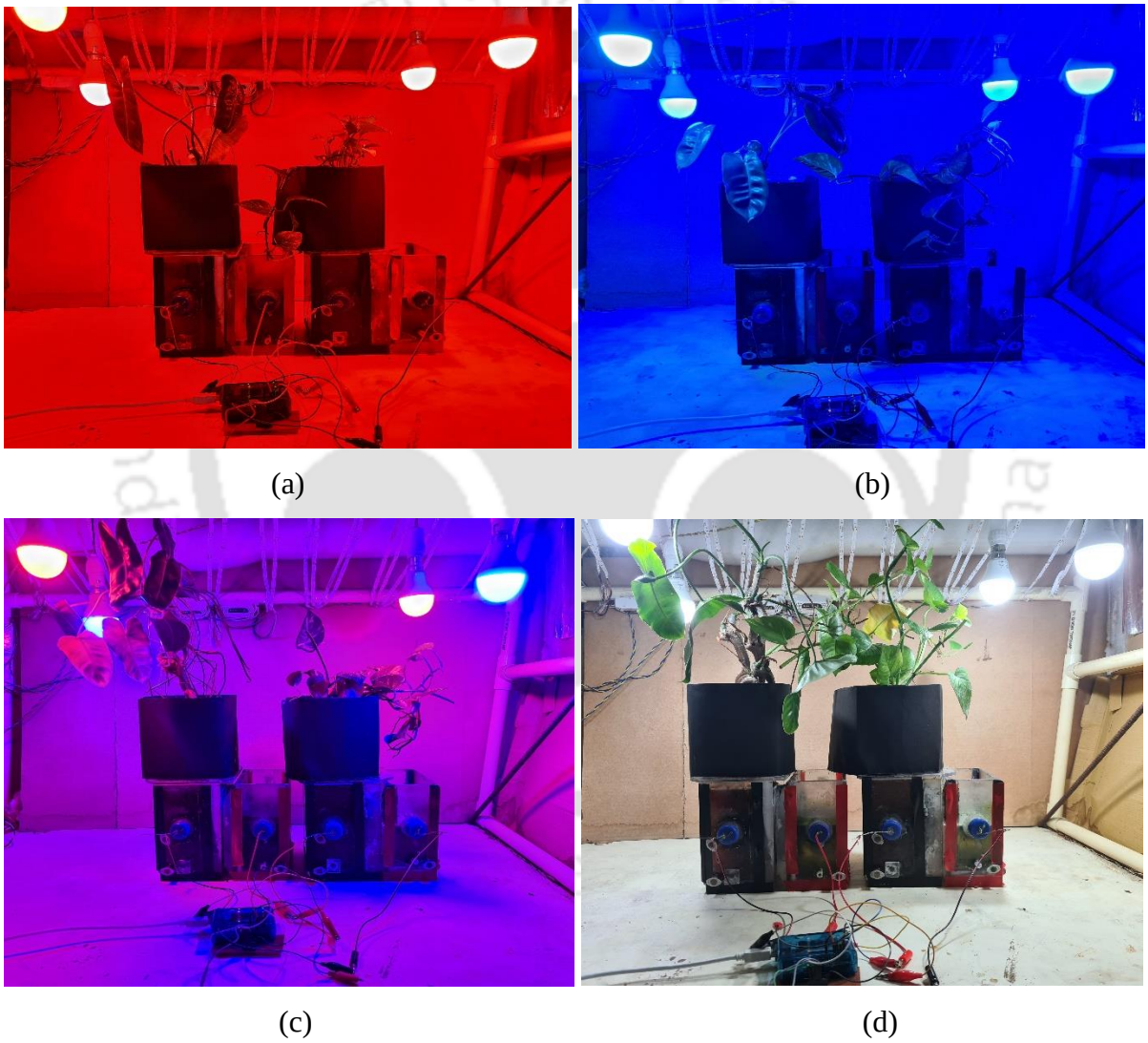

(a) (b)

(c) (d)

Fig. 3.2 Lab scale setup of PMFCs with plant *E. aureum* and *P. erubescens* under different lighting condition. (a) Red light (b) Blue Light (c) Red-Blue Light (d) White light.

3.2.4 Effect of plant growth medium on power output of PMFC

To understand the effect of growth medium on the power output of a PMFC, different types of plant growth inducing substances containing all the necessary macronutrients, micronutrients, hormones, vitamins, proteins etc., were mixed together to form a novel composite media to be used for the first time in a PMFC study. A 1000 mL solution was prepared by dissolving all the plant nutrients as per Table 1. 10 mL of the prepared nutrient solution was sprayed at the plant thrice a week.

For this study, two different three chamber PMFC were setup containing indoor plant *P. Erubescens*. To make a comparison analysis of effect of growth medium on plant growth and in turn bioelectricity generation, growth media was not sprayed in PMFC-I while plant assembly of PMFC-II was enriched by spraying 10 mL of growth media thrice a week. At the end of the study, plant biomass growth was measured in both the PMFC. This involves manually calculating number of branches and leaves. To evaluate the roots development, plants were removed from the plant assembly and roots were washed with water to remove soil particles and then measurements were taken.

Table 3.1 Composition of plant growth medium

Nutritional Ingredients	% by weight
Seaweed Extract	12
Amino acid + Fulvic acid + Humic acid	9
Nitrogen (N_2) + Phosphorus (P_2O_5) + Potassium (K_2O)	9
Calcium (Ca) + Magnesium (Mg) + Cupper (Cu) + Zinc (Zn)	64
Boron (B) + Sulphur (S) + Iron (Fe) + Sodium (Na) Molybdenum (Mo)	4
Vitamins + Brassinolide	2
Auxin + Gibberellins + Alginic acid + Cytokinines	1.5

3.2.5 Effect of electrode location on bioelectricity generation

Positioning of anode inside in a PMFC is very crucial for its performance. Placing anode away from the vicinity of roots, helps in creating better anaerobic conditions for microbes as plants are known to release oxygen via their roots (Liu et al., 2018). Plants are known to release oxygen through their roots in to the rhizosphere region and causes reduction in PMFC performance through root induced oxygen loss effect if anode is placed at the vicinity of roots (Liu et al., 2018). Therefore, in this study, three different positioning of the anode was tested as shown in the Fig. 3.3. Three different PMFCs were constructed with plant

Philodendron erubescens. Carbon fibre brush anode of size 5 cm in diameter was placed at three different locations i.e., 3cm, 7cm and 11cm respectively in three individual PMFCs as shown. Carbon fibre brush cathodes in all the PMFCs were fixed at 7 cm perpendicular to the membrane. The anode and cathode chambers of the PMFCs were inoculated with anaerobic and microalgal cultures respectively, and the chambers were separated by clay based ceramic membranes.

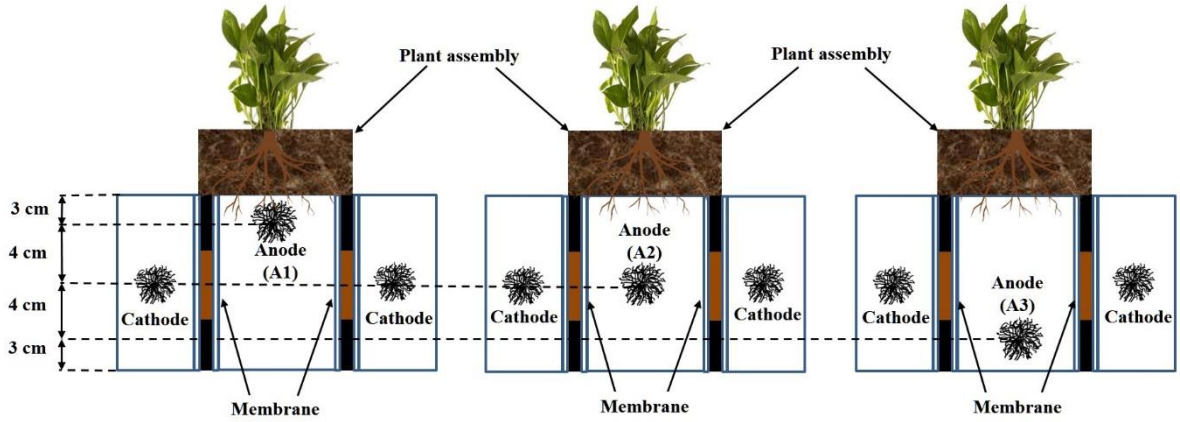

Fig.3.3 PMFCs setup with different positioning of anode A1, A2, A3.

3.2.6 Design, modification and characterization of the electrode

Electrode are the heart of a fuel cell, allowing development of microbial biofilm over it surface either at anode or cathode (bio-cathode). As previously discussed in chapter-II, the carbon fiber is known to be a suitable material for use in PMFC considering its cost effectiveness and eco-friendliness and particularly suited for PMFC operation and incorporating it in soil do not hamper root growth and development (Maqsud et al., 2015). The carbon fibre modification is an essential requirement for achieving improvement in biofilm development and bioelectricity generation capabilities of PMFCs.

Carbon fibre (Hindoostan Mills Limited, India) was used for making the electrodes. The carbon fibre surface modification was carried out by sonication using the ultra-sonication bath (50 Hz) containing H_2SO_4 and HNO_3 (3:1 v/v) for 1 h. Carbon fibre was thereafter washed with distilled water several times until pH of the washing solution reached 7. It was air dried prior to its use as brush anode (Numfon et al., 2012). For development of carbon fibre brush, the carbon fibre cloth was cut into the desired length and twisted to form brush with the help of copper wire for effective surface area development.

Morphological characterization of electrode surface was studied under Field Emission Scanning Electron Microscopy (FESEM Gemini 300, ZEISS). Elemental composition was determined by using Energy dispersive spectroscopy (EDX) coupled with FESEM. The KBr pellet technique was employed to record the Fourier transform-infrared (FTIR) spectra over a wavenumber range of 400-400 cm^{-1}. Raman spectra were recorded with LabRAM HR Raman microscope (laser: 514 nm).

3.2.7 Bacterial community structure analysis of bio anode

For analysis of microbial communities present in the anodic chamber of the PMFC, biofilm samples were collected from the surface of the brush anode and analyzed using 16S rRNA gene amplicon high-throughput sequencing. The analysis was carried out for closed-circuit PMFC during the consistent power generation period.

The hypervariable V3 and V4 regions of microbial 16S rRNA genes were amplified using universal primers: 341F (5′-CCTACGGGNGGCWGCAG-3′) and 805R (5′-GACTACHVGGGTATCTAATCC-3′). The 16S rRNA gene amplicons were sequenced on a MiSeq platform (Eurofins Pvt Ltd, Bengaluru, India). The resulting community of 16S rRNA gene sequence data were processed using QIIME (Milner et al., 2016). The sequences were assigned to operational taxonomic units (OTUs) with a 97% pair-wise identity threshold and classified taxonomically according to the Ribosomal Database Project (RDP) for use in the taxonomic analysis. Since each OTU may be made up of many sequences, therefore OTUs were subsequently picked by using the UCLUST clustering method against a closed reference table. A representative sequence from each OTU was determined based on the most abundant sequences in each OTU, and their taxonomic affiliation was assigned using the Green genes OTU database (version 13_8). This resulted in different chart figures at different taxonomical levels. The raw sequence was submitted to NCBI sequence read archive (SRA) database with the accession number PRJNA750906.

For phylogenetic analysis, the representative sequences of each OTU's, i.e., a single FASTA file containing one sequence per OTU's were extracted. Phylogeny was constructed using 50 most abundant representative sequences based on Multiple Sequence Alignment (MSA) via "MUSCLE" algorithm in QIIME, and maximum likelihood distance generated using 'FastTree' algorithm in QIIME (Arulmani et al., 2021).

3.2.8 Analysis and calculations

The start-up process of all the PMFCs was carried out under open circuit potential (OCP). This helps microbes and plants get acclimatized to its new environment and accelerate biofilm development at anode and cathode, respectively, during start-up. Close monitoring of the start-up phase was carried out by a multimeter (Fluke 17B+, Everett, WA, USA). Gradually, when stable cell potentials were obtained, all the PMFCs were connected to a data acquisition system (Arduino, Atmega 328P) linked to a personal computer. The potentials were recorded at regular intervals for the entire duration of the experiment. Once stable cell potentials were achieved continuously for a few days, PMFCs were connected in closed circuit configuration through an external resistance of 100 Ω for continuous measurement of operational voltage (OV). Using Ohm's law, the current I in Amperes (A) was calculated against OV

$$I = V/R \tag{3.4}$$

where V is the operating voltage in volts (V), and R is the external resistance in Ohms. The Power yield of the PMFCs was calculated by taking the square of the multiplication of current and known resistance (Provost et al., 2011).

$$P = I^2R \tag{3.5}$$

The polarization curve was then plotted by changing the external resistance values from 15 KΩ to 50 Ω using variable resistance. Power density and current density were normalized to anode surface area. During the 8th week of the experiment, after 18,000 s (5 h) of a closed circuit, polarization curve and power density curve was plotted for determining the maximum output power by prepared manually by adapting a series of external resistances, i.e., 15,000, 10,000, 1000, 560, 470, 330, 220, 150, 100 and 56, every 10 min from open circuit voltage. The equations (5.9) and (5.10) obtained current density and power density, respectively.

$$I = \frac{V}{\alpha R} \tag{3.6}$$

$$P = \frac{V^2}{\alpha R} \tag{3.7}$$

Where, α is the surface area of the anode. in our case anode surface area was taken into consideration. The total energy generation per week during the entire duration of the experiment was measured in Joules by using Eq (5.11)

$$(\mathrm{J/m^2}) = \Sigma P * t \tag{3.8}$$

Where, P = average power density in Wm^{-2} during a week and t = one week containing 604,800 sec.

All data measurements were done in triplicates and expressed as mean ± standard deviation (SD). Statistical analysis was carried out using Origin 9.0.

3.3 Results and discussion

3.3.1 Effect of plant species on bioelectricity generation

All the four PMFCs were operated for an extended period of over six months, to access long term durability and reliability as a sustainable source of bioelectricity. During this period, constant monitoring was done without adding any inoculum. The potentials were continuously recorded using an Arduino-based data logging system. The four plants grown in the PMFC reactors showed a significant increase in size and weight during the six-month operational period which confirmed that plant growth was unaffected by long term bioelectricity generation in a PMFC system. The plant *E. aureum* had grown from ≈ 15 cm to 75 cm whereas, *P. erubescens, A. Andreanum* and *D. braunii* had grown from ≈ 18 cm to 40 cm, ≈ 10 cm to 24 cm, and ≈ 17 to 23 cm respectively. The plant *E. aureum,* a climber, showed maximum increase in height followed by *P. erubescens,* whereas the other two plants did not show any significantly increase in height. However, among all the four plants number, three plants viz., *E. aureum, P. erubescens, A. Andreanum* showed increase in number of branches, whereas in case of *D. braunii,* the growth was almost stagnant as seen in Fig. 3.4a. The voltage generation pattern remained almost constant at around 1V from the 12^{th} week onwards in case of PMFC with *P. erubescens* with a highest power density of 32.21 mW m^{-2} among all (Fig. 3.4a, Table 3.2). The results show that the PMFC can sustain bioelectricity generation for an extended period. Whereas, a low voltage in case of *D. braunii* can be attributed to its stagnant growth. During the stable state condition, the total energy production per week was almost constant, with *P. erubescens* being the species with the best performance at 234 J. This is followed by *E. aureum, A. Andreanum* and *D. braunii* with 204 J and 187 J, 155 J respectively. This stable energy generation was possible because of the continuous nutrient supply from plants' thereby sustaining the microbial biofilm and its metabolic activity and resulting in higher and prolonged energy generation. Here, the plant's root hairs elongation in the anodic chamber plays a pivotal role in ensuring proper plant nutrient availability for the microbes. All the measured electrical parameters were summarised in Table 3.2.

Table 3.2 Performance of different PMFCs.

Electrical parameters	*A. andreanum*	*D. braunii*	*E. aureum*	*P. erubescens*
Open circuit potential (mV)	810 ± 8	626 ± 6	900 ± 10	1020 ± 8
Operating voltage (mV)	468 ± 8	312 ± 6	510 ± 4	586 ± 4
Max. current density (mA m^{-2})	49 ± 1.6	32 ± 1.4	57 ± 1.4	63 ± 1.2
Max. Power density (mW m^{-2})	22.37 ± 0.6	18.6 ± 0.8	27.63 ± 0.6	32.21 ± 0.4
Internal Resistance(ohm)	220 ± 5	263 ± 5	210 ± 5	189 ± 5

The long-term study was significant to analyze the behavior of all these plants species. The difference in power generation in *P. erubescens* with respect to other species could be due to different types of root systems. *P. erubescens* has a thick root system, while the *E. aureum* and *A. Andreanum* have finer root systems. Moreover, roots development is progressive in the order *P. erubescens* > *E. aureum* > *D. braunii* > *A. Andreanum* (Fig. 3.4b). *A. Andreanum* was more difficult to maintain among all plants because of its low tolerance to moisture conditions. On the other hand, *P. erubescens* and *E. aureum* did not require much maintenance and responded more efficiently to moisture conditions, which was needed to enhance performance in PMFC environments (Apollon et al., 2020). As a result, *P. erubescens* and *E. aureum* survived for a more extended period of time exceeding six months while *A. Andreanum* died gradually. Long term growth of all the four plants were also monitored outside PMFC condition in the same indoor environment. Growth pattern of *P. erubescens*, *E. aureum* and *D. braunii* were almost similar both inside and outside PMFCs, however *A. Andreanum* being a slow growing plant stays heathy outside PMFC environment. A few comparative performance analysis of different PMFCs by various researchers incorporating various plants were summarized in Table 3.3.

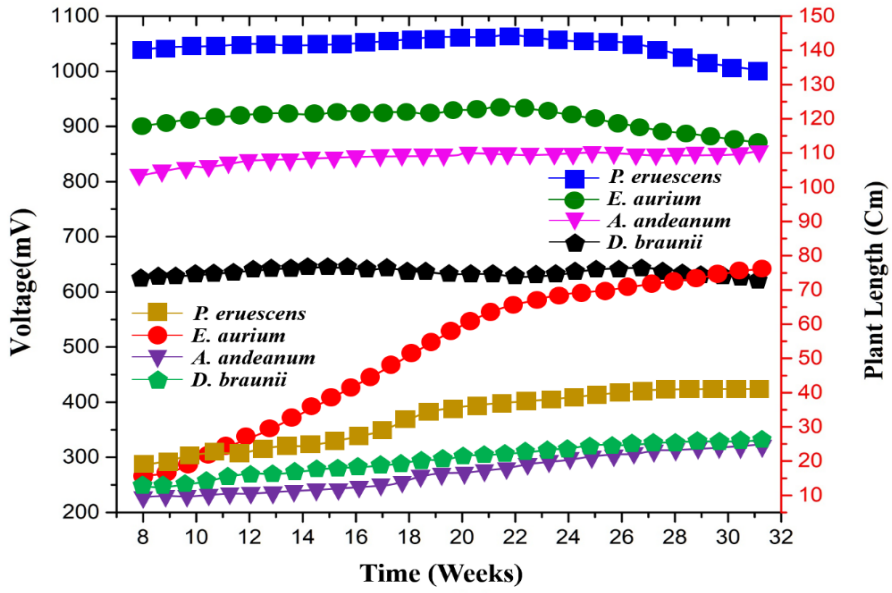

(a)

(A) (B) (C) (D)

(b)

Fig. 3.4 (a)Long term performance with voltage generation and plant growth for all PMFCs (b) Roots development after 32nd Week [(A) *P. erubescens* (B) *E. aureum* (C) *A. Andreanum* (D) *D. braunii*].

Table 3.3 Comparision of various PMFCs performance

Plants used	Membrane used	Operation time (days)	Electrode used	Max. voltage (mV)	Max. Power Density (mW m^{-2})	Electron acceptor (catalyst)	Reference
S. anglica	CEM	180	graphite felt	-	222	Potassium ferric cyanide	Helder et al., 2010
A.anomala				400	22		
Rice plant	Soil		Carbon fiber	700	23	O_2	Moqsud et al., 2015
I. aquatic	Gravel	40	granular activated carbon (anode)	650	12.42	O_2	Liu et al., 2013
			stainless steel mesh (cathode)				
L. minuta	Water filter	45	carbon felt	700	380	O_2	Hubenova and Mitov, 2012
Rice plant	soil	120	graphite felt	300	6	O_2	Kaku et al., 2008
S. anglica	CEM	703	graphite felt	600	440	Potassium ferric cyanide	Helder et al., 2012
S. anglica	BPM	151	graphite felt	600	679	O_2(bacteria)	Wetser et al., 2015
P. australis	UFM	136	graphite felt	~600	22	O_2	Wetser et al., 2017
S. anglica					82		
G. maxima	Tubular	85	Graphite felt	-	10	Potassium ferric cyanide	Timmers et al., 2013
	UF		Graphite granules	-	12		

3.3.2 Effect of Photoperiodism on bioelectricity generation

Photosynthesis is a light driven process, hence duration of photoperiod is crucial for plant productivity. To understand the best photoperiod among the three, that improves PMFCs electricity production, the power densities were compared considering 21 days' experimental period in a two chamber PMFC. Since excessive light induces photo inhibition resulting in decrease in photosynthetic efficiency, hence photoperiod was not increased beyond 16 h. The average power density over three photoperiods of 16/8 h, 12/12 h and 8/16 h was found to be 24.38 ± 0.8 mW m^{-2}, 23.64 ± 1.4 mW m^{-2} and 21.38 ± 0.4 mW m^{-2}, respectively. The power output during photoperiods of 16/8 h and 12/12 h showed nearly similar results however, when the PMFCs were exposed to lesser duration of lights i.e., photoperiods of 8/16 h the power output decreases (Fig. 3.5). There was no adverse effect of drop in power density observed while shifting from one photoperiod to another as change in photoperiod was done in very gradual manner. Since photoperiod of 12/12 h light and dark cycle closely resembles natural lighting process considering the geographical location of the study, therefore for optimum utilization of both the plants at bio anode and microalgae at the bio cathode the said photoperiod was used for all succeeding studies. There was no significant variation in power output was observed during light and dark phase in all photoperiods. This may be because of the fact that bioelectricity generation process in a PMFC is not only dependent on plant photosynthesis process rather a mutual operational process of plants and microbes which works day and night.

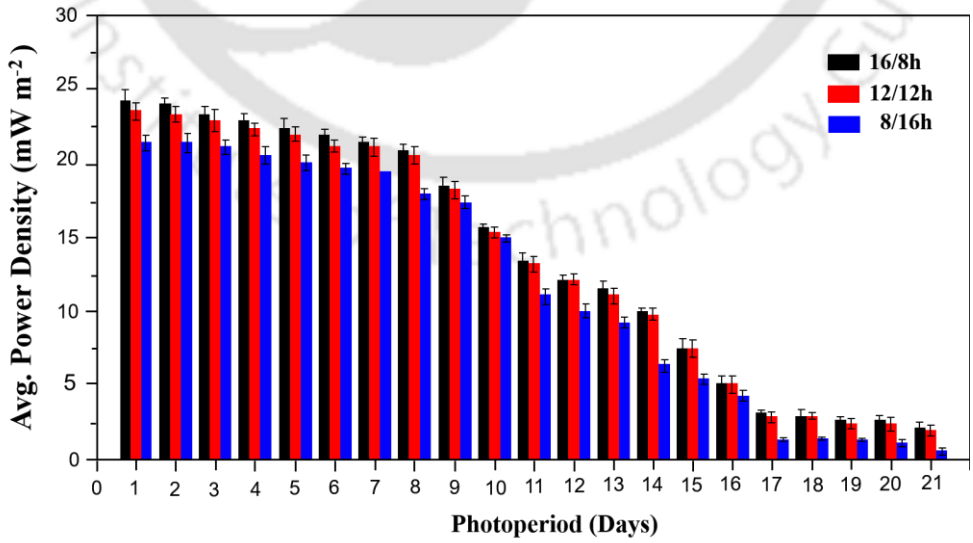

Fig. 3.5 Bioelectricity generation under different photoperiod with plant *P. erubescens*.

3.3.3 Effect of Red-Blue spectral light of PMFC performance

The voltage generation pattern by two indoor plant *E. aureum* and *P. erubescens* were studied under different lighting conditions. The behaviour of both the plants were similar with respect to the change in lightening condition. For ease of representation, OCV generated by PMFC with plant *P. erubescens* is presented in Fig.3.6a during two months' study period. Among the two different lights tested blue light alone had a significant effect on performance of the PMFC as compared to red light. On another instant when blue light is supplemented with red lights the voltage generation is further increased. The white light on other hand shows highest PMFC performance among all. PMFC arrangements under different lightening conditions can be seen in Fig. 3.6a and corresponding power densities were documented in Table 3.4. The max power density obtained from PMFC with *P. erubescens* exceeds PMFC with *E. aureum* and the respective values were 26.42 ± 0.4 mW m^{-2} and 22.38 ± 0.4 mW m^{-2}. The two indoor plants viz., *E. aureum* and *P. erubescens* have different morphological features in terms of growth characteristics. The *E. aureum* plant being a climber shows rapid elongation of stems as compared to *P. erubescens*. However, *P. erubescens* has extensive root system as compared to *E. aureum* which may help in easy release of nutrients through root exodus resulting in a higher performance delivered by PMFC with *P. erubescens* as compared with plant *E. aureum* under similar conditions. The biomass increase was seen in both the plants, which is highest in case of white light and least in case of red light. A detail long term effects of red and blue light on plant growth and development and understanding plant physiological response to changes in lights can be found elsewhere (Zheng et al., 2017; Pennisi et al., 2019).

The variation in lightening condition not only affect the growth of plants but also the photosynthetic organism present at the bio cathode i.e., *Chlorella sorokiniana*. Initially during the start of the experiment, the cathode chamber looked light green, while the chlorophyll concentrations measured were 3.09 ± 0.046 µg mL^{-1} (Chlorophyll a=1.36 µg mL^{-1}, chlorophyll b=1.73 µg mL^{-1}). The photosynthetic activities of the microalgae were reflected by chlorophyll concentrations which carry out photolysis of the water that releases oxygen needed as terminal electron acceptor. During the later operational period, the cathodic chamber culture turned dark green as a result of increased chlorophyll content with time, however maximum chlorophyll concentration of 29.36 ± 1.6 µg mL^{-1} (chlorophyll a=13.76 µg mL^{-1}; chlorophyll b=15.58 µg mL^{-1}) was obtained under white light conditions at the end of two months. However, a much

thicker concentration of algal biomass limits light penetration inside the chamber due to self-shedding effects (Yadav et al., 2020). The values of initial and final chlorophyll concentration were summarized in Table 3.4 considering an average value among the two PMFCs. It can be seen that a single source of white light enhances plant and microalgal biomass at the same time, which results in increase in power density as compared to other light sources.

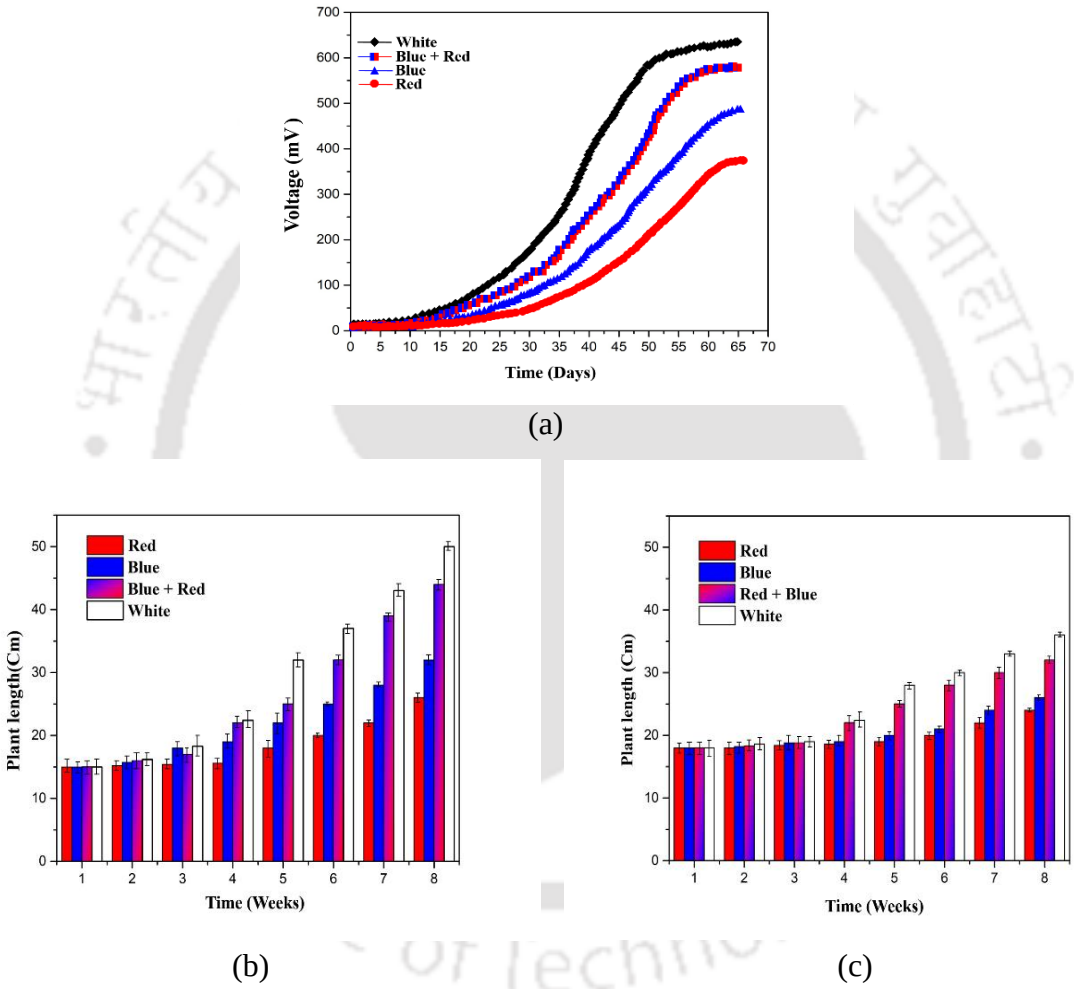

Fig. 3.6 (a) Variation of voltage generation with time under different lighting condition. Plant growth pattern under different lighting conditions (b) *E.aureum* and (c) *P.erubscence*.

Table 3.4 Effect of light quality on plant growth and chlorophyll concentration of *C. sorokiniana* and variation in power densities of PMFCs.

Plant Species	Light Quality	Plant Length (cm)	Power Density (mW m^{-2})	Total Chlorophyll (µg mL^{-1})	
				Initial	Final
E.aureum	Red	25 ± 1.5	12.46 ± 1.4	3.09 ± 0.046	19.36 ± 2.0
	Blue	32 ± 1.6	16.21 ± 0.6		22.42 ± 1.6
	Red + Blue	44 ± 1.5	20.26 ± 1.1		26.67 ± 1.2
	White	51 ± 1.2	22.38 ± 0.4		28.42 ± 1.4
P. erubescens	Red	23 ± 0.5	15.32 ± 1.2	3.09 ± 0.046	20.12 ± 1.8
	Blue	25 ± 0.8	17.20 ± 0.8		21.46 ± 1.4
	Red + Blue	32 ± 0.6	22.86 ± 1.6		27.56 ± 1.0
	White	36 ± 1.0	26.42 ± 0.4		29.36 ± 1.6

3.3.4 Effect of plant growth medium on power output of PMFC

It was observed that the during the whole experimental period, the PMFC-II was performing better than the PMFC-I owing to healthier condition of the plant in PMFC-II as compared to PMFC-I. Fig. 3.7A represent the initial period of PMFC-I and PMFC-II, where growth of both the plants were identical. From the shoot and root development of both the plants during the end of the experiment, it was seen that, *P. erubescens* plant in PMFC-II has large number of leaves and better roots development as compared to PMFC-I (Fig. 3.7B) owing to the use of growth media. The bioelectricity generation pattern in both the PMFCs were presented in Fig. 3.7B.

It can be seen that the initial period (first 40 days) both the PMFCs performed similarly, however during the steady state period, PMFC-II has higher voltage generation of 846 ± 5 mV as compared to PMFC-I 768 ± 5 mV (OCV). This phase indicates a high amount of energy accumulated inside anodic biofilm. During this steady state, PMFCs were connected to an external resistor of 1000 Ω resulting in drastic voltage drop and power density and current density increases as the bacteria captures low energy (Khudzari et al., 2018). The maximum power density of 27.41 mW m^{-2} and a current density of 51.60 mA m^{-2} was obtained from PMFC-II, which was an overall 31% increase in power generation with respect to PMFC-I with a corresponding value of 21.30 mW m^{-2} and of 44.52 mA m^{-2} respectively. The higher power and current density obtained during the steady state (starts from the scale marked as zero) also confirms that the nitrate and sulphate reduction do not significantly affect voltage generation as reported in literature. This may be

because of the fact that a heathy plant releases sufficient nutrients through root exodus for the bacteria to breakdown and release electron at the anode to be supplied at the cathode side. However, over time due to the depletion of carbon source, the voltage drops quickly in both the cells. In this phase also PMFC-II performs better due to good root exodus as compared to PMFC-I under similar condition. Thus, voltage generation is not affected. However, a lot of study need to be carried out in near future to confirm this fact.

(a)

(b)

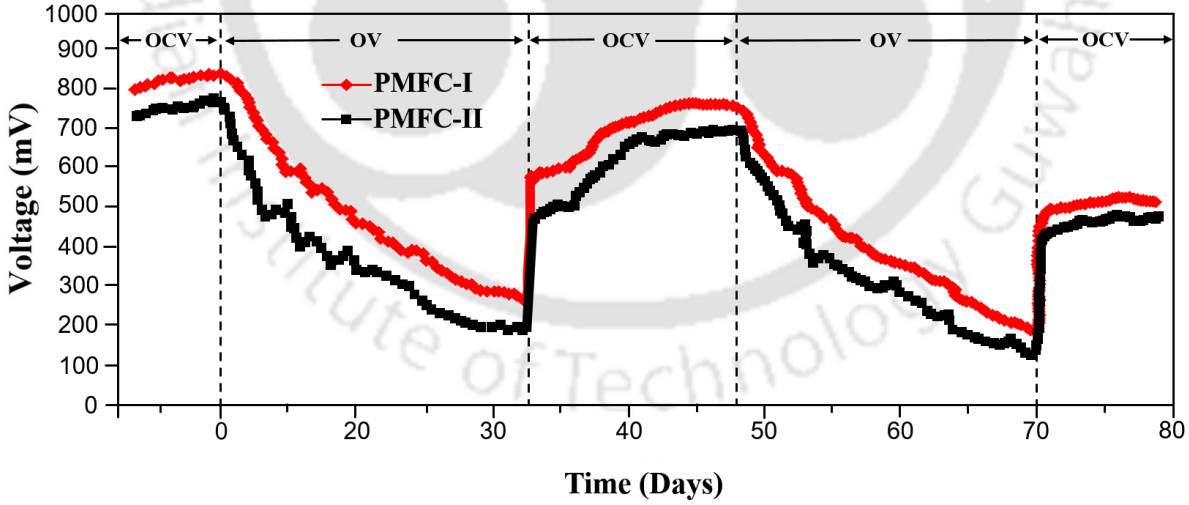

(c)

Fig. 3.7 (a) PMFCs setups at the start of the experiment (Left side: PMFC I, Right side: PMFC II) (b) Shoot and roots growths at the end of the experiment (A) PMFC I (B) PMFC II. (c) Voltage generation pattern of PMFC I and PMFC II under OV and OCV condition during steady state.

3.3.5 Effect of electrode location on bioelectricity generation

To study the effect of anode positioning, all the PMFCs were initially operated under open circuit voltage (OCV) condition until a constant stable voltage starts to appear after 6th week to be considered as steady state. All the PMFCs were then connected to a 1k Ω resistor to measure operating voltage (OV). It was interesting to note that anode potential measured against Ag/AgCl electrode increases with the depth of positioning of anode from A1 to A2 but decreases slightly at A3 (Fig. 3.8a). However, cathode potential remains almost similar. Therefore, OCV differences were caused by anode potential. The maximum OCV and OV were obtained in case of PMFC with anode A2 and not with PMFC with A3. To further investigate the reason for this voltage difference, the oxygen profiles of all the three PMFCs were measured quantitatively using an electrochemical O_2 microsensor (Unisense OX-25). The O_2 concentration significantly decreases as we go down from 3 cm to 11 cm resulting in more anoxygenic environment which is favourable for anaerobic oxidation of organic matter. However, at the same instance, the positioning of electrode and membrane in a cell plays a significant role in proton exchange which in turn drives reduction reaction at cathode. In the PMFC with anode A3, the positioning of the anode is far away from the membrane surface as compared to PMFC with anode A2, thereby increasing solution and mass transfer resistance, whereby protons have to travel a longer distance from anode to cathode as mentioned by Logan (2008). Also the reason for lower electrogenic activity near A3 region might be because of lesser availability of root exodus. Therefore, it may be confirmed that the positioning of electrode and membrane is very critical for PMFC performance and in this study PMFC with anode A2 shows one of the favourable configurations where in anode, membrane and cathode are aligned in a single line and are nearest to one another. The power density and current density of the PMFC with anode A2 (at a 7 cm depth) respectively were 2.2 times and 3.5 times higher, as compared to PMFC with anode A1 (at a 3 cm depth) (Table 3.5).

Also, it was observed that, PMFC with anode A1 had relatively greater variation in OCV as compared to PMFC with anode A2 and anode A3. This may be because of influence of leakage of oxygen due to inter-junction transition from plant assembly to anode chamber or plant roots causing continuous changes in pH and oxygen content which is relatively less as we move deeper. Therefore, placing anode into the soil containing plant roots or near to roots as in anode A1 may shows difference in the PMFC performance because of root induced oxygen loss effect (Fig. 3.8b).

Therefore, anode and membrane positioning inside a PMFC plays an important role to obtain best performance in terms of bioelectricity generation.

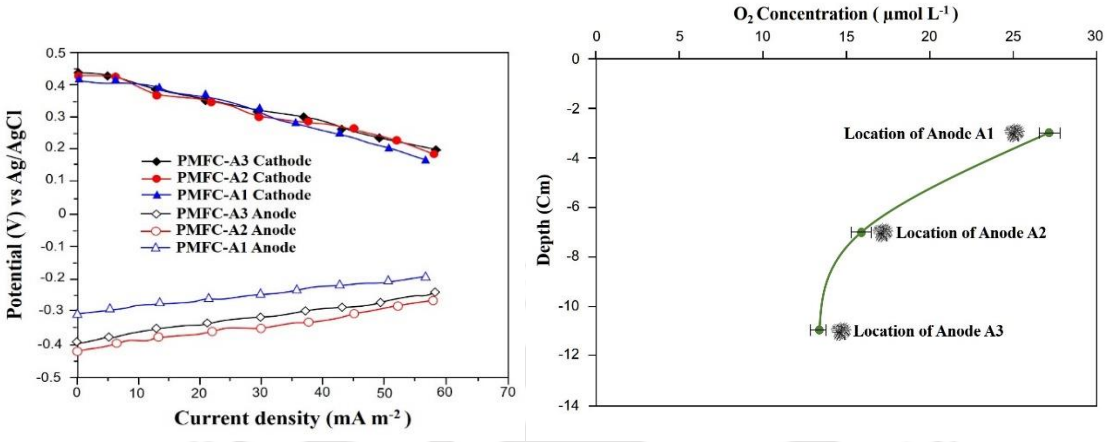

(a) (b)

Fig. 3.8 (a) Bio-electrochemical behavior of three PMFCs showcasing anode and cathode cell potential (b) Oxygen concentration profiles at different anode depth A1, A2, A3.

Table 3.5 Performance analysis of PMFCs with anodes at different depth.

Electrical parameters	PMFCs with different Anode Position		
	A1	A2	A3
Open circuit voltage (mV)	780 ± 2	842 ± 5	806 ± 2
Operating voltage (mV)	376 ± 2	486 ± 2	440 ± 2
Max. current density (mA m^{-2})	15.04 ± 0.2	52.65 ± 1.2	45.46 ± 1.8
Max. Power density (mW m^{-2})	12.46 ± 0.6	27.21 ± 0.8	24.30 ± 0.6
Internal Resistance(Ω)	280 ± 5	220 ± 5	266 ± 5
O_2 Profile at bottom (µmol L^{-1})	27.25 ± 1.4	15.4 ± 2.0	13.6 ± 2.0

3.3.6 Morphological characterization of electrode

3.3.6.1 FTIR analysis

To examine the change in chemical properties of the carbon fiber before and after the acid treatment, the FTIR studies of carbon fiber were carried out. FTIR spectra of acid treated carbon fiber and untreated carbon fiber were presented in Fig. 3.9a. The broad band obtained at 3436 cm^{-1} and 1590 cm^{-1}, can be ascribed to stretching vibration of OH and C=O of ketone and carboxyl

groups, respectively. The Presence of a notable peak at 1036 cm^{-1}, confirmed the bending vibration of –OH. The relative intensities of the peaks listed above were increased after the electrochemical oxidation treatment of carbon fiber cloth, indicating the formation of alcohol and carboxyl functional groups on its surface. These functional groups helped to enhance the electron transfer between electro-catalytic surface of bacteria and the electrode, owing to the formation of hydrogen bonding between these functional groups of electrode with peptide bonds present in bacterial cytochrome (Crittenden et al., 2006). They also demonstrated that the carboxylic acid terminus of the modified electrode can facilitate binding of bacterial cytochrome on its surface, thereby increasing the current production owing to the enhanced transfer of electrons from the interior of the cells.

3.3.6.2 Raman analysis

The structures of the carbon fibre were analyses before and after acid treatment and the resulting changes in structural features were compared using Raman spectroscopy. Raman spectroscopy is a powerful non-destructive tool for distinguishing ordered and disordered crystal structures of carbon. As shown in Fig. 3.9b, characteristic carbon peaks were observed at 1349 and 1585 cm^{-1}, demonstrating that the presence of carbon in a disordered structure. The D band around 1349 cm^{-1} is associated with the disordered microstructure of carbon materials, while the G band at about 1585 cm^{-1} corresponding to the E_{2g} mode of graphite is assigned to graphitic carbon (Sun et al., 2013). The ID/IG ratio, which derives from the peak intensities of D and G bands, is used to evaluate the graphitic degree and analyse the structural features of carbonized materials. The ID/IG of treated carbon fibre is 0.89, which is lower than the untreated portion (1.02), indicating that acid modified carbon fibre has higher graphitic degree and lower disordered structure, that was beneficial for electrode performance (Chen et al., 2018).

3.3.5.3 FESEM- EDS analysis

The morphological characterization of carbon fibre were carried out by FESEM analysis wherein finer details of the carbon fibres were observed. Acid treatment of carbon fibre resulted in enhancement of the fibrous nature of the material. FESEM images confirms development of favourable environment for bacterial attachment to the electrode, which may have resulted from

hydrogen bonding between the bacterial cytochrome and carboxyl group of the electrochemically oxidized carbon fibre.

A comparative performance analysis of acid treated and untreated carbon fibre brush anode was carried out in a two chamber membrane less PMFC using plant *E. aureum* and *D. braunii*. The detail description of the PMFC setup is presented in Chapter-V. The results confirm higher bioelectricity generation using acid treated electrodes as compared to untreated one (Table 3.6). Therefore, the electrochemically active bacteria that colonized on the anode surface appeared to facilitate the electron transfer from bacteria to anode. It was seen that small quantities of bacterial colonies were formed on the surface of the untreated carbon fibre brush anode, whereas significantly large, thick, and dense biofilms were formed on the surface modified anode.

The carbon fibre is very well suited for soil micro environment (Maqsud et al., 2015) therefore it helps to achieve a stable long term performance in PMFC system. Fig. 3.9d showed carbon fibre brush electrode enclosed by plants roots (*E. aureum*), from which it was clear that carbon fibre does not affect the root development process as an electrode, thereby ensuring proper plant nutrient availability in the chamber. Also, a higher concentration of root development resulted in release of surplus substrates for microorganism to metabolize and thus enhanced metabolic activity resulting in higher bioelectricity generation.

EDS attached to FESEM revealed the carbon content of both acid treated and untreated carbon fibre. It can be seen that after acid treatment, carbon content decreases from 91.80 to 87.02 wt%. whereas concentration of constituents such as O, Al, S increase marginally (Fig. 3.9d).

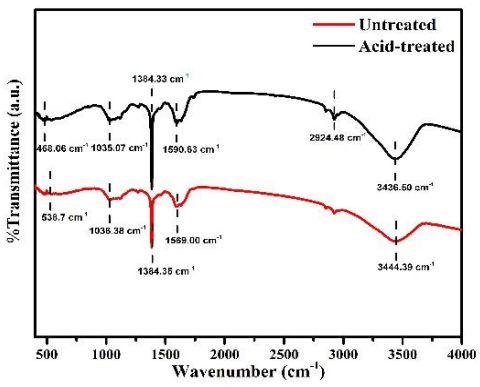

(a)

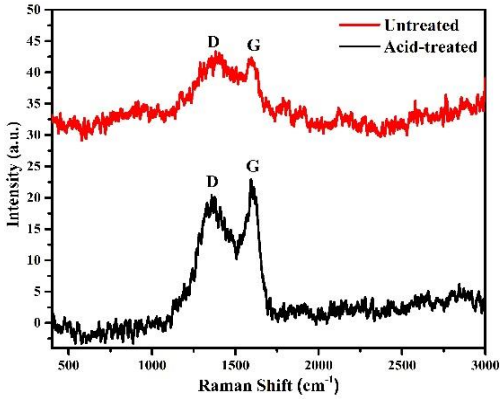

(b)

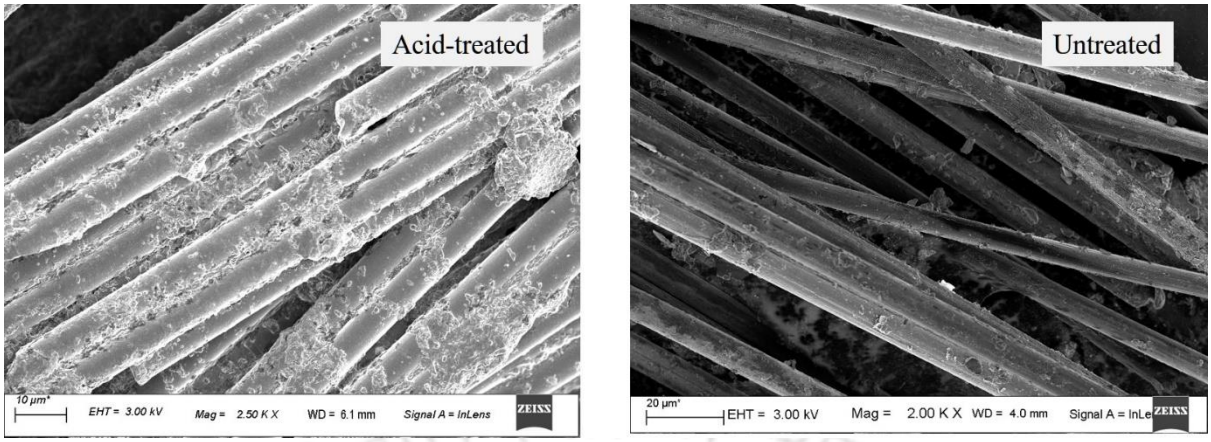

(c)

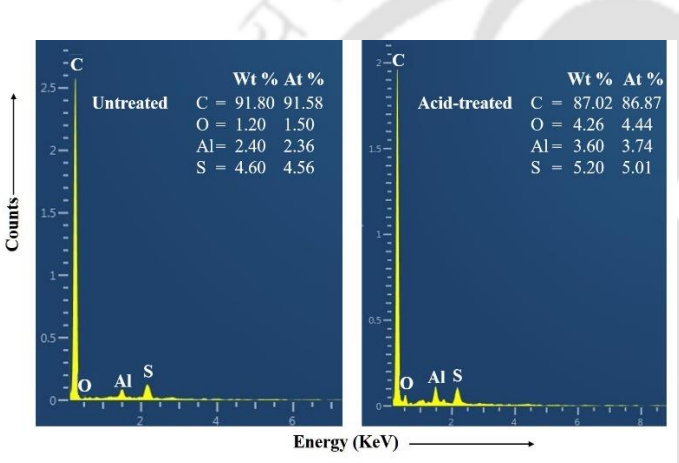

(d)

(e)

Fig. 3.9 Surface compositions of the carbon fibre electrode (a) FTIR spectrum (b) Raman spectrum (c) FESEM image of carbon fibre showing microbial biofilm development and (d) EDS spectrum (e) Plant root development enclosed around anode.

Table 3.6 Comparision of voltage, power and current generation with modified and unmodified electrodes.

PMFCs	Peak Voltage (mV)	Max. Power density (mWm^{-2})	Max. Current density (mAm^{-2})
Epipremnum aureum (acid treated)	620	15.38	38.46
Epipremnum aureum (untreated)	466	14.06	20.76
Dracaena braunii (acid treated)	432	12.42	16.23
Dracaena braunii (untreated)	276	10.60	7.54

3.3.7 Bio-anode microbial community analysis

The microbial community distribution over the biofilm was obtained, and 16S rRNA gene pyrosequencing libraries of our bacterial sample KMPJS were constructed with around 178,754 high-quality reads for each library. A total base of 70,850,454 was generated, resulting in 70.85 Mb Data. The Good's Coverage estimator indicated that the sizes of libraries were sufficient to cover 97%-99% of the bacterial communities.

The distribution of relative abundance profiles of OTUs in samples with taxonomic assignments was carried out from the data and plotted at various taxonomic levels. The various pie charts showed the absolute abundance of each division within each bacterial community. From Fig. 3.10a, it can be inferred that the most abundant phyla are Firmicutes (56.84%) and Bacteroidetes (38.45%). The most commonly reported phyla obtained from BES with a high level of dominance are known to be Proteobacteria, Firmicutes, and Bacteroidetes. The presence of these phyla is also known to produce higher performance in an MFC [4]. Among these, the most widely reported one is Firmicutes, a dominant integral member among bacterial communities favoring electron shuttling mechanism. Within the phylum Firmicutes, the most abundant class obtained is Clostridia (43.4%), belonging to order Clostridiales (42.96%). The most abundant family of bacteria obtained were Porphyromonadaceae (38.37%) belonging to Bacteroidetes phyla. However, the abundant genus remains unclassified from Porphyromonadaceae Family (38.32%). The second most dominant bacteria obtained was *Sporanaerobacter* (13.71%), belonging to phylum Firmicutes. The phylogenetic tree was constructed based on 16s rRNA gene sequences data of anodic biofilm (Fig. 3.10b). Top 50 OTUs were aligned in the form of a phylogenetic profile where most microbes belong to phylum Firmicutes, Bacteroidetes.

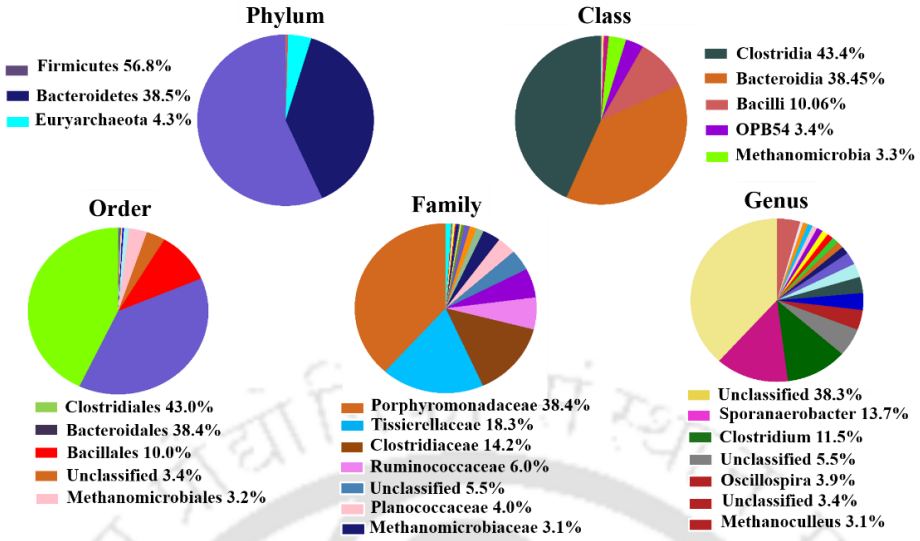

(a)

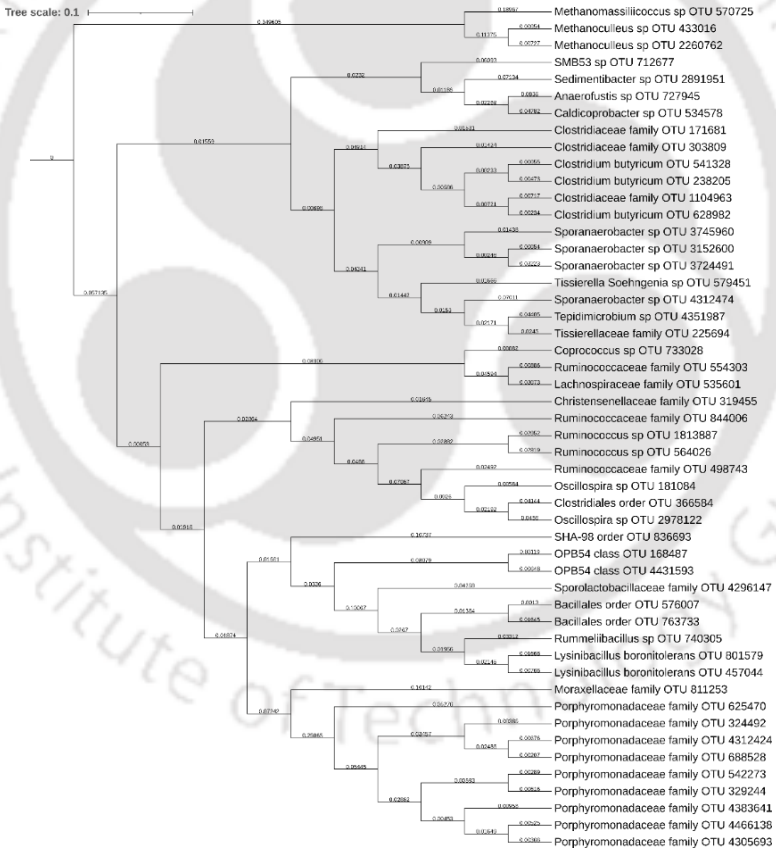

(b)

Fig. 3.10 (a) Taxonomical distribution of microbial community at different level (b) Phylogenetic tree of Top 50 OTUs for "KMPJS".

3.4 Conclusion

This study signifies the importance of different operating parameters playing a crucial role in growth and development of plants in a PMFC. The photoperiod in a PMFC operated with microalgal bio cathode is an important factor where in an optimum duration of light-dark period is highly essential for growth of both the organisms. The study demonstrated that 12/12 h light and dark phase was optimum to extract maximum performance from PMFCs without creating operational stress. Also, the addition of novel plant growth media can influence plant growth and power generation in a PMFC. The study also demonstrated that white light is more effective than any other source of light for enhancing plant growth and increasing microalgal chlorophyll concentration at the bio cathode. Electrode modification is an important criterion for biofilm development and enhancing performance of PMFCs. The power density and current density increased significantly when carbon fibre was modified by acid treatment. The configuration of PMFC setup and placement of electrodes and membranes are highly important criteria affecting utilization of anaerobic environment necessary for PMFC performance. Plant species also plays an important role in performance of PMFC. Among all the plants' species, *Philodendron erubescens* showed the best performance as compared to the other species with a maximum power density of 32.21 mW m^{-2}. A long-term performance study showed that the better root development and adaptability of plant species under moist conditions enhanced PMFC performance and stability, reducing the cell's internal resistance. Anode microbial community structure shows Firmicutes (56.84%) and Bacteroidetes (38.45%) as the most dominating bacteria present.

References

Apollon W, Kamaraj SK, Espino SH, Segovia CP, Montero LV, Ruelas VM, Marco AV, Medina RO, Silvia FB, Juan FG (2020) Impact of Opuntia species plant bio-battery in a semi-arid environment: demonstration of their applications. Applied Energy 279:115788

Arulmani SRJ, Gnanamuthu HL, Sabariswaran KC, Govindarajan G, Alsehli M, Ashraf EA, Pugazhendhi A, Zhang H (2021) Sustainable bioelectricity production from *Amaranthus viridis* and *Triticum aestivum* mediated plant microbial fuel cells with efficient electrogenic bacteria selections. Process Biochemistry 107: 27–37

Bantis F, Ouzounis T, Radoglou K (2016) Artificial LED lighting enhances growth characteristics and total phenolic content of *Ocimum basilicum*, but variably affects transplant success. Sci. Hortic. 198: 277–283

Carvalho SD, Schwieterman ML, Abrahan CE, Colquhoun TA, Folta KM (2016) Light quality dependent changes in morphology, antioxidant capacity, and volatile production in sweet basil (*Ocimum basilicum*). Frontiers in Plant Science 71328

Chen S, Tang J, Jing X, Liu Y, Yuan Y, Zhou S (2016) A hierarchically structured urchin-like anode derived from chestnut shells for microbial energy harvesting. Electrochimica Acta 212: 883–889

Claudio L (2011) Indoor air quality. Planting Healthier Indoor Air Environmental Health Perspectives 119(10), 426-427.

Crittenden SR, Sund CJ, Sumner JJ (2006) Mediating electron transfer from bacteria to a gold electrode via a self-assembled monolayer. Langmuir 22: 9473-9476

Helder M, Strik DPBTB, Hamelers HVM, Kuhn AJ, Blok C, Buisman CJN (2010) Concurrent bio-electricity and biomass production in three Plant-Microbial Fuel Cells using *Spartina anglica, Arundinella anomala* and *Arundo donax*. Bioresource Technology 101: 3541–3547

Helder M, Strik DPBTB, Hubertus VMH, Cees JNB (2012) The flat-plate plant-microbial fuel cell: the effect of a new design on internal resistances. Biotechnology for Biofuels 5: 70-80

Hubenova Y, Mitov M (2012) Conversion of solar energy into electricity by using duckweed in Direct Photosynthetic Plant Fuel Cell. Bioelectrochemistry 87: 185–191

Kaku N, Yonezawa N, Kodama Y, Watanabe K (2008) Plant-microbe cooperation for electricity generation in a rice paddy field. Appl. Microbiol. Biotechnol. 79: 43–49

Khudzari J M, Kurian J, Gariépy Y, Tartakovsky B, Raghavan GSV (2018) Effects of salinity, growing media, and photoperiod on bioelectricity production in plant microbial fuel cells with weeping alkaligrass. Biomass and Bioenergy 109: 1–9

Lan JCW, Raman K, Huang CM, Chang CM (2013) The impact of monochromatic blue and red LED light upon performance of photo microbial fuel cells (PMFCs) using *Chlamydomonas reinhardtii* transformation F5 as biocatalyst. Biochemical Engineering Journal 78: 39–43

Liu B, Ji M, Zhai H (2018) Anodic potentials, electricity generation and bacterial community as affected by plant roots in sediment microbial fuel cell: Effects of anode locations. Chemosphere 209: 739–747

Liu S, Song H, Li X, Yang F (2013) Power generation enhancement by utilizing plant photosynthate in microbial fuel cell coupled constructed wetland system. Int. J. Photoenergy, 1–11

Logan BE (2008) Microbial Fuel Cells. John Wiley & Sons, New York

Malakar B, Das D, Mohanty K (2022) Evaluation of banana peel hydrolysate as alternate and cheaper growth medium for growth of microalgae *Chlorella sorokiniana*. Biomass Conv. Bioref.

Milner EM, Popescu D, Curtis T, Head IM, Scott K, Yu EH (2016) Microbial fuel cells with highly active aerobic biocathodes. Journal of Power Sources 324:8–16

Moqsud MA, Yoshitake J, Bushra QS, Hyodo M, Omine K, Strik DPBTB (2015) Compost in plant microbial fuel cell for bioelectricity generation. Journal of Waste Management 36: 63–9

Numfon E, Dooil K, Lee JW, Park KY, Kim HS (2012) Enhancement of Electron Transfer by Electrochemical Treatment of Electrode in the Microbial Fuel Cell. International Conference on Chemical Environmental Science and Engineering (ICEEBS)

Pennisi G, Blasioli S, Cellini A, Maia L, Crepaldi A, Braschi I, Spinelli F, Nicola S, Fernandez JA, Stanghellini C, Marcelis LFM, Orsini F, Gianquinto G (2019) Unraveling the Role of Red:Blue LED Lights on Resource Use Efficiency and Nutritional Properties of Indoor Grown Sweet Basil. Front. Plant Sci. 10: 305

Piovene C, Orsini F, Bosi S, Sanoubar R, Bregola V, Dinelli G (2015) Optimal red: blue ratio in led lighting for nutraceutical indoor horticulture. Sci. Hortic. 193: 202–208

Provost J, Van Vooren G, Le Gouic B, Couzinet-Mossion A, Legrand J (2011) Systematic investigation of biomass and lipid productivity by microalgae in photobioreactors for biodiesel application. Bioresour. Technol. 102:150–158

Shuai W, Xiaodi W, Xiangbin S, Baoliang W, Xiaocui Z, Haibo W, Fengzhi L (2016) Red and Blue Lights Significantly Affect Photosynthetic Properties and Ultrastructure of Mesophyll Cells in Senescing Grape Leaves. Horticultural Plant Journal 2 (2): 82–90.

Sun X, Wang X, Feng N, Qiao L, Li X, He D (2013) A new carbonaceous material derived from biomass source peels as an improved anode for lithium ion batteries, J. Anal. Appl. Pyrolysis 100:181–185.

Timmers RA, Strik DP, Hamelers HV, Buisman CJ (2013) Electricity generation by a novel design tubular plant microbial fuel cell. Biomass Bioenergy 51: 60-67

Wang S, Wang Xi, Shi Xi, Wang B, Zheng Xi, Wang H, Liu F (2016) Red and Blue Lights Significantly Affect Photosynthetic Properties and Ultrastructure of Mesophyll Cells in Senescing Grape Leaves. Horticultural Plant Journal 2 (2): 82–90

Wetser K, Sudirjo E, Buisman CJN, Strik DPBTB (2015) Electricity generation by a plant microbial fuel cell with an integrated oxygen reducing biocathode. Applied Energy 137: 151–157

Wetser K, Dieleman K, Buisman C, Strik DPBTB (2017) Electricity from wetlands: Tubular plant microbial fuels with silicone gas-diffusion biocathodes. Apenergy 185: 642-649

Wolverton BC, Johnson A, Bounds K (1989) Interior landscape plants for indoor air pollution abatement. NASA, John C. Stennis Space Center, Mississippi

Yadav G, Sharma I, Ghangrekar M, Sen R (2020) A live bio-cathode to enhance power output steered by bacteria-microalgae synergistic metabolism in microbial fuel cell. Journal of Power Sources 449: 227560

Zheng L and Van Labeke M-C (2017) Long-Term Effects of Red- and Blue-Light Emitting Diodes on Leaf Anatomy and Photosynthetic Efficiency of Three Ornamental Pot, Plants. Front. Plant Sci. 8:917

Chapter-IV

Development and Comprehensive Characterization of Low-cost Hybrid Clay Based Ceramic Membrane

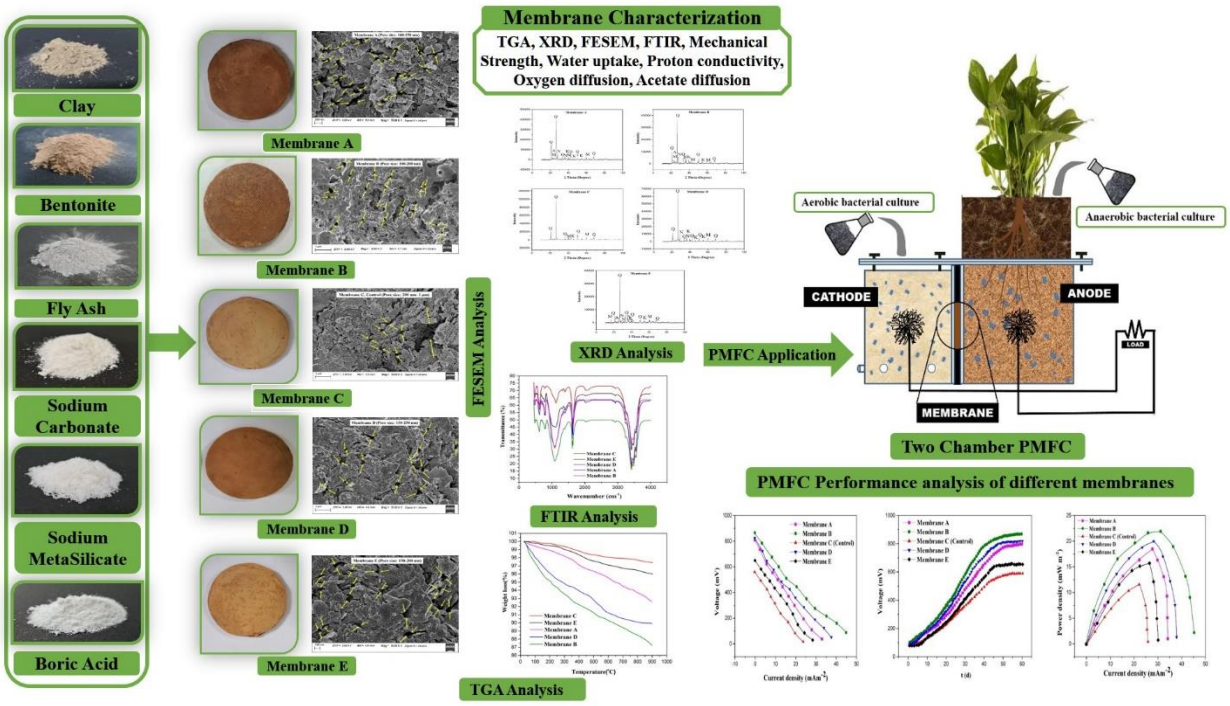

4.1 Overview

A considerable amount of development has been made in MFC technology in terms of electricity generation in the recent past (Kondaveeti et al., 2014); however, it suffers from various constraints, viz., high cost of materials including an electrode, membranes, catalysts, etc. Further, MFCs also suffer from unstable performance and low energy harvesting efficiency, which limits their large-scale practical application (Gajda et al., 2015; Kabutey et al., 2019; Shaikh et al., 2020;). However, an ion-selective separator's role is indispensable for the efficient and stable operation of MFCs. Commercialization of MFCs is one of the main challenges due to the cost of the materials involved in the operation of the MFCs, especially the electrodes and membranes. 38% of the total capital cost of an MFC is borne by the membrane alone (Tiwari et al., 2016). Nafion is a preferred choice as far as cation exchange membranes are concerned for its higher proton conducting ability due to the presence of negatively charged sulfonate groups (Chae et al., 2008). However, certain drawbacks, such as high cost, oxygen back diffusion into the anodic chamber, and permeability to cations like Na^+ and K^+, hinder nafion's proton transfer ability and thrive researchers to look for cheaper alternatives (Behera and Ghangrekar, 2011; Neethu et al., 2019; Ghadge and Ghangrekar, 2015). In recent years, researchers have gained significant interest in the ceramic membrane because of its unique thermal, chemical, and mechanical characteristics and offers a significant advantage over polymeric membranes (Ghadge and Ghangrekar, 2015; Flores et al., 2016; Winfieldet al., 2013; Chakraborty et al., 2020). The performance of terracotta and earthen pot materials was also tested as a low-cost PEM separator in an MFC (Ajayi and Weigele, 2012; J. Winfield et al., 2012; Behera et al., 2010).

One of the advantages of plant-based MFCs is that it does work without a membrane separator, as the soil in which a plant grows carries out the role of a membrane for ion transport. Although membrane-less PMFCs reduce the design process's complexity and material cost to some extent, their performance is compromised due to the diffusion of oxygen from outside to the anode. Thus growth and bioactivity of the anaerobic bacteria are hindered and result in the loss of organic matter excreted by the plants (Tiwari et al., 2016). Also, it was found that electrodes inserted directly into the soil were preoccupied with soil particles. Hence, less surface area is available for biofilm formation leading to a decrease in PMFC (Detail in Chapter-V). Therefore, membrane-assisted PMFCs are preferred as they physically separate anode and cathode compartments in an

aqueous system and help to maintain electro-neutrality by allowing only protons to pass through to the cathodic chamber and restricting the backflow of oxygen (Behera and Ghangrekar, 2011; Neethu et al., 2019).

Natural clay is already known to have ion exchange capabilities; however, natural clay is very soft and does not possess enough strength for long-term usage as a membrane in PMFCs. Various studies have investigated natural clay membranes and shown them to perform better than costly Nafion membranes (Ghadge et al., 2015). However, it has not been used in PMFC research to date. The motivation behind this study was to develop a low-cost ceramic membrane that can be an excellent substitute for the commercially available Nafion 117 for actual time application in a PMFC with enhanced shelf life. Therefore, this chapter focuses on the potential of natural clay along with other ingredients viz., bentonite, flyash, sodium carbonate, sodium metasilicate and boric acid in different concentrations to fabricate ceramic membranes. The presence of sodium metasilicate helps create silicate bonds with clay particles thus increases mechanical strength while sodium carbonate improves dispersion properties, creating homogeneity in membranes. The application of boric acid helps creates metaborates during the sintering process, thereby increasing mechanical strength (Reed, 1995; Jana et al., 2010). The presence of bentonite clay in a membrane provides excellent cationic exchange and semi-permeable properties (Tang et a., 2014; Bohac et al., 2019). In contrast, fly ash is known to provide high porosity, superior specific surface area (SSA), enhanced chemical and thermal stability, resistance to high pressure, and excellent catalytic properties due to its intrinsic nature. Therefore, the presence of fly ash enhances life of a ceramic membrane thus making it an ideal ingredient in manufacturing PEM for MFC applications (Namburath et al., 2015). Physiochemical characterization was carried out by using TGA, XRD, FESEM, FTIR, flexural strength test, water uptake, proton conductivity, oxygen and acetate diffusion and compared with Nafion117. Performance of ceramic membranes in PMFCs were evaluated by using the plant *E. aureum* with carbon fiber brush electrode.

4.2 Materials and Methods

4.2.1 Fabrication of Membranes

Natural clay was collected from the neighborhood of IIT Guwahati campus in Assam, India. It was dried in an oven, and uniform powder were selected by passing through a 150 mesh screen. The basic properties of the clay such as pH and bulk density was measured by using

standard protocols (Chesworth, 2008). For the casting of the membranes, clay was mixed with varying concentrations (weight percent) of sodium carbonate, sodium metasilicate, boric acid, bentonite, and fly ash, as shown in Table 1. As per membrane type, ingredients are adequately mixed with an optimum quantity of water to make the clay soft and form a dough. The dough is then rolled into a sheet and cut into a circular plate size of 12 cm diameter and 8 mm thick. The raw circular plates were sun-dried for 8-10 h to remove moisture. In a muffle furnace, sintering was done in a step-by-step incremental temperature (50 ^{o}C in 15 min) from 800 ^{o}C - 900 ^{o}C for 6 h. On cooling to room temperature, the membrane was removed, washed with distilled water, and dried before being used in different PMFCs. The final size obtained was 10 cm diameter and 6 mm thickness (Fig. 4.1).

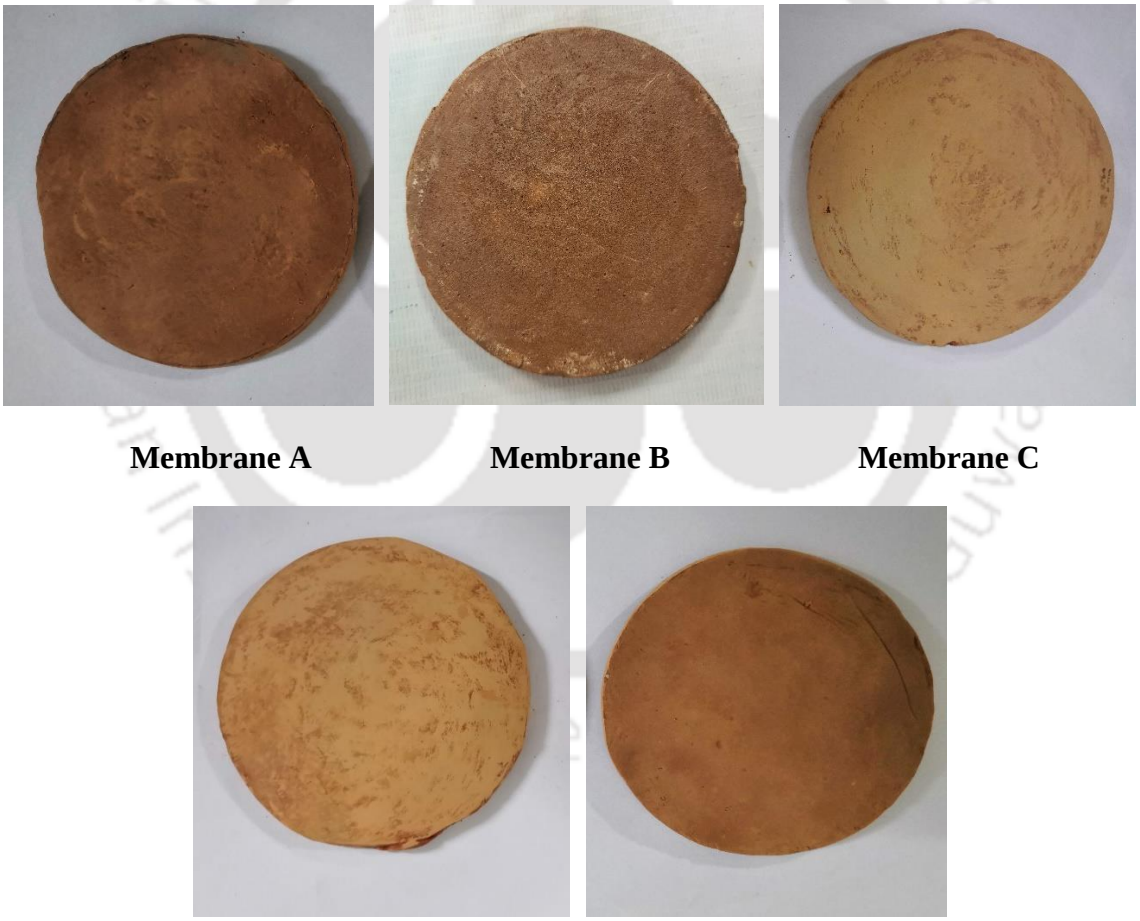

Fig.4.1 Different types of ceramic membranes.

Table 4.1 Compositions of different types of membranes.

Materials	Membrane A	Membrane B	Membrane C	Membrane D	Membrane E
Clay (%)	95-80	70-40	100	50	Nil
Sodium Carbonate(%)	3-10	5-10	Nil	Nil	Nil
Sodium Metasilicate(%)	1-3	2-3	Nil	Nil	Nil
Boric acid(%)	1-7	3-7	Nil	Nil	Nil
Bentonite(%)	Nil	10-20	Nil	25	50
Flyash(%)	Nil	10-20	Nil	25	50

4.2.2 Characterization of membranes

4.2.2.1 Component, structural and morphological analysis

The component analysis of all the membranes were carried out by X ray diffraction (XRD) technique. The membrane surface was cleaned, dried and placed into the sample holder to identify inorganic components with Cu-Kα irradiation (λ =1.543 Å) using X'pert-pro high-resolution diffractometer (Smartlab, Rigaku, Japan). The Bragg angle (2θ) was varied from 10° to 120° at a scan rate of 0.12°/s during analysis.

The thermal transformation of the membranes during the whole sintering process was evaluated between 30 ^{o}C to 900 ^{o}C temperature range through thermogravimetric analysis (TGA) (Hitachi STA7200, Japan).

The functional groups associated with the structures of all the membranes were analyzed by Fourier Transform Infrared Spectrometer (FTIR) (Spectrum Two, Perkin-Elmer, Singapore). To carry out the analysis, KBr was mixed with dry powder samples of membranes in a mortar pestle and a flat round pellet was made by hydraulically pressing it. The pellet was placed under the IR beam, and FTIR spectra was recorded between 400 cm^{-1} and 4000 cm^{-1}.

Morphological characteristics of all the membrane surfaces containing different types of pores and its distributions were observed using Field Emission Scanning Electron Microscopy (FESEM) (Gemini 300, ZEISS). A small portion of all the ceramic membranes was taken for analysis and entirely dried in a hot air oven overnight at 100 °C. Samples were uniformly sputter coated with carbon particles, and images were obtained by incident electron beam energy of 10KeV.

4.2.2.2 Water uptake and swelling ratio

The water-absorbing capabilities of all the membranes were determined and compared by the difference in the weight of the membranes before and after soaking with water (Jiang and Jiang, 2012). Similarly, the swelling ratio (%) was determined by observing the change in the thickness of membranes upon water uptake by using following Eq (1).

$$\text{Swelling ratio} = \frac{((D2 - D1) \times 100)}{D1} \tag{4.1}$$

where, D_2 (in mm) and D_1 (in mm) are the thickness of membrane under wet and dry conditions, respectively.

4.2.2.3 Proton conductivity and transfer coefficient

The proton conducting ability of all the membranes were abiotically determined in a two-chambered MFC, each chamber having an equal volume (v, cm^3). The chambers were separated by the membrane of interest having an exposed surface area (a, cm^2). Deionized water containing different proton concentrations (Ca and Cc) was used to fill the chambers. Chambers were maintained at two different pH, i.e., 10.5 and 6.5, by adding NaOH and deionized water, respectively. The change in pH from one chamber to another was monitored continuously by using a pH probe to determine the proton mass transfer coefficient (K_H, cm s^{-1}) and proton diffusion coefficient (D_H, cm^2s^{-1}) as per Eq (2) and (3) respectively (Neethu et al., 2019; Chae et al., 2008; Ghadge and Ghangrekar, 2015).

$$K_H = \frac{(-v)}{2at}.\ln\frac{(Ca + Cc - 2Cct)}{Ca} \tag{4.2}$$

$$D_H = K_H \times d \tag{4.3}$$

Where a is the exposed surface area of the membrane, and v is the volume of the deionized water inside the chambers. C_a and C_c are the initial concentration of protons in the anode and the cathode chamber, respectively; C_{ct} is the concentration of protons in the cathode chamber at time t, and d is the average thickness of the membrane.

4.2.2.4 Oxygen diffusion coefficient

To understand the diffusion of oxygen from one chamber to another across the membrane, anaerobic condition was maintained in one of the chamber by sparging nitrogen; whereas, in the second chamber, an adequate concentration of oxygen (O_{ad}, mg L^{-1}) was retained by continuously aerating the deionized water. The change in dissolved oxygen (DO) concentration in the anaerobic chamber (O, mg L^{-1}) was constantly monitored by using a DO meter (Extech DO700) to determine the change in DO value. The oxygen mass transfer coefficient (K_o, cm s^{-1}) and diffusion coefficient (D_o, $cm^2 s^{-1}$) of the membranes were calculated using Eq (4) and (5), respectively (Neethu et al., 2019; Kondaveeti et al., 2014; Ghadge and Ghangrekar, 2015).

$$K_o = \frac{(-v)}{2at} ln \frac{(Osat - O)}{Osat} \quad (4.4)$$

$$Do = K_o \times d \quad (4.5)$$

4.2.2.5 Acetate diffusion coefficient

Acetate crossover from one chamber to another across a membrane in an MFC was measured using the same experimental setup as above. In one of the chambers, acetate was added, while the change in acetate concentration in the adjacent chamber was measured using a gas chromatograph. (GC, Agilent Technology, USA) (Ghadge and Ghangrekar, 2015). The diffusion coefficient (D_A, $cm^2 s^{-1}$) of all the membranes was calculated by Eq (6)

$$D_A = \frac{(-v.d)}{2at} . \ln \left[\frac{(Ca - 2Cb)}{Ca}\right] \quad (4.6)$$

where v is the volume of liquid inside the chamber, d is the average thickness of the membrane in cm, a is the exposed surface area of the membrane, t is time in sec, C_a is the initial acetate concentration in the chamber. C_b is the acetate concentration in the other chamber at a certain time interval t.

4.2.3 Application of membranes in a PMFC

For evaluating the performance of the casted membranes in a PMFC, a two-chamber PMFC setup was made with poly-acrylic sheets (Fig. 4.2a). The ceramic membrane was fixed in between anodic and cathodic chambers. To make a performance comparison, the PMFC with membrane C containing only clay was considered as a control. Therefore, five different PMFC setups were

configured using different membranes (Fig. 4.2b). The electrode used in the setup was a carbon fiber brush electrode. Cathode and anode chambers were inoculated with aerobic and anaerobic bacterial cultures, respectively. For the study, *Epipremnum aureum* plant was chosen, considering it to be well suited for PMFC conditions and easy to grow with low maintenance. The plant has also shown excellent bioelectricity generation abilities.

The start-up process of all the PMFCs was carried out under open circuit potential (OCP). This helps microbes and plants acclimate to their new environment and accelerate biofilm development at anode and cathode, respectively. Close monitoring of the start-up phase was carried out by a multimeter (Fluke 17B+, Everett, WA, USA). Gradually, when stable cell potentials were obtained, all the PMFCs were connected to a data acquisition system (Arduino, Atmega 328P) linked to a personal computer. The potentials were recorded at regular intervals for the entire duration of the experiment. Once stable cell potentials were achieved continuously for a few days, PMFCs were connected in closed circuit configuration through an external resistance of 100 Ω for continuous measurement of operational voltage (OV).

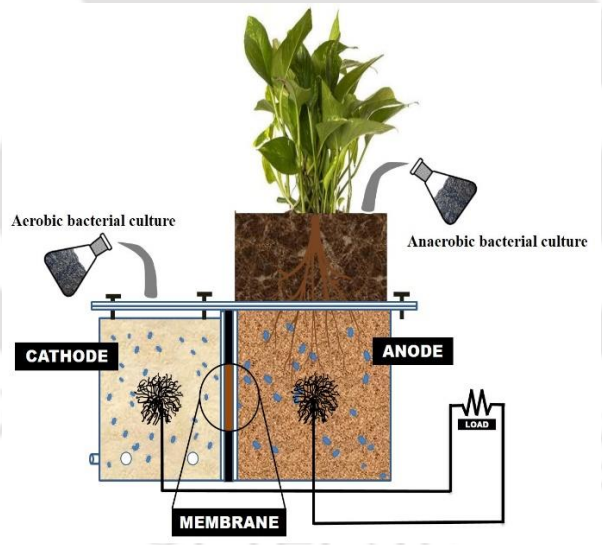

(a)

(b)

Fig. 4.2 (a) Schematic representation of PMFC design (b) Experimental setup of PMFCs.

4.2.4 Measurement of voltage, current, and power density

Continuous monitoring of the open circuit voltage (OCV) and the potential across a resistor i.e., operating voltage (OV) was measured using a data acquisition unit (Arduino, Atmega 328P). Power output of the PMFCs was calculated by taking the square of the multiplication of current and known resistance $P = I^2R$. The behavior of the PMFCs were studied by polarization curve and power density curve prepared manually by varying a series of external resistances from 15000 Ω to 50 Ω during the steady state period. In this way, the cell's maximum current density and power density can be obtained, respectively. The current density and power density were obtained by the equations $I = \frac{V}{\alpha R}$ and $P = \frac{V^2}{\alpha R}$ respectively normalized to anode surface area α.

4.2.5 Electrochemical kinetics

To understand the mechanism of oxidation and reduction in any MFC, cyclic voltammetry (CV) remains an established and straightforward technique. The response of the redox current peak under CV can provide information about the electrocatalytic reactions going on the surface of the anodic biofilm (Gunaseelan et al., 2021). Therefore, the CV technique was carried out in three-electrode setups employing an Ag/AgCl reference electrode coupled to a potentiostat. The electrode characterization was done during the bio electrocatalytic (turnover) condition using anode as the working electrode, Ag/AgCl as the reference electrode, and cathode as the counter electrode. CV was performed in the potential range of -0.5 V to + 0.5 V at a slow scan rate of 10

mV s^{-1} at 25 ^{o}C, and the resulting response current peaks were recorded by using potentiostat PGSTAT 302N (Metrohm, Autolab) (Martinez et al., 2011).

Electrochemical Impedance Spectroscopy (EIS) technique measured the cell's internal resistances. It was carried out in two-electrode setups where the cathode acts as a reference/auxiliary electrode in the frequency range of 100 kHz to 10 MHz with 10 mV amplitude of AC signal using potentiostat PGSTAT 302N (Metrohm, Autolab) (Ghadge and Ghangrekar, 2015; Gunaseelan et al., 2021).

4.3 Results and Discussion

4.3.1 Properties of clay and chemical characterization of membranes

The basic properties of clay obtained were pH (7.2), bulk density (1370 kg m^{-3}), organic matter (0.96%), and soluble matter (3.0%).

4.3.1.1 X-ray diffraction (XRD) analysis

The powdered samples of all the membranes were analyzed by XRD technique which shows the presence of various hygroscopic oxides viz., SiO_2, Al_2O_3, Fe_2O_3, FeO, CaO, Na_2O, K_2O, MgO, etc. Among all, the major peaks corresponded to SiO_2, Al_2O_3, $Al_2(SO_4)_3$, and Al_2SiO_5, which is a major constituent of quartz and mullite present in clay, thus seen in the case of membrane C. These hygroscopic oxides are known to improve the hydration property of the membrane along with its strength (Jana et al., 2010; Neethu et al., 2018), and facilitate proton transport through Grotthuss and vehicle mechanisms (Grancha, et al., 2016; Neethu et al., 2019; Chae et al., 2008). Therefore, these oxides are incorporated in the case of the Nafion membrane to increase proton conductivity and retain bound water. A major constituent of flyash is mullite and quartz, along with other oxides such as TiO_2, Fe_2O_3, CaO, etc. On the other hand, bentonite consists of quartz and mullite as major constituents along with nepheline (Na_2O, Al_2O_3, $2SiO_2$), albite ($NaAlSi_3O_8$) and kaolinite ($Al_2(OH)_4Si_2O_5$). The corresponding peaks of all these constituents are seen in XRD patterns of Fig. 4.3. In the case of a composite membrane consisting of clay, bentonite, fly ash, Na_2CO_3, Na_2SiO_3, and H_3BO_3, the intensity of all these peaks increased, which may further assist in proton transport.

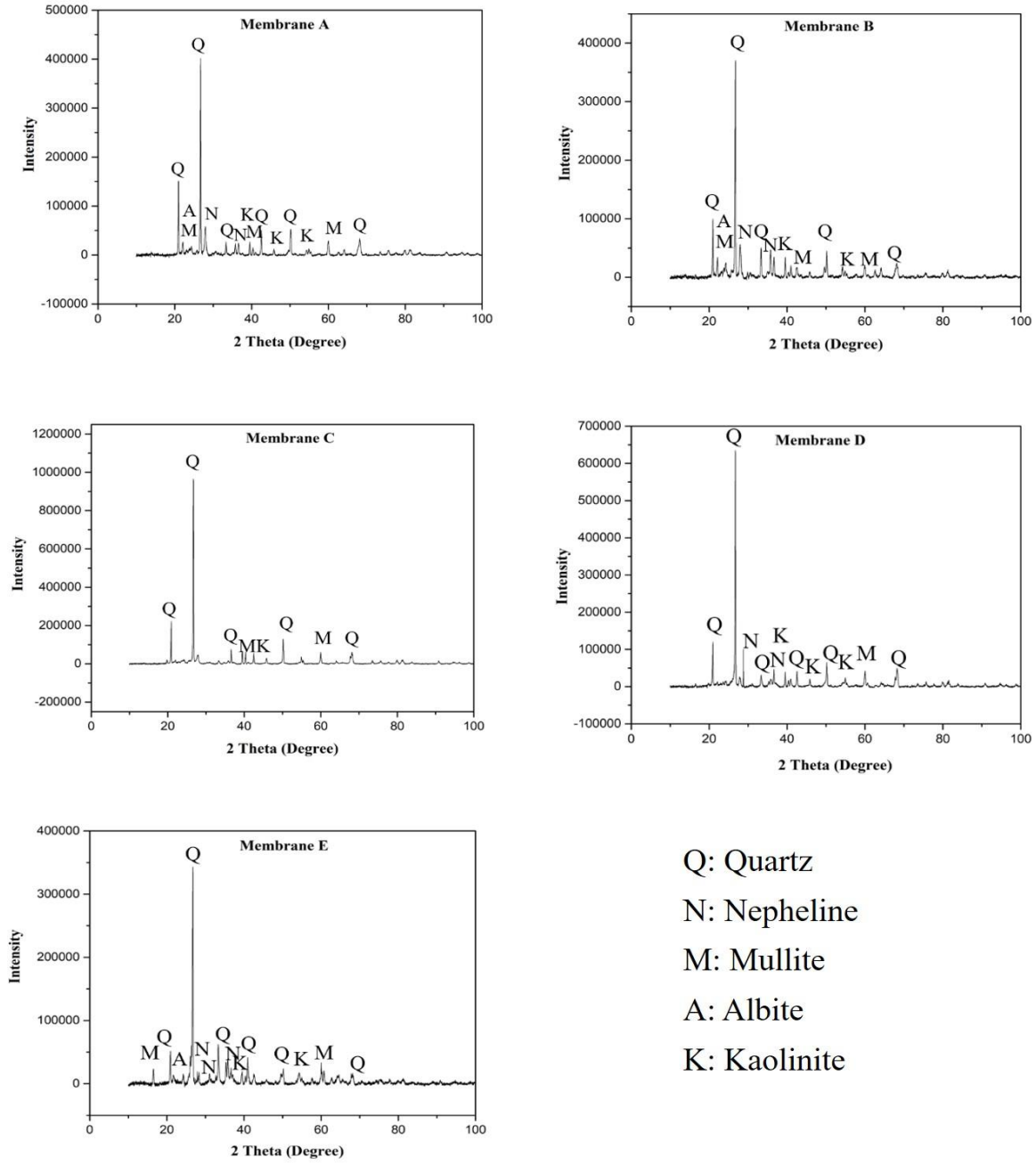

Fig. 4.3 XRD analysis of the membranes.

4.3.1.2 Thermogravimetric analysis

During the heating process, the mass loss in the case of membrane A and membrane B was more than in other membranes (Fig. 4.4a). In the first phase, up to 150 °C the, membrane A and membrane B lose 2.8% and 3.6% of their mass, whereas a mass loss of 0.12%, 0.23%, and 0.46%

was seen for membrane D, membrane C, and membrane E respectively. These mass losses can be attributed to the loss of loosely bound water molecules (Jana et al., 2010). In the second phase, from 50-350°C, the evaporation of crystal water in the interlayers occurs. The presence of hygroscopic components in sodium metasilicate and boric acid may have led to higher mass loss in membrane B. By comparing all TGA curves (Fig. 4.4a), it was observed that between 300 °C to 500 °C a higher mass loss occurred in case of membrane A and membrane B. This mass loss may be attributed to the boiling point of boric acid as a component of these membranes is around 300 °C. Finally, negligible weight loss in the range of 350–700 can be attributed to the structural dehydration of the neighboring hydroxyl group. However, mass loss for membrane C containing clay is negligible throughout the heating process. After 600 °C, marginal mass change was observed for all the compositions. Thus, the minimum sintering temperature for all membranes were kept above 600 °C.

4.3.1.3 FTIR analysis

FTIR spectra of all the membranes are represented by Fig. 4.4b, where strong absorptions were obtained around 1030 cm^{-1} for membrane B and deviated towards 1100 cm^{-1} following the order: membrane B> membrane D> membrane A> membrane E> membrane C. A relatively higher peak intensity around 1030 cm^{-1} corresponded to the presence of a sulphonic acid group (-SO_3H) similar to Nafion 117 (Jiang and Jiang, 2012; Neethu et al., 2018), which is known to enhance the proton conductivity of a membrane. Bands around 2320 cm^{-1} have appeared due to the NH group of amine salts in all the membranes. The peaks around 3416 cm^{-1} - 3551 cm^{-1} in all the membranes showed (-NH) stretch. The presence of peaks around wave number of ~3600 cm^{-1} was associated to the stretching vibration of the hydroxyl group which proved the ease of proton transfer (Tiwari et al., 2016). A sharp intensity obtained by membrane B makes it a good candidate for proton exchange. Also, sharp peaks are seen around 779 cm^{-1} - 797 cm^{-1} and 1600 cm^{-1} in all membranes, showing complexity of ceramic membranes as compared to Nafion 117.

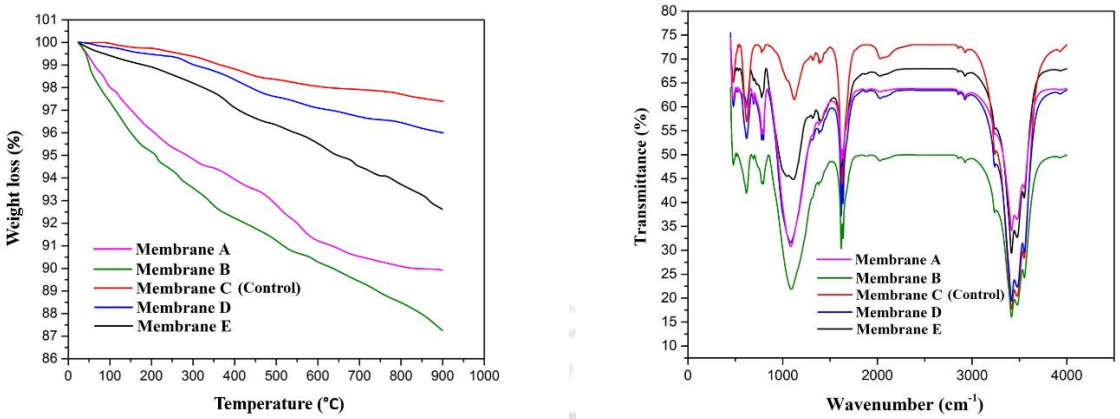

(a) (b)

Fig. 4.4 (a) Thermogravimetric analysis of different membranes (b) FTIR spectra of all the membranes.

4.3.2 Physical characterization of membranes

4.3.2.1 Water uptake and swelling ratio

The mobility of the proton is known to be strongly affected by the membrane's water content or water uptake capacity. The presence of water inside the membrane is generally known to enhance the ion conductivity of membranes in many instances (Neethu et al., 2018). The presence of bentonite, flyash and other chemical ingredients, viz., Na_2CO_3, Na_2SiO_3 and H_3BO_3, used in membrane A and membrane B increases hydrophilicity of the membranes. The water absorption capabilities and swelling ratios of different membranes, casted with different proportions of bentonite, fly ash, Na_2CO_3, Na_2SiO_3 and H_3BO_3, are presented in Table 2. An increasing trend in water absorption was observed in membrane A with an increase in the concentration of Na_2CO_3, Na_2SiO_3 and H_3BO_3 from 3-10%, 1-3% and 1-7% (w/w) respectively, while water absorption decreases beyond this weight percentage. The decrease in water absorption with further increased concentration of Na_2CO_3, Na_2SiO_3 and H_3BO_3 may have resulted in reduction of effective surface area due to the aggregation with clay particles. This further resulted in the reduction of interspace volume responsible for the channeling of water. However, in the case of membrane B, an increase in water absorption from 21.4 ± 1.7 to 26.4 ± 1.7 was observed with an increase in the concentration of bentonite and fly ash from 10 to 15%. However, with a further

increase in the concentration of the same ingredients from 15 to 20% a proportional increase in water absorption was not observed (Table 4.2).

The stability of the membrane can be easily understood by membrane swelling behavior when placed under water. All the membranes were examined in terms of their water uptake capacity to understand their swelling nature. Keeping aside the trend observed in water absorption pattern, the swelling ratio was found to increase with an increase in concentration of Na_2CO_3, Na_2SiO_3 and H_3BO_3. The swelling ratio increases from 1.1%, to 2.0% in membrane A with increasing concentration of Na_2CO_3, Na_2SiO_3 and H_3BO_3 from 3-10%, 1-3% and 1-7% (w/w) respectively. Similarly, with increased bentonite and fly ash concentrations from 10% to 20% in membrane B, the swelling ratio increases from 2.1% to 2.9% respectively. However, when concentration of bentonite and fly ash increased from 15% to 20%, a very tiny increase in water absorption and swelling ratio was observed in membrane B. In case of membrane D as well, water absorption and swelling ratio was found to increase with increasing concentration of bentonite and fly ash (Table 4.2).

Therefore, considering water absorption and swelling pattern; membrane B casted using concentration of bentonite, fly ash, Na_2CO_3, Na_2SiO_3 and H_3BO_3 at 15%, 15%, 8%, 2%, 5%, respectively was used for application in PMFCs.

4.3.2.2 Proton conductivity and proton transfer coefficient

The proton mass transfer coefficient (K_H) of membrane C (100 % clay) was found to be 2 ± 0.20×10^{-5} cm s^{-1}. However, when clay concentration was decreased by 5% in membrane A by addition of Na_2CO_3, Na_2SiO_3 and H_3BO_3, no change in K_H value was observed. Further increasing concentration of Na_2CO_3, Na_2SiO_3 and H_3BO_3 with 80% clay concentration increases the value of K_H up to 7.2 ± 0.46×10^{-5} cm s^{-1} in membrane A (Detail in Table 4.2). The corresponding proton diffusion coefficients are also listed in Table 2. Similarly, membrane B decreases clay concentration further to 70 % by adding bentonite, fly ash, Na_2CO_3, Na_2SiO_3 and H_3BO_3 at 10%,10% 5%,2%,3% increases proton mass transfer coefficient to 7.6 $\times10^{-5}$ cm s^{-1}. The proton mass transfer coefficient further increases to 8.2×10^{-5} cm/sec when clay concentration decreases to 55%, however further decrease in clay concentration up to 40%, the proton mass transfer coefficient decreased slightly to 7.8×10^{-5}cm s^{-1} due to reasons not known (For detail please refer Table 2).

The values in Table 4.2, depict that the addition of Na_2CO_3, Na_2SiO_3 and H_3BO_3, bentonite and fly ash at specific concentrations enhances the water absorption capacity and proton transfer efficiency of the membranes significantly at the same time. The proton mass transfer coefficient of Nafion 117 is much higher (24.0×10^{-5} cm s^{-1}) as compared to membrane B (8.2×10^{-5} cm s^{-1}) probably because of a thin thickness of Nafion membrane (0.18 mm) as compared to the casted ceramic membrane (6 mm). However, considering the thickness of the membranes, membrane B has a higher proton diffusion coefficient, D_H ($50.84 \pm 0.30\times10^{-6}$ cm^2 s^{-1}) as compared to Nafion 117 (4.32×10^{-6} cm^2 s^{-1}). The water absorbing capacity was controlled by the presence of hygroscopic oxides like SiO_2 and other functional groups associated with clay, bentonite and fly ash in the membrane. Thus this induces water uptake and supports the proton transfer process through the Grotthuss mechanism due to the presence of hydrogen bonds in water molecules (Grancha et al., 2016; Ghadge and Ghangrekar, 2015; Neethu et al., 2018).

4.3.2.3 Oxygen and substrate diffusion coefficient

Oxygen and acetate diffusion across the chamber through the membrane will experience a detrimental outcome on the performance of MFC since the presence of oxygen at an anodic chamber act as an electron acceptor and causes aerobic oxidation of organic matter, thus reducing performance efficiency. A greater diffusion of oxygen into an anodic chamber can cause direct aerobic oxidation of the organic matter, thus reducing the power generation from the PMFC (Neethu et al., 2019; Ghadge and Ghangrekar, 2015; Neethu et al., 2018).

Oxygen diffusion from cathode to anode across the membrane was monitored over time using a DO probe (Fig. 4.5). Among all the ceramic membranes tested, membrane B with a concentration of bentonite, fly ash, Na_2CO_3, Na_2SiO_3 and H_3BO_3 at 15%, 15%, 8%, 2%, and 5% respectively resulted in relatively smaller oxygen mass transfer coefficient of 2.09×10^{-4} cm s^{-1} (Table 4.2); whereas the clay separator showed much higher oxygen mass transfer coefficient of 8.24×10^{-4} cm s^{-1}. The other membranes had intermediate oxygen mass transfer coefficients. On the other hand, Nafion showed an oxygen mass transfer coefficient of 3.0×10^{-4} cm s^{-1} (Table 4.2). The respective oxygen diffusion coefficient of all the membranes are listed in Table 4.2. Therefore, it can be seen that even after being a thinner membrane, Nafion showed greater oxygen diffusion than membrane B. The ceramic membrane on the other hand, being a compact structure due to the presence of bentonite and fly ash, acts as filler material and may hinder oxygen diffusion.

Similar to oxygen diffusion, the performance of an MFC is severely affected by the diffusion of the substrate from the anodic chamber to the cathodic chamber. To evaluate any acetate diffusion, samples were collected from the cathodic chamber twice a day at an interval of 12 hours. PMFC with Membrane B showed the lowest acetate diffusion coefficient among others with a value of $5.96 \pm 0.28 \times 10^{-6}$ cm s^{-1} (Table 4.2). The said value was 1.6 times lower than the control. On the other hand, the Nafion membrane having very fine and uniform porosity showed much less acetate diffusion than all ceramic membranes in this study (Table 4.2).

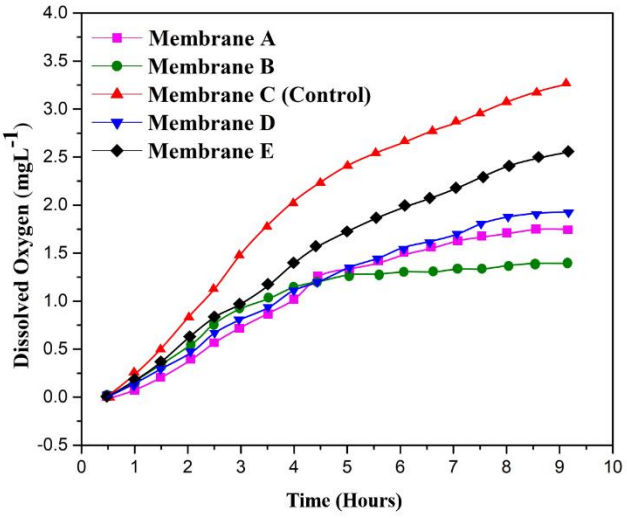

Fig. 4.5 Dissolved oxygen profile of ceramic membranes.

4.3.2.4 Mechanical strength

The physical strength of all the membranes were measured by a three point bending flexural strength test (Instron-Dynamic UTM 8801). The flexural strength of membranes increases with elevating sintering temperature without change in composition (Jana et al., 2010). For membrane A, flexural strength increased from 2.54 MPa (800 °C sintered) to 3.79MPa (900 °C sintered). In the case of composite membrane B, consisting of clay, bentonite, fly ash, Na_2CO_3, Na_2SiO_3 and H_3BO_3 the highest flexural strength is obtained. Membrane B's flexural strength further increases from 3.56 MPa (800 °C sintered) to 6.79 MPa (900 °C sintered). This was due to the formation of nepheline as indicated by XRD which is known to impart higher mechanical strength to ceramic materials (Kiran et al., 2020). However, among all the membrane C with 100%

clay has the lowest flexural strength. Similarly, increasing percentage content of bentonite, fly ash Na_2CO_3, Na_2SiO_3 and H_3BO_3 to clay enhances the flexural strength as represented in Table 4.2. During membrane manufacturing, it was also observed that, with increasing concentrations of Na_2CO_3, Na_2SiO_3, and H_3BO_3 beyond 10%, 3%, and 7% (w/w), respectively, and sintering at 900 °C, abnormal cysts-like lesions developed over the membrane surface resulting in creaking the surface, which becomes non useful (Fig. 4.6).

Fig. 4.6 Picture showing abnormal cysts like lesions developed over the surface of membrane.

Table 4.2 Comparison of characteristics of casted membrane separator used in this study

Membranes	Water absorption %	Swelling ratio %	K_H (cm/sec) $\times10^{-5}$	D_H (cm^2/sec) $\times10^{-6}$	K_O (cm/sec) $\times10^{-4}$	D_O (cm^2/sec) $\times10^{-4}$	D_A (cm^2/sec) $\times10^{-6}$	Flexural strength (MPa)
Membrane A Clay-95% , Na_2CO_3-3%, Na_2SiO_3-1%, H_3BO_3-1%	5.2 ± 0.7	1.1	2 ± 0.18	12.24 ± 0.40	6.60 ± 0.46	4.09 ± 0.80	3.60 ± 0.46	2.76
Membrane A Clay-90%, Na_2CO_3-5%, Na_2SiO_3-2%, H_3BO_3-3%	12.0 ± 1.3	1.7	3.2 ± 0.24	19.86 ± 0.42	5.74 ± 0.36	3.55 ± 0.76	3.20 ± 0.30	3.09
Membrane A Clay-80%, Na_2CO_3-10% Na_2SiO_3-3%,H_3BO_3-7%	19.4 ± 1.2	2.0	7.2 ± 0.46	44.64± 0.80	3.48 ± 0.20	2.15 ± 0.42	2.80 ± 0.12	3.79
Membrane B Clay-70% Bentonite-10%, Flyash-10%, Na_2CO_3-5% Na_2SiO_3-2% H_3BO_3-3%	21.4 ± 1.7	2.1	7.6 ± 0.48	47.12 ± 0.84	3.20 ± 0.18	1.98 ± 0.36	3.20 ± 0.20	5.60
Membrane B Clay-55% Bentonite-15%, Flyash-15%, Na_2CO_3-8%, Na_2SiO_3-2%, H_3BO_3-5%	26.4 ± 1.7	2.7	8.2 ± 0.56	50.84 ± 0.30	2.09 ± 0.10	1.29 ± 0.24	2.26 ± 0.2	6.79
Membrane B Clay-40% Bentonite-20% Flyash-20% Na_2CO_3-10%, Na_2SiO_3-3%, H_3BO_3-7%	27.0± 1.2	2.9	7.8 ± 0.47	46.36 ± 0.68	2.0 ± 0.08	1.20 ± 0.20	2.50 ± 0.3	6.55
Membrane C Clay-100%	6.0 ± 1.7	1.1	2 ± 0.20	12.40 ± 0.16	8.24 ± 0.54	4.09 ± 0.60	5.60 ± 0.5	1.24
Membrane D Clay-80% Bentonite-10% Flyash-10%	8.2 ± 1.5	1.2	2.9 ± 0.24	17.98 ± 0.28	3.31 ± 0.18	2.05 ± 0.16	3.05 ± 0.5	2.29
Membrane D Clay-70%,, Bentonite-15%, Flyash-15%,	9.8 ± 1.1	1.6	3.0 ± 0.26	18.60 ± 0.24	2.98 ± 0.26	4.78 ± 0.40	2.86 ± 0.32	3.29
Membrane D Clay-50% Bentonite-25% Flyash-25%	10.6 ± 1.4	2.0	3.8 ± 0.32	23.56 ± 0.26	2.60 ± 0.22	5.02 ± 0.48	2.60 ± 0.24	4.02
Membrane E Bentonite-50% Flyash-50%	7.6 ± 1.6	1.4	2.6 ± 0.24	16.12 ± 0.20	4.23 ± 0.36	2.62 ± 0.20	4.47 ± 0.54	3.24
Nafion 117	28.0 ± 2.4	5.6	24.0 ± 1.6	4.32 ± 0.20	3.0 ± 0.24	0.54 ± 0.08	0.47 ± 0.20	--

K_H: Proton mass transfer coefficient; D_H: Proton diffusion coefficient; K_O: Oxygen mass transfer coefficient; D_O: Oxygen diffusion coefficient; D_A: Acetate diffusion coefficient

4.3.2.5 FESEM analysis

After performing characterization of all the membranes for proton conductivity, oxygen and acetate diffusion, field emission scanning electron microscopy (FESEM) was performed to observe the surface structure of the best performing membranes from each category (Fig. 4.7). The thickness of the all membranes was around 0.62 cm. Among all the membranes, the most uniform distribution of pores was seen on the surface of membrane B with pore size of 100-200 nm, followed by membrane A, membrane D and membrane E (Fig. 4.7). The presence of little larger but uniform pore size of 100-250 nm are seen on the surface of membrane A and membrane D with more uniform distribution seen on membrane A rather than membrane D. This might be because of the addition of sodium carbonate, boric acid and sodium metasilicate, which resulted in uniform cross linkage between clay, bentonite and fly ash particles present in membrane A and membrane B respectively by acting as conductive filler material thus obtaining uniform and narrow pore sizes. This helps in inhibiting oxygen diffusion from cathode to anode chambers as well. However, pores present on the surface of membrane C is very non-uniform and are larger in size starting from 200 nm to 1µm thus increasing oxygen entry in the anodic chamber while minimizes electrogenesis and reducing power harvested by PMFC. Pore size ranging from 150-200 nm were also seen on the surface of membrane E containing bentonite and fly ash only. However, in case of Nafion membrane the pore sizes were quite smaller (10-20 nm) (Ghadge and Ghangrekar, 2015). Sintering temperature is known to play a vital role in determining pore size, however from a small section of membrane under FESEM, not much difference was observed with increase in temperature from 800 °C to 900 °C.

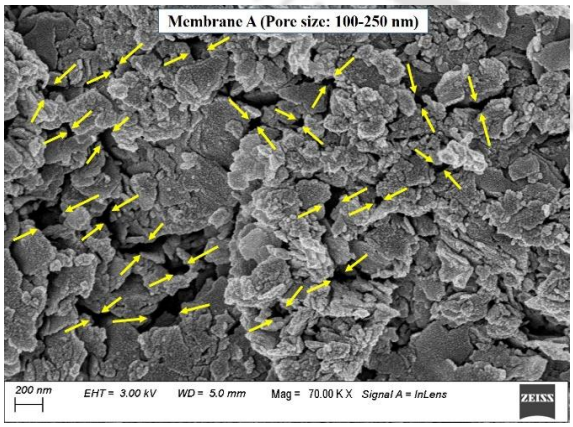

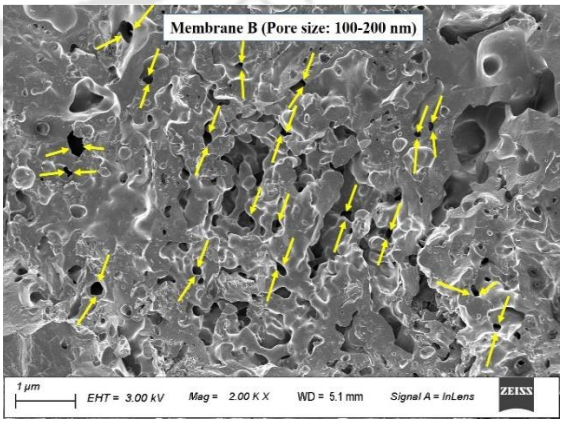

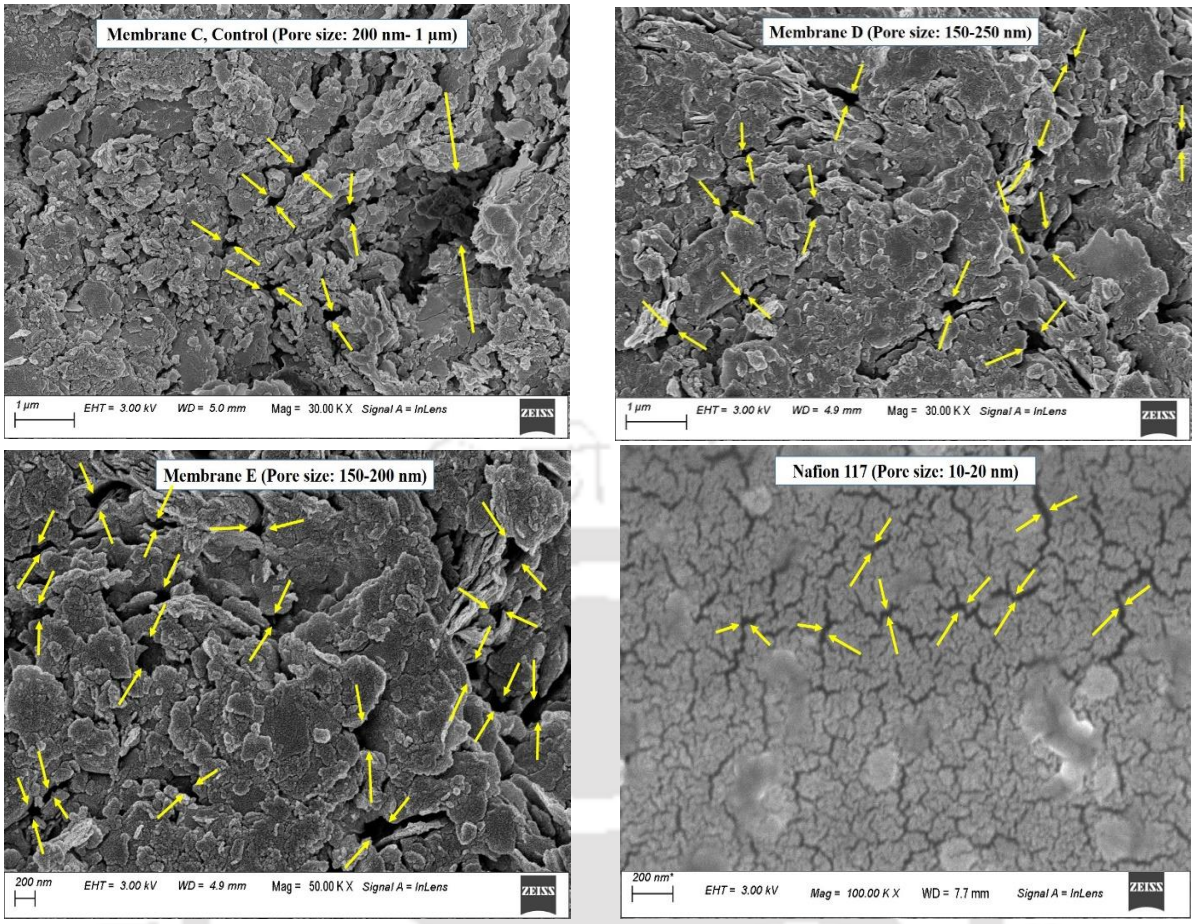

Fig. 4.7 FESEM pictures of membranes.

4.3.3 PMFC application and performance comparisons

After characterization of all the eleven membranes, the best performing membranes from each category of membrane A, B and D viz., Membrane A (Clay-80%, Na_2CO_3-10%, Na_2SiO_3-3%, H_3BO_3-7%), Membrane B (Clay-55%, Bentonite-15%, Flyash-15%, Na_2CO_3-8%, Na_2SiO_3-2%, H_3BO_3-5%) and Membrane D (Clay-50%, Bentonite-25%, Flyash-25%) were used for application in PMFCs grown with plant *E. aureum*. The performance of all three membranes were compared with Membrane C (Clay-100%) and Membrane E (Bentonite-50%, Flyash-50%).

All the five PMFCs behavior was similar during the start-up period, showing voltage fluctuations at 180 ± 10 mV (OCP) for two weeks due to new environmental conditions and the slow growth rate of microorganisms. Gradually stable voltage started to appear after 20 days of inoculations, typically in the range of 200 ± 10 mV to 400 ± 10 mV from all PMFCs (Fig. 4.8a) implying the presence and colonization of electrodes by exoelectrogenic bacteria.

At this stage, all the PMFCs were connected with a 100 Ω external resistance to measure the operating voltage (OV), thus assessing the real electricity generation potential.

The open-circuit voltage (OCV) generation pattern in all five PMFCs was almost similar with the maximum voltage obtained during 49^{th} -56^{th} days. It remained almost constant until the end of the experiment, with plants maintained under healthy conditions. However, PMFC with Membrane B shows the highest OCV of 780 ± 6 mV, followed by Membrane D (742 ± 2 mV), Membrane A (710 ± 2 mV) and Membrane E (655 ± 2 mV) (Fig 7a). The control PMFC with Membrane C showed a lower voltage of 586 ± 2 mV during the steady state.

The OCV and the respective OV, as seen in Table 4.3, clearly showed that the PMFC with Membrane B produced higher OCV and OV than the rest of the PMFCs. This signifies superior ion transport across Membrane B leading to significant enhancement in the performance of the said PMFC as compared to others.

Polarization curves (Fig. 4.8b) and power curves (Fig. 4.8c) were obtained during steady-state on the 8^{th} week. The maximum power density of 22.38 mW m^{-2} with a current density of 45.24 mA m^{-2} was obtained from PMFC with Membrane B, showing an overall 78% increase in power generation with respect to control PMFC. A more significant voltage drops in the case of membrane C (control) can be witnessed from the voltage vs. current curve (Fig. 7b) compared to other PMFCs, mainly in the region of the ohmic and concentration polarization range. This voltage drop may have resulted because of ohmic loss and mass transfer losses due to resistance provided by the membranes and inefficient transfer of oxidized compounds towards the cathode. The trend of power densities of PMFCs with different membranes was in the order of Membrane B > Membrane D > Membrane A > Membrane E > control. This difference in power densities might be due to differences in the physical characteristics of the membranes, such as diffusivity, conductivity, porosity etc. From the slope of the polarization curve, the internal resistance of all the PMFCs were calculated. The parameters obtained from all the PMFCs are reported in Table 4.3.

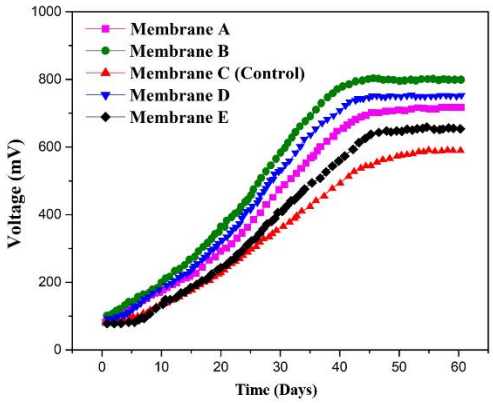

(a)

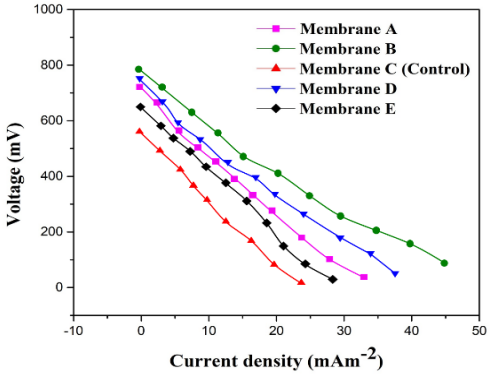

(b)

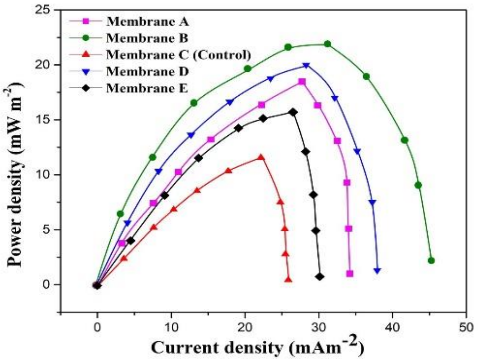

(c)

Fig. 4.8 (a) Cell voltage curve (b) Polarization curves (c) Power curves of different PMFCs assembled with different membranes.

Table 4.3 Performance analysis of different membranes.

Electrical parameters	PMFC 1 with Membrane A	PMFC 2 with Membrane B	PMFC 3 with Membrane C	PMFC 4 with Membrane D	PMFC 5 with Membrane E
Open circuit potential (mV)	710 ± 2	780 ± 6	586 ± 2	742 ± 2	655 ± 2
Operating voltage (mV)	276 ± 2	366 ± 2	220 ± 2	279 ± 2	236 ± 2
Max. current density (mA m^{-2})	33.62 ± 1.2	45.24 ± 1.4	23.46 ± 0.8	37.26 ± 1.2	29.34 ± 0.8
Max. Power density (mW m^{-2})	18.46 ± 0.6	22.38 ± 0.4	12.6 ± 1.2	20.21 ± 1.1	16.26 ± 1.4
Internal Resistance (Ω)	310 ± 5	234 ± 5	346 ± 5	257 ± 5	280 ± 5

The practical application of clay-based ceramic membranes in MFCs has been seen for a while (Winfield et al., 2013; Gunaseelan et al., 2021). However, its use in a PMFC is a very new

concept and not very widely used. However, Table 4.4, compares different types of PMFC operated with a clay-based ceramic membrane.

Table 4.4 Comparison of various PMFCs performance based on the application of clay-based ceramic membranes.

Plants Used	Membrane Used	Electrode used	Max. Power Density (mW m^{-2})	Internal Resistance (Ohm, Ω)	Reference
Rice Plant (*Oriza Sativa*)	Clay Based terracotta tube	Graphite felt	16.8	188	Kiran et al., 2020
Brassica juncea *Trigonella foenum-graecum* *Canna stuttgart*	Clay-mix container (Clay, kaolinite, Montmorillonite)	Carbon brush (Anode) carbon cloth (Cathode)	69.32 80.26 222.54	138 33 23	Sophia and Sreeja, 2017
Rice plant (*Oriza Sativa*)	Earthenware	Carbon fibre	60		Regmi and Nitisoravut, 2017
O. ficus-indica O. joconostle O. robusta O. albicarpa	Ceramic stick	Graphite felt (Anode) Zinc sheet (Cathode)	6.60 5.76 2.01 5.47		Apollon et al., 2020
Vetiver plants (*Vetiveria zizaniodes*)	Cylindrical earthen pot	graphite fiber	68	60	Regmi et al., 2018

4.3.4 Electrochemical analysis

Cyclic voltammetry (CV) is a wonderful technique for the characterization of the electron transfer interactions in fuel cells. CV analysis was carried out for all the PMFCs during steady state operation on 49th day which revealed higher redox current in PMFC incorporated with Membrane B (Fig. 4.9a). A peak current of 21 mA, 20 mA, 17 mA, 13 mA were obtained from PMFC with Membrane B, Membrane D, Membrane A and Membrane E respectively. On the other hand, a lesser faradaic current (11 mA) was obtained from the control PMFC with Membrane C (100% clay). The higher current generation in the case of PMFC with Membrane B is because of the optimum translation of microbial activities into end product due to efficient proton diffusion across the membrane resulting in lesser ohmic polarization. The CV current obtained was in the order of PMFCs with Membrane B > Membrane D > Membrane A > Membrane E > control PMFC. Also, the width of the graphs progressively decreased in similar order indicating decreasing current density trends, which also correlates with the polarization curves. In addition to the presence of a superior membrane in a PMFC, an efficiently growing

biofilm on the surface of the electrode with membrane-bound electron transfer proteins attached to bacterial cells produces higher bioelectrocatalytic activity, leading to an increase in current. In the case of membrane B, adding Na_2CO_3, Na_2SiO_3, H_3BO_3, bentonite, and flyash increases the surface uniformity. It reduces the overall porosity of Membrane B, which helps in resisting oxygen diffusion from the cathode chamber thereby providing an efficient environment for exoelectrogenic biofilm formation on anode surface. Similarly, it also reduced acetate crossover from anodic to cathodic chamber. Therefore, PMFC with Membrane B proved to be superior among others while comparing the bioelectricity generation capabilities.

The Nyquist plot acquired by EIS techniques also describes internal resistance predominating in these PMFCs. The curved semi-circular portion of the graph (Fig. 4.9b) symbolizes the redox process occurring on the surface of the biofilms as a result of nutrients breakdown into electrons and protons representing solution and charge-transfer resistance. On the other hand, the linear portion of the graph manifests the mass transfer process at the electrode-electrolyte interface (Ghadge and Ghangrekar, 2015). The biofilm formation over the surface of the electrodes, nutrient solution inside the chambers, and the membrane structure significantly influenced the overall internal resistance of the cell. Among all the PMFCs, lowest internal resistance was obtained from PMFC with Membrane B, indicating the maximum number of ions passing through the membrane, which increases the rate of reduction at the cathode and reduces the over potential at the same time. While for the control PMFC, a higher internal resistance was noticed. EIS was interpreted by using an equivalent circuit diagram which shows ohmic resistance R_Ω of PMFCs due to variations in the charge transfer ability of membrane and electrolyte solutions. The rate of transfer of ions from electrolyte solution and biofilm to the electrode is affected by charge transfer resistance R_{CT}. Diffusion resistance from the electrolyte solution to microbial biofilm can be represented by Warburg element (W_d). An electric double layer exists between electrode and membrane, equivalent to a capacitor. C_{dl} can represent its capacitance. The values of all the parameters obtained by the equivalent circuit are presented in Table. It can be seen that compositional changes in Membrane B enhance its physical and chemical properties leading to improve charge transport and higher reduction kinetics resulting in reduced charge transfer resistance R_{CT}. The decrease in the magnitude of R_{CT} may be because of well-developed biofilm development at the electrode and higher proton transfer through membranes. The capacitance of a capacitor is inversely proportional to its impedance. In this case, higher C_{dl} indicated the ability to pass more current to charge the capacitor faster. Higher W_d values (Table 5) indicates higher mass transfer losses which are

maximum in PMFC with Membrane C. The internal resistance values acquired from the EIS data also support the data achieved through the polarization curve in section 4.3.3.

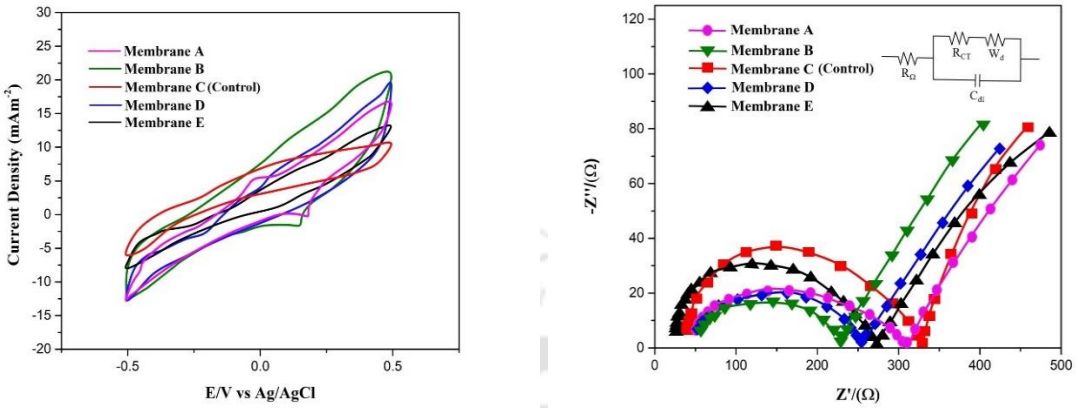

(a) (b)

Fig. 4.9 Electrochemical characterization of PMFCs (a) with anode as the working electrode. (b) Nyquist plots of ceramic membranes.

Table 4.5 Different components of PMFC impedance.

PMFC Types	R_Ω (Ω)	R_{CT} (Ω)	W_d (Ω S^{-2})	C_{dl} (µF)
Membrane A	48.4	261.56	610.4	1.88
Membrane B	53.2	181.2	464.1	2. 36
Membrane C	44.6	301.10	670.5	1.68
Membrane D	51.3	205.7	489.3	2.08
Membrane E	24.1	256	572.7	1.87

4.3.5 Long term stability of membranes

The long-term stability of the membranes was also tested for a period of over six months' duration. It was found that the presence of sodium metasilicate, sodium carbonate, and boric acid makes a membrane more stable underwater with an improved life span. Similar is the case with bentonite and flyash being present as ingredients of the clay membrane. In our study, we have found that over six months, there has been little to no degradation in the physical structures of these membranes. However, in the case of the membrane with clay as the only ingredient, the physical structure looks weaker over time. It loses its firmness either due to microbial degradation or continuous water absorption. Accumulation of biomass in the

membranes was seen, leading to clogging of the pores due to fouling. This may be one of the reasons for reduction in power generation over time, indicating the necessity of replacement. In our study, it was seen that the membrane fouling was very evident in case of Membrane C (with 100% clay), however with the inclusion of bentonite, flyash, sodium carbonate, sodium metasilicate and boric acid with clay, fouling was comparatively less evident, probably due to shinny surface structure of the membrane restricting attachment of biomass. However, as the cost of making a membrane is significantly less than the commercially available Nafion membrane, the problem can be easily solved by easily replacing it after use.

4.3.6 Cost analysis

One of the prime objectives of this study was to develop a ceramic membrane that gives superior performance in an MFC with respect to the already existing polymeric membranes in the market without compromising in its durability and at a lower cost. The cost of manufacturing a ceramic PEM is comparatively very low and can be further lowered if produced in large quantity. A major portion of total cost of fabrication in any MFC goes towards manufacturing membranes. Therefore, making a low-cost membrane was necessary to lower the production cost of a PMFC setup. At the same time, it was a challenge to make a ceramic membrane with superior qualities and performance that can take on the widely used commercially available Nafion membrane. Therefore, a cost comparison was made for the best-performing membrane in this study with respect to the Nafion membrane. The breakdown of cost analysis was done considering the combined cost for materials, transportation charges and manufacturing process involved in membrane casting (Table 6). The cost of certain materials viz., clay, bentonite and fly ash could be further lowered in certain locations where transportation cost is very low. It can be seen that final cost of the ceramic membrane was significantly less than the Nafion membrane, and considering its superior performance, it qualifies as a potential candidate for any MFC application and can easily replace costly Nafion membrane.

Table 4.6 Cost breakup for fabrication of membranes.

Ingredients	Price g^{-1} (₹)	g reqd ft^{-2}	Price ft^{-2} (₹)
Clay	10	1100	11
Sodium Carbonate	873	160	140
Sodium Metasilicate	583	40	23
Boric Acid	1017	100	102
Bentonite	5	300	1.5
Fly ash	5	300	1.5
Membrane Casting cost (Labour, Electricity, etc)			1000
Total Cost			1,279
Nafion 117			80,580

4.4 Conclusion

The study demonstrated the development of low-cost ceramic membranes which can potentially replace extremely expensive commercial membrane without much compromise on properties and performance of PMFCs. Different types of ceramic membranes were developed by blending natural clay with bentonite, flyash, Na_2CO_3, Na_2SiO_3, H_3BO_3 at various composition. Membrane characterizations revealed that the presence of bentonite, flyash, Na_2CO_3, Na_2SiO_3, H_3BO_3 improved the performance of MFC by supplementing its cation transport ability and reducing the oxygen diffusion and substrate crossover. The addition of bentonite, fly ash, Na_2CO_3, Na_2SiO_3 and H_3BO_3 at a concentration of 15%, 15%, 8%, 2%, and 5%, respectively to clay in membrane B improves the conductivity of the membrane. Hence, higher bioelectricity generation and superior performance was achieved by its application in a PMFC. Long-term study showed that the membranes were able to sustain PMFC operation for more than six months with little to no compromise in the bioelectricity generation capabilities. Beyond this time frame, the replacement of membrane is recommended mainly due to fouling. The cost of making the ceramic membrane was estimated to be extremely low at ₹1,279 ft^{-2} in comparison to nafion117 (₹80,580 ft^{-2}), and it represent economically viable alternative to commercially available proton exchange membranes due to its ease of use in modular PMFCs. However, there is always a scope to improve properties of ceramic membranes using other ingredients and cation exchangers in the future for large scale PMFC applications and building a road map for further advancement in terms of scale-up of PMFC technology.

References

Ajayi FF, Weigele PR (2012) A terracotta bio-battery. Bioresource Technology 116: 86-91

Apollon W, Kamaraj SK, Espino SH, Segovia CP, Montero LV, Ruelas VM, Marco AV, Medina RO, Silvia FB, Juan FG (2020) Impact of Opuntia species plant bio-battery in a semi-arid environment: Demonstration of their applications. Applied Energy 279 115788

Behera M, Ghangrekar MM (2011) Electricity generation in low cost microbial fuel cell made up of earthenware of different thickness. Water Sci. Technol. 64: 2468

Behera M, Jana PS, Ghangrekar MM (2010) Performance evaluation of low cost microbial fuel cell fabricated using earthen pot with biotic and abiotic cathode. Bioresource Technology 101: 1183–1189

Bohac P, Delavernhe L, Zervas E, Koniger F, Schuhmann R, Emmerich K (2019) Cation exchange capacity of bentonite in a saline environment. Applied Geochemistry 100: 407–413.

Chae KJ, Choi M, Ajayi FF, Park W, Chang IS, Kim IS (2008) Mass transport through a proton exchange membrane (Nafion) in microbial fuel cells. Energy Fuels 22: 169-176

Chakraborty I, Das S, Dubey BK, Ghangrekar MM (2020) Novel lowcost proton exchange membrane made from sulphonated biochar for application in microbial fuel cells. Materials Chemistry and Physics 239: 122025

Flores GH, Poggi-Varaldo HM, Solorza-Feria O (2016) Comparison of alternative membranes to replace high cost Nafion ones in microbial fuel cells. International journal of hydrogen energy 41: 23354-23362

Gajda I, Stinchcombe A, Greenman J, Melhuish C, Ieropoulos I (2015) Ceramic MFCs with internal cathode producing sufficient power for practical applications. International journal of hydrogen energy 40: 14627-14631

Ghadge AN, Ghangrekar MM (2015) Development of low-cost ceramic separator using mineral cation exchanger to enhance performance of microbial fuel cells. Electrochimica Acta 166: 320–328

Ghadge AN, Jadhav DA, Pradhan H, Ghangrekar MM (2015) Enhancing waste activated sludge digestion and power production using hypochlorite as catholyte in clayware microbial fuel cell. Bioresource Technology 182: 225-231

Grancha T, Ferrando-Soria J, Cano J, Amoros P, Seoane B, Gascon J, Bazaga- Garcia M, Losilla ER, Cabeza A, Armentano D, Pardo E (2016) Insights into the Dynamics of Grotthuss Mechanism in a Proton-Conducting Chiral *bio*MOF. Chem. Mater. *28*: 4608-4615

Gunaseelan K, Jadhav DA, Gajalakshmi S, Pant D (2021) Blending of microbial inocula: An effective strategy for performance enhancement of clayware Biophotovoltaics microbial fuel cells. Bioresource Technology 323: 124564

Jana S, Purkait MK, Mohanty K (2010) Preparation and characterization of low-cost ceramic microfiltration membranes for the removal of chromate from aqueous solutions. Applied Clay Science 47: 317–324

Jiang ZQ, Jiang ZJ (2012) Preparation of proton exchange membranes with highperformance by a pulsed plasma enhanced chemical vapor deposition technique (PPECVD). RSC Adv. 2: 2743–2747

Kabutey FT, Zhao Q, Wei L, Ding J, Antwi P, Quashie FK, Wang W (2019) An overview of plant microbial fuel cells (PMFCs): Configurations and applications. Renewable and Sustainable Energy Reviews 110: 402–414

Kiran KV, Manmohan K, Sreelakshmi PM, Manju P, Gajalakshmi S (2020) Resource recovery from paddy field using plant microbial fuel cell. Process Biochemistry 99: 270–281

Kondaveeti S, Lee J, Kakarla R, Kim HS, Min B (2014) Low-cost separators for enhanced power production and field application of microbial fuel cells (MFCs). Electrochimica Acta 132: 434–440

Martinez AAC, Harnisch F, Fitzgerald LA, Biffinger JC, Ringeisen BR, Schroder U (2011) Cyclic voltammetric analysis of the electron transfer of *Shewanella oneidensis* MR-1and nano filament and cytochrome knockout mutants. Bioelectrochemistry 81(2): 74-80

Namburath M, Joshi GN, Cholemari M, Shet C, Sreekrishnan TR, Veeravalli S (2015) Feasibility Study of Indigenously Developed Fly Ash Membrane in Municipal Wastewater Treatment, Aquatic Procedia 4: 1492–1499

Neethu B, Bhowmick GD, Ghangrekar MM (2018) Enhancement of bioelectricity generation and algal productivity in microbial carbon-capture cell using low cost coconut shell as membrane separator. Biochemical Engineering Journal 133: 205–213

Neethu B, Bhowmick GD, Ghangrekar MM (2019) A novel proton exchange membrane developed from clay and activated carbon derived from coconut shell for application in microbial fuel cell. Biochemical Engineering Journal 148: 170–177

Reed JS (1995) Principles of Ceramics Processing. John Wiley & Sons

Regmi R, Nitisoravut R (2017) Effect of configuration and growth stages on bioenergy harvest in the paddy type microbial fuel cell under greenhouse condition. Proceedings of 2017 International Conference on Green Energy and Applications, ICGEA:109–112

Regmi R, Nitisoravut R, Charoenroongtavee S, Yimkhaophong W, Phanthurat O (2018) Earthen pot-plant microbial fuel cell powered by vetiver for bioelectricity production and wastewater treatment. Clean - Soil, Air, Water 46(3):1700193

Shaikh R, Rizvi A, Quraishi M, Pandit S, Mathuriya AS, Gupta PK, Singh J, Prasad R (2020) Bioelectricity production using plant-microbial fuel cell: Present state of art. South African Journal of Botany 000:1-16

Sophia AC, Sreeja S (2017) Green energy generation from plant microbial fuel cells (PMFC) using compost and a novel clay separator. Sustainable Energy Technologies and Assessments 21: 59–66

Tang Q, Katsumi T, Inui T, Li Z (2014) Membrane behavior of bentonite-amended compacted clay. Soils and Foundations 54(3): 329–344

Tiwari BR, Noori MT, Ghangrekar MM (2016) A novel low cost polyvinyl alcohol-Nafion-borosilicate membrane separator for microbial fuel cell. Materials Chemistry and Physics 182 86-93

Winfield J, Chambers LD, Rossiter J, Ieropoulos I (2013) Comparing the short and long term stability of biodegradable, ceramic and cation exchange membranes in microbial fuel cells. Bioresource Technology 148: 480–486

Winfield J, Ieropoulos V, Greenman J (2012) Investigating a cascade of seven hydraulically connected microbial fuel cells. Bioresource Technology 110: 245-250

Chapter-V

PMFC Design Evolution and Performance Comparison of Bacterial and Microlagal bio-cathode

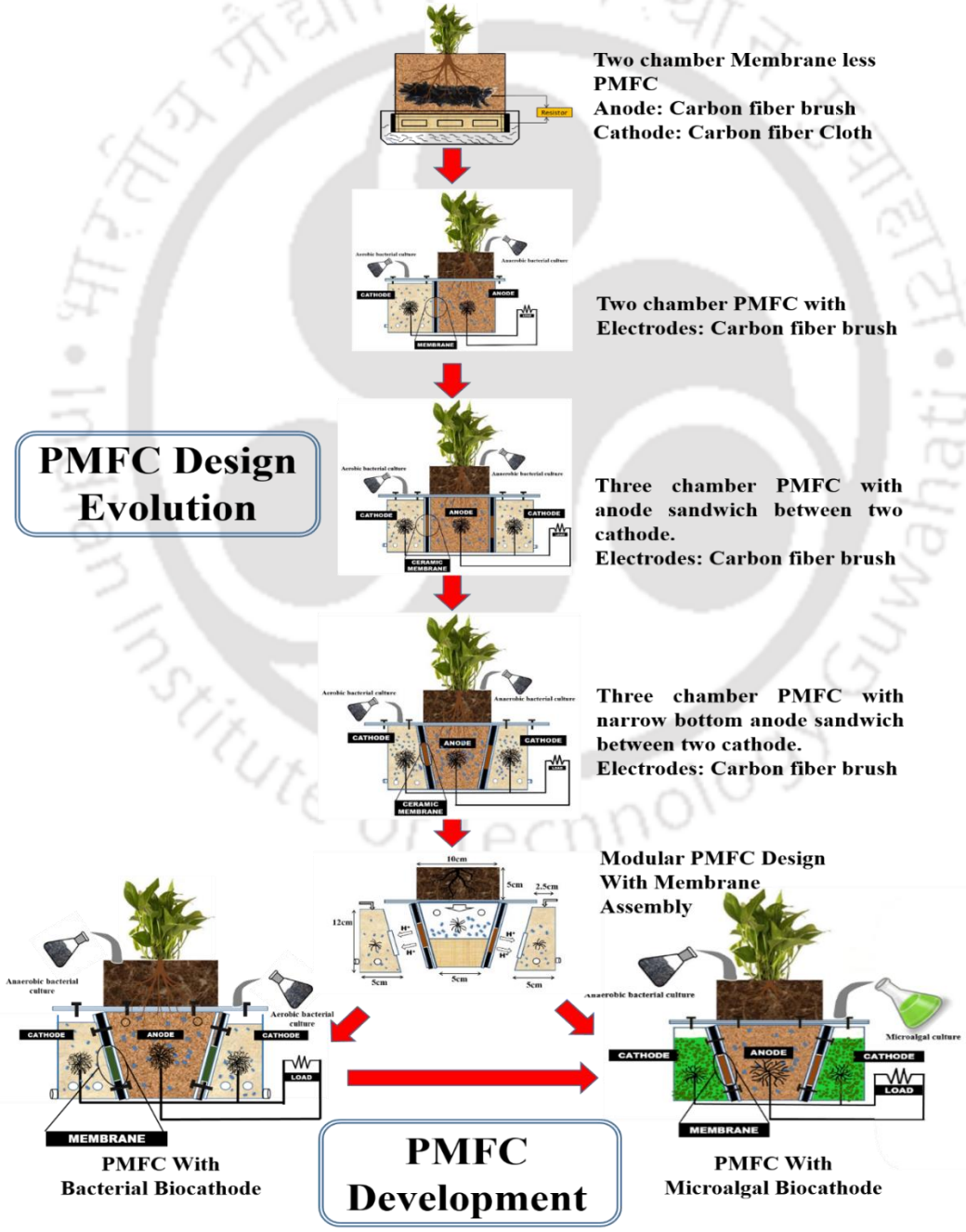

5.1 Overview

To bring microbial fuel cells nearer to practical application is a challenge because of their low power output, higher cost of materials and scale-up difficulties, and difficulty in maintenance over an extended period (Hubenova and Mitov, 2012). Some significant and essential criteria that can significantly affect the performance of a PMFC is its overall design (Wetser et al., 2017). Technology scale-up is most important when it comes to the design of a PMFC setup. Researchers around the globe have incorporated various MFC reactor design approach and structural modifications from time to time. This includes single and multiple chamber configurations (Wetser et al., 2015, 2017; Timmers et al., 2013; Helder et al.,2012), different materials for electrodes (Khudzari et al., 2019; Zhou et al., 2017; Chen et al., 2018), membrane and membrane-less arrangements (Ghadge and Ghangrekar, 2015; Chakraborty et al., 2020; Lu et al., 2020), anodic and cathodic modifications (Gulamhussein et al., 2020), different types of inoculum (Wu et al., 2017) as well as focusing on the use of low tech and low-cost raw materials while designing MFCs (Ghadge and Ghangrekar, 2015).

Ever since the MFC technology was developing, only half of the system, i.e., the anodic chamber, was biological, involving microbial oxidation of organics. In contrast, the cathodic chamber was abiotic, involving chemical catalysts (e.g., Pt, CuO). Using a chemical catalyst as a terminal electron acceptor for reduction reaction at the cathode improves the performance. However, they are expensive and are not eco-friendly. However, now researchers worldwide are carrying out studies involving complete biological setups (Wu et al., 2017; Milner et al., 2016; Rusli et al., 2019; Hubenova and Mitov, 2012). This consists of using microorganisms at the cathode, representing a "biocathode". The use of biocathode presents significant advantages over abiotic and chemical cathodes minimizing investments and operational costs. Also, the use of microorganisms creates an eco-friendly environment rather than the use of hazardous chemical catalysts.

The presence of oxygen for the cathodic reactions in any MFCs is the most favorable option as a terminal electron acceptor because of its high redox potential and infinite presence in the atmosphere. The mixed culture aerobic microorganisms are known to perform better oxygen reduction than pure cultures because of their ability to rapidly form biofilm on the electrode surface. This has resulted in higher power output due to its ability to adapt to changing environmental conditions with less substrate specificity, thus making the process economically viable. Moreover, their easy availability, robustness and sustainability make them an ideal candidate for bio cathode. However, despite its advantages, additional mechanical aeration is

required at the cathode chamber, which seems costly, thus increasing the expenditures by approximately 50% of the total operational costs (Wu et al., 2017; Milner et al., 2016).

Replacing chemical catalysts and mechanical aeration processes with photosynthetic microalgae species in an MFC is also promising to improve cathodic performance. Among the various possible configurations, the microalgal biocathodes represent a more attractive and effective solution to overcome the limiting aspects of oxygen (O_2) reduction and other limitations caused by abiotic and general biocathodes in MFCs. This helps avoid the need for energy-intensive mechanical aeration and its subsequent energy costs. The microalgae generate O_2 via photosynthesis at the biocathode resulting in the enhancement of PMFCs performance in an environmentally sustainable way. This, in turn, helps reduce the overpotentials caused by various losses. The microalgae absorb CO_2 from air or the anode chamber for their growth (Rusli et al., 2019; Hubenova and Mitov, 2012). There have been reports where CO_2 generated by anaerobic degradation of organics can get diffused through pores of the separator and reach the cathodic chamber for utilization by microalgae (Timmers et al., 2013). The applications of microalgal biocathodes in MFCs require knowledge of both engineering and science to provide a suitable environment to have an efficient CO_2 sequestration, *in-situ* O_2 generation, wastewater treatment (nutrient uptake), biomass for biofuel, biofertilizer, and other value-added products generation. Therefore, utilizing microalgal biomass or living algae directly for power generators can become a promising approach.

This chapter describes the evolution journey of PMFCs from a two-chamber membrane less design to a three-chamber modular structure. A bio cathode performance comparison study was carried out between a bacterial and a microalgal assisted bio cathode. The performance of the PMFCs were appraised in terms of their power generation capabilities, biofilm development at anode and cathode, and ease of operation.

5.2 Materials and Methods

5.2.1 Design, development and performance evolution of PMFCs

The design of PMFC setup plays an essential role in its performance; therefore, continuous improvements in design configurations become vital for obtaining long-term sustainable bioelectricity generation capabilities. The study goes through a series of upgradation in setup design from a two-chamber PMFC to a three-chamber PMFC to find out the role of chamber architecture on the bioelectricity generation capabilities.

For this study, four different PMFC designs were incorporated to find out the role played by chamber architecture on the bioelectricity generation capabilities. In all the PMFCs, a bacterial bio cathode was used. The PMFC-1 is a membrane-less design, whereas in the case of others, the chambers were separated by a ceramic membrane made up of Clay-55%, Bentonite-15%, Flyash-15%, Na_2Co_3-8%, Na_2Sio_3-2% and H_3Bo_3-5%. The size of the membranes used was 10 cm in diameter and 6 mm in thickness with a surface area of 78.6 cm^2. The said membrane has already shown the best performance among all ceramic membrane tested previously (Chapter-IV), therefore, it was used in all subsequent studies. The plant of interest for the study was *Philodendron erubescens*, which showed excellent bioelectricity generation potential due to its ability to adapt in a moist environment and develop an excellent root network system (Section 3.3.7, Chapter-III). For all PMFCs, the plants were grown in a mixture of soil, cow dung and compost in a ratio 3:2:1. While planting, 50 g of dried roots of each plant cut in the length 4-8 cm were added to the soil of the new plant assembly setup. The presence of dried roots in the chamber is known to reduce soil compactness and help the bacterial community to grow and accelerate the start-up process (Wetser et al., 2015). The plants were grown under indoor conditions in the temperature range of 22 ± 3°C. Artificial lighting was provided using light-emitting diode LED grow lights (9W, Bajaj Electricals Ltd. India), and 12 h day/night condition mimic conditions were maintained mimicking natural conditions using an automatic timer. Sisalation was used at the top to reflect light on plants mimicking outdoor growing conditions. To eliminate any potential surface contamination, the electrode brushes were washed with acetone and ethanol and finally rinsed with deionized water before placing them inside their respective chambers. At the start of the experiment, the anode and cathode of all PMFCs were inoculated with anaerobic and aerobic media mentioned later in sections 5.2.3.1 and 5.2.3.2, respectively.

5.2.1.1 Two chamber membrane-less PMFC

In this preliminary design, the PMFC experimental setup were made up of two different plastic containers with anode and cathode chambers having dimension (diameter × height) 10 cm × 14 cm and 14 cm × 5 cm, respectively. The design is a membrane-less arrangement, wherein a bentonite clay layer of thickness 1 cm was prepared and used at the base of the anode chamber in PMFC to act as a separator between soil and catholyte. At the bottom of the anode chamber segmented perforation was made all around the perimeter for effective movements of cations from anode to the chambers across the bentonite clay layer.

PMFC experiment was initiated by growing plant in the anode chamber and allowed to be acclimatized to the new conditions for at least 10 days. The basic properties of soil and separator used in the experiments are summarized in Table 5.1. Acid-treated carbon fibre was used as electrodes. The anode was made up of carbon fibre brush using copper wire (4 cm in diameter and 6 cm in length and weight of 4.7 g) for effective surface area development and was placed perpendicular to the growth of plant roots just above the bentonite clay layer (separator) in close proximity to the roots. The cathode comprises carbon fibre cloth (2 cm in width and 21 cm in length and weight 4.2 g) wrapped outside the lower perforated segmented of the anode chamber. The anode chamber is placed inside the cathode chamber, as shown in Fig. 5.1. The electrodes were connected externally by epoxy copper wire with an external resistance of known value.

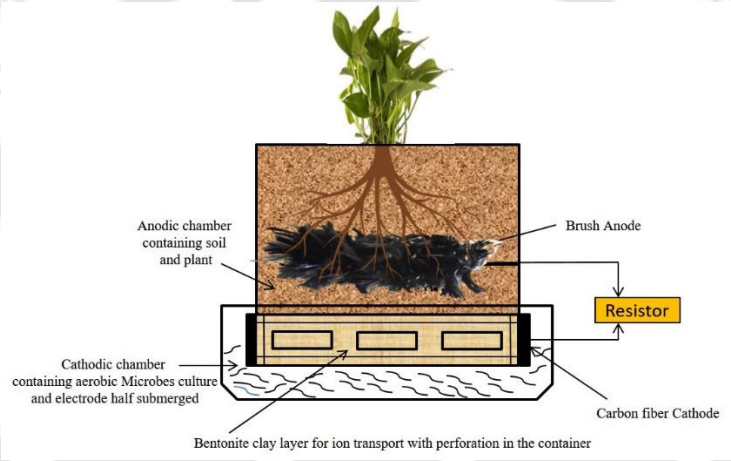

Fig. 5.1 Schematic representation of PMFC-1 with membrane less design setup.

Table 5.1 Basic properties of Soil and Separator used in the experiment.

Parameters	Soil	Separator
pH	7.4	8.2
Moisture content (%)	~ 65	<10
Density of particle (g cm^{-3})	3.256	2.635

5.2.1.2 Two chamber PMFC

To further improve the performance of a PMFC and to address the flaws of existing setup, a new two-chamber PMFC setup was made with poly-acrylic sheets of 8 mm thickness for higher stability (Fig. 5.2). The anode chamber has a 1000 mL capacity and a cathode chamber with 800 mL working volume. In this design, plants were not grown directly in the anode chamber as in the previous design; instead, the anode chamber of the previous design (Section 5.2.1.1) is used as plant assembly having a same dimension of 10 cm × 14 cm and

placed inside newly made anode chamber. In the plant assembly, perforations were made at the lower portion for effective root elongation, thus enhancing nutrient transportation and movements of microbes. Unlike the use of a bentonite clay layer in the previous design, here, a proper novel ceramic membrane was introduced for the first-time separating anode and cathode chamber. Unlike carbon fibre cloth used as cathode in the previous design, here in this design setup, both the electrodes were made up of carbon fibre brush. The electrode material used in the study is an acid-modified carbon fibre cloth, to enhance roughness and hydrophilicity as mentioned in our previous chapter (Chapter-III). This will enable better bacterial cell distribution and would enhance biofilm development and mass transfer process. The carbon fibre was then cut into the desired length and twisted to form a brush with the help of titanium wire for effective surface area development and used as both anode and cathode with a dia of 5 cm and 2.5 cm for anode and cathode, respectively. The anode was placed perpendicular to the direction of plant roots growth in the anode chamber. Unlike the previous design (Section 5.2.1.1**)**, this allows the surface of the anode not to be preoccupied with the soil particles and instead allows more surface area for microbes for biofilm formation under wet conditions. The wet environment helps in the growth of exoelectrogenic bacteria compared to dry environments. In the present design, the electrodes were made with titanium wire (1.0 mm in diameter) instead of the copper wire used previously. The titanium wire is non-corrosive and well suited for wet and moist environments and decreased internal resistance to ion transport.

After inoculating the anodic chamber with anaerobic culture, plant assembly was placed inside it and edges were sealed. To remove any unwanted O_2, nitrogen purging was done to maintain anaerobic conditions.

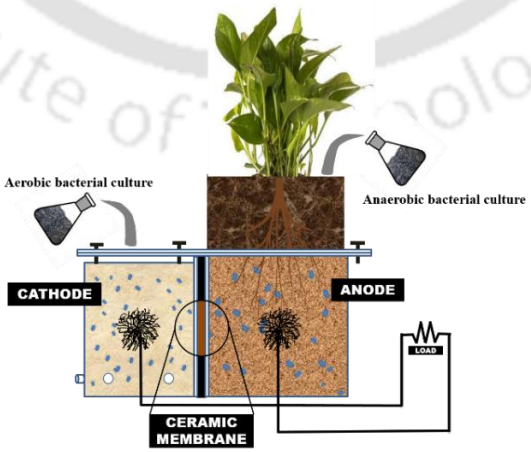

Fig. 5.2 Schematic representation of PMFC-2 incorporating ceramic membrane.

5.2.1.3 Three chamber PMFC

This design further extends to the two-chamber PMFC described in section 5.2.1.2. Here an anode chamber is sandwiched between two cathode chambers. The PMFCs has an overall dimension of 16 × 30 cm with an anode chamber capacioty of 1000 mL and two cathode chambers with 400 mL each working volume of catholyte. The three-chamber configuration enhances the performance of a PMFC compared to the two chamber PMFC. Hence, this configuration was used in this study. Both the cathodes were connected as a single unit while operating.

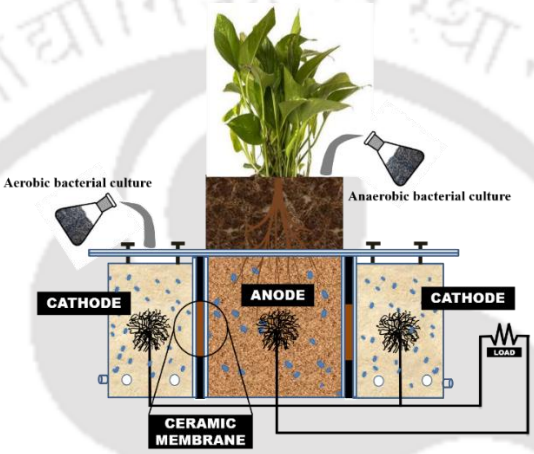

Fig. 5.3 Schematic representation PMFC-3 with three chamber design setup.

5.2.1.4 Three chamber narrow bottom anode PMFC

In this design, PMFC setups were designed using a similar polyacrylic sheet as before for high stability. Here the shape of the anodic chamber was designed in "V" shaped with 1000 mL capacity with a narrow bottom to favour the development of anaerobic conditions for the microbes. On either side of the anodic chamber, two cathodic chambers were fixed, separated by a ceramic membrane, each with 400 mL capacity. The cathode chambers have wider bottom for easy circulation of air. However, the overall size remains the PMFC remains same as in Section 5.2.1.3.

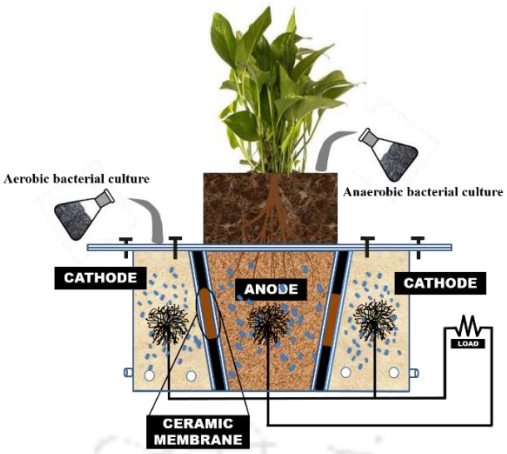

Fig. 5.4 Schematic representation PMFC-4 with three chamber design setup having narrow bottom anode.

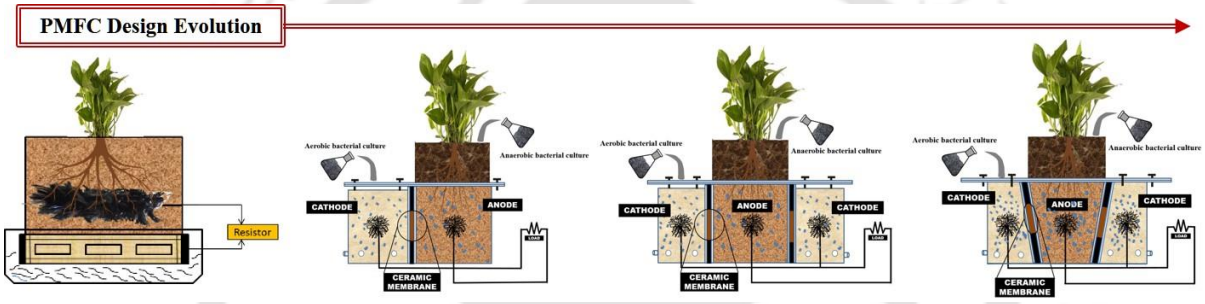

(a) (b) (c) (d)

Fig. 5.5 Schematic representations of PMFC designs evolution from a two chamber PMFC to a three chamber PMFC (a) Two chamber PMFC with anode integrated into soil. (b) Two chamber PMFC with plant assembly is separated from anode. (c) Three chamber PMFC with anode sandwich between two cathodes. (d) Three chamber PMFC with a narrow bottom anode.

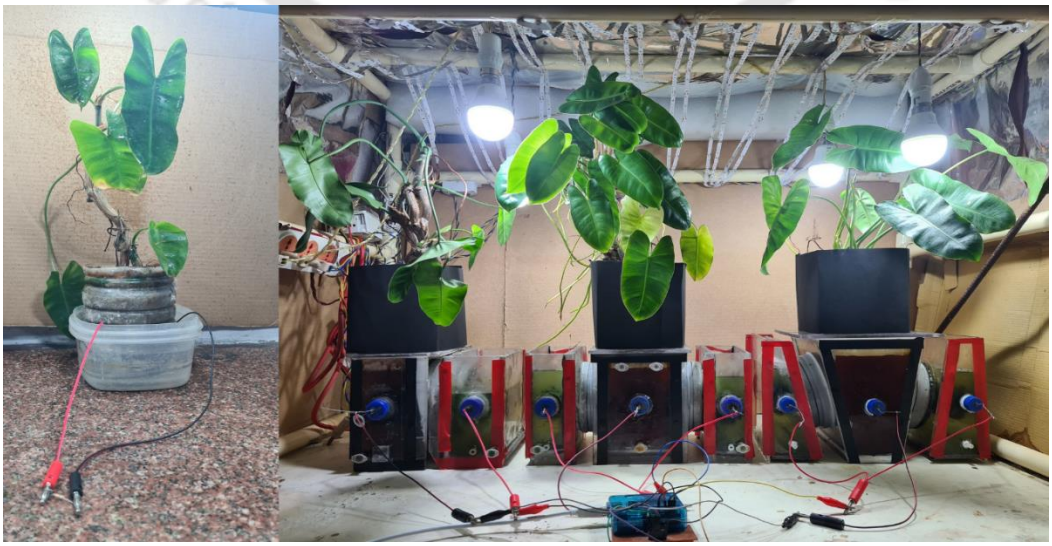

Fig. 5.6 Laboratory arrangement of all the four different PMFC setup design.

5.2.2 Design of a modular PMFC setup

To make regular operational and maintenance work easier, an upgradation in the design of the three chamber PMFC i.e., PMFC-3 was carried out. The modular PMFC was designed using same polyacrylic sheet of 8 mm thickness for higher stability. The working volume of chambers remains same as PMFC-3 with a narrowed bottom anodic chamber to enhance the development of an anaerobic environment. On the other hand, a wider base at the cathodic chamber will help in the aeration, supplemented by the use of silicon rubber tubes (Fig.5.7) for easy diffusion of outside air into the section (Wetser et al., 2017). The three chambers PMFC has been made completely modular in design, thus, provides ease of changing and assembling every part without any hassle. The membrane assembly is uniquely designed to easily change and replace membranes, and the setup can be easily assembled.

Similarly, changing and replacing plants, electrodes and nutrient media in the PMFC setup is easy and convenient. With this design concept, the plant assembly is also a separate entity where plants were allowed to grow in a separate plastic container, which was later incorporated into the anode chamber without disrupting the setup. The PMFC design provides an advantage of changing the plants in case they die or become non-performing. The carbon fiber brush electrodes were fitted with screw caps with an interior thread design, making them easy to fit inside the chamber and remove at the same time to replace them due to fouling.

The placement of an exhaust valve at the base of each chamber is a part of our modular design PMFC which helps the user to replace spent media from each chamber easily and independently of other chambers and without disturbing the other chambers or the whole setup. A complete schematic representation is laid in Fig. 5.7(a) and (b) for better understanding.

In the new modular design, the membrane assembly is uniquely structured (described in Fig. 5.7) to affix different types of ceramic membrane in the junction between anode and cathode chambers. Since membranes are fixed between anode and cathode chambers, its placement is critical for PMFC stability so that liquid content of the chambers do not leak from one chamber to another and outside.

In any conventional MFC design setup, a membrane has to be fixed permanently at the junction of chambers, making it difficult to open at the end of operation cycle. Also assembling a new membrane is the same place was tedious and thus work is delayed. In case of the new modular design, the membrane assembly is a slide-in-out mechanism wherein ceramic membrane is placed and locked in place (to make non-movable) by using a rotating circular dice inside the assembly. The membrane assembly consist of two parts, one part is fixed in

anode chamber and another in the cathode chamber (Fig. 5.7). The chambers are fixed by sliding cathode chamber part inside anode chamber part without using any screw or glue to fix chambers. The rubberized gasket placed inside makes the entire setup leak proof. This process makes working with PMFC very easy as chambers can be easily opened and membrane can be easily replaced.

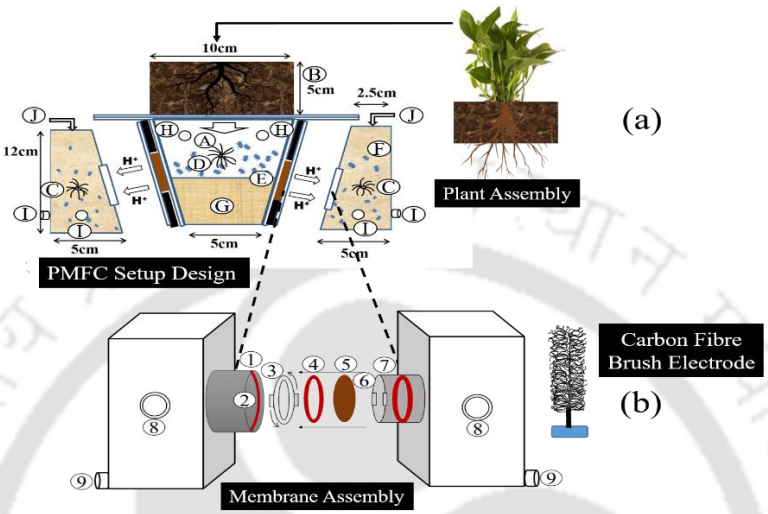

Fig. 5.7 The modular design of the Plant microbial fuel cell (PMFC)with breakup explanation of every components (a) PMFC setup design (b) Membrane assembly design
[(A) Photosynthetic Substances Expelled by Roots (B)Upper cavity (Soil Layer) (C)Brush Cathode (D) Brush Anode (E)Active Anaerobic Microbes (F)Active Aerobic Microbes (G)Solid Phase Nutrient (H) Nitrogen Purging (I) Silicon Tubing (J)Air In (1) Outer Cpvc Casing 11 cm dia (2) Inner Rubber Gasket (3) Casted Acrylic Ring with Rotational Lock (4) Outer Rubber Gasket (5) Ceramic Membrane (6) Inner Cpvc Casing 10.7 cm dia (7) Inner Fixed Gasket (8) Site for Electrode Placing with internal thread (9) Outlet for Removal of Nutrient Media].

5.2.3 Performance comparison of Bacterial and Microalgal Bio-cathode

For this comparison study, the PMFC-4 architecture was used with the plant of interest being *P. erubescens* and *E. aureum* grown under the same condition in a plant assembly setup as mentioned in section 5.2.1.

5.2.3.1 PMFC inoculation and operation

A biological sludge sample was collected from the bottom sediment extract of the sewage treatment plant of IIT Guwahati for culturing anaerobic microorganisms. Mixed liquid suspended solid (MLSS) and mixed liquid volatile suspended solids (MLVSS) analysis were out as per protocol described elsewhere (APHA, 1985). 10 mL of this sewage sample were cultured in artificial media containing 8 g L^{-1} sodium acetate, 7 g L^{-1} glucose 7 g L^{-1} fructose, 10 g L^{-1} peptone 8.2 $Na_2HPO_4.2H_2O$, 5.2 g L^{-1} $NaH_2PO_4.H_2O$ (Tommasi et al.,2016). For

faster biofilm development, pre-acclimatization of the brush electrodes in the respective anodic and cathodic microbial media was carried out for at least 7 days before insertion into the PMFC chamber. Nitrogen gas purging was carried out in the culture bottle to maintain the anaerobic condition and the cultures were maintained at 37 ^{o}C.

One of the key reasons for using mixed culture anaerobic microbes instead of pure cultures is to avoid contamination by other organisms. Pure culture microbes are known to be superior in the degradation of organics; however, they need to be monitored continuously, and different contamination avoiding techniques are required, which results in higher operational costs. Hence, mixed cultures microbes which are naturally occurring are more suited for the study as it offers faster biofilm development and better synergetic interaction during the electron transfer mechanisms than the pure culture (Gunaseelan et al.,2021).

To reduce start-up period in a PMFC, a solid-state nutrient (SSN) source was prepared similar to that of Tommasi et al., (2016), containing all the mentioned nutrients and a solidifying agent called agar. The prime idea is to convert liquid nutrient source into a solid one, which will store nutrients for extended periods of time, increasing their density and a slow release over time. Once the SSN was put into the cell, mixed culture bacterial solution grown under anaerobic condition was poured over it (Fig. 5.8c). Chemical oxygen demand (COD) was measured at the start of the experiments and in case of decline in cell potential.

(a) (b) (c)

Fig. 5.8 (a) Carbon brush electrode (5 cm i.d.) (b) dried roots used during PMFC setup (c) Picture of the agar-based solid-state nutrient (SSN) inside the anodic chamber.

5.2.3.2 Development of Bacterial Biocathode

For inoculation of biocathode, the same anodic media mentioned in section 5.2.3.1 was used. However, instead of sodium acetate, 0.94 g L^{-61} $NaHCO_3$ was used (Wu et al., 2017). For the development of the aerobic condition, air circulation is done using an aquarium air

pump, and fresh media was introduced twice a week into the cathode chamber. The pH was maintained at 7 ± 0.5 throughout the experiment by adding dilute NaOH and HCl. For the study, two best performing indoor plant i.e., *P. erubescens* and *E. aureum* were in PMFCs with and without SSN. Further, these PMFC perfornmance were compared with a control setup without plant but containing bacterial biocathode. The cathode chamber was agitated periodically for maintainance of aerobic culture using an aquarium pump (SOBO, SB548A). Fig. 5.9 shows the experimental setup.

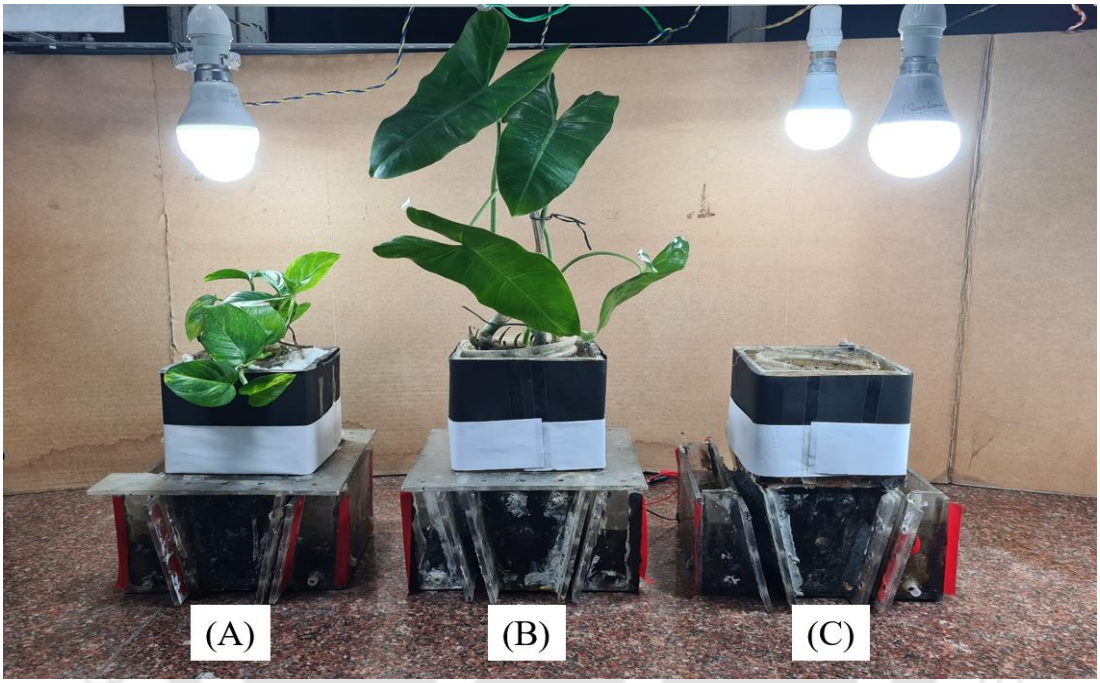

Fig. 5.9 Experimental setup of PMFCs with bacterial biocathode [(A) *E. aurium* (B) *P. erubescens* (C) Control without plant].

5.2.3.3 Development of Microlagal Biocathode

For biocathode development using microalgae, a locally isolated strain i.e., *Chlorella sorokiniana* KMBM_K, was used for the study. The microlagal strain was isolated from a water body in IIT Guwahati identified and maintained in our laboratory in the traditional BG11 growth medium. The BG11 nutrient medium comprises of 0.075 g L^{-1} magnesium sulfate ($MgSO4.7H_2O$), 0.036 g L^{-1} calcium chloride ($CaCl_2.2H_2O$), 0.006 g L^{-1} citric acid ($C_6H_8O_7$), 0.006 g L^{-1} ferric ammonium citrate (C_6H_5 + $4yFexNyO_7$), 0.006 g L^{-1} EDTA ($C_{10}H_{14}N_2Na_2O_8.2H_2O$), 0.02 g L^{-1} sodium carbonate (Na_2CO_3), 1.5 g L^{-1} sodium nitrate ($NaNO_3$), 0.04 g L^{-1} dipotassium hydrogen phosphate (K_2HPO_4), and 1 mL L^{-1} trace element mix. The trace element mixture contains 2.86 g L^{-1} boric acid (H_3BO_3), 1.81 g L^{-1} manganese

chloride ($MnCl_2.4H_2O$), 0.222 g L^{-1} zinc sulfate ($ZnSO_4.7H_2O$), 0.39 g L^{-1} sodium molybdate ($Na_2MoO_4.2H_2O$), 0.079 g L^{-1} copper sulfate ($CuSO_4.5H_2O$), and 0.0494 g L^{-1} cobalt nitrate ($Co(NO_3)_2.6H_2O$). The microalgae were maintained by artificial illumination through white fluorescent tube light (around 5000 lux) at a temperature of approximately 25 °C, with a light: dark cycle of 12:12 h. Culture media used in anode and cathode is shown in Fig.5.10 (c) and (d).

When the algal biomass concentration reached 0.8 g L^{-1} and was visibly green during the exponential growth phase, it was used as the inoculum for the cathode chamber. Microalgal growth, biofilm development, and electrode colonization were monitored periodically. The two indoor plant viz., *P. erubescens* and *E. aureum* was used for the study in two different PMFC. To analysis the performance of biocathode, these PMFCs were compared with control PMFCs (without plant and absence of microalgal biocathode, wherein tap water was used in the cathode chamber) Schematic representation of PMFCs with microalgal biocathode and experimental setup is shown in Fig. 5.10 (a) and (b). It was agitated periodically using an aquarium pump (SOBO, SB548A). To understand the sustainability of microalgal biocathode a PMFC setup without a plant was also used a control.

The microalgal growth profile in the cathodic chamber of the PMFC was monitored by measuring the optical density of the microalgal culture at A_{680} nm in a UV-Vis spectrophotometer (Thermo Fisher Scientific, USA) at an interval of every 24 h. The biomass concentration in dry cell weight (DCW) was estimated by proper calibration between the absorbance value at 680 nm and the dry cell weight.

The overall biomass productivity (P_W, mg L^{-1} d^{-1}), specific growth rate (μ, d^{-1}), and the cell doubling time (D_T, d^{-1}) was estimated by the following equations:

$$P_W = (W_f - W_0)/ (T_f - T_0) \quad (5.1)$$

$$\mu = \ln (Y_2 - Y_1) / (T_2 - T_1) \quad (5.2)$$

$$D_T = \ln 2/\mu \quad (5.3)$$

Where Y_2 and Y_1 are the biomass concentration (g L^{-1}) at time T_2 and T_1 respectively, and W_f and W_0 are the biomass concentration (g L^{-1}) at cultivation time T_f and T_0, respectively (Malakar et al., 2022a, 2022b).

The chlorophyll a and b were extracted using pure methanol by a previously reported spectrophotometric-based method (Provost et al., 2011). The concentration of chlorophyll in the sample was calculated by using 3.1-3.3 mentioned in section 3.2.2 (Chapter-III).

To speed up the initial start-up process, both anode and cathode were pre-acclimatized in their respective media for ten days prior to placing inside PMFCs. In this way, microbes get extra time to acclimatize to a new environment. The biofilm development process is faster once the electrodes are placed inside PMFCs.

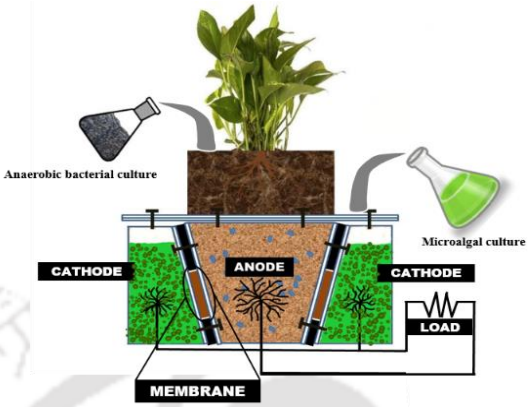

(a)

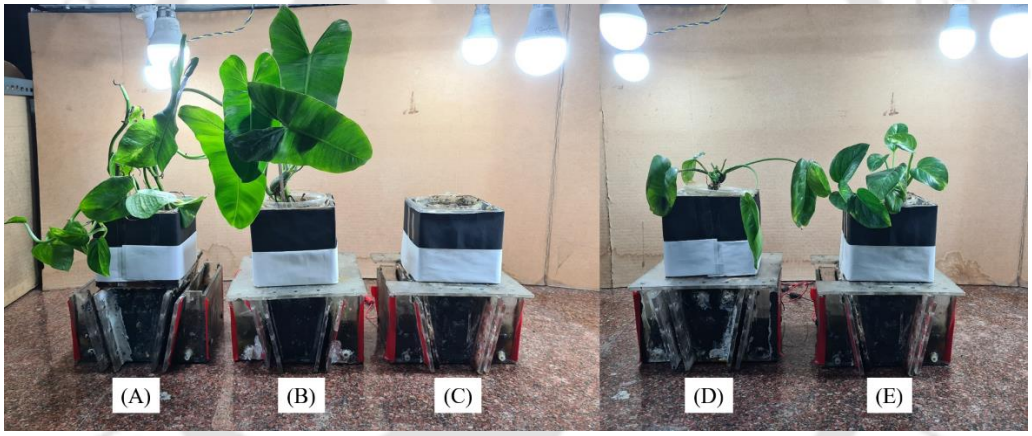

(b)

(c) (d)

Fig. 5.10 (a) Schematic representation of PMFC with microalgal bio cathode (b) Experimental setup of PMFCs [(A) *E. aurium* (B) *P. erubescens* (C) Control without plant (D) Control with

P. erubescens (E) Control with *E. aurium*] (c) Mixed culture of anaerobic microbes (d) Culture of *Chlorella sorokiniana*.

5.2.3.4 Electrochemical kinetics

To understand the mechanism of oxidation and reduction in any MFC, cyclic voltammetry (CV) remains an established and straightforward technique. The response of redox current peak under CV can provide information about the electro catalytic reactions going on the surface of the anodic biofilm (Alessandro et al., 2011). Therefore, the CV technique was carried out in three-electrode setups employing an Ag/AgCl reference electrode coupled to a potentiostat. The electrode characterization was done during the initial period (non-turnover) and in bio electro catalytic (turnover) conditions to understand and analyze the transition of electrodes towards biofilm development and its bio electro catalytic behaviour with the help of redox current peak response.

For the analysis of the entire cell, the anode was used as the working electrode, Ag/AgCl as the reference electrode, and the cathode as the counter electrode. Similarly, bio cathode characterization was also executed by engaging cathode as working electrode, Ag/AgCl as the reference electrode positioned inside the cathodic chamber. The anode, in this case is the counter electrode. CV was performed in the potential range of -0.5 V to +0.5 V at a slow scan rate of 10 mV s^{-1} at 25^{o} C. While varying the potential, the resulting response current peaks were recorded by using potentiostat PGSTAT 302N (Metrohm, Autolab) (Gunaseelan et al.,2021).

Electrochemical Impedance Spectroscopy (EIS) technique was used to measure the cell's internal resistances. EIS being a powerful and non-destructive technique, works without disturbing the biological functions of PMFCs. It was carried out in two-electrode setups where cathode acts as reference/auxiliary electrode in the frequency range of 100 kHz to 10 mHz with 10 mV amplitude of AC signal using potentiostat PGSTAT 302N (Metrohm, Autolab) (Alessandro et al., 2011; Zhou et al., 2015).

5.2.3.5 Electrode surface analysis using SEM

To observe the presence and formation of anodic and cathodic biofilm on the electrodes surface, a portion of the electrode surface was cut and was washed with sterile water, followed by fixation using 3% glutaraldehyde and PBS buffer (pH 7.0). Subsequently the surface was dehydrated using ethanol (10%, 25%, 50%, 75%, and 100%) to observe the biofilm formation

under Field Emission Scanning Electron Microscopy (FESEM Gemini 300(ZEISS)) (Abbas et al., 2018).

5.3 Results and Discussion

5.3.1 Effect of PMFC design structure on bioelectricity generation

The design of a PMFC setup is an important criterion, as it plays a significant role on the bioelectricity generation capabilities of PMFCs. The design evolution of PMFC setup shows substantial improvement in bioelectricity generation capabilities. The behavioral response and bioelectricity generation pattern from all the four PMFCs are shown in Fig. 5.9 and the obtained parameters are presented in Table 5.2. During the initial period i.e., 10-15 days, the output from all the PMFCs were similar; however, with the progress of time, an apparent variation in power generation pattern was observed among all the PMFCs (Fig.5.11a). The voltage output pattern from PMFCs having a membrane (PMFC-2, PMFC-3, PMFC-4) were almost similar during 15-30 days' period with PMFC-2 having least values. However, in case of membrane less PMFC initially voltage output was less but increases sharply during 18-24 days to around 580mv and was maintained till 40th day before declining. The voltage generation rises again after second inoculum was fed of 45th day. This type of response may be because of effective ions with less resistance due to absence of a membrane. However, the decline in voltage was because of depletion of nutrients. Polarization curves (Fig. 5.11b) and power curves (Fig. 5.11c) obtained during steady-state on the 8th week shows the maximum power density of 29.12 mW m^{-2} and a current density of 53.23 mA m^{-2} from PMFC-4, showing an overall increase of 8 %, 29 % and 60 % in power generation with respect to PMFC-3, PMFC-2 and PMFC-1 respectively. From the polarization curve's slope, the systems' internal resistance was calculated and presented in Table 5.2. The performance enhancement can be attributed to upgradation in design aspects and materials used in PMFC.

The results show superiority of new design PMFCs (PMFC-2, PMFC-3 and PMFC-4) in terms of power generation as compared to membrane less PMFC (PMFC-1). The incorporation of liquid media in the anode chamber and presence of a membrane makes it becomes easier for the protons to travel through the nearest PEM towards the cathode side and reduced itself. Therefore, a consistent increase in voltage generation was observed and its sustainability is maintained without addition of external media. While in case of PMFC-1, the incorporation of anode directly inside the soil results in preoccupation of a large amount of surface area of brush anode by soil particles. This reduces the number of active sites for biofilm

formation. Also inside the anode chamber in PMFC-1, the O_2 concentration was found to be in the range of 45-35 µmol L^{-1}, which is relatively high as compared to other PMFCs (Fig.5.12). Therefore, incorporation of anode in the vicinity of roots restricting the anaerobic bacterial biofilm development dur to predominating oxygen loss from roots (Liu et al., 2018).

Similarly, reduction rates also increase with the incorporation of membrane based PMFCs. This can also be seen from the CV curves with anode as working electrode in Fig.5.11d with an obtained current densities of 19.6 mA m^{-2}, 28.8 mA m^{-2}, 34.4 m A m^{-2} and 39.6 mA m^{-2} from PMFC-1, PMFC-2, PMFC-3 and PMFC-4 respectively. Incorporation of two cathodes on either side of anode also improves reduction rates in PMFC-3 and PMFC-4. Among the three chamber PMFCs, a slight improvement in bioelectricity generation was also observed in PMFC-3 as compared to PMFC-2 probably because of having a narrow bottom anode chamber which restrict mixing of the content of the chamber and helps in creating necessary anaerobic environment. On the other hand, having a wider bottom cathode chamber eases out air circulation at the bottom thus creating aerobic environment. To ascertain this fact, the oxygen profile was determined quantitatively using an electrochemical O_2 micro sensor (Unisense OX-25, Denmark). The maximum O_2 concentration in all the PMFC was approximately 25-27.5 µmol L^{-2} at a depth of 3 cm from the junction of the plant assembly.

In contrast, the O_2 concentration at a depth of 14 cm was lowest in the case of PMFC-4 with a narrow bottom anode with a value of 11.25 µmol L^{-1} (Fig 5.12). In the case of anode chamber in PMFC-1, the O_2 concentration decreases with depth; however, the presence of roots at the lower portion of the chamber, a rise in O_2 concentration was seen. A higher concentration of O_2 was also found at a significant depth below the exposed soil surface, i.e., 2-4 cm from the inter-junction of anode chamber and plant assembly in the case of PMFC-2, PMFC-3, and PMFC-4 predominantly because of oxygen loss by the roots exodus. The O_2 profile for all four PMFCs is summarised in Table 5.2. It was observed that O_2 concentration at the bottom of the anode chamber in PMFC-4 was nearly 26% less than PMFC-2 and PMFC-3 owing to its narrow button design, which significantly enhanced the development of necessary anaerobic conditions and proved to be superior for bioelectricity generation among all PMFCs.

Therefore, it was confirmed that the design criteria of a PMFC play an essential role in its performance, wherein the position of the plant root and the anode chamber's depth influence the development of anaerobic conditions and, subsequently the power generation in PMFCs.

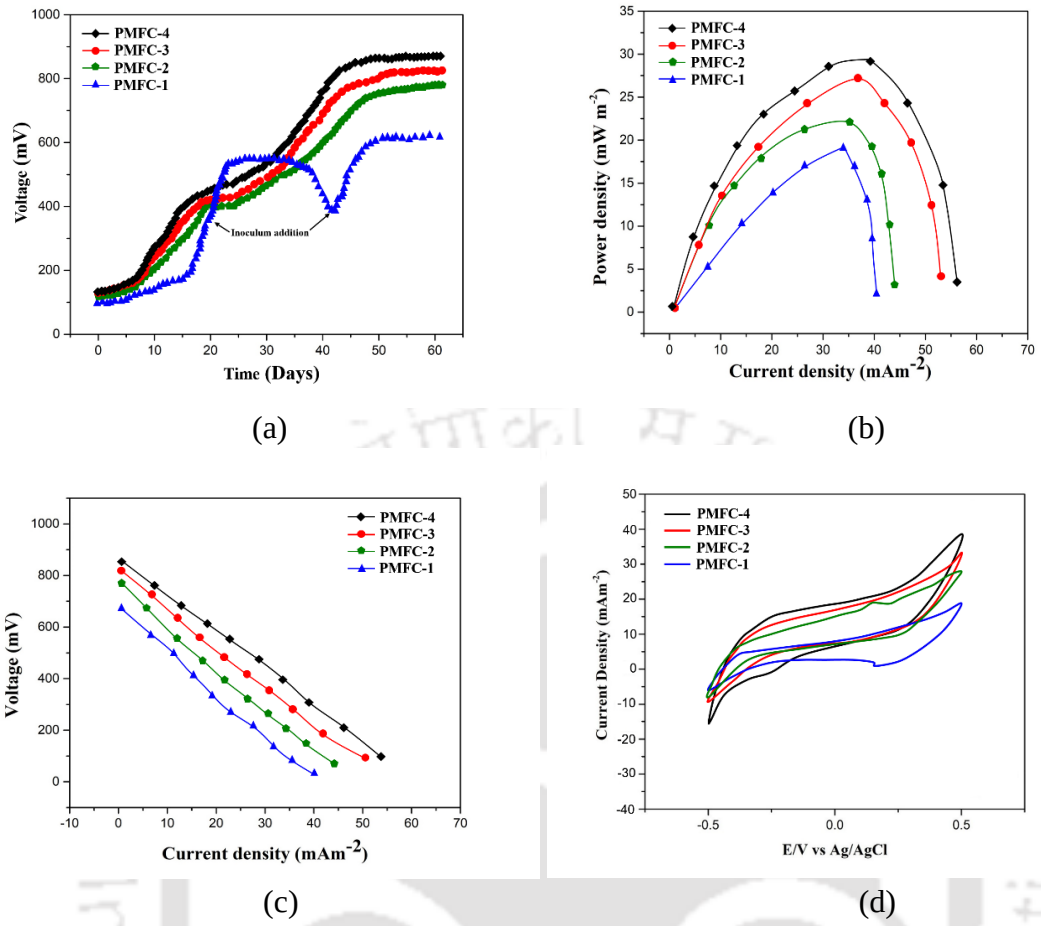

Fig. 5.11 (a) Cell voltage curve (b) Polarization curves (c) Power curves of different PMFCs (d) Electrochemical characterization of PMFCs with anode as the working electrode.

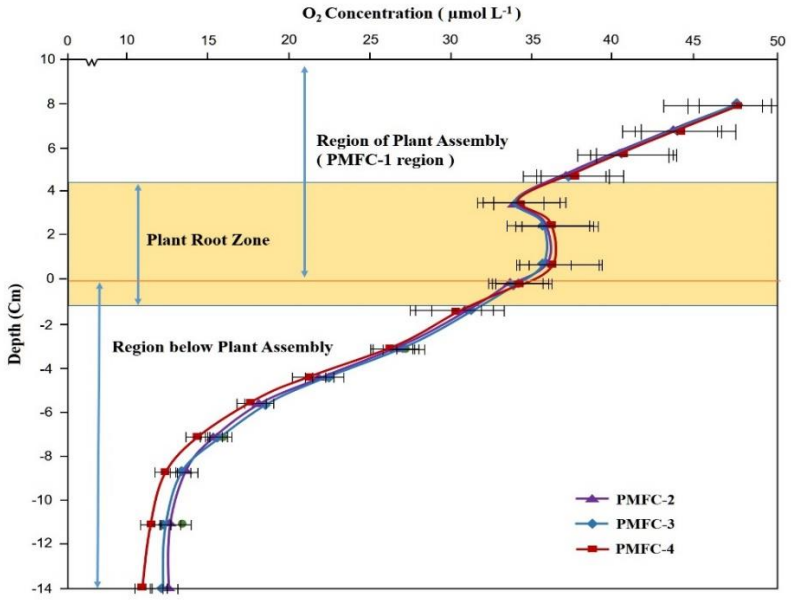

Fig. 5.12 Oxygen concentration profiles of anode chamber at different depth in PMFC-1, PMFC-2, PMFC-3 and PMFC-4. (The point with a depth of 0 cm was the interface between plant assembly and anode chamber in PMFC-2, PMFC-3 and PMFC-4).

Table 5.2 Performance analysis of PMFCs.

Electrical parameters	PMFCs with different Setup Configurations			
	PMFC-1	PMFC-2*	PMFC-3#	PMFC-4@
Open circuit voltage (mV)	680 ± 10	780 ± 6	816 ± 5	856 ± 5
Operating voltage (mV)	285 ± 2	370 ± 2	486 ± 2	492 ± 2
Max. current density (mA m^{-2})	41.67 ± 0.8	44.83 ± 1.4	52.65 ± 0.8	53.23 ± 0.8
Max. Power density (mW m^{-2})	18.23 ± 0.3	22.49 ± 0.6	27.21 ± 0.8	29.12 ± 0.4
Internal Resistance(Ω)	260 ± 5	238 ± 5	220 ± 5	182 ± 5
O_2 Profile in anode (µmol L^{-1})	35.23 ± 2.0	12.36 ± 2.0	12.4 ± 2.0	11.25 ± 2.4

*Two chamber PMFC, # Three chamber PMFC, @ Three chamber PMFC with narrow bottom anode chamber

5.3.2 Effect of the new modular design on working performance of PMFCs

The new design PMFC have proved to be very useful for easy assembling and disassembling of chambers at the start and end of the experiments respectively. Therefore, the modular nature of the setup makes operation easy and significantly reduces time for assembling multiple PMFCs at a time. The new design has been used extensively for more than 180 days. The performance of PMFCs decreases after 180 days, owing to accumulation of spent organic matters inside the chamber leading to fouling of surfaces of membranes and electrodes. Therefore, the modular design helps to replace these parts easily and the PMFCs can be made ready for next cycle at the earliest as compared to previous designs. Also the modular design helps to replace individual components i.e., plant assembly, electrodes, membranes etc. as per requirements without disturbing the whole setup thereby improving the efficiency of the PMFCs.

In recent times many novel works have been highlighted by the research community around the world. However, it is very difficult to compare results in terms of power output, as different researchers use different configurations and techniques to calculate power densities. However, a summary of a few of them is reported in Table 5.3.

Table 5.3 Comparision of various MFCs performance.

Sl. no	PMFC type	Design Criteria and its influence	Plants Used	Electrode used	Max. Power generation	References
1	Three chambers	A modular design which is easy to assemble and disassemble. The design makes operation and maintenance easy.	*E. Aurium*	Carbon fiber brush	24.56 (mW m^{-2})	This study
2	Three chambers	A biocathode was intergrated for the first time in a PMFC	*S. anglica*	Graphite felt	240 (mW m^{-2})	Wetser et al., 2015
2	Single Chamber	Soil mixture and thickened WAS used as substrate. Use of a complete wet chamber helped in the growth of electrogenic bancerial and also aids in hydrogen ion transport.	*W. thyrsiflora* *C. papyrus*	GAC (Anode) Carbon sheet coated with Pt. (Cathode)	1036 (mW m^{-3}) 510 (mW m^{-3})	Gulamhussein and Randall, 2020
3.	Single Chamber	A membrane-electrode assembly (MEA) was incorporated into stem coupled PMFC. Mutualism between the bacteria and plant stem was established.	*P. macrocarpa* *P. alba*	Graphite felt as anode. Graphite paper coated with Pt. (Cathode)	7.61 (mW m^{-2}) 3.60 (mW m^{-2})	Lu et al., 2020
4	Single Chamber	Vertically integrated plug-in ceramic stick-based PMFCs. It reduced the top-soil surface occupation of the cathode.	*O. ficus-indica* *O. joconostle* *O. robusta* *O. albicarpa*	Graphite felt (Anode) Zinc sheet (Cathode)	6.60 (mW m^{-2}) 5.76 (mW m^{-2}) 2.01 (mWm^{-2}) 5.47 (mW m^{-2})	Apollon et al., 2020
5	Single Chamber	PMFCs as green roofs in a subtropical metropolis. It provides cooling effect to buildings and regulate urban heat island (UHI).	*R. rotundifolia* *T. angustifolia* *P. alopecuroides*	Carbon felts	0.02 (mW m^{-2}) 2.86 (mW m^{-2}) 1.31 (mW m^{-2})	Guan and Yu, 2021
6	Single Chamber	Green renewable energy harvesting system with simultaneous food crop productions.	*A. viridis* *T. aestivum*	Carbon fiber brush (Anode) Stainless steel (Cathode)	1471.68 (mW m^{-3}) 1731.64 (mW m^{-3})	Arulmani et al., 2021
7	Single Chamber	Membrane-less light-driven PMFC and its ability to harvest energy from moss.	*Pleurocapous* moss	Carbon felt (Anode) Glass coated with CuO-Cu2O photocatalyst (Cathode)	2.5 (mW m^{-3})	Castresana et al., 2019

8	Single Chamber	Horizontal and vertical designs of terracotta-based ceramic-PMFCs	*Rice Plant*	Graphite Felt	9.1 (mW m^{-2}) 16.8 (mW m^{-2})	Kiran et al., 2020

5.3.3 Development of Bacterial Biocathode

5.3.3.1 Start-up and MFC performance

During the start-up phase, the behavior of all the PMFCs were quite similar. The (MLSS) and (MLVSS) values of the anaerobic biological sludge were obtained to be 1537 mg L^{-1} and 1110 mg L^{-1}, respectively. The obtained MLVSS/MLSS ratio of 1.38 reflected the very good quality of seed organisms and COD values were in the range of 167 ± 27 mg L^{-1}. Many voltage fluctuations were observed at 200 ± 10 mV due to the slow growth rate of microorganisms that retarded the growth of proper biofilm on electrode surfaces. After 15 days of inoculations, a stable voltage of 460 ± 10 mV was produced from all the five types of PMFCs (Fig. 5.13a), which shows that exoelectrogenic bacteria had been acclimated on the surface of the anode. However, within the next 10+ days, the cell voltage of three PMFCs, i.e., without solid-state nutrient (SSN) and without plant, started to decline, as shown in Fig. 5.11a. This might be due to the depletion of nutrients for the microorganisms since new inoculum was not added to any of these PMFCs. The COD values for PMFCs without SSN (*P. erubescens* and *E. aurium*) and without plant were obtained to be 128 ± 18 mg L^{-1}, 126 ± 22 mg L^{-1} and 117 ± 23 mg L^{-1} respectively on 25th day, confirming nutrient loss. The two PMFCs with solid-state nutrient (SSN) maintained the stable voltage for the next 20 days with a steady increase. The voltage in the cell reached 856 ± 5 mV and 830 ± 5 mV on the 49th day for *P. erubescens* and *E. aurium* respectively. On the other hand, it required around 60 days to achieve the same maximum cell voltage for the PMFC without solid-state nutrient. The difference in voltage generation pattern between PMFC with and without SSN clearly showed the advantage of using SSN to enhance the cell's initial performance. However, in the later period (after 60 days), both the PMFCs performed similarly. On the other hand, the control MFC (without plant) operated for around 45 days and finally being discarded due to low voltage output (Fig 5.13a). Thus, it was observed that the incorporation of solid-state media helped to maintain the constant nutrient requirements for the microbes and acted as a nutrient bridge between synthetic nutrients fed to the chamber and plant root exodus.

All the PMFCs were operated under open circuit potential for the initial 60 days and then switched into close circuit mode by connecting a resistor of 100 Ω (ohm) after stabilizing

voltage for a week. Upon stabilization of voltage, polarization curve was obtained on 8th week by utilizing methods as mentioned in section 3.2.8 (Chapter-III). Subsequently, the maximum power density of 29.12 mW m^{-2} and 25.56 mW m^{-2} with a current density of 53.23 mA m^{-2} and 52.45 mA m^{-2} was obtained from *P. erubescens* and *E. aurium* respectively (Fig 5.13b). Pre-activation of electrodes helped in the development of bio-electrode both at anode and cathode in a shorter time. It may have helped to enhance the performance along with a lower internal resistance of 180 as obtained from the polarization curve.

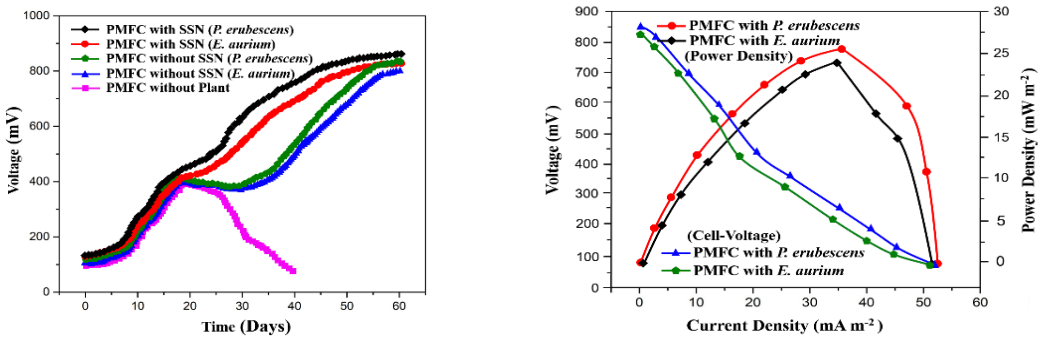

(a) (b)

Fig. 5.13 Cell voltage curve (a) of different PMFCs (b) Polarization and power density curve of PMFC with SSN.

5.3.3.2 Electrochemical characterizations (CV and EIS)

To evaluate the performance of the PMFC system, total cell cyclic voltammetry (CV) was carried out on the 35th day of operation. For PMFCs with solid-state nutrient (SSN) a current density of 36 mA m^{-2} and 33 mA m^{-2} was obtained for *P. erubescens* and *E. aurium* respectively. On the other hand, for PMFCs without SSN the current density obtained were 32 mA m^{-2} and 27 mA m^{-2} respectively. However, the control PMFC without plant achieved a current density of 19 mA m^{-2} (Fig 5.14a). The higher current in solid-state nutrient PMFC showed the active presence of electroactive microorganisms during nutrient transition state, which helped in faster biofilm development. The presence of redox peaks in PMFCs with and without SSN at the potential -0.25 and +0.26 confirms the presence of exogenous mediators produced by microbes. This suggests electrons transfer through the nutrient solution in the chamber due to enhanced microbial actions. The decrease in current in the PMFC without SSN was due to depletion in nutrient in the chamber and non-availability of plant nutrients during that period as seen from the voltage generation pattern from Fig. 5.14. On the other hand, the CV graph for control PMFC signified the non-availability of nutrients, and hence no significant

redox peaks were generated (Fig. 5.14a). The CV curve obtained on 60th day of operation shows increase in current density to 44 mA m^{-2} and 39 mA m^{-2} for *P. erubescens* and *E. aurium* respectively.

The electrochemical behaviour of the biocathode was also studied on the first week as well as on the 60th day of installation. CV analysis of the biocathode (Fig. 5.14b) showed a reducing current density of -29 m Am^{-2} and -27 m Am^{-2} at around -0.5 V for *P. erubescens* and *E. aurium* respectively. This shows catalyzing oxygen reduction due to biofilm development on the electrode surface. A significant difference was seen from the graph on zero (0) day vs 60th day, showcasing proper biofilm development on the cathode surface. CV analysis was also done on the 35th day; however, difference was negligible compared to the initial days, concluding that proper biocathode development is a time-consuming process. The enhancement of anodic and cathodic current can be attributed to the microstructure of carbon fibre brush electrodes, as seen in FESEM images (Fig. 5.14), which significantly enhanced specific surface area for biofilm development.

To further probe the electrochemical properties of the PMFCs, an EIS analysis was carried out. The Nyquist plot obtained through EIS techniques provides detailed information about prevailing internal resistance in the PMFC. The biofilm formation over the electrodes' surface significantly influenced the cell's overall internal resistance. Also, the presence of nutrient solution inside the chambers and the membrane structure induces ohmic and charge transfer resistance incrementing the overall internal resistance of the cell. The curved semi-circular portion of the graph corresponded to the redox process occurring on the biofilm surface due to the breakdown of nutrients. In contrast, the linear section showed the mass transfer process at the electrode-electrolyte interface (Zhou et al., 2015). The overall internal resistance obtained from Fig. 5.14c shows around 200 Ω for two PMFCs with SSN and around 250 Ω for PMFCs without SSN, whereas the PMFC without plant shows a value above 300 Ω. The internal resistance value obtained from the EIS curve coincides with the values obtained through the polarization curve. EIS was interpreted by using an equivalent circuit diagram similar to section 4.3.4 (Chapter-IV). The values of all the parameters of the equivalent circuit are presented in Table 3. In the presence of SSN in two PMFCs, an improved charge transport with higher reduction kinetics was observed in the initial (25th day) period, resulting in reduced charge transfer resistance R_{CT}. However, after the 60th day, the behaviour of all four PMFCs was similar, with overall internal resistance under 200 Ω. In the case of the control PMFC without plant, a higher R_{CT} value was observed due to the deficiency of nutrients. Also, a higher W_d value (Table 3) indicates higher mass transfer losses which are maximum in control PMFC.

The internal resistance values acquired from the EIS data also support the data achieved through the polarization curve in Fig.5.13b.

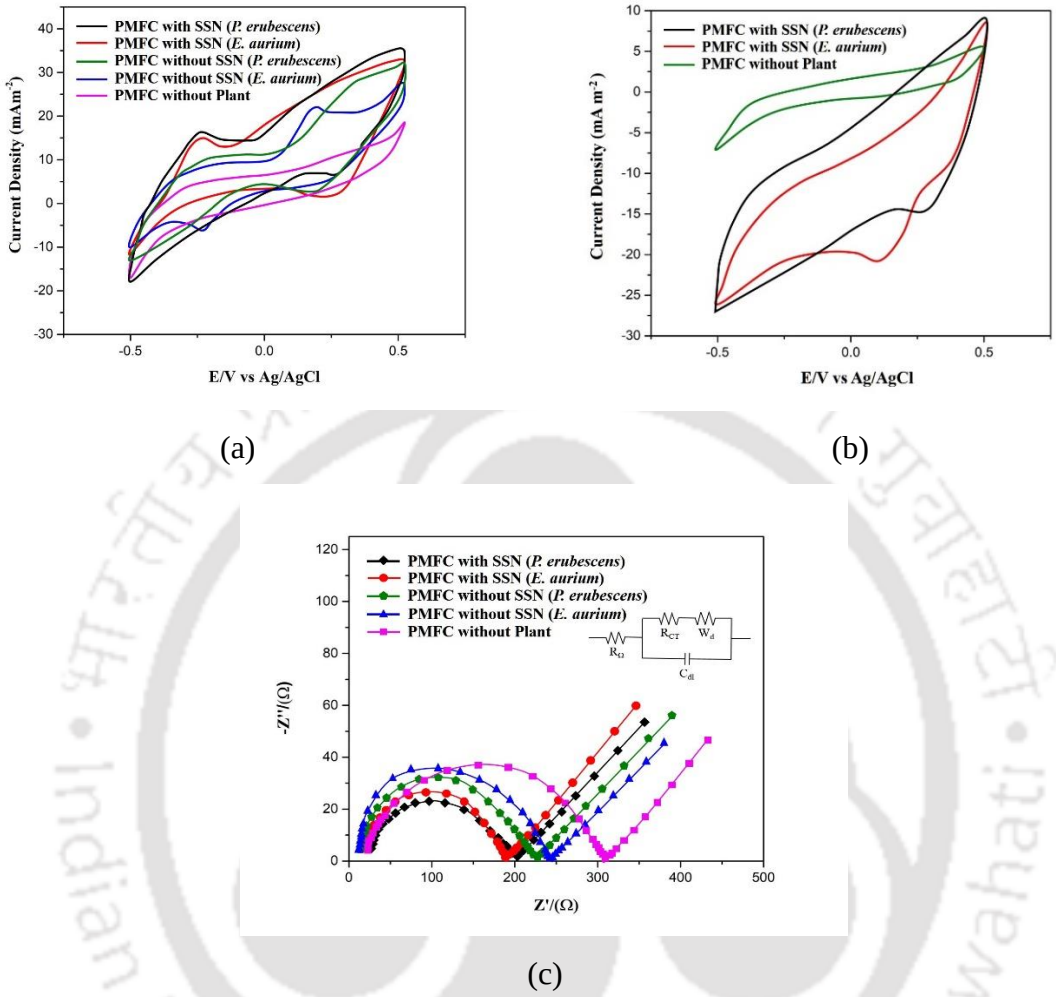

Fig. 5.14 Electrochemical characterization of PMFC (a) with anode as working electrode (b) with cathode as working electrode (c) Nyquist plots of biofilm carbon electrodes.

5.3.3.3 Long term performance and biofilm development

The biofilm development on the electrode surface influences the long-term performance of the PMFC system (Timmers et al., 2010). The carbon fibre surface is continuous, smooth, and non-porous. However, the FESEM image of acid-modified carbon fibre showed a longitudinal wavy surface, increasing the fiber's roughness, promoting microbial colony formation and biofilm development. Our previous investigation (Chapter-III) aimed to increase the power density of PMFCs by tailoring and optimizing carbon fibre material to increase the bacteria loading. The electrode modification helped provide a

microenvironment for improving electron transfer and promoting long-term stability of interfacial bacterial biofilm at the electrode surface, thus resulting in improved power density.

During the long-term performance of PMFCs for nearly six months, a well-developed biofilm formation was seen both on the anode and cathode surfaces during the initial three months. PMFCs were kept under constant observation during this period without adding any external microbial inoculum. The voltage generation pattern was monitored continuously using an Arduino-based data logging system. The performance of all the PMFCs remained almost constant at around 880-900 mV from 55-60 days onwards, which showed that the PMFC could produce bioelectricity sustainably for an extended period. Continuous plant health monitoring was carried out, and a similar growth pattern was seen, as mentioned in section 3.3.7 chapter-III. A stable and well-developed anodic biofilm resulted in higher and prolonged energy generation. The biofilm structure and morphology were observed by high-resolution Field emission scanning electron microscope (FESEM) images obtained per the protocol mentioned elsewhere (Jagna, 2009). Fig. 5.15a showed the presence of microbial biofilm on the surface of the anode, confirming the availability of nutrients in the plant rhizosphere region. The microfibre structure with rough groves formation after acid modification helped the biofilm to adhere to its surface. Fig. 5.15b shows the development of a well-defined biocathode with biofilm growth on the carbon fibre surface.

The performance of PMFCs starts decreasing after three months, probably because of the development of white patches on the cathode (Fig 5.15c), indicating the commencement of cathode fouling, which resulted in increased internal resistance and declined performance. The power generation decreased by 40% from the maximum power that was obtained steady state. Similar fouling was seen on the membrane surface on the cathode side. Surface of the membrane showing anode and cathode side can be seen in Fig 5.15d taken on 24th week. White fungal patches were seen on cathode side, while on the anode side a slime layer was observed due to organic matter attachment thereby clogging the pores. Applying an antifungal agent, fluconazole reduced biofouling; however, further in-depth investigation is needed to mitigate such fouling and restore PMFC performance.

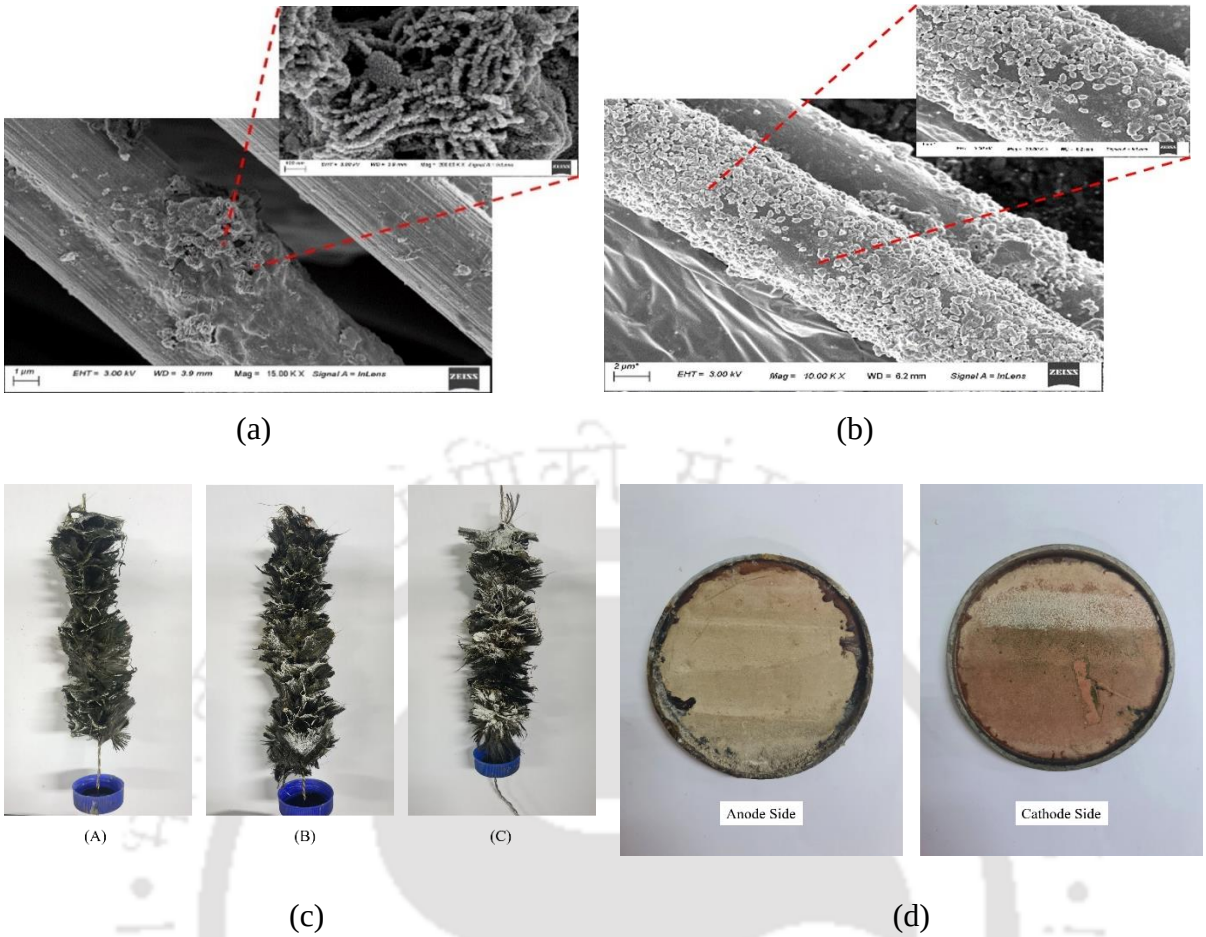

Fig. 5.15 Biofilm development on the surface of (a) anode and (b) cathode (c) biofouling of cathode [(A) 14th week (B) 18th week (C) 22nd week] (d) biofouling of membrane.

5.3.4 Development of Microlagal Biocathode

5.3.4.1 Start-up and PMFC Performance

During the start-up period, the behaviour of all four PMFCs was similar, considering their performance. The (MLSS), (MLVSS), and COD values of the anaerobic biological sludge were similar to the previous experiment (Section 5.3.3). The COD values of the anodic compartment decreased a bit by the end of two weeks and then again increased and remained almost constant at 130 ± 22 mg L^{-1} throughout the experiment. This showed that a constant source of nutrients was available from plants even after synthetic nutrients had been exhausted. During the initial 15 days, OCV was measured, and it showed voltage fluctuations at 200 ± 10 mV due to new environmental conditions and the slow growth rate of microorganisms. Gradually stable voltage started to appear from 15-18 days' period of inoculations, typically in the range of 450 ± 10 mV from all PMFCs (Fig. 5.16a). This showed that exoelectrogenic bacteria and the microalgae had been acclimated on the respective electrode surfaces. In the control setup without a plant, the voltage generation started to decline from the 27th day

onwards; however, the PMFC ran till the 57th day with low power output due to exhaustion of nutrients.

The initial open-circuit voltage (OCV) generation pattern in all five PMFCs was almost similar. However, after 2nd week the voltage started to increase for PMFCs with *P. erubescens* and *E. aurium,* and the highest OCV of 1020 ± 5 mV and 900 ± 10 mV, respectively, was obtained on the 56th day (Fig. 5.16a). The increase in power generation is due to continuous nutrient supply as plant exodus and microalgal biocathode. The control PMFCs with *P. erubescens* and *E. aurium* showed a lower voltage of 586 ± 10 mV and 504 ± 6 during the steady state, probably because of ineffective reduction at the cathode. The OCV and the respective OV, as seen in Table 5.4, clearly showed that the PMFCs having bio-cathode produced higher OCV and OV than the control PMFCs. This signified that the biocathode presence significantly enhanced the performance of an MFC compared to a conventional MFC.

Polarization curves (Fig. 5.16b) and power curves (Fig. 5.16c) were obtained during steady-state on the 8th week. The maximum power density of 32.21 mW m^{-2} and a current density of 63 mA m^{-2} was obtained from *P. erubescens*, showing an overall 17% increase in power generation with respect to bacterial bio-cathode. From the polarization curve's slope, the system's internal resistance can be calculated. The parameters obtained from all the PMFCs are reported in Table 5.4

The performance enhancement in the new PMFCs can be accredited to the chambers' new design and the use of microalgal biocathode in PMFC. Also, the pre-activation of electrodes was instrumental in developing bio-electrode at the anode and cathode within a short period, thus enhancing PMFCs performance.

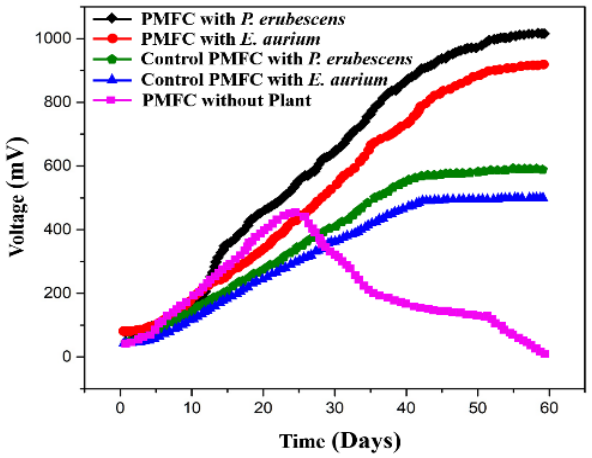

(a)

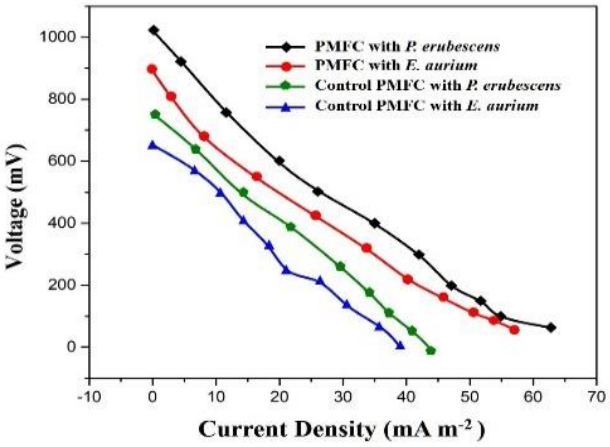

(b)

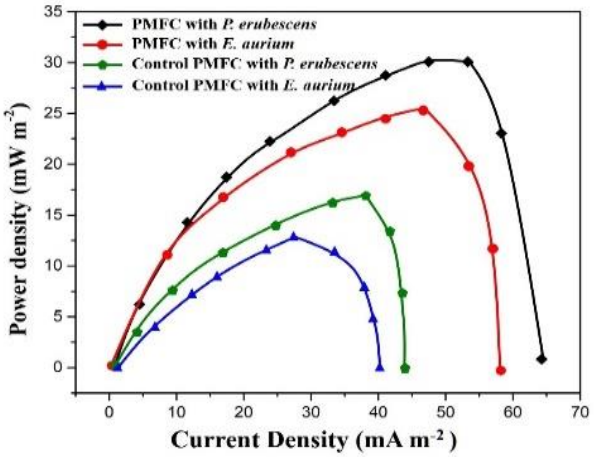

(c)

Fig. 5.16 (a) Cell voltage curve (b) Polarization curves (c) Power curves of different PMFCs.

Table 5.4 Performance analysis of PMFCs with Bacterial and Microalgal Biocathode.

Electrical parameters	Bacterial Biocathode			Microalgal Biocathode			Control With *E. aurium*	Control With *P. erubescens*
	E. aurium PMFC-II	*P. erubescens* PMFC-II	Control (without Plant)	*E. aurium* PMFC-I	*P. erubescens* PMFC-I	Control (without Plant)		
Open circuit voltage (mV)	830 ± 5	856 ± 5	446 ± 5	900 ± 10	1020 ± 4	450 ± 5	504 ± 6	586 ± 10
Operating voltage (mV)	486 ± 2	492 ± 2	234 ± 5	510 ± 4	534 ± 2	230 ± 5	241	267
Max. current density (mA m^{-2})	52.45 ± 0.8	53.23 ± 1.8	-	57 ± 1.4	62.23 ± 0.8	-	23	25
Max. Power density (mW m^{-2})	25.56 ± 0.4	27.12 ± 0.6	-	27.63 ± 0.6	31.40 ± 0.4	-	11.7	12.6
Internal Resistance(Ω)	186 ± 5	182 ± 5	-	210 ± 5	190 ± 5	-	329	352

5.3.4.2 Electrochemical characterizations (CV and EIS)

The extracellular electron transfer process of the electroactive microbial biofilm was evaluated by performing total cell cyclic voltammetry (CV) during the initial period (1st week) and at the high-performance steady state (8th week) (Fig. 5.17). All four PMFCs performed similarly, and a significant difference was seen between the 1st and the 8th week graph. During the 1st week (7th day) of operation, no redox peak was obtained in any of the PMFCs, and the graph obtained was almost flat; hence, only one PMFC was shown in Fig. 5.17. The PMFCs were still not stabilized, and the microbial biofilm development was nascent.

The CV results on the 8th week showed that the oxidation current started at about -0.25 V and reached a plateau of about 0.25 V. The exogenous mediators produced by microbes were reflected by prominent redox peaks obtained for *P. erubescens* and *E. aureum* at 0.25 and 0.1, suggesting enhanced electron transfer due to enhanced microbial actions. However, redox peaks were not evident in the rest of the PMFCs. The current densities of 42m A m^{-2} and 36 mA m^{-2} were obtained for PMFC with *P. erubescens* and *E. aureum*, respectively (Fig. 5.17a). However, in the control PMFC with *P. erubescens,* the current density obtained was 32 mA m^{-2}. The decrease in current in control PMFC with respect to the others may be because of an inferior oxygen reduction reaction compared to bio-cathode (Fig. 5.17a). Also, the width of the graphs progressively decreased from *P. erubescens* > *E. aureum* > Control PMFC with *P. erubescens* > Control PMFC with *E. aureum*, indicated decreasing current density trends, which does correlate with the polarization curves as well. All four plants were growing optimally and in very healthy conditions, providing a sustainable nutrient supply to the electroactive microorganisms resulting in higher current. This helped in faster biofilm growth and development.

The oxygen reduction characteristics of all the PMFCs were analyzed by studying the electrochemical behavior of the biocathode during the first week (7th day) and on the 8th week of the experiment. A noticeable difference was seen between the 7th day vs. 56th day graph, thus inferencing the active biofilm development on the cathode surface. The maximum current was obtained from the bio-cathode of *P. erubescens* in both forward scan (12.7 mA m^{-2}) and reverse scan (-16.2 mA m^{-2}), followed by *E. aureum* with (10.1 mA m^{-2}, -7.1 mA m^{-2}). A relatively lower current output was obtained from control abiotic cathodes viz., *P. erubescens* (9.7 mA m^{-2}, -5.6 mA m^{-2}) and *E. aureum* (7.6 mA m^{-2}, -6.8 mA m^{-2}) (Fig. 5.17b). These results indicated that in addition to the electrode material's microfibrous structure, biocathode development with *Chlorella sorokiniana* played a vital role in the catalytic behavior of the oxygen reduction reaction.

Additionally, the Nyquist plot acquired by EIS techniques simulated by the equivalent circuit describes internal resistance predominating in a PMFC. The biofilm formation over the surface of the electrodes significantly influenced the overall internal resistance of the cell. Also, the presence of nutrient solution inside the chambers and the membrane structure induces ohmic and charge transfer resistance incrementing the overall internal resistance of the cell. The overall internal resistance was obtained under 200 Ω for PMFC with *P. erubescens* and *E. aureum*. While for the control PMFCs, the internal resistance of nearly 240 Ω was noticed. The internal resistance values acquired from the EIS data were tallied with that obtained through the polarization curve in Fig. 5.16b.

It can be seen that the PMFCs having a microalgal biocathode, an improve charge transport and higher reduction kinetics was observed resulting in reduced charge transfer resistance R_{CT}. However, in the control PMFCs with *P. erubescens* and *E. aureum* a comparatively higher value of R_{CT} values was observed due to improper reduction kinetics because of absence of a well-developed biocathode. The capacitance of a capacitor is inversely proportional to its impedance. Therefore, a higher C_{dl} indicated the ability to pass more current to charge the capacitor faster. Higher W_d values (Table 5.5) indicates higher mass transfer losses which are higher in control PMFCs.

Table 5.5 Different components of PMFC impedance

Bacterial Biocathode				
PMFC Types	R_Ω (Ω)	R_{CT} (Ω)	W_d (Ω S^{-2})	C_{dl} (µF)
PMFC with SSN *(P. erubescens)*	28.5	177.5	410.7	2.05
PMFC with SSN (*E. aurium*)	24.8	165.2	418.4	1.90
PMFC without SSN *(P. erubescens)*	22.6	211.1	450.5	1.67
PMFC without SSN (*E. aurium*)	19.3	225.7	560.3	1.46
PMFC without Plant	25.1	280.0	673.2	1.44
Microalgal Biocathode				
PMFC Types	R_Ω (Ω)	R_{CT} (Ω)	W_d (Ω S^{-2})	C_{dl} (µF)
PMFC with *P. erubescens*	25.6	165.2	380.4	2.80
PMFC with *E. aurium*	38.2	181.5	410.7	2.08
Control PMFC with *P. erubescens*	36.4	210.7	560.3	1.60
Control PMFC with *E. aurium*	23.3	243.8	576.2	1.46

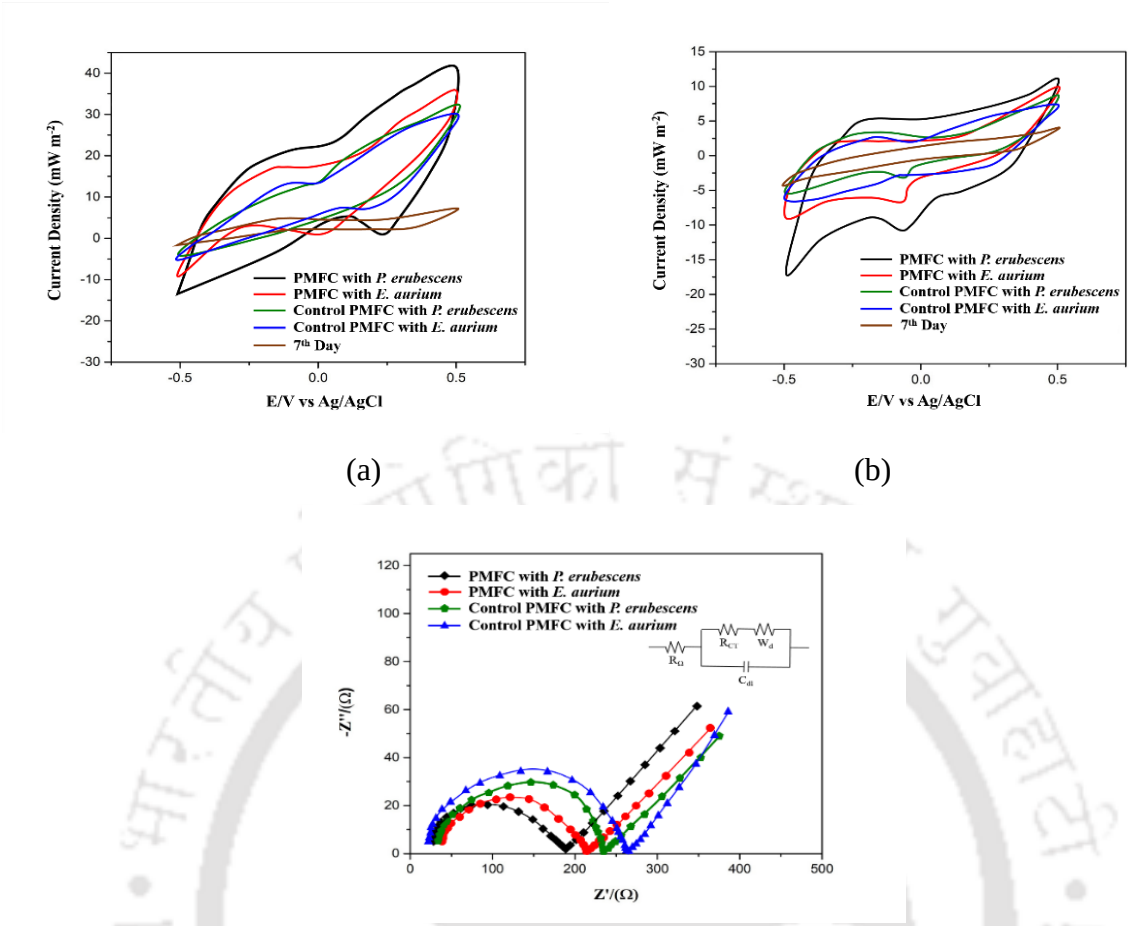

Fig. 5.17 Electrochemical characterization of PMFCs (a) with anode as the working electrode (b) with cathode as the working electrode (c) Nyquist plots of biofilm carbon electrodes.

5.3.4.3 Microalgal growth at the cathode

Regular monitoring of the growth of microalgal biomass at the cathode was done to correlate with the power output. An initial algal biomass concentration of 0.8 g L^{-1} was used as a catholyte in all PMFCs except control; however, the maximum biomass concentration was obtained during the steady-state operational stage in all PMFCs. Other growth-related kinetic parameters are presented in Table 5.6. The dissolved oxygen (DO) concentration at the cathode plays a significant role in the performance of the PMFCs. At the start of the light phase, CO_2 was bubbled to stimulate microalgal growth at 10 am for 5 min every day. As a result, both DO and cell voltage decrease sharply due to the stripping process (Araceli et al., 2015). The algae carried out photosynthesis during the light phase absorbing light, capturing carbon dioxide, and releasing oxygen. After that, the DO and cell voltage gradually increase and reaches the daytime maximum, and remain stable throughout the day. However, once the dark phase starts,

the DO level and cell voltage decrease to the day time lowest. This happens because microalgae consume oxygen and carry out respiration during the dark phase. The trend was similar with both the PMFCs, and for representation purposes, the change in DO and cell voltage for PMFC with *P. erubescens* during a single day was shown in Fig. 15.18a. The increase in DO during the light phase does help to enhance microbial electrogenic activities, and it translates into an increase in MFC performance. Light-dependent performance variations were reported by other studies as well, including cyanobacteria (Enamala et al., 2020; Mostafa et al., 2021). However, in our previous studies it was seen that anodic microorganism metabolism was not much affected by light/dark cycles. Therefore, day/night variation in voltage generation capabilities was almost similar.

In the PMFC with *P. erubescen*, a maximum DO concentration of 10.7 mg L^{-1} was obtained, 57% higher than the control (6.8 mg L^{-1}). However, after reaching the maximum value, the DO level decreased when the maximum biomass growth was achieved, as depicted in Fig. 15.18b. It was probably because of nutrient exhaustion in the cathode chamber and the self-shading effect. This was when the fresh microalgal culture was introduced to the cathode chamber. The pH of both chambers is also very crucial for the performance of PMFC, and therefore pH was closely monitored. A decrease in cathodic chamber pH was seen when CO_2 was bubbled. The pH decreased down to 5.0 and then increased up to 7.0 during a later period in the day.

Therefore, it can be said that the DO concentration significantly influences the cell voltage generation at the cathodic chamber since oxygen is the electron acceptor. This type of cell behaviour was observed by other researchers as well (Zou et al., 2009; Pisciotta et al., 2010). Diurnal cell voltage difference was very negligible in all our studies when microalgae were not used in the cathode. Over a period of 30 days, the microalgae biomass also increased, and the maximum biomass obtained in PMFC is shown in Fig. 15.18b.

Initially, during the start of the experiment, the cathode chamber looked light green, while the chlorophyll concentrations measured were 2.92 ± 0.023 µg mL^{-1} (Chlorophyll a=1.20 µg mL^{-1}, chlorophyll b=1.72 µg mL^{-1}). The photosynthetic activities of the microalgae were reflected by chlorophyll concentrations which carry out photolysis of the water that releases oxygen needed as terminal electron acceptor. During the later operational period, the cathodic chamber culture turned dark green as a result of increased chlorophyll content with time, and it reached a maximum of 27.43 ± 1.2 µg mL^{-1} (chlorophyll a=3.60 µg mL^{-1}; chlorophyll b=5.07 µg mL^{-1}) at the end of cycle operation as summarized in Table 5.6 This resulted in light limitation due to the self-shading effect (Zhou et al., 2015). All the parameters studied in two

PMFCs shows similar results, hence for ease of representation an average value is presented in Table 5.6.

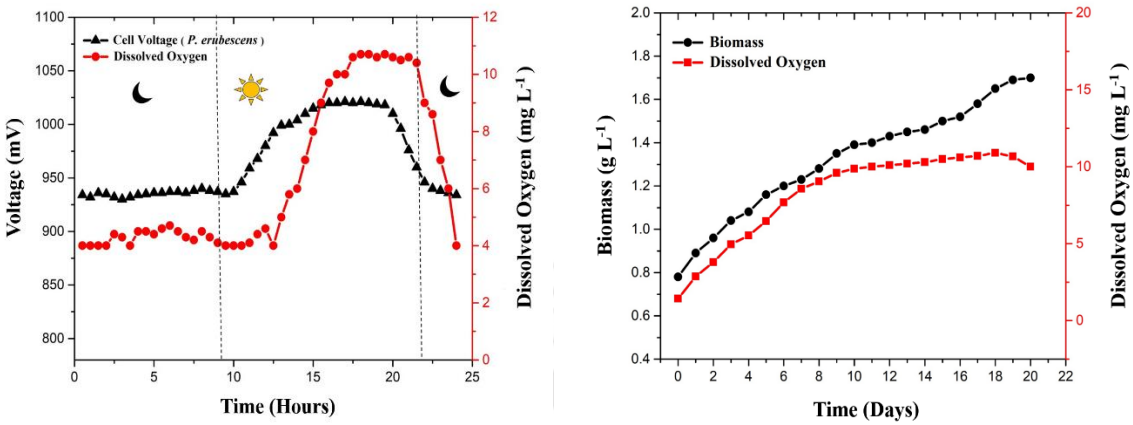

(a) (b)

Fig. 15.18 (a) Cell voltage and dissolved oxygen at the cathode during one day (b) Time course profile of biomass growth and DO level of microalgae *Chlorella sorokiniana*.

Table 5.6 Consolidated data related to the microalgal performance at biocathode.

Parameters	Units	Values#
Biomass concentration	g L^{-1}	1.61 ± 0.08
Biomass productivity (P_W)	mg L^{-1} d^{-1}	0.153 ± 0.04
Specific growth rate (μ)	d^{-1}	0.25 ± 0.03
Doubling time (D_T)	d^{-1}	2.77 ± 0.04
Total Chlorophyll (a+b)	µg mL^{-1}	27.43 ± 1.2
DO Concentration	mg L^{-1}	10.7 ± 0.26

#The values are an average of all the two PMFCs.

5.3.4.4 Biofilm development and long term performance

After about 30 days' time, a portion of anode and cathode brush microfiber was taken out, and a visual inspection of the microfibers confirmed that they were covered with light brown and green biofilm, respectively. To ascertain this, the biofilm morphology and structure were observed under high-resolution FESEM. Dense microbial biofilm growth on the anode surface can be seen (Fig. 5.19a), confirming the nutrient availability near the plant rhizospheric zone, which helped enhance the long-term performance of the PMFCs (Timmers et al., 2010).

While FESEM images confirmed the bio-anode formation, the microscopic observation of the bio-cathode (Fig. 5.19b) showed the presence of a dominant green microalgal biocommunity. Cathode surfaces on all PMFCs have shown well-developed biofilms of

photosynthetic green microalgal. However, on the control cathode's surface, photosynthetic organisms' microbial growth was visible to the naked eye during long-term MFC operation, making it serendipitously biotic, as reported earlier (Gajda et al., 2015). These microbes in the control cell may have helped in the bioelectricity generation process in small magnitude; however, further study was not done in the control PMFC.

The rough groves structures formed after acid modification in carbon microfibers helped to enhance the surface area for easy microbial cell adhesion. Fig. 5.19 (a) and (b) showed a well-defined biofilm growth and bio-anode and bio-cathode development, respectively, on the carbon fiber surface. The microscopic images of bio-electrodes development were similar in all the PMFCs; hence for representation, only PMFC with *P. erubescens* was shown as it showed higher bioelectricity generation.

Further, while the operational period was increased beyond the six-month period, an increase in biofilm thickness due to the presence of bulky green layers on the cathode surface was seen with time. This indicated the commencement of fouling of the cathode, limiting oxygen diffusion with an increase in internal resistance and a decline in performance. However, unlike bacterial biocathode, very limited white patches were seen with the naked eyes. Similarly, anode fouling also occurred due to the deposition of dead microbial film over the surface. In the case of the membrane, no visual biofouling was seen on the cathode side, however on the anode side, a slimy layer was developed; however, no mechanical degradation was seen with time. The power generation decreased gradually after a six-month time, indicating the time to change the membranes and electrodes.

Therefore, the incorporation of microalgal biocathode proved beneficial and superior in terms of maintenance of PMFC, considering its long-term sustainability. Biofouling of bacterial cathode was found to be one of the major hurdles affecting long-term PMFC performance, whereas microalgal biocathode contamination was not very evident. Unlike bacterial biocathode, the microalgal biocathode helps in the development of both plant and microalgal biomass under a single light source, as mentioned in section 3.3.7 chapter-III. Microalgal biocathode proved superior, with a 17% improvement in power generation capability with respect to bacterial biocathode. Overall incorporation of microalgal biocathode in PMFC-4 resulted in a 72% increase in power out with regard to membrane-less PMFC in section 5.2.1.1. Also, it helped to cut down the energy-intensive mechanical aeration process as required in bacterial biocathode. Instead, the presence of microalgae helps to increase O_2 concentration in the cathode chamber of the control with a maximum DO concentration of 10.7 ± 0.26 mg L^{-1}.

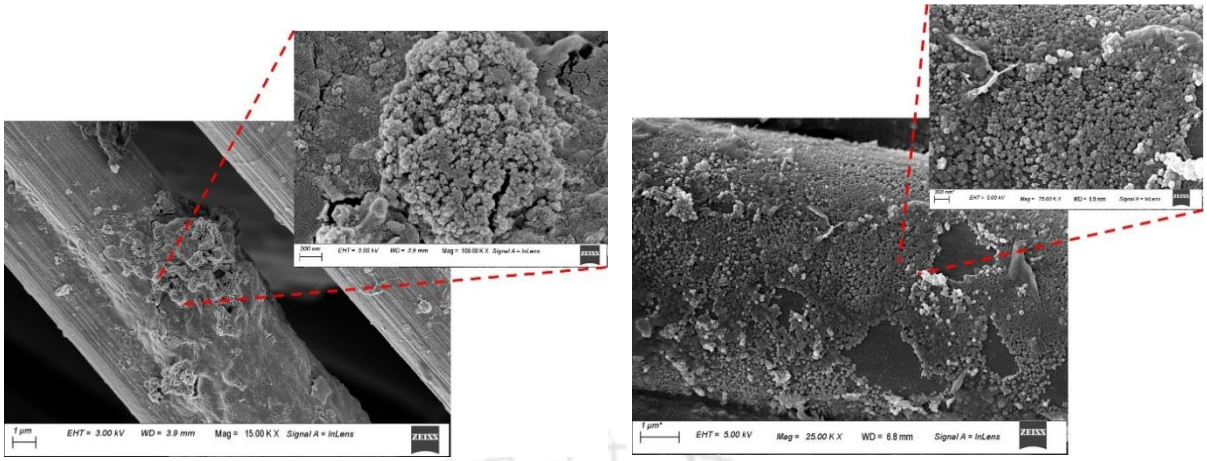

(a) (b)

Fig. 5.19 Biofilm development on the surface of (a) anode and (b) cathode.

5.4 Conclusion

The study demonstrates the design evolution process of four different PMFCs, starting from a membrane less two chamber design to a modular three chamber structure. The final design strucure resulted in overall 72% increase in power generation owing to improved anaerobic condition inside anode chamber, increased in ion transport across the chamber and higher ORR at the biocathode due microalgal biofilm development as compared to bacterial biofilm. The new modular design of PMFC plays a significant role for ease of operation and maintenance of PMFCs during long term usage. The start-up time was significantly reduced because of the pre-acclimatization of electrodes. The voltage generation pattern between the initial 20-60 days' time was very crucial as it depicted the nutrient transition period from synthetic nutrient to plants released nutrients through rhizodeposits. The use of SSN in PMFCs provided a smooth nutrient transition for microorganisms which in turn helped to maintain a smooth and continuous power generation pattern.

A three-chamber PMFC was successfully integrated with bacterial bio cathode and a microalgae bio-cathode incorporating plants *P. erubescens* and *E. aureum*. A comparative performance analysis was also carried between the two system to find out best performing PMFC system. The integration of microalgae bio-cathode into the PMFC system significantly improves the power generation capabilities with respect to bacterial bio-cathode and makes it an economically viable option as mechanical aeration can be avoided. Unlike bacterial biocathode wherein energy intensive mechanical aeration is required the presence of microalgal

biocathode help to increase O_2 concentration in the cathode chamber with a maximum DO concentration recordes to be 10.7± 0.26 mg L^{-1}.

Furthermore, microalgae bio-cathode leads to a 17 % increase in power generation as compared to bacterial counterpart. This signified the self-sustainable nature of PMFC, where plants-bacteria-microalgae mutual collaborative approach leads towards a better PMFC performance. However, a lot of research is yet to be channelized towards understanding the biocathode reaction mechanism for power management in PMFCs.

References

Abbas SZ, Rafatullah M, Khan MA, Siddiqui MR (2018) Bioremediation and electricity generation by using open and closed sediment microbial fuel cells. Front Microbiol 9:3348

Alessandro A, Carmona M, Falk H, Lisa AF, Justin CB, Bradley RR, Uwe S (2011) Cyclic voltammetric analysis of the electron transfer of Shewanella oneidensis MR-1and nano filament and cytochrome knockout mutants. Bioelectrochemistry 81(2):74–80

APHA, AWWA, and WEF: Standard methods for the examination of water and wastewater, 16th ed. American Public Health Association, Washington, DC (1985)

Apollon W, Kamaraj SK, Espino SH, Segovia CP, Montero LV, Ruelas VM, Marco AV, Medina RO, Silvia FB, Juan FG (2020) Impact of Opuntia species plant bio-battery in a semi-arid environment: Demonstration of their applications. Appl. Energy 279: 115788

Araceli GC, Jose F, Pablo C, Manuel AR, Francisco JF, Justo L (2015) Characterization of light/dark cycle and long-term performance test in a photosynthetic microbial fuel cell. Fuel140:209–216

Arulmani SRB, Gnanamuthu HL, Kandasamy S, Govindarajan G, Alsehli M, Elfasakhany A, Pugazhendhi A, Zhang H (2021) Sustainable bioelectricity production from *Amaranthus viridis* and *Triticum aestivum* mediated plant microbial fuel cells with efficient electrogenic bacteria selections. Process Biochem. 107: 27–37

Castresana PA, Martinez SM, Freeman E, Eslava S, Lorenzo MD (2019) Electricity generation from moss with light-driven microbial fuel cells. Electrochim. Acta 298: 934–942

Chakraborty I, Das S, Dubey BK, Ghangrekar MM (2020) Novel lowcost proton exchange membrane made from sulphonated biochar for application in microbial fuel cells. Materials Chemistry and Physics 239: 122025

Chen W, Feng H, Shen D, Jia Y, Li N, Ying X, Chen T, Zhou Y, Guo Y, Zhou M (2018) Carbon materials derived from waste tires as high-performance anodes in microbial fuel cells. Science of the Total Environment 618: 804–809

Enamala MK, Dixit R, Tangellapally A, Singh M, Dinakarrao SMP, Murthy C, Sudhakar RP, Ak V, Kadier A, Chandrasekhar K (2020) Photosynthetic microorganisms (Algae) mediated bioelectricity generation in microbial fuel cell: concise review. Environ Technol Innov 19:100959

Gajda I, Greenman J, Melhuish C, Ieropoulos I (2015) Self-sustainable electricity production from algae grown in a microbial fuel cell system. Biomass Bioenergy 82:87–93

Ghadge AN, Ghangrekar MM (2015) Development of low-cost ceramic separator using mineral cation exchanger to enhance performance of microbial fuel cells. Electrochim. Acta 166: 320–328

Guan CY, Yu CP (2021) Evaluation of plant microbial fuel cells for urban green roofs in a subtropical metropolis. Sci. Total Environ. 765: 142786

Gulamhussein M, Randall DG (2020) Design and operation of plant microbial fuel cells using municipal sludge. Journal of Water Process Engineering 38: 101653

Gunaseelan K, Jadhav DA, Gajalakshmi S, Pant D (2021) Blending of microbial inocula: an effective strategy for performance enhancement of clayware Biophotovoltaics microbial fuel cells. Bioresour Technol 323:124564

Hartmut K, Lichtenthaler HK (1987) Chlorophylls and carotenoids: pigments of photosynthetic biomembranes. Meth Enzymol 148:350–882

Helder M, Strik DP, Hamelers HV, Buisman CJ (2012) The flat-plate plant-microbial fuel cell: the effect of a new design on internal resistances. Biotechnology for Biofuels 5: 70

Hubenova Y, Mitov M. (2012) Conversion of solar energy into electricity by using duckweed in Direct Photosynthetic Plant Fuel Cell. Bioelectrochemistry 87: 185–191

Jagna K (2009) Standard preparation of biological material for SEM analysis. Laboratory of scanning electron microscopy, University of Silesia, Poland

Khudzari JM, Gariepy Y, Kurian J, Tartakovsky B, Raghavan GSV (2019) Effects of biochar anodes in rice plant microbial fuel cells on the production of bioelectricity, biomass, and methane. Biochemical Engineering Journal 141: 190–199

Kiran KV, Manmohan K, Sreelakshmi PM, Manju P, Gajalakshmi S (2020) Resource recovery from paddy field using plant microbial fuel cell. Process Biochem. 99: 270–281

Liu B, Ji M, Zhai H (2018) Anodic potentials, electricity generation and bacterial community as affected by plant roots in sediment microbial fuel cell: Effects of anode locations. Chemosphere 209: 739-747

Lu Z, Yina D, Chena P, Wanga H, Yanga Y, Huanga G, Caia L, Zhanga L (2020) Power-generating trees: Direct bioelectricity production from plants with microbial fuel cells. Applied Energy 268: 115040

Malakar B, Das D, Mohanty K (2022a) Utilization of waste peel extract for cultivation of microalgal isolates: a study of lipid productivity and growth kinetics. Biomass Conv Bioref.

Malakar B, Das D, Mohanty K (2022b) Evaluation of banana peel hydrolysate as alternate and cheaper growth medium for growth of microalgae Chlorella sorokiniana. Biomass Conv Bioref.

Milner EM, Popescu D, Curtis T, Head IM, Scott K, Yu EH (2016) Microbial fuel cells with highly active aerobic biocathodes. Journal of Power Sources 324: 8-16

Mostafa EE, Zabed HM, Yun J, Zhang G, Qi X (2021) Recent insights into microalgae-assisted microbial fuel cells for generating sustainable bioelectricity. Int J Hydrog Energy 46:3135–3159

Pisciotta JM, Zou YJ, Baskakov IV (2010) Light-dependent electrogenic activity of cyanobacteria. PLoS One 5(5):10821

Rusli SFN, Bakar MHA, Loh KS, Mastar MS (2019) Review of high-performance biocathode using stainless steel and carbon-based materials in Microbial Fuel Cell for electricity and water Treatment. International Journal of Hydrogen Energy 44: 30772-30787

Timmers RA, Strik DPBTB, Hamelers HVM, Buisman CJN (2010) Long-term performance of a plant microbial fuel cell with Spartina anglica. Appl. Microbiol. and Biotechnology 86:973–981

Timmers RA, Strik DPBTB, Hamelers HVM, Buisman CJN (2013) Electricity generation by a novel design tubular plant microbial fuel cell. Biomass and Bioenergy 51: 60–67

Tommasi T, Salvador GP, Quaglio M (2016) New insights in Microbial Fuel Cells: novel solid phase anolyte. Scientific Reports 6: 29091

Wetser K, Sudirjo aaaE, Buisman CJN, Strik DPBTB (2015) Electricity generation by a plant microbial fuel cell with an integrated oxygen reducing biocathode. Applied Energy 137: 151–157

Wetser K, Dieleman K, Buisman C, Strik D (2017) Electricity from wetlands: tubular plant microbial fuels with silicone gas-diffusion biocathodes. Applied Energy 185: 642–649

Wu J, Chen W, Yan Y, Gao K, Liao C, Li Q, Wang X (2017) Enhanced oxygen reducing biocathode electroactivity by using sediment extract as inoculum. Bioelectrochemistry 117: 9–14

Zhou S, Tang J, Yuan Y (2015) Conduction-band edge dependence of carbon-coated hematite stimulated extracellular electron transfer of Shewanella oneidensis in bioelectrochemical systems. Bioelectrochemistry 102:29–34

Zhou Y, Tang L, Liu LTZ, Hou J, Chen W, Li Y, Sang L (2017) A novel anode fabricated by three-dimensional printing for use in urine-powered microbial fuel cell. Biochemical Engineering Journal 124: 36–43

Zou YJ, Pisciotta JM, Billmyre RB, Baskakov IV (2009) Photosynthetic microbial fuel cells with positive light response. Biotechnol Bioeng 104:939–946

Chapter-VI

Efficient Energy Harvesting from Plant Microbial Fuel Cells (PMFCs) and Development of a Power Management System (PMS) to Power Small Electronic Devices

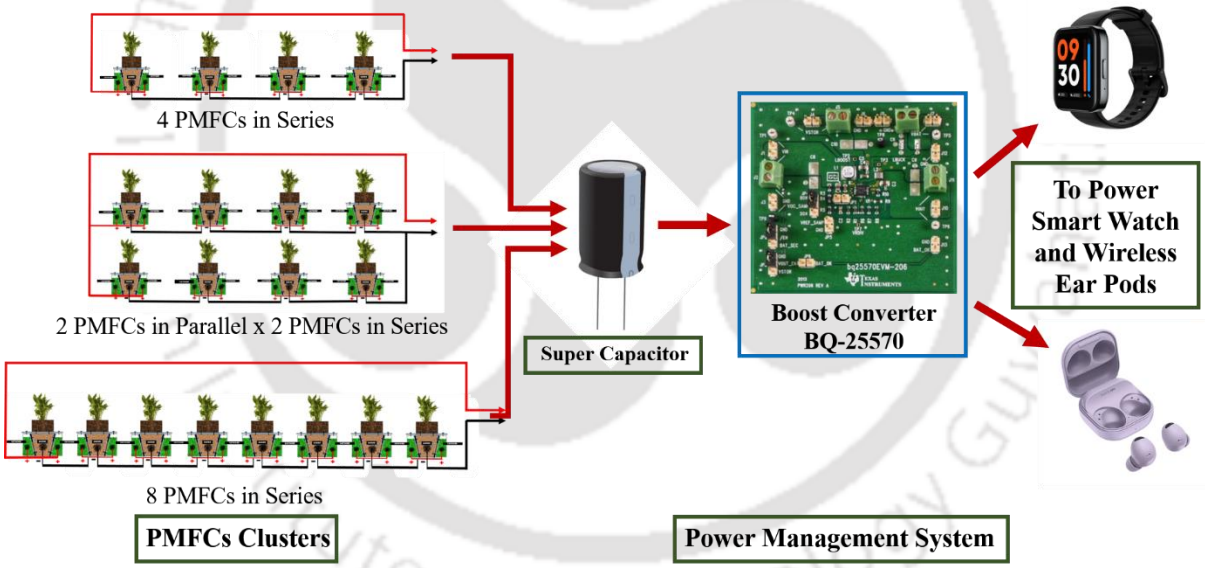

6.1 Overview

Plant microbial fuel cell is a promising renewable, self-sustainable, eco-friendly, and green technology that offers long-term power generation by harnessing the photosynthetic ability of plants (Limbergen et al., 2022; Chiranjeevi et al., 2019). Unlike other electrochemical systems, PMFCs provide dual benefits of bioelectricity generation by combining plant and microbial physiology and conserving nature by purifying air simultaneously. PMFC technology has an exceptional potential to be implemented in large-scale bioelectricity generation in urban areas, including rooftops, wherein we are rapidly losing green cover (Helder et al., 2013a; Tapia et al., 2017). Apart from these, PMFCs can be easily integrated into agricultural land, and the vast majority of wetlands can be turned into a powerhouse of energy without compromising food production (Wetser et al., 2015).

Many studies have deciphered the potential advantages of MFC technology, including PMFCs. Over the years, many advancements and innovations were made to increase power generation using MFCs in general and PMFCs in particular, including electrode and membrane modifications, MFC design structure, improvement in growth media composition, etc. (Maddalwar et al., 2021; Apollon et al., 2021). However, despite all this efforts, MFCs still exhibit low output voltages to be used for any practical application. The maximum production of open circuit voltage (OCV) in a typical MFC range is 0.3-1.0 ± 0.2 V. In addition, when an external load is applied, the operating voltage (OV) obtained from a single MFC is between 0.2 - 0.6 ± 0.06V owing to various losses (Limbergen et al., 2022). However, the minimum output voltage required for real-world applications is greater than 3V. In our study, the highest OCV achieved was 1020 V from a single PMFC with plant *P. erubescens* (Section 5.3.4, Chapter-V). Also, during the operational period, it is difficult to maintain a constant voltage in an MFC due to constantly changing microbial metabolic activities and environmental conditions; hence the power output from MFCs fluctuates frequently (Park and Ren, 2012).

Several researchers have various quantified approaches to address the problem of low output voltage hindering MFCs' practical use. Connecting MFCs in a stack of series can increase the voltage as an algebraic sum of individual cells, whereas connecting MFCs in parallel can increase current in same fashion. Min and Logan in 2004, could obtain a maximum OCV of 2.02 V and power density of 228 Wm^{-3} by connecting 6 MFCs in a series-parallel connection. Bombelli et al., in 2016, connected 10 pot-based MFCs in series to obtain a power of 6.7 ± 0.6$mWm^{-2,}$ which was used to charge a rechargeable battery of 3.6 V to power a radio just for 80 s. However, series–parallel connections suffer from the problem of voltage reversal

if the load rating is increased or if the device needs to be used for a prolonged period resulting in the failure of the entire MFC system (Oh and Logan, 2007; Kim et al., 2019). Also, the performance of a PMFC is affected by various conditions such as plant type, soil, microbial inoculum, light source, temperature, use of electrode and its placement etc. Therefore, optimization of different operating conditions is necessary to obtain higher performance from PMFCs. A study on the effects of various operating conditions on PMFC performance was presented in chapter-III.

It is essential to step-up voltage to obtain consistent power output from PMFCs for practical application as the energy generated from PMFCs is not sufficient to meet practical applications due to low and inconsistent voltage generation patterns. Therefore, introducing a power management system (PMS) becomes indispensable. However, it was seen that output voltage and output power dramatically declined when a DC/DC boost converter was directly connected to the MFC stack. A higher current was drawn by DC/DC boost converter, which the MFCs stack can't handle for a long time, leading to voltage overshoot and the circuit becoming dysfunctional (Li et al., 2022; Watson and Logan, 2011; Winfield et al., 2011). Therefore, such a circuit needs a supercapacitor to be connected (in between MFC and DC/DC converter) to store the energy produced by the MFCs. In this way, the supercapacitor is charged by MFCs and function as an input source for the PMS (DC/DC converter) (Kim et al.,2019). A PMFC stack was recently established by installing multiple anodic chambers in an algal raceway pond. During long-term operation, the highest power density of the stack with capacitors reached 2.34 Wm^{-3}, which was 77% higher than that without capacitors (1.32 Wm^{-3}) (Yang et al., 2019). Prasad and Tripathi in 2020, charged a 12 V battery using 210 MFCs in series-parallel connection using a DC/DC boost converter (XL6009IC). The charged battery was used to glow a 7W LED bulb.

Therefore, this study brings in a novel approach to develop an efficient energy harvesting system for indoor plant-based PMFCs to run small electronic devices requiring low power input. The PMFCs were connected in different arrays of series and parallel connections to determine the best possible combination for higher and usable power generation without voltage reversal. This study will provide a new direction for energy harvesting from indoor plant-based PMFCs. A power management system (PMS) was developed based on DC/DC boost converter to supply a constant voltage to charge a rechargeable lithium-polymer battery.

In today's world of advanced lifestyle, electronic gadgets are becoming widespread in daily life. Unlike our mobile phones, a smartwatch can make everyday life more accessible because of its multi-functionality including daily health monitoring. Similarly, a missing

headphone jack in our mobile phones has pushed people to use True Wireless Stereo (TWS) to talk and stream music or listen to audiobooks using Bluetooth. Therefore, this study is an effort to power these two crucial day-to-day use gadgets using energy stored in a rechargeable lithium-polymer battery powered by PMFC clusters.

6.2 Materials and Methods

6.2.1 MFC setup and operation

For this study, 8 modular design three chamber PMFCs were made similar to Chapter-V. Anode and cathode were made of acid treated carbon fibre brush made up of titanium wire similar to our previous study. The anode and cathode were being separated by a ceramic membrane of 6 mm thickness made up of Clay-55%, Bentonite-15%, Flyash-15%, Na_2Co_3-8%, Na_2Sio_3-2%, and H_3Bo_3-5%. The said membrane is a low-cost membrane, and its characterization and behavioral study were carried out previously in Chapter-IV and compared with a commercially available Nafion 117 membrane. The distance between the electrodes were kept at minimum to minimise internal resistance. Two different indoor plants viz., *P. erubescens* and *E. aureum*, which have already shown very good performance in previous studies have been used in this study along with *Chlorella sorokiniana* based microalgal bio cathode.

6.2.2 Stacking of PMFCs

PMFCs were arranged in three different cluster arrangements to increase power generation and to understand the role of series parallel connections. In Cluster I (4 series connected PMFCs), Cluster II (2 Parallel ×4 series connected PMFCs) and Cluster III (8 series connected PMFCs) as shown in Fig 6.1. To connect PMFCs in series, anode of PMFC-I was connected to cathode of PMFC-II and the series was continued by connecting multiple PMFCs in similar fashion. On the other hand, in a parallel arrangement, the connections are reversed.

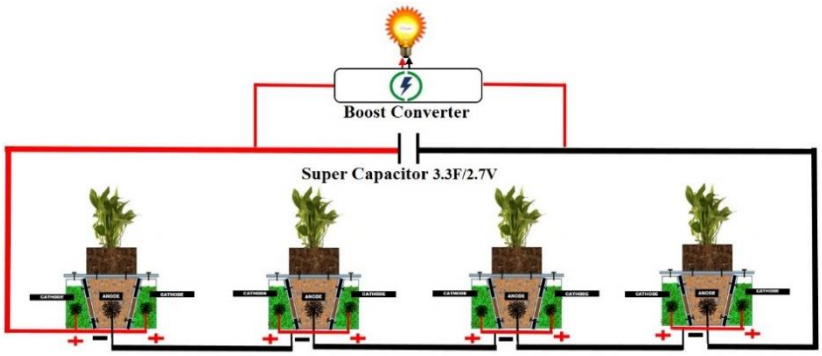

(a)

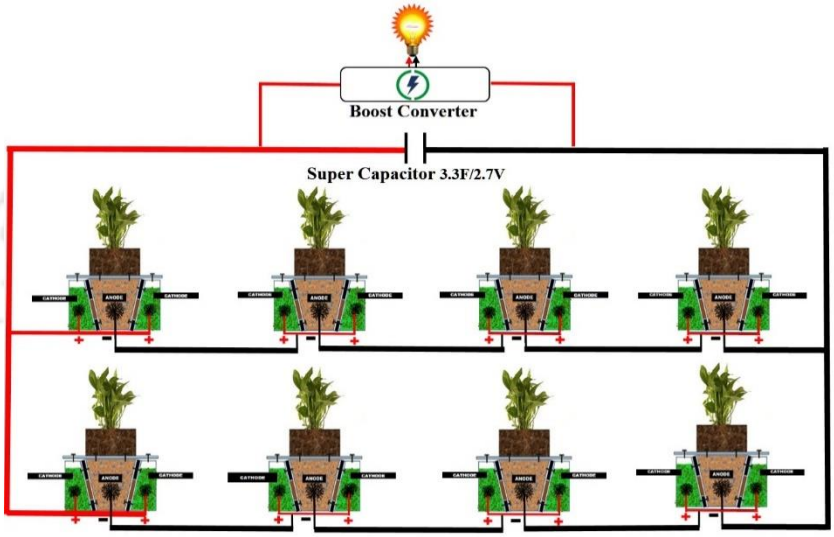

(b)

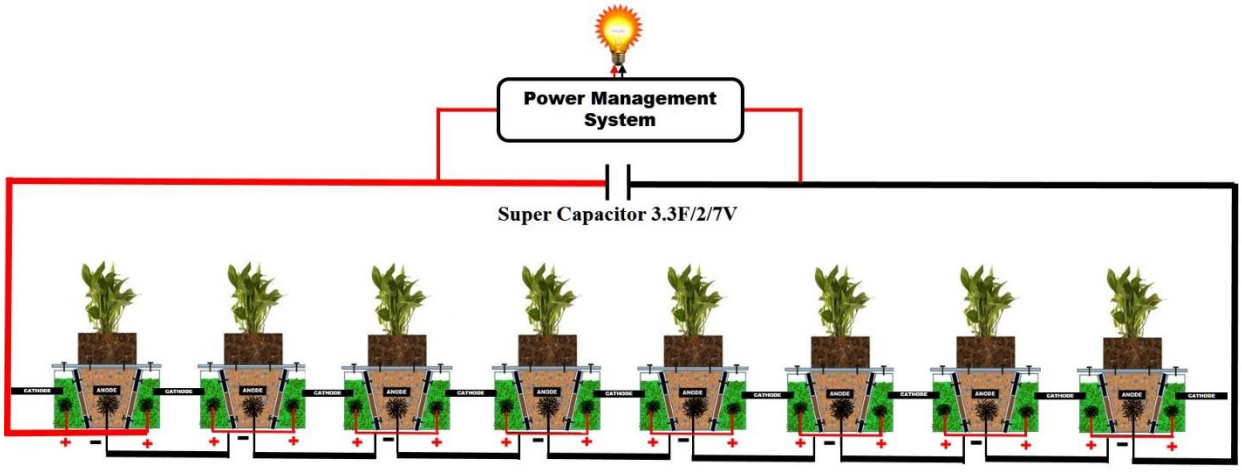

(c)

Fig 6.1 Schematic electrical connection of different cluster: (a) Cluster I (4 series connected PMFCs), (b) Cluster II (2 Parallel ×4 series connected PMFCs) and (c) Cluster III (8 series connected PMFCs).

6.2.3 Implementation of Power management systems (PMS) to improve PMFCs performance

In this study we have used a power management systems (PMS) as shown in block diagram of Fig. 6.2. These PMS has boost converters to boost the input voltage from a supercapacitor (already connected to PMFCs clusters). The PMS, consist of a boost converter BQ-25570 (Texas Instruments, USA) which is a nano-power boost charger and buck converter for energy harvester powered applications that manages energy from an input voltage as low as 100 mV, which allows to use this device in thermoelectric generators, small solar cells, piezoelectric generators, among others. Also, this device was specifically designed to efficiently acquire and manage microwatts (μW) to milliwatts (mW) of power generated from a variety of high output impedances. The BQ-25570 implements a programmable maximum power point tracking (MPPT) module for maximizing the transfer of power from the storage supercapacitor linked to PMFCs cluster to the battery. The boost converter has an internally referenced voltage called V_{STOR} which is not utilised. When the V_{STOR} is less than 1.8 V, it works under cold start mode. Once the V_{STOR} output reaches ~1.8 V, the main boost converter extracts the power more efficiently from the supercapacitor connected to the PMFCs cluster. It provides a constant regulated output voltage in the range of 4.5-5V for the battery to charge, till the supercapacitor discharges to ~100mV.

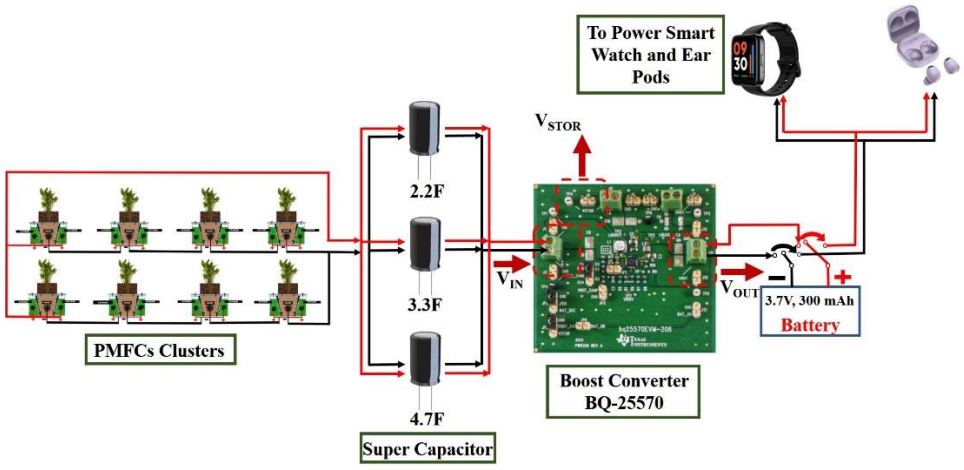

Fig 6.2 Block diagram of the power management system (PMS) with boost converter BQ-25570.

6.2.4 Electrochemical measurements of PMFCs

The output voltage from PMFCs cluster were measured using Arduino connected to a PC. The power output from PMFCs cluster were calculated as

$$P_{IN} = V_{IN} \times I_{IN} \quad (6.1)$$

where P_{IN}, V_{IN}, and I_{IN} are the input power, the input voltage and the input current for the PMSs, respectively. The energy stored (E_C) in the supercapacitor can be measured by

$$E_C = \frac{1}{2} C (V_D^2 - V_C^2) \quad (6.2)$$

Where, charging voltage (V_C) to the discharging voltage (V_D) and C is the capacitance of the supercapacitor in Farad. The average power provided by the individual PMFCs cluster to charge the supercapacitor can be calculated as

$$P_{av} = E_C / T_C \quad (6.3)$$

Where, T_C time taken to charge the supercapacitor. The input power provided by the charged supercapacitor to the PMS can be calculated as

$$P_{IN} = E_C / T_D \quad (6.4)$$

Where, T_D is the discharging time of the supercapacitor. The charging-discharging of the battery was monitored by IoT based battery monitoring system using ESP8266 in the Think Speak IoT platform. The charging time for the battery was measured by:

$$The\ charging\ time\ for\ battery\ (hours) = \frac{The\ battery\ capacity\ (mAh)}{The\ charging\ Current\ (mA)} \quad (6.5)$$

6.3 Results and Discussion

6.3.1 Performances of PMFCs clusters

For all the PMFCs, it takes around 2-3 weeks to acclimatize to the new condition and deliver a stable open circuit voltage (OCV). The modular design of PMFC was beneficial in assembling many PMFCs in a short period. During the initial 20 days, the PMFCs were connected in OCV mode as a continuous fluctuating potential increase was observed. The start-up phase depends on plant and microbes' adaptability, availability, and degradation of organic matter by microbes. After 20 days, when stable OCV was obtained, the individual PMFCs were connected across a load to obtain operating voltage. After that, the PMFCs were connected in different cluster arrangements, as shown in Fig. 6.1. The maximum open circuit voltage obtained in all three clusters was represented in Table 6.1, with cluster-III showing the highest values of 5.69 ± 0.23 (OCV). However, there are variations in power generation among PMFCs

because of variations in the internal resistance of individual cells due to variations in the internal mechanism of cells affected by biofilm growth. These include factors such as mass transfer loss, activation loss, and ohmic loss. The individual PMFC performance also depends on biofilm behaviour on both the anode and cathode. When the individual PMFCs cluster are connected to charge a supercapacitor of 3.3F/2.7 V, the maximum short circuit current (SCC) obtained are 0.87 ± 0.23 mA, 1.45 ± 0.23 mA, 0.94 ± 0.23 mA for Cluster-I, Cluster-II, Cluster-III respectively (Table 6.1). The parallel connections in the Cluster-II lead to the generation of higher current compared to other clusters. The polarization curve and power curve for all three clusters are obtained, and the maximum power derived from Cluster-I, Cluster-II, and Cluster-III are 1.788, 2.95, and 2.80 mW at an operating voltage of 2.054, 2.056, and 2.97 V, respectively. The power derived from Cluster II is higher due to the higher current generation of parallel connections.

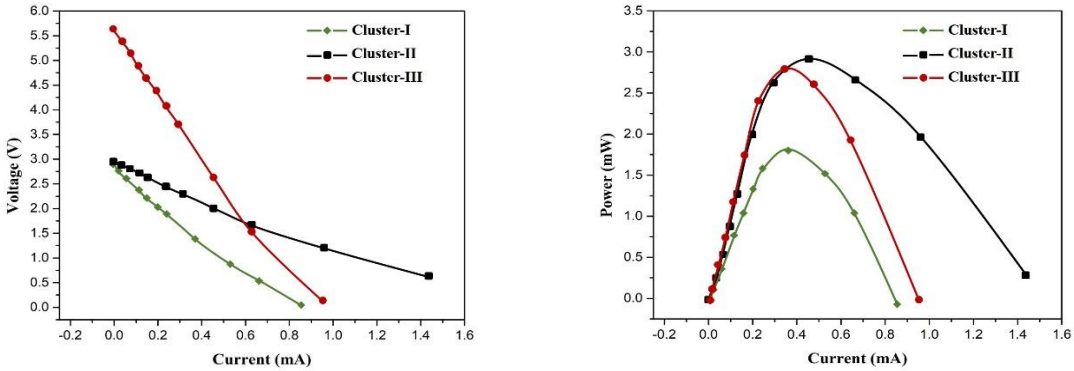

(a) (b)

Fig.6.3 (a) Polarization curve and (b) Power curve of all three PMFC clusters.

Table 6.1 Performance of different PMFC clusters.

PMFCs	Configurations	Max. Voltage (V)	Max. Power (mW)	Max. Current (mA)
Cluster-I	4 PMFCs in Series	2.87 ± 0.04	1.78 ± 0.10	0.87 ± 0.04
Cluster-II	4 PMFCs in Series × 2 Parallel	2.89 ± 0.06	2.95 ± 0.08	1.45 ± 0.04
Cluster-III	8 PMFCs in Series	5.69 ± 0.04	2.80 ± 0.08	0.94 ± 0.04

6.3.2 PMFCs recovery profile

The study of plant recovery profile is essential to understand the sustainability of PMFCs. During the supercapacitor charging period (typically 18-19 h) a significant voltage drop was noticed at the output from PMFCs. The PMFCs clusters were disconnected and OCV

was measured. The OCV values were obtained to be 1.5 ± 0.6 V, 1.5 ± 0.6 V and 2.6 ± 0.4 V for Cluster-I, Cluster-II, Cluster-III, respectively. The PMFCs cluster recovery time is studied throughout the experiment period and is represented for 10 continuous days in Fig. 6.4. It can be seen that for Cluster-I, it took nearly ~8.5 h to fully recover the voltage to its starting point of 2.7 V.

Similarly, time taken for recovery Cluster-II was ~8.5 h, with a maximum voltage level of 2.7 V. In case of Cascade-III, within ~8.5 h, the voltage recovery was 5.5 V. The plant recovery time is very consistent, representing the sustainable nature of PMFC technology without adding any external nutrients for microbes. However, for healthy growth of the plants in PMFCs, plant growth media is regularly sprayed, as mentioned in Chapter-III. A more in-depth study is currently going on regarding changing dynamics of plant and microbes' physiology and its co-relation with bioelectricity generation during the PMFC recovery period.

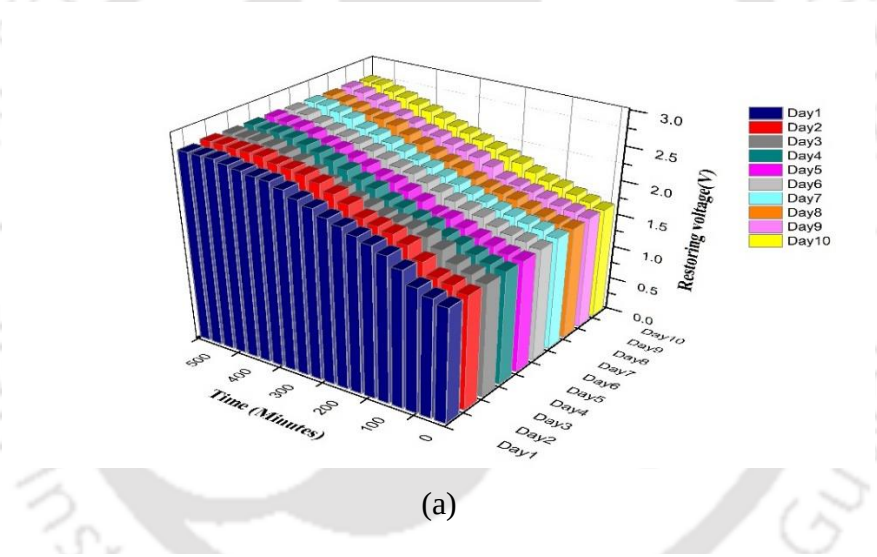

(a)

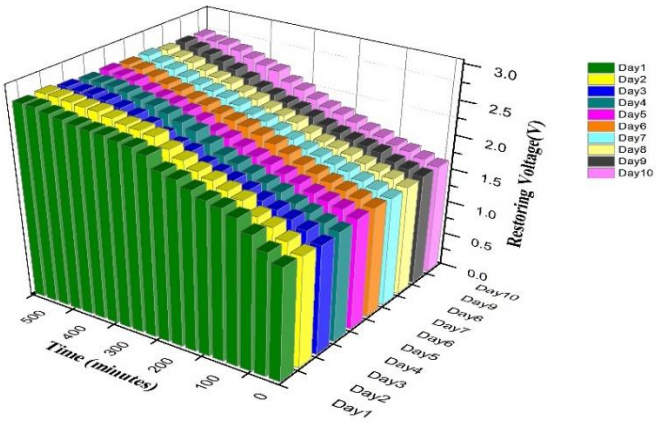

(b)

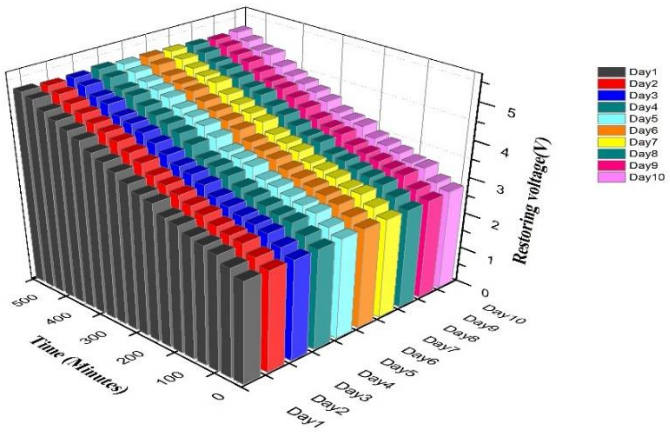

(c)

Fig.6.4 PMFCs cluster revival time (a) 4PMFCs in Series (b) 4 PMFCs in series × 2 Parallel (c) 8 PMFCs in Series.

6.3.3 Supercapacitors charging using PMFC cluster

The power output generated by cluster-II supersedes the other two clusters; therefore, Cluster-II was used in subsequent studies for charging supercapacitors. In this study, three different supercapacitors, viz., 2.2 F, 3.3F, and 4.7F, were connected to cluster-II to conduct a comparative analysis through a repeated charging-discharging cycle. A long-term stability study is carried out by performing the experiments for more than two months, involving at least 15 charging-discharging cycles for all three supercapacitors. To step up the voltage, the supercapacitor is connected to DC/DC boost converter BQ25570 throughout the process to see how output voltage varies with time. It was noticed that the initial charging process is very quick; however, to reach the steady state conditions, it takes around 13 h for both 2.2 F and 3.3F supercapacitors, while it takes a longer duration of 17.5 h for 4.7 F supercapacitors (Fig. 6.5). The supercapacitors are connected to the PMFC cluster for around 18-19 h to understand the complete charging profile (Fig. 6.5). The energy stored in the is obtained to be 8.05 J, 8.72 J, and 9.4 J once the maximum steady state voltage is attained as 2.7 V, 2.3 V, and 2.0 V in the 2.2 F, 3.3 F, and 4.7 F supercapacitor respectively.

While the supercapacitor is getting charged, at the same time, BQ25570 starts boosting the input voltage. From Figure 6.4, it can be seen that during the initial stage (0-0.6 V) the BQ25570 works under cold start mode showing the adaptability of boost converter to amplify input voltage coming from the supercapacitor. The cold start behaviour of BQ25570 varies with input sources. In the case of all three supercapacitors, it took around 45 minutes to overcome cold start mode. The BQ25570 converter only requires microwatts of power at the

input of the circuit to begin operating in cold-start mode. Once the cold start operation ends, the boost converter starts accumulating voltage in its internal storage called $V_{STOR.}$ The advantage of using BQ25570 is that it can deliver a consistent output voltage of 4.9 V through a wide range of input voltage range from 2.7 V to as low as 100 mV from the supercapacitor (Fig. 6.5).

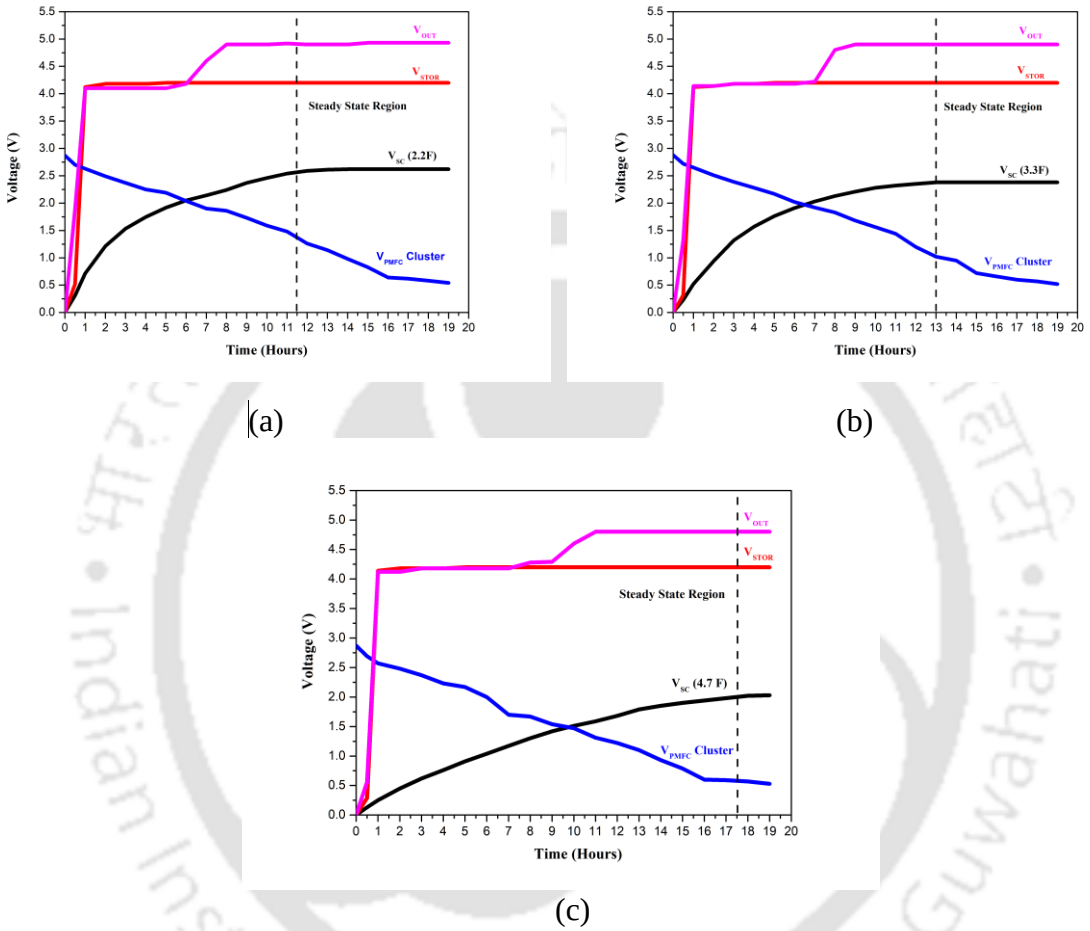

Fig.6.5 Charging behaviour of supercapacitor of (a) 2.2 F (b) 3.3 F (c) 4.7 F and the corresponding boosted output voltage (V_{OUT}) from BQ25570.

6.3.4 Discharge behaviour of supercapacitor and analysis of battery charging

To study the discharge behaviour of all three supercapacitors, a 300 mAh battery was connected to the output terminal of the boost converter BQ25570. The supercapacitor discharging behaviour and battery charging curve is represented in Fig. 6.6. The charging of the battery takes place once the V_{STOR} reaches ~1.8 V, and the main boost converter extracts the power in MPPT mode more efficiently from the supercapacitor connected to the PMFCs cluster. The MPPT mode of the board enables while V_{STOR} value reaches 4.2 V and provide 5 V at V_{OUT}. The boost converter provides a continuous output of 4.8-5V (V_{OUT}) till the supercapacitor voltage drops below 100 mV (Fig.6.6). The discharge time of the supercapacitor

varies and depends on the energy stored in each supercapacitor. Compared to 2.2F and 3.3F supercapacitors, the 4.5F supercapacitor provides a high discharge current and lowering discharging time due to the accumulation of higher charge from the PMFC cluster. The discharging time of the supercapacitor was 256 ± 6 s, 182 ± 2 s, and 157 ± 5 s for 2.2 F, 3.3F and 4.7 F supercapacitors, respectively. During this time interval, the battery voltage increases by 0.218 ± 0.016 V, 0.248 ± 0.010 V, 0.260 ± 0.008 V by fully discharging a supercapacitor of 2.2 F, 3.3F and 4.7 F, respectively.

The PMFC cluster recovery study in the previous section shows that for complete recovery of PMFCs to their highest OCV potential, it takes nearly 8.5 h. Therefore, once a supercapacitor gets discharged, it has to wait for another 26 h to fully charge itself (8-8.5 h plant recovery time + 18 h supercapacitor charging time). The battery percentage drops by 3-5 % in this time interval. Therefore, fully charging the battery takes little more than 7 days when a 4.7 F supercapacitor is used as an input. The complete battery charging profile when all three supercapacitors is used as input source can be seen in Fig.6.7. The charging time duration can be easily reduced if multiple set of cluster-II PMFCs can be brought to use similar to Prasad and Tripathi in 2020. Also, PMFCs can use solar cells in hybrid mode to increase efficiency.

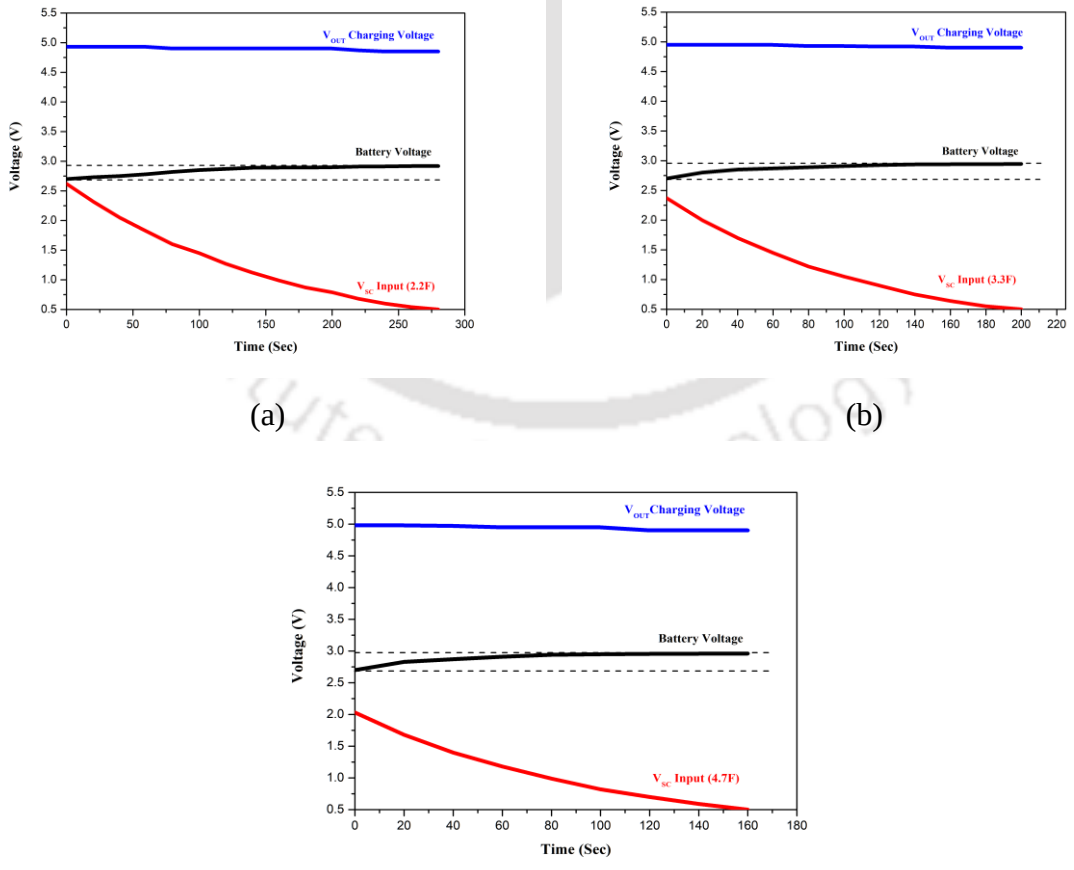

(a) (b)

(c)

Fig.6.6 Discharge behaviour of the super capacitor of (a) 2.2 F (b) 3.3 F (c) 4.7 F for BQ25570.

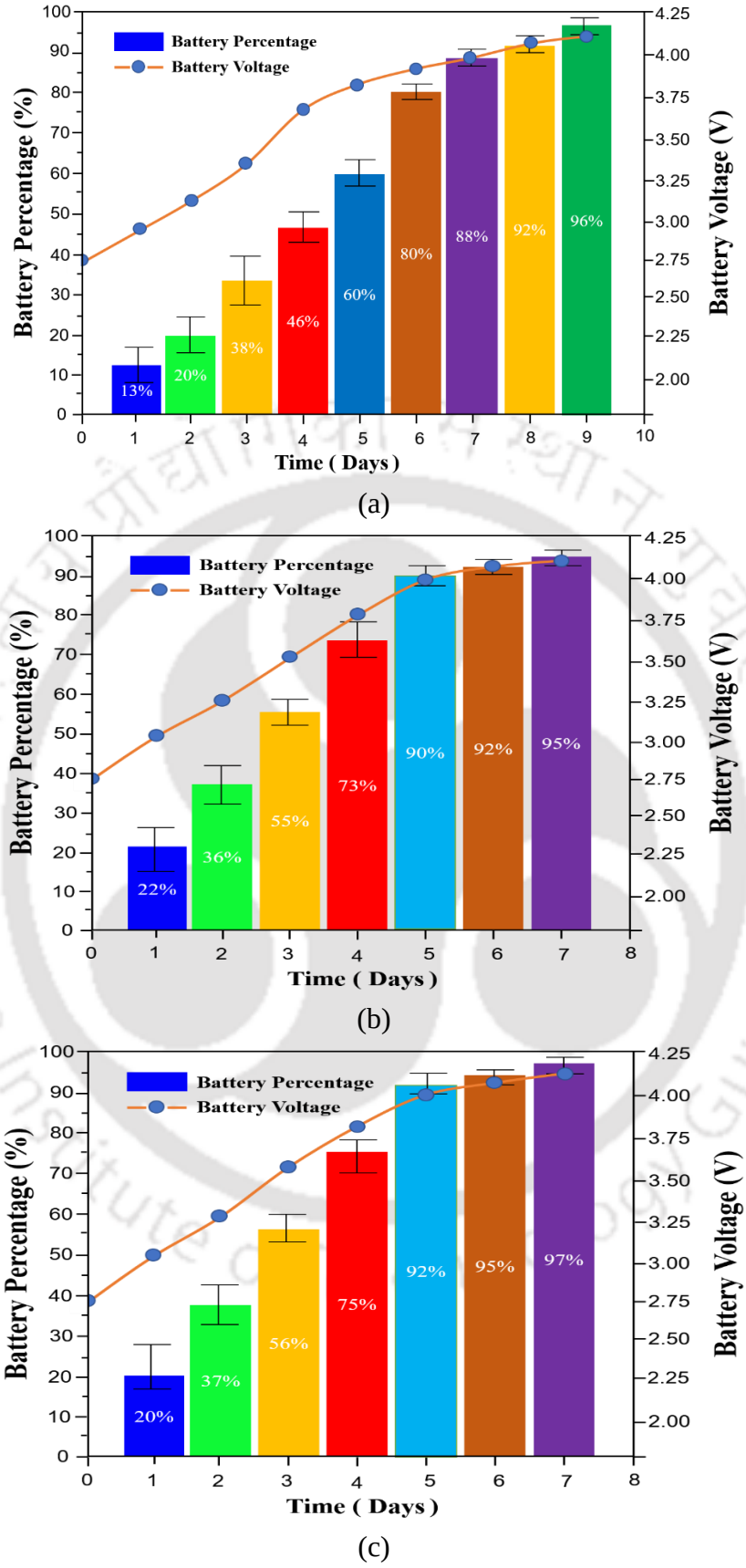

Fig.6.7 Variation of battery percentage and voltage with respect to time during charging of 3.7 V lithium polymer battery using (a) 2.2 F (b) 3.3 F (c) 4.7 F super capacitor.

6.3.5 Powering a smartwatch and a wireless ear buds

To drive out the functionality of a 300mAh charged battery, it was disconnected manually and connected again as input to the boost converter BQ25570 to act as an input source for charging a 170 mAh smart watch and a pair of ear pod having a combined 43mAh battery (charged through its housing case). As per manufacturer information of these two product, it requires a minimum voltage of 4.2 V for charging these devices. Therefore, a fully charged battery having voltage of ~3.7 V needs to be connected to the boost converter to charge the devices. For simplicity, the whole process of powering the electronic gadgets was divided into two steps (Stage-I and Stage-II), as represented in Fig. 6.8a. In the Stage-I supercapacitor was charged by using the PMFC cluster. The energy stored in the supercapacitor is used to charge the Li-Polymer battery through DC/DC boost converted BQ25570 in successive steps. In case of Stage-II, the fully charged battery is connected to the input of the DC/DC boost converted BQ25570 to charge a Smartwatch and a wireless ear buds. In the process, the rechargeable battery is discharged from ~ 4.2 V to ~ 2.7 V. A digital display battery tester was used to measure battery capacity. The voltage variation and change in battery capacity is shown in Fig. 6.8b. It can be seen that; it took nearly 120 minutes to fully charge the smartwatch from 0 to 100 % with 60% decrease in battery capacity in the process. For charging of wireless ear buds having a capacity of 43 mAh, it took around 60 minutes, and in the process the rechargeable battery percentage further decreased up to 96%, finally leaving a 6 % battery charge. After the battery was fully discharged, it was again charged by BQ25570 multiple times to reach better conclusion. During the entire study, no voltage reversal issue was noticed.

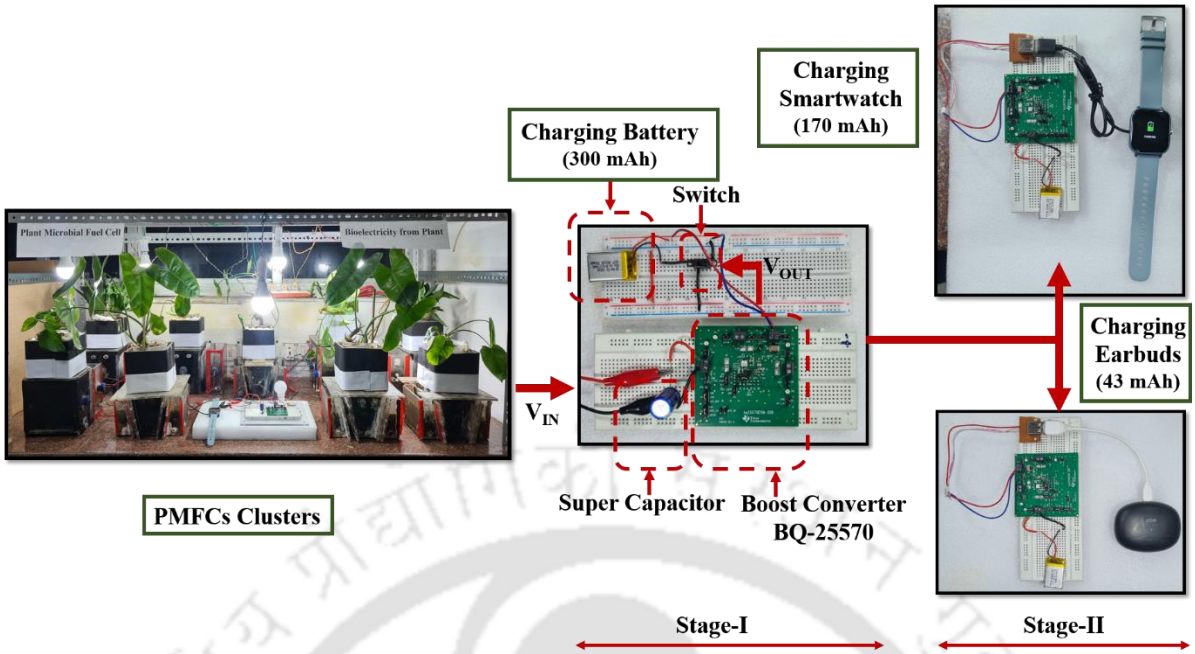

(a)

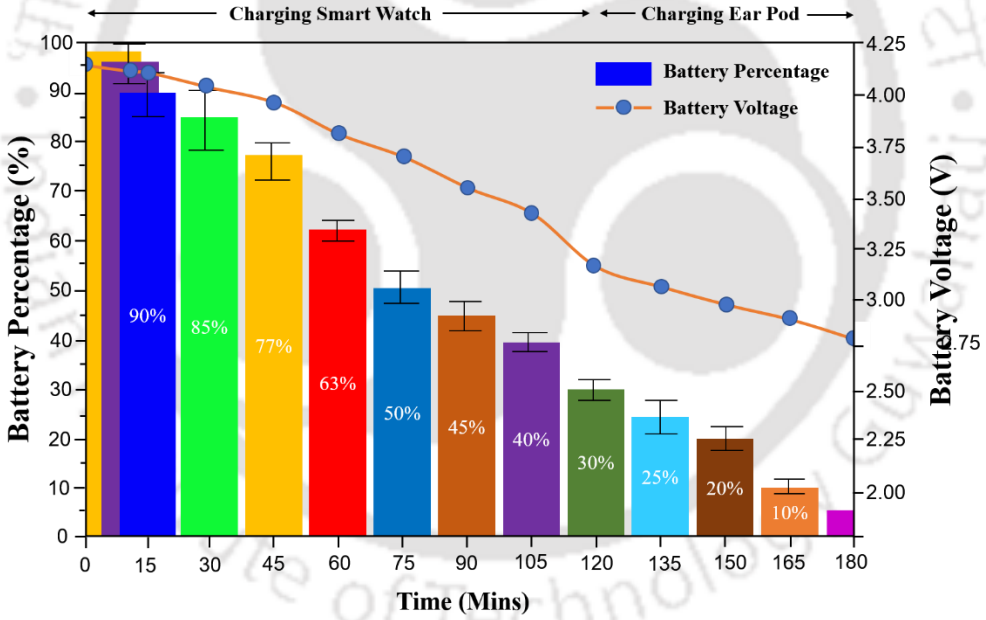

(b)

Fig.6.8 (a) PMFC Cluster Powering Smartwatch and Earbuds(b) Variation of battery percentage and voltage with respect to time when powering Smartwatch and Ear pod.

6.3.6 Driving the application modules

There is a diverse application of PMFC for large-scale energy generation systems starting from wetlands (Wetser et al., 2015; Schievano et al., 2017) to engineered rooftop (Helder et al., 2013; Guan and Yu, 2021) as most plant species are suited for such environment as mentioned in section 2.2 (Chatper-II). This also represents a benefit over other biomass

energy (Strik et al., 2008). Besides large-scale primary electricity production, the PMFC technology was also used to run low-power devices such as wireless sensors for environmental monitoring. Recently a graphene quantum dots (GQDs) embedded PMFC-WIFI device was designed by Xu et al., 2021 with indoor plants to provide a power supply for the Internet of Things (IoT) and 5G signal amplification application. Table 6.2 represents a few studies with PMFC, where a PMS was built using DC/DC boost converted BQ25570 to power wireless sensors.

Table 6.2 PMFC comparative analysis.

MFC Type	Plant Type	OCV (V)	Input Power (mW)	Output Voltage (V)	Output Power (mW)	Application	Ref.
			Boost Converter BQ-25570				
Single PMFC	*Sansevieria asparagaceae*	0.8	--	3.3	2.92	WSN-Smart City	[27]
Three PMFC	*Dypsis lutescens*	1.7	1.8	4.2	--	IoT-WSN	[28]
Three PMFC	*Stenotaphrum secundatum*		1.8	3.3	2.14	IoT LoRa Network	[29]
Eight PMFC	*Philodendron erubescens, Epipremnum aureum*	5.9	2.89	4.8	--	Power smart watch and wireless ear pod	This study

6.4 Conclusion

Indoor plant-based PMFCs can be a source to power various low-power electronic devices and has the potential to meet the increasing demand for green energy. Eight PMFCs in different cluster arrangements show that the voltage generation increases in case of a series connection; however, connecting PMFCs both in series and parallel helps to increase voltage and current simultaneously. Among the three different arrangements, it is observed that Cluster-II generates the highest current, 1.45 mA, and therefore helps to charge the supercapacitor faster. Three different supercapacitors, viz., 2.2 F, 3.3F, and 4.7 F, were charged using Cluster-II, and it took around 13 h to fully charge the 2.2F, 3.3F supercapacitor from 0V to 2.7V. In contrast, it took 17.5 h to charge the 4.7 F supercapacitor fully. Every time a supercapacitor is charged, the PMFC cluster voltage decreases, taking around 8.5 h to recover fully. The DC/DC boost converter (BQ25570) provides a constant regulated output voltage in the range of 4.5-5V for 256 ± 6 s, 182 ± 2 s, 157 ± 5 s for a rechargeable battery to charge when

connected to 2.2 F, 3.3F and 4.7 F supercapacitors respectively. In the process, to completely charge a battery (3.7V) up to 100 %, it took 8 days, 7 days and 7 days while using 2.2 F, 3.3F, and 4.7 F supercapacitors, respectively. The fully charged battery could charge a smartwatch and wireless earbuds in 120 minutes and 60 minutes, respectively. Therefore, this study offers to exploit the potential of PMFCs to power electronic gadgets for day-to-day application.

References

Apollon W, Maldonado AIL, Kamaraj SK, Contreras JAV, Fuentes HR, Leyva JFG, Ruiz JA (2021) Progress and recent trends in photosynthetic assisted microbial fuel cells: A review. Biomass and Bioenergy 148: 106028

Bombelli P, Dennis RJ, Felder F, Cooper MB, Madras Rajaraman Iyer D, Royles J, Harrison ST, Smith AG, Harrison CJ, Howe CJ (2016) Electrical output of bryophyte microbial fuel cell systems is sufficient to power a radio or an environmental sensor. R Soc Open Sci. 3(10): 160249

Chiranjeevi P, Yeruva DK, Kumar AK, Mohan SV, Varjani S (2019) Chapter 3.8 -plant-microbial fuel cell technology. In: Mohan SV, Varjani S, Pandey A (Eds.), Microbial Electrochemical Technology. Biomass, Biofuels and Biochemicals. Elsevier 549–564

Guan CY, Yu CP (2021) Evaluation of plant microbial fuel cells for urban green roofs in a subtropical metropolis. Science of the Total Environment 765: 142786

Helder M, Chen WS, Harst EJ (2013a) Electricity production with living plants on a green roof: environmental performance of the plant microbial fuel cell. Biofuels, Bioproducts and Biorefining 7: 52–64

Helder M, Strik DP, Timmers RA, Raes SMT, Hamelers HVM, Buisman CJN (2013b) Resilience of rooftop plant-microbial fuel cells during Dutch winter. Biomass Bioenergy 51: 1–7

Kim T, Yeo J, Yang Y, Kang S, Paek Y, Kwon JK, Jang JK (2019) Boosting voltage without electrochemical degradation using energy harvesting circuits and power management system-coupled multiple microbial fuel cells. Journal of Power Sources 410–411: 171–178

Li S, Zhao Z, Li B, Wei T, Jiang H, Yan Z (2022) Supercapacitors accumulating energy harvesting from stacked sediment microbial fuel cells and boosting input power for power management systems. International Journal of Hydrogen Energy 47: 10689-10700

Limbergen TV, Bonne R, Hustings J, Valcke R, Thijs S, Vangronsveld J, Manca JV (2022) Plant microbial fuel cells from the perspective of photovoltaics: Efficiency, power, and applications. Renewable and Sustainable Energy Reviews 169: 112953

Lopez JJE, Castillo JV, Atoche AC, Rosa EO, Lozano JH, Atoche AC (2023) A Sustainable Forage-Grass-Power Fuel Cell Solution for Edge-Computing Wireless Sensing Processing in Agriculture 4.0 Applications. Energies16(7):2943

Maddalwar S, Nayak KK, Kumar M, Singh L (2021) Plant microbial fuel cell: Opportunities, challenges, and prospects. Bioresource Technology 341: 125772

Min B, Logan BE (2004) Continuous electricity generation from domestic wastewater and organic substrates in a flat plate microbial fuel cell. Environ. Sci. Technol. 38: 5809-5814

Oh SE, Logan BE (2007) Voltage reversal during microbial fuel cell stack operation. Journal of Power Sources 167: 11–17

Park JD, Ren Z (2012) High efficiency energy harvesting from microbial fuel cells using a synchronous boost converter. Journal of Power Sources 208: 322–327

Prasad J, Tripathi RK (2020) Voltage control of sediment microbial fuel cell to power the AC load. Journal of Power Sources 450: 227721

EO Rosa, Castillo JV, Atoche AC, Lozano JH, Atoche AC, Nunez GB, Barbosa R (2021) Arrays of Plant Microbial Fuel Cells for Implementing Self-Sustainable Wireless Sensor Networks, *IEEE Sensors Journal* 21(2): 1965-1974

Ruiz DA, Atoche AC, Ibarra ER, Rosa E, Castillo JV (2019). A Self-Powered PMFC-Based Wireless Sensor Node for Smart City Applications. Wireless Communications and Mobile Computing 2019: 1-10

Schievano A, Colombo A, Grattieri M, Trasatti SP, Liberale A, Tremolada P, Pino C, Cristiani P (2017) Floating microbial fuel cells as energy harvesters for signal transmission from natural water bodies. Journal of Power Sources 340: 80–88

Strik DPBTB, Hamelers HVM, Snel JFH, Buisman CJN (2008) Green electricity production with living plants and bacteria in a fuel cell. Int. J. Energy Res. 32: 870–876

Tapia NF, Rojas C, Bonilla CA, Vargas IT (2017) Evaluation of Sedum as driver for plant microbial fuel cells in a semi-arid green roof ecosystem. Ecological Engineering 108: 203–210

Watson VJ, Logan BE (2011) Analysis of polarization methods for elimination of power overshoot in microbial fuel cells. Electrochem Commun 13: 54–6

Wetser K, Liu J, Buisman C, Strik D (2015) Plant microbial fuel cell applied in wetlands: spatial, temporal and potential electricity generation of *Spartina anglica* salt marshes and Phragmites australis peat soils. Biomass Bioenergy 83: 543–50

Winfield J, Ieropoulos I, Greenman J, Dennis J (2011) The overshoot phenomenon as a function of internal resistance in microbial fuel cells. Bioelectrochemistry 81: 22–7

Yang Z, Zhang L, Nie C, Hou Q, Zhang S, Pei H (2019) Multiple anodic chambers sharing an algal raceway pond to establish a photosynthetic microbial fuel cell stack: voltage boosting accompany wastewater treatment. Water Research 164: 114955

Xu Y, Lu Y, Zhu X (2021) Toward Plant Energy Harvesting for 5G Signal Amplification. ACS Sustainable Chemistry & Engineering 9(3): 1099-1104

Chapter-VII

Overall Conclusion and Future Scope

7.1 Overall conclusion

Climate change is the biggest challenge the world is facing today because of continuous use of fossil fuel. At the same time, there is a tremendous rise in energy demand globally on a regular basis. Therefore, a shift towards alternative form of energy is highly in demand and it should be renewable, sustainable, non-polluting, eco-friendly and economical in nature. Over a period of time, the PMFC technology has turned to be a promising one and has the potential to be an equally important form of renewable energy in near future for large scale implementation in both rural and urban areas. It has the advantage of being a sustainable form of bioenergy, which can work 24 × 7 throughout the year. Therefore, it helps to conserve biodiversity, mitigate environment pollution and bioelectricity generation at the same time.

Many indoor plants are known for their ability to mitigate various indoor pollutions and are widely used in every household, office establishments, etc. Therefore, the present study is an effort to harness the bioelectricity generation potential of various indoor plants while mitigating indoor air pollution at the same time. The study is an integrated process involving design and development of PMFC setup to improve bioelectricity generation potentials by optimising different operating parameters. The entire process is illustrated in the following steps:

I. Studies on the effect of different operating parameters viz., photoperiod, light sources, growing media, electrode placement etc.
II. Study of bioelectricity generation potential of different indoor plants and understanding its long-term performance.
III. Study of electrode modification and its effect on PMFC performance.
IV. Study of the microbial community associated with bioelectricity generation.
V. Development and characterization of low-cost clay based ceramic membranes for PMFC application.
VI. PMFC setup design improvement to enhance its performance.
VII. Development of modular PMFC for ease of operation and maintenance.
VIII. Comparative analysis of bacterial and microalgal biocathode development for enhance bioelectricity generation.

IX. Scaling up of PMFCs and development of PMS for application of PMFCs to power small electronic devices.

Various indoor plant species have different mechanisms to release nutrient into soil as rhizodeposits which affect PMFC performance. Therefore, four different indoor plants viz., *Epipremnum aurium*, *Anthurium andreanum*, *Dracaena braunii*, *Philodendron erubescens* were tested in a PMFC setup. Among all the plants' species, *Philodendron erubescens* showed the best performance as compared to the other species with a maximum power density of 32.21 mW m^{-2}. Performance of a PMFC is significantly affected by various operational parameters such as photoperiod, light source and plant growth media. The study demonstrated that 12/12 h light and dark phase was optimum to extract maximum performance from PMFCs without creating operational stress. Also, the addition of novel plant growth media can influence plant growth and power generation in a PMFC. The study also demonstrated that white light is more effective than any other source of light for enhancing plant growth and increasing microalgal chlorophyll concentration at the bio cathode.

Development of biofilm on the electrode's surface is crucial for bioelectricity generation. For this study, carbon fibre material was used, which is known to be cost effective and has good adaptability for PMFC environment. Carbon fibre was modified by acid-based treatment, which helped increase surface area and improve its properties for enhanced biofilm development as evident from FESEM-EDS, Raman, FTIR analysis.

Developing low-cost ceramic membranes was one of the objective of this study, which can potentially replace extremely expensive commercial membrane without compromising the properties and performance of PMFCs. Different types of ceramic membranes were developed by blending natural clay with bentonite, flyash, Na_2Co_3, Na_2Sio_3, H_3Bo_3 at various composition. Membrane characterizations revealed that the presence of bentonite, flyash, Na_2Co_3, Na_2Sio_3, H_3Bo_3 improved the performance of MFC by supplementing its cation transport ability and reducing the oxygen diffusion and substrate crossover. The cost of making the ceramic membrane was estimated to be extremely low at ₹1,279/ ft^2 in comparison to nafion117 (₹80,580/ ft^2), and it represent economically viable alternative to commercially available proton exchange membranes.

The configuration of PMFC setup and electrode and membrane placement are important criteria affecting PMFC performance. Throughout the study, four different PMFC setups were used, from a membrane-less two chamber design to a modular three chamber structure. The design evolution process resulted in an overall 72% increase in power generation due to improved anaerobic condition inside anode chamber and improvement in ion transport across

the chamber. The three chamber PMFC design with placement of electrodes close to the membrane proved to be superior than a two chamber PMFC design enhancing transmembrane ion transport. Also development of anaerobic condition at the bio anode is favourable with a narrow bottom chamber configuration, which significantly decreases O_2 concentration at the bottom, thus enhancing power generation in PMFCs.

A comparative analysis study of biocathode development with respect to bacterial and microalgal based biocathode was also carried out. PMFCs with microalgae bio-cathode leads to a 17 % increase in power generation as compared to bacterial counterpart. The highest voltage generated was 1020 ± 4V from plant *P. erubescens.* Microbial community analysis of anode biofilm shows the presence of Firmicutes (56.84%) and Bacteroidetes (38.45%) as the most dominating bacteria present.

The new modular design of PMFC plays a significant role for ease of operation and maintenance of PMFCs during long term usage. The modular design of PMFCs also helped to assemble large number of cells in a small period of time.

As a final phase of this study, an energy harvesting system was developed with the help of a power management system to store energy from PMFCs and use it to power small electronic gadgets of day to day use. The energy generated was first stored in a supercapacitor, which was then connected to a DC/DC boost converter BQ25570 to boost the voltage for charging a 300mAh battery. The charged battery was used to charge a smartwatch and a pair of wireless earbuds.

7.2 Limitations and Future Scope

The current research tries to address the potential of indoor plants in generation of bioelectricity. The indoor plants are known for their ability to mitigate various pollutants inside close doors and purify air. The current study was limited to lab-scale under control environment. Therefore, further research can be oriented towards the design and development of a PMFC based on practical applicability with ease of operation and maintainance.

During the research period, it was found the power generation from individual PMFCs were low. After a load is attached to the PMFC clusters the power generation reduces significantly with a higher plant recovery time. Also fouling of membranes and electodes leads to further reduction in performance of individual PMFC.

Therefore, considering the above limitations, following are some of the areas where more improvements can be made.

- Anode modification can be done by impregnation with semiconducting metal, non-metal and their oxide nanoparticles to reduce ohmic resistance and enhance exo-electrogenic microbes' attachment on the anode's surface.
- To increase the rate of oxygen reduction reaction (ORR) and improve performance of carbon cloth, incorporation of low cost activated carbon and doping with non-pt based catalyst may be done for cathode.
- Proton transport across the chamber can be improved by incorporating new and novel ingredients with more sulphonic acid (SO_3H) groups. Membrane manufacturing process can be mechanised to achieve a more uniform pore size distribution.
- Species identification of biofilm-forming microorganisms can be done and their genetic modification or alteration may be carried out to enhance bioelectricity generation potential.
- Improvement in design aspect of PMFCs with the help of 3D printing technology to provide a more robust and user friendly device.
- For commercialising indoor PMFCs and large-scale bioelectricity generation, an aesthetically designed PMFC housing arrangement needs to be made, which can incorporate many PMFCs that occupy less space.

List of Publications

Peer-reviewed Journals:

1. P.J. Sarma, K. Mohanty, *Epipremnum aureum* and *Dracaena braunii* as indoor plants for enhanced bio-electricity generation in a plant microbial fuel cell with electrochemically modified carbon fiber brush anode, ***Journal of Bioscience and Bioengineering*** 126 (2018) 404–410, DOI: https://doi.org/10.1016/j.jbiosc.2018.03.009.
2. P.J. Sarma, K. Mohanty, A novel three-chamber modular PMFC with bentonite/flyash based clay membrane and oxygen reducing biocathode for long term sustainable bioelectricity generation, ***Bioelectrochemistry*** 144 (2022) 107996, DOI: https://doi.org/10.1016/j.bioelechem.2021.107996.
3. P.J. Sarma, Malakar B, Mohanty K. Self-sustaining bioelectricity generation in photosynthetic plant-based microbial fuel cells (PMFCs) with microalgae assisted oxygen reducing bio cathode, ***Biomass Conversion and Biorefinery*** (2023) DOI: https://doi.org/10.1007/s13399-023-03848-z.
4. P.J. Sarma, K. Mohanty, Development and comprehensive characterization of low-cost hybrid clay based ceramic membrane for power enhancement in plant based microbial fuel cells (PMFCs) ***Materials Chemistry and Physics*** 296 (2023): 127337, DOI: https://doi.org/10.1016/j.matchemphys.2023.127337.
5. P.J. Sarma, K. Mohanty, Effect of photoperiod, light source, growing media, anode placement and setup design on performance of a plant microbial fuel cells (PMFCs) with oxygen reducing microalgal biocathode, ***Biomass Conversion and Biorefinery*** (2023) DOI: https://doi.org/10.1007/s13399-023-04265-y.
6. P.J. Sarma, J. Pathak, K. Mohanty, Efficient energy harvesting from plant microbial fuel cells (PMFCs) using a power management system (PMS) to charge a smartwatch and a pair of wireless earbuds, (*Journal of power sources*, under review)

Book chapters:

1. S. Sevda, P. J. Sarma, K. Mohanty, T. R. Sreekrishnan, D. Pant, Microbial fuel cell technology for bio electricity generation from wastewater. In: Singhania, R., Agarwal, R., Kumar, R., Sukumaran, R. (eds) ***Waste to Wealth. Energy, Environment, and Sustainability,*** Springer, Singapore (2018) 237-258. DOI: https://doi.org/10.1007/978-981-10-7431-8_11.

2. P. J. Sarma, K. Mohanty, Bioelectricity from municipal wastes. In: Singh L, Mahapatra DM (eds) ***Waste to Sustainable Energy: MFCs – Prospects through Prognosis,*** CRC Press (2019) 204-210. DOI: https://doi.org/10.1201/9780429448799-11.
3. P. J. Sarma, K. Mohanty, An insight into plant microbial fuel cells. In: Krishnaraj RN, Sani RK (eds) ***Bioelectrochemical Interface Engineering***, John Wiley & Sons, Inc. (2019) 137-148. DOI: https://doi.org/10.1002/9781119611103.ch8.

Conferences:

1. P. J. Sarma, K. Mohanty, Bioelectricity Generation potentials of Indoor plants in a Microbial fuel cell, Indo-Japan bilateral symposium on future prospective of Bio resource utilization in North-East India, IIT Guwahati, Assam, India Feb 1-4, 2018.
2. P. J. Sarma, K. Mohanty, Generation of bio-electricity by indoor plant based microbial fuel cell, International Conference on Biotechnological Research and Innovation for Sustainable Development (BioSD-2018), CSIR-Indian Institute of Chemical Technology, Hyderabad, India, November 24-25, 2018
3. P. J. Sarma, K. Mohanty, An insight into plant microbial fuel cells, International Conference on Renewable & Alternate Energy (ICRAE-2018), Assam Science and Technology University (ASTU), Guwahati, Assam, India, December 04-06, 2018
4. P. J. Sarma, K. Mohanty, Self-sustaining bioelectricity generation in photosynthetic plant-based microbial fuel cells (PMFCs) to power small electronic devices, International conference on Biotechnology for Sustainable Bio resource and Bio economy (BSBB-2022) Indian Institute of Technology Guwahati, Assam, India, 7-11 December, 2022.

Patent:

1. Design and development of a modular plant microbial fuel cell (PMFC) for ease of operation and enhance bioelectricity generation. App No: 202231032009.
   (Status: Examination report submitted)

Achievements:

1. Quarterfinalist in **DST & Texas Instruments India Innovation Challenge Design Contest 2017**, Anchored by IIM Bangalore
2. **2nd Prize, Technophilia-2022,** Royal Global University, Guwahati.
3. **Runner-up at Scientifique-Model Presentation,** Research and Industrial Conclave-2023, IIT Guwahati

Journal of Bioscience and Bioengineering
VOL. 126 No. 3, 404–410, 2018
www.elsevier.com/locate/jbiosc

Epipremnum aureum and *Dracaena braunii* as indoor plants for enhanced bio-electricity generation in a plant microbial fuel cell with electrochemically modified carbon fiber brush anode

Pranab Jyoti Sarma[1] and Kaustubha Mohanty[1,2,*]

Bioelectrochemistry 144 (2022) 107996

Contents lists available at ScienceDirect

Bioelectrochemistry

journal homepage: www.elsevier.com/locate/bioelechem

A novel three-chamber modular PMFC with bentonite/flyash based clay membrane and oxygen reducing biocathode for long term sustainable bioelectricity generation

Pranab Jyoti Sarma[a], Kaustubha Mohanty[a,b,*]

[a] School of Energy Science and Engineering, Indian Institute of Technology Guwahati, Guwahati 781039, India
[b] Department of Chemical Engineering, Indian Institute of Technology Guwahati, Guwahati 781039, India

Materials Chemistry and Physics 296 (2023) 127337

Contents lists available at ScienceDirect

Materials Chemistry and Physics

journal homepage: www.elsevier.com/locate/matchemphys

Development and comprehensive characterization of low-cost hybrid clay based ceramic membrane for power enhancement in plant based microbial fuel cells (PMFCs)

Pranab Jyoti Sarma[a], Kaustubha Mohanty[a,b,*]

Biomass Conversion and Biorefinery
https://doi.org/10.1007/s13399-023-03848-z

ORIGINAL ARTICLE

Self-sustaining bioelectricity generation in plant-based microbial fuel cells (PMFCs) with microalgae-assisted oxygen-reducing biocathode

Pranab Jyoti Sarma[1] · Barasa Malakar[1] · Kaustubha Mohanty[1,2]

Biomass Conversion and Biorefinery
https://doi.org/10.1007/s13399-023-04265-y

ORIGINAL ARTICLE

Effect of photoperiod, light source, growing media, anode placement and setup design on performance of plant microbial fuel cells (PMFCs) with oxygen reducing microalgal bio-cathode

Pranab Jyoti Sarma[1] · Kaustubha Mohanty[1,2]